Stratigraphic evolution of the North Levant Platform (Syria) during Aptian to Early Turonian

Dissertation
zur Erlangung des Doktorgrades der Naturwissenschaften
(Dr. rer. nat.)
am Fachbereich Geowissenschaften
der Universität Bremen

Hussam Ghanem

Bremen, September 2012

University of Bremen
Department of Geosciences
PhD thesis
Supervisor: Prof. Dr. Hans-Joachim Kuss

ACKNOWLEDGMENTS

First and foremost, I would like to thank the staff of the Geochronology and Basin analysis department of Bremen University. In particular, I thank my supervisor, Prof. H. Jochen Kuss, who provided the opportunity for me to study in Bremen. I benefitted from his motivated support, valuable discussions, critical review and constructive comments on the manuscript. I am really grateful to many people who have encouraged me during my PhD times and kept me away from procrastinating. Especially, Christian Scheibner, Maria Petrogiannis, Stefan Höntzsch, Ralf Bätzel, Matthias Heldt, Ahmed Abdel Naby, and Salwa Bey for their professional and amicable support and the comfortable working atmosphere. I would like to extend special thanks to PD Dr. Jens Lehmann (Bremen) for discussing stratigraphic questions and for his support and encouragement

At this place I would like to thank the General Establishment of Geology and Mineral Resources (GEGMR) and the Syrian Petroleum Company (SPC) in Damascus for their support especially of the Mapping and the subsurface data, fieldwork would not have been possible. Furthermore I want to thank the colleagues for their willingness to aid the fieldwork.

My deep thanks for assistance and pleasant cooperation go to Prof. Mikhail Mouty and to Prof. Mahmoud Ibrahem for their help and kindness during the post-graduate period. I would like to extend my thanks Prof. Esmiralda Cuas for discussion on benthonic foraminiferal taxonomy.

My thesis was financially supported by the “Deutsche Akademische Austauschdienst” (DAAD), which I gratefully acknowledge.

My friends from home "Syria" should all be thanked for their friendship and constant belief that I wouldn’t be a student for the whole of my life!!! I would also like to thank my brother Ali, for his support.

Without the help of my parents, I would not be here today writing these acknowledgements. I would like to thank them from the bottom of my heart for giving me the opportunities in life and always believing I would get the goal in the end.

ABSTRACT

The Levant margin includes the easternmost part of the Eastern Mediterranean in a region where the oceanic (Tethyan) plates and the Arabian, African and Eurasian crustal plates interact. The tectonic events in relation with these plate deformations resulted in the division of the Levant into several provinces; the Southern, the Middle and the Northern. The studied area forms the Northern part of the Levant Platform.

The combination of relative sea changes, tectonics, volcanism and local, regional and global environmental perturbations in the North Levant left imprints on the Aptian - Early Turonian carbonate platform configuration and depositional settings. The latter are reconstructed within a nimproved stratigraphic framework, based on field observations, high resolution biostratigraphy, geochemical analysis, detailed microfacies distribution and sequence stratigraphy.

The Aptian – Early Turonian succession of the North Levant in the South Palmyrides and Coastal Range of Syria represents two different depositional environments of the intra platform rifting basin (Palmyrides) and passive marginal basin (Coastal Range). Deposition was controlled by terrigenous input and/or nutrition resources, syn-depositional volcanic activity, climatic and sea level change which gives the Aptian and the Albian – Early Turonian its characteristic features.

The high resolution stratigraphic calibration of the Aptian - Early Turonian strata of the Coastal Range and South Palmyrides is based on the integrated identification of benthonic and planktonic foraminifera, in comparison with carbon isotope signals and (subsurface) logs. The abundant larger benthonic foraminifera in all outcrops of both areas allow to subdivide the Aptian - Early Turonian succession into 7 biozones in the Coastal Range and five in the South Palmyrides. Locally abundant planktonic foraminifera allow the subdivision of the latest Aptian - Cenomanian succession into seven biozones in the South Palmyrides, comparing to seven biozones range from the latest Albian to Early Turonian.

Carbon isotope fluctuations record significant perturbations that are well comparable with several global changes of the carbon cycle: OAE1c, OAE1d, LCE I-III, MCE, and OAE2. The carbon isotope record is calibrated by high resolution biostratigraphic data, especially during rising sea levels.

The stratigraphic interpretation shows that the depositional systems correspond very well with deepening-up, maximum flooding surfaces (mfs) and shallowing-up cycles that were applied to support the sequence stratigraphic model. Based on high resolution microfacies and gamma ray logs of five wells, the Aptian-Early Turonian succession was subdivided into eleven 3rd order (Syrian) depositional sequences, bounded by major unconformities. Three Aptian sequences of

the Coastal Range and the South Palmyrides with mfs K80, K81S, K82S correlate partly with “Arabian” mfs (v. Buchem et al., 2012); four Albian sequences of the Coastal Range and two of the South Palmyrides with mfs K83S, K100, K110, K120 and five Cenomanian sequences (mfs K121S, K130, K131 S, K140) are defined.

ZUSAMMENFASSUNG

Der Levant Plattenrand umfasst den östlichsten Teil des östlichen Mittelmeers, wo die ozeanischen (Tethys) Platten und die arabischen, afrikanischen und eurasischen Krustenplatten einander beeinflußen. Im Zusammenhang mit diesen Plattenverform-ungen führten tektonische Ereignisse zur Unterteilung der Levant Region in eine südliche, mittlere und nördliche Provinz. Das untersuchte Gebiet bildet den nördlichen Teil der Levant Platform.

Das Zusammenspiel von relativen Meeresspiegelveränderungen, Tektonik, Vulkanismus und lokaler, regionaler und globaler Umweltveränderungen führte in der nördlichen Levant während des Apt - Unterturon zu differenzierten Plattform-konfigurationen und Ablagerungsbereichen. Letztere wurden in einem verfeinerten stratigraphischen Rahmen rekonstruiert, basierend auf Geländebeobachtungen, hochauflösender Biostratigraphie, geochemischen Analysen, detaillierter Mikrofazies-verteilung und Sequenzstratigraphie.

Die Abfolgen des Apt - Unterturon der südlichen Palmyrides und der Coastal Range Syriens sind zwei verschiedenen Ablagerungsräumen zuzuordnen: einem intra-Plattform Riftbecken (Palmyriden) und einem Becken am passiven Kontinentalrand (Coastal Range). Die Sedimentation wurde während des Apt - Unterturon vom terrigenen Eintrag, vulkanischer Aktivität, klimatischen- und Meeresspiegeländer-ungen gesteuert.

Die hochauflösende stratigraphische Kalibrierung der Apt - Unterturon Abfolgen der Coastal Range und der südlichen Palmyriden basiert auf einem integrierten Ansatz von Biostratigraphie (benthische und planktonische Foraminiferen) im Vergleich mit Kohlenstoffisotopen-Signalen und (Bohrungs) logs. Die anschnittsweise in allen Aufschlüssen reichlich vorhandenen Großforaminiferen beider Gebiete ermöglichten die Apt - Unterturon Abfolgen in sieben (Coastal Range) bzw. fünf Biozonen (Südliche Palmyriden) zu unterteilen. Die abschnittsweise häufigen planktonischen Foraminiferen erlauben die Unterteilung der Oberapt - Cenoman Abfolgen in sieben Biozonen (Südliche Palmyriden) bzw. in sieben Biozonen des Oberalb-Unterturon (Coastal Range).

Signifikante Schwankungen der Kohlenstoffisotopgehalte sind gut vergleichbar mit globalen Veränderungen des Kohlenstoff-Kreislaufs während: OAE1c, OAE1d, LCE I-III, MCE und OAE2. Der Datensatz zu den Kohlenstoffisotopen wurde mit hochauf-lösenden biostratigraphischen Daten kalibriert, vor allem während der Zeiten des Meeresspiegelsanstiegs.

Die stratigraphische Interpretation zeigt, dass die Ablagerungssysteme sehr gut mit Vertiefungszyklen, maximale. Überflutungsflächen (mfs) und Verflachungszyklen korrelieren, die angewendet wurden, um das sequenzstratigraphische Modell zu unterstützen. Basierend auf Mikrofazies und hochauflösenden Gamma-ray-Daten von fünf Bohrungen, wurde die Apt-Unterturon Abfolge in elf Ablagerungssequenzen 3. Ordnung (Syrian) unterteilt, die von großen Diskordanzen begrenzt sind. Drei Apt- Sequenzen der Coastal Range und der Südlichen Palmyriden (mfs K80, K81S K82S) korrelieren teilweise mit den "Arabian" mfs (v. Buchem et al, 2012.), ebenso wie vier Alb- Sequenzen der Coastal Range und zwei der Süd Palmyriden (mfs K83S, K100, K110, K120) bzw. fünf Cenoman-Sequenzen (mfs K121S, K130, K131S, K140).

TABLE OF CONTENTS

LIST OF FIGURES

I. INTRODUCTION AND SUMMARY

The stratigraphic evolution of the Aptian Early Turonian of North Levant carbonate platform is studied with specific emphasis on the lithostratigraphy, biostratigraphy, chemostratigraphy, facies distribution and sequence stratigraphy. During the Lower – Middle Cretaceous multiple parameters are used as proxy for the interpretation of the stratigraphic evolution of the eastern Mediterranean platform. Global, regional and local factors such as sea level fluctuations, terrigenous input and/or nutrition resources, climatic change, and mantle plume activities led to characteristic depositional features (Brew et al., 1999; Krasheninnikov et al., 2005; Mouty and Sait-Marc, 1982; Segev, 2009; Schulze et al., 2005; Homberg and Bachmann, 2010; Bachmann et al., 2003; Kazmin, 2002; Gardosh et al., 2010a; Gardosh et al., 2010b; van Buchem et al., 2011). The sediment composition of the North Levant Platform during Aptian to early Cenomanian is a function of three different depositional sources: 1) terrigenous input 2) production of skeletal grains 3) (hemi-)pelagic marls and marly limestones with plankton in the latest Aptian, Early Albian, latest Albian and Cenomanian.

The present study has concentrated on the interpretation of the stratigraphy of eastern Mediterranean and the linked impact of sea level change, the local volcanism and the global perturbations. This study aims to fill a major gap of information on the Northern Levant Platform and will introduce more details on the Aptian to Early Turonian stratigraphy. It contributes to a improved knowledge on the lateral facies variability and the age-contribution of sedimentary units in this area, by means of high-resolution integrated stratigraphy (biostratigraphy, lithostratigraphy, carbon isotope and sequence stratigraphy). Furthermore, the reconstruction of the depositional environments based on detailed bed-by-bed investigation, and succeeding analysis of litho-, bio-, and microfacies is attempted.

II. GEOLOGICAL SETTING AND TECTONOSTRATIGRAPHY OF SYRIA (NORTH LEVANT PLATFORM)

The investigated area, located to the Eastern Mediterranean Sea, geologically belongs to the Northwestern Arabian Plate (Figure II.1). It was a vast carbonate platform, formed on a passive margin attached to Tethys from Cambrian to recent. The geological evolution of the Eastern Mediterranean (Syria) is characterized by complex deformation episodes (Kazmin, 2002), as a consequence of the nearby plate- movements (Brew et al., 2001; Gardosh et al., 2010). Various authors subdivide the geological evolution of Syria into three major periods; the **Cambrian - Late Carboniferous** Pre-rifting period; the **Permian - Late Cretaceous** Syn-rifting period; **the late Cretaceous - recent** compressional period. The latter led to folding and the currently observed topographic uplifts.

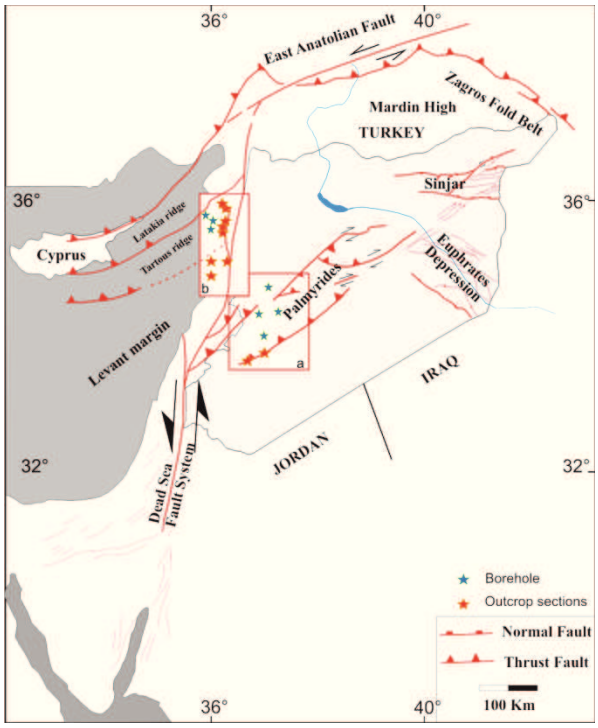

Figure II.1 - Regional map of the Eastern Mediterranean showing the major tectonic units of the Syrian Arc (modified after Bowman, 2011, Brew et al., 2002) including the localities of the studied outcrops (red asterisks) and boreholes (blue asterisks).

Pre-rifting period:

The Proterozoic Basement is directly overlain by the Paleozoic clastics, shales and limestones, defined as the oldest sediments of Syria (Brew et al., 2001). Significant thicknesses of the Cambrian Syrian Deposits reflect a N-facing passive margin (Stampfly 2002, Saber et al., 1993; Brew et al., 2001). While the clastics are probably derived from the granitic basement of the Arabian Shield to the South (Figure II.2). The thickness of the Ordovician deposits increases to ca. 2 km to ca 5 km, with A maximum thickness in southeast Syria (beneath Rutba uplift) (John et al., 1993). The Carboniferous is characterized by the Sinjar trough crossing central Syria, associated

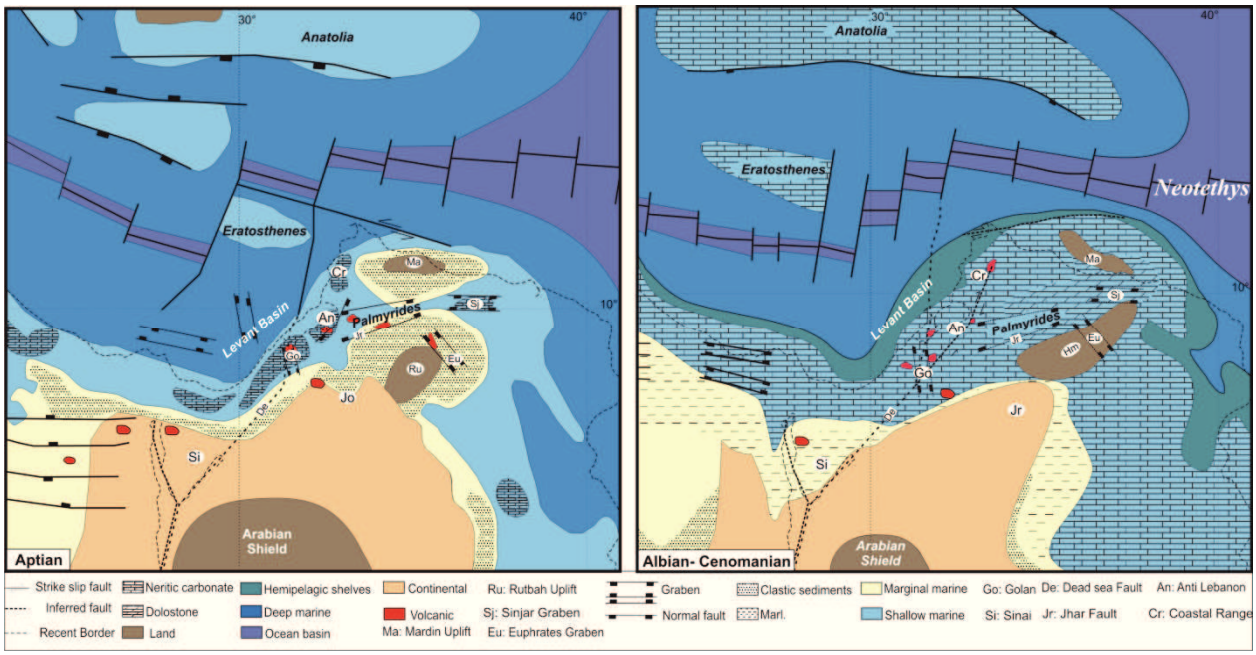

Figure II.2 - Palaeogeographic maps of the Aptian and Albian – Cenomanian after Philip (2003) and Gardosh et al. (2010).

with the reactivation of a zone of crustal weakness (Gardosh et al., 2010). The Sinjar trough is in trend with the Palmyrides Basin during the Early Paleozoic and represents the continuation of the Proterozoic rifting in the crystalline basement (George et al., 2011, Figure II.3.a). The Carboniferous rocks reflect the eastern facing of the passive margin (Brew et al., 2001).

Syn-rifting (Late Carbonefrous – Early Cretaceous):

The syn-rifting period of Syria is marked by a thick succession of Late Carboniferous-Permian shallow marine rocks (clastics and carbonates), coinciding with active rifting in the Sinjar/Palmyrides trough (Brew et al., 1999; Chaimov et al., 1992) including the Euphrate Graben (Kazmin, 2002, Figure II.2). This rifting is correlated with extensional processes along the North Africa margin during the continental breakup of Gondwana and Tethyan rifting; it led to spreading in the eastern Mediterranean and the Late Permian - Early Triassic opening of the Neo-Tethys (Figure II.2) (Stampfli and Borel, 2002). The Triassic of the North Arabian plate is characterized by two different periods of renewed extension and rifting: in the late Early Triassic, and in the Late Triassic (Brew et al., 2001; Kazmin, 2002; Wood, 2011).This period is characterized by a thick

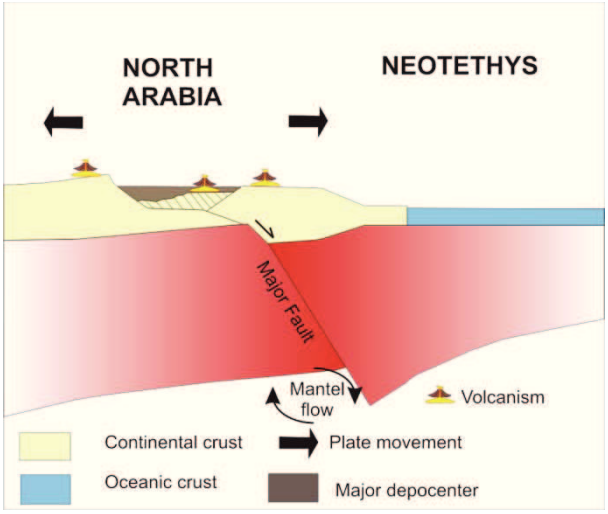

Figure II.3.a - Schematic diagrams for the volcano tectonic model of the North Arabian plate during Early Cretaceous (modified after Ma et al., 2011).

Early Triassic section in the Palmyrides-Sinjar trough. Syria changed during the Permian to Triassic from a East-facing to a West-facing passive margin (Best et al., 1993, Figure II.3.a).

The major episode of postrift subsidence of North Arabia occurred in the Early Cretaceous, following a period of erosion during the Neocomian gap. Three rifting episodes are distinguished in three individual tectonic basins: the Palmyrides Basin, the Euphrate Graben and the Sinjar Trough. Rifting in the Early Cretaceous was associated with volcanic activity in the Palmyrides, Coastal Range, Anti-Lebanon, Euphrate Graben, and South Levant (Kazmin, 2002; Segev and Rybakov, 2010, George et al., 2011, Figure II.2).

Plate Collision and Folding episode

Plate-tectonic convergence between the African and Eurasian plates are indicated by small compressional structures and deformations in the Northern Arabian Platform during Senonian (Brew et al., 2001; Kasmin, 2002; Segev and Rybakov, 2010). The initial closure of the Neo-Tethys is marked by the collision of the Northern Arabian platform with an intraoceanic subduction. This event is associated with the obduction of ophiolites during the Late Maastrichtian (Garfunkel, 2004) that is marked by a major rise in sea level (Bowman, 2011, Figure II.3.a). During this Event, minor compression and uplift are observed in the South Coastal Range, Sinjar and some parts of the North Palmyrides (Bishri Block).

The Paleocene is characterized by marine environments with extensive pelagic deposition, but uplift and compression continued during the Eocene as part of the “Syrian Arc”, corresponding to the plate collision along the northern Arabian margin (Brew et al., 2001; Gardosh et al., 2010; Bowman, 2011, Figure II.3.a).

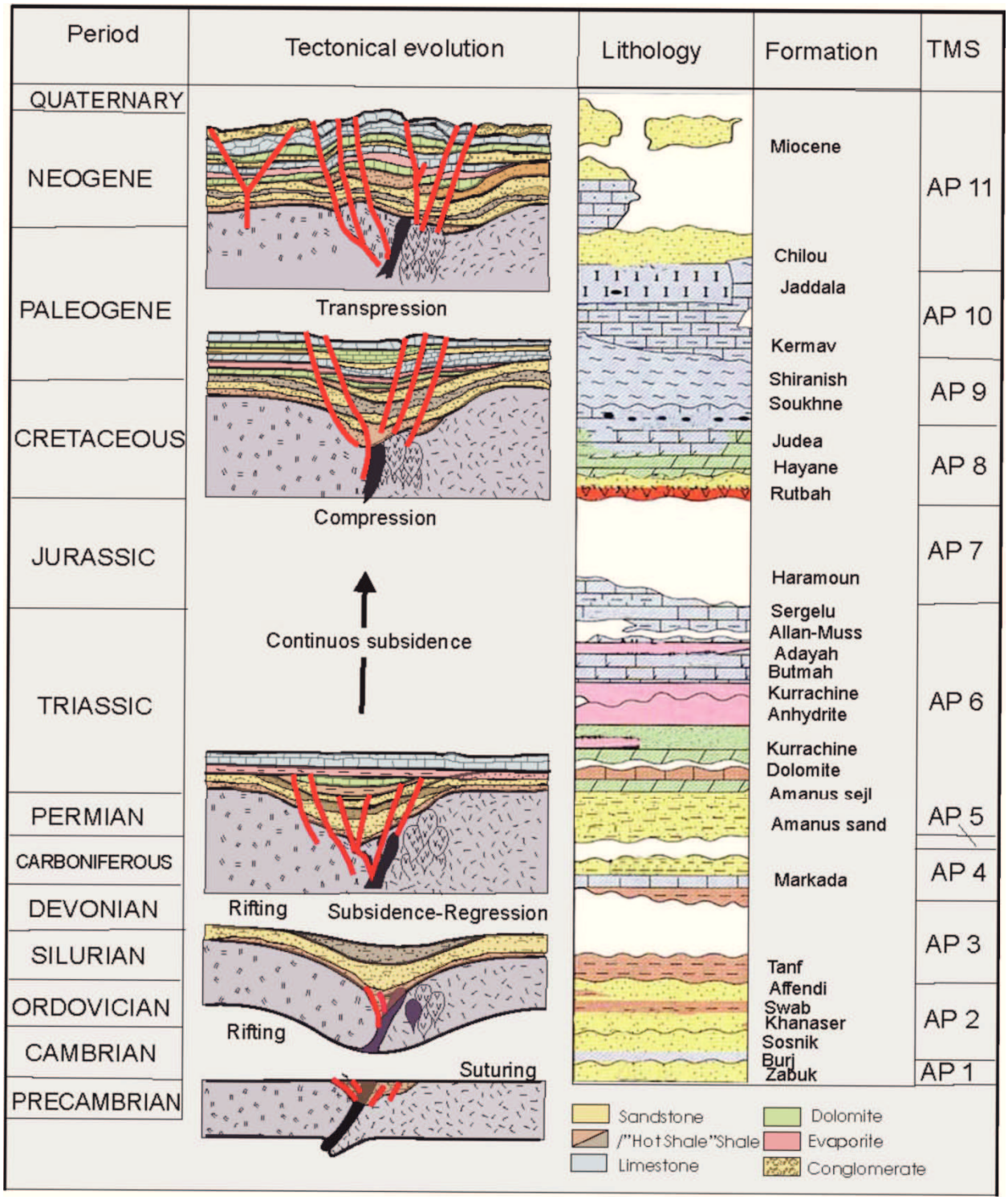

Figure II.3.b - Schematic tectonic evolution of the intra-platform baisn (Palmyrides) of Syria modified after Lucic (2002). Generalized lithostratigraphy of Syria based on surface observations and drilling records. Time intervals not to scale; relative dates of Arabian Plate (AP) tectono-stratigrahic megasequence boundaries (Sharland et al., 2001).

Tectonic uplifts and compressional events from the Middle-Miocene to Quaternary resulted in the present day structure and geomorphology (Brew et al., 2001; Gardosh et al., 2010). The Palmyrides geomorphology is a system of elongated ridges (anticlines) and intermontane depressions (synclines) (El-Motaal and Kosky, 2003, Figure II.3.a). During the Middle Miocene, the maximum stress direction changed from a compressional regime to a sinistral strike-slip regime, separating the Arabian Plate from the African Plate by the Dead Sea Transform fault system. The latter resulted in the Coastal Range uplift and its present geomorphologic features (Bowman, 2011).

III. OBJECTIVES

This study aims to fill the gap of information on the eastern Mediterranean (South Palmyrides and Coastal Range), and introduces details of a combined approach of litho-bio-, and carbon-isotope stratigraphy with facies interpretations to establish a sequence stratigraphic framework, adopted from outcrop data and borehole records.

Creating a bio-stratigraphic zonation for the Aptian - Early Turonian allows to improve the correlation of the here established sequence stratigraphic frameworks of both, Palmyrides and Coastal Range of Syria. In this study various surface and subsurface sections in different geotectonic units are analyzed in order to reconstruct the stratigraphic evolution of the Levant margin carbonate platform. High resolution microfacies, biostratigraphy, carbon isotope, gamma ray log and sequence stratigraphy as well as the correlation with the other Tethyan and global (sequences and biozones) helped to understand the evolution of the Aptian - Early Turonian of Syria

<u>The main goals of my phD-project are</u>:

- Building a deeper understanding of the sedimentary conditions on the carbonate platform during climate changes.
- Sorting the different types of microfacies and noticing the biotic and abiotic evolution of carbonate platforms to better understand the stratigraphic succession.

- Detailed field work in Syria to study and collect mid-Cretaceous outcrops. A 3D-network of several high-resolution stratigraphic sections allows to understand the sedimentologic interrelationships as well as to explain the stratigraphic evolution of the platform.
- Comparing surface and subsurface data of various log-data from several wells in the Palmyrides Basin and Coastal Chain (onshore) will be integrated in a sequence stratigraphic interpretation to compare local, regional and global processes controlling the platform sedimentation during the mid-Cretaceous of Syria.

IV. WORKING AREA AND GEOLOGICAL SETTING

West-Syria represents part of the carbonate platform surrounding the Levant margin from the Late Permian to the Late Eocene. In this study sequence stratigraphic interpretations of a relatively monotonous succession of limestones, marls, and dolostones of Aptian-Early Turonian age in West Syria are presented that form the northwestern edge of the Levant Platform. The stratigraphic evolution and different depositional settings was analyzed with respect to regional comparisons of neighboring surface data.

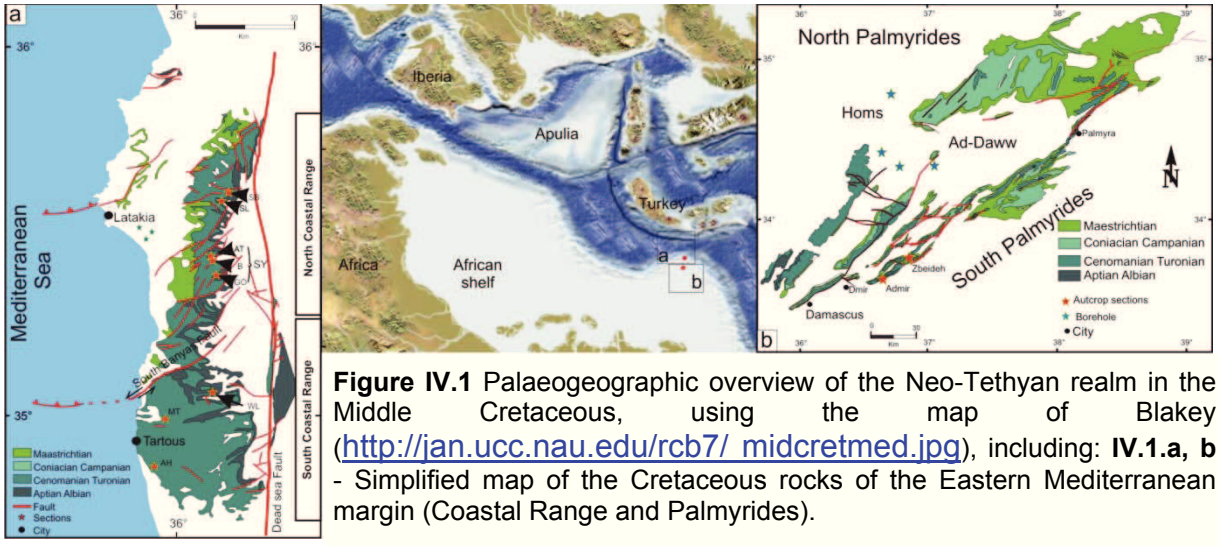

Figure IV.1 Palaeogeographic overview of the Neo-Tethyan realm in the Middle Cretaceous, using the map of Blakey (http://jan.ucc.nau.edu/rcb7/_midcretmed.jpg), including: **IV.1.a, b** - Simplified map of the Cretaceous rocks of the Eastern Mediterranean margin (Coastal Range and Palmyrides).

South Palmyrides

The Late Aptian to Cenomanian succession of the South Palmyrides is characterized by the deposition of shallow-water carbonates, in addition to Late Albian pelagic sediments and hemipelagic Late Cenomanian strata. Surface exposures of the Cretaceous succession are located in the cores of anticlinal folds and domelike structures of the South Palmyrides Chain (Krasheninnikov et al., 2005; Mouty et al., 1983; Ponikarov et al., 1966; Figure 1). These folds were cut by large faults that produce a scarp- and-cliff ridge landscape (Al-Maleh et al., 2000). The investigated area is located northeast of Damascus and extends approximately 15–17 km between the Admir and Zbeideh sections in the southwestern part of the South Palmyrides.

Coastal Range

The western slopes of the Coastal Range gradually dip to the west in the Mediterranean Sea, while its eastern slopes are cut by the Dead Sea Fault (Mouty and Saint-Marc, 1982; Krasheninnikov et al., 2005). The Aptian to Early Turonian succession is characterized by passive continental margin depositional sequences, commonly passing upward into alluvial to carbonate shelf or pelagic ramp settings (Mouty and Saint-Marc, 1982; Alsharhan and Nairn, 1997; Sharland, 2001; Gerdes et al., 2010).

Subsurface Data

Subsurface data are based on 4 boreholes from The Ad-Daww and Homs Depressions and 3 boreholes from the Latakia Basin (onshore) of the Coastal Range. The wire-line logs include sonic, gamma ray, and lithologic descriptions with few microfacies and biostratigraphic data some cored intervals. The stratigraphic data are based on the stratigraphic correlation of drilling records and outcrops. For the first time, were consider all the data in total to establish a detailed stratigraphic model of the Aptian to Early Turonian succession of west/central Syria.

V. METHODS

V. 1. Field work

The fieldwork of this study was undertaken in four separate field trips: April 2009, December 2009, December to January 2010; as all samples of the latter fieldtrip became lost, a fourth trip was conducted from February to March 2011). During these field campaigns 10 sections of the North Levant platform were collected from two different tectonic regions (Palmyrides and Coastal Range) and more than 1300 samples were taken.

Field work included the description of sedimentary structures, detailed documentation of bed by bed sections, and the description of rocks including lithology, bed thickness, colour, composition, facies and grains (fauna and clastic), and textural classification (using Dunham, 1962).

The exposure of the studied successions was variable; therefore, a dense sampling regime was needed for the chemical collections from marls and limestones. Whereas, there was perfect limestone exposure, the samples were collected for thin-section analysis (microfacies analysis and fossil identification). Photographing was part of the field work and deposit documentation presents the marker parts of the sedimentary recorded sections.

V.2. Biostratigraphy

A high resolution stratigraphic calibration of the Aptian – Early Turonian strata is based on the identification of benthonic and planktonic foraminifera. Furthemore, the foraminifera in this study were used as paleoenvironmental indicators and as proxies for the interpretation of sea level fluctuations on the platform. After identification they were described systematically and used to define local biozones of the southeastern Tethyan realm. Their importance for environmental studies is recorded by their wide range of marine environments, from coastal marshes to abyssal plains. Whereas their variety and distribution is applied as proxy for different parameters (i.e. nutrients and oxygen

availability, temperature). The biozonation schemes allow for a much improved regional understanding of particular phylogenetic lineages of benthonic and planktonic foraminifera. Planktonic foraminiferal biostratigraphy coincided with periods of sea level rising, while shallow-benthonic species dominate shallow marine environments with grained limestones.. The high diversity of Syrian foraminiferal assemblages record many faunal similarities with those of the South European platforms, described e.g. from

Section	Latitudes	Longitudes	Samples	Stratigraphic range
South Palmyrides Chain				
Admir (AM)	33°69'45"N	36°89'55"E	**172** (62 TS, 110 loose)	Late Albian Cenomanian
Zbeideh(ZB)	33°78'36"N	36°98'73"E	**190** (78 TS, 83 loose)	Aptian Cenomanian
Coastal Range				
Slenfeh(SL)	35°35'74"N	36°12'05"E	**95** (48 TS, 47 loose)	Late Albian Early Cenomanian
Bab Abdallah (SB)	35°37'11"N	36°10'25"E	**160** (79 TS, 82 loose)	Cenomanian- Early Turonian
Gobet Al-Berghal (GO)	35°29'23"N	36°09'50"E	The composed section Sayno (SY) **146** (137 TS)	Aptian Cenomanian
Ain Tina(AT)	35°59'92"N	36°11'62"E		
Al-Bragh(B)	35°32'39"N	36°10'34"E		
Wadi-Layoun(WL)	34°59'53"N	36°11'57"E	**87** (32 TS)	Aptian Early Cenomanian
Al-Meten(MT)	34°59'27"N	35°55'23"E	**106** (57 TS, 12 loose)	Late Cenomanian- Early Turonian
Wadi Al- Haddah (AH)	34°49'18"N	35°59'23"E	**143** (110 TS, 23 loose)	Middle Late Cenomanian

Table IV. 1 – List of the recorded sections, including GPS coordinates, numbers of samples and stratigraphic range. Abbreviations: TS. Samples for thin sections, loose. loose marl samples. The bold numbers indicate the total number of recorded samples.

the Adriatic Plate. As a consequence, a standardized classification was achieved with the correlation of Tethyan Aptian – Early Turonian planktonic zonation of Ogg and Ogg (2008) and Premoli Silva and Verga (2004) and shallow benthonic zonation after Velić (2007) and minor comparison with eastern Arabian platform.

V.3. Litho- Microfacies and log response

The detailed bed-by-bed field observations allow to subdived seven major litofacies types. A more detailed limestone classification is based on a microfacies analysis (including component analysis and textural descriptions) sensu Dunham (1962). and followed the. A total of 603 TS thin-sections have been prepared and grouped in 16 MFTs (standard microfacies types of Flügel, 2004), representing the Aptian – Early Turonian succession of the Levant platform.

The gamma-ray logs of seven boreholes of the Ad-Daww, Homs Depressions and the Latakia Basin show distinctive signatures that are useful for identifying the microfacies and its log response. Correlation of these signatures between boreholes may be inaccurate due to lateral facies changes, which have been well documented in neighboring outcrops.

V.4. Carbon isotopes

A total of 520 pure limestone and marl samples were analyzed for $\delta^{13}C$ isotopes. These analyses were performed at the MARUM Research Center at Bremen University. The studied isotope samples are from five sections of the Coastal Range and South Palmyrides, spanning a late Albian to Early Turonian interval. The contribute to a high-resolution biostratigraphic calibration and contributed to an Albian to Turonian reference $\delta^{13}C$ curve that was correlated with Jarvis et al. (2006). The latter authors documented boreal bioevents and global oceanic perturbations in correlation with carbon isotope excursions.

V.5. Sequence stratigraphy

Sea level fluctuations are reflected by various facies records in unique depositional environments. The field observations, thin-section analyses, and microfacies distributionare used to characterize the metre-scale cyclicity which is so pervasive in the studied lagoonal to deep marine deposits. The Aptian-Early Turonian strata are represented by deepening/ shallwing-up cycles. Cyclicity was defined by assessing the vertical stacking of microfacies in the successions. The base of a cycle was identified by

hardgrounds and/or from the sharp facies changes. A multitude of high frequency cycles and (half) cycles are defined by changes of the depositional environments that are expressed in different sedimentary facies associations. Comparisons were done with the “global sequence stratigraphy” (Hardenbol et al., 1998; Ogg, 2004; Ogg et al., 2008; Gradstein et al., 2012) and with the “Arabian Platform sequence stratigraphy” (Sharland et al., 2001, 2004; van Buchem et al., 2010, 2011).

VI. THESIS OUTLINE

The major results of this PhD thesis are summarized in three chapters, representing three separate manuscripts which are in process to be published (VII, VIII) or which have been already published (IX).

1) **Sequences, Facies and log response a case study from NW Syria**
   The North Levant platform is studied to reconstruct the stratigraphic evolution of the Aptian – Early Turonian Sea. Ten outcrop sections and seven boreholes along the shallower platform to the basin transect are studied, concentrating on lithofacies interpretations of field observations and of lithofacies interpretations of log responses. Microfacies analysis of both surface and subsurface sections form the most important outcome of that study.The distribution of floral and faunal assemblages, reflect sea level fluctuations that were interpreted to correlate all sections across the Northeastern Levant Platform.

2) **Biostratigraphy and carbon isotope stratigraphy of the uppermost Aptian to Upper Cenomanian strata of South Palmyrides, Syria.**
   The South Palmyrides has been the focus and the latest Aptian – Cenomanian transition has been studied in detail. The biostratigraphy, dating and lithostratigraphic terms for the latest Aptian - Cenomanian are discussed, with a detailed overview of the regional description of the carbon isotope curve and sequence stratigraphy.

Ghanem H., Mouty M., Kuss J. 2012 Biostratigraphy and carbon isotope stratigraphy of the uppermost Aptian to Upper Cenomanian strata of South Palmyrides, Syria. GeoArabia, v. 17, no. 2, p.155-184.

3) **Stratigraphic control of the Aptian - Early Turonian sequences of the Levant Platform (Northwest Syria - Coastal Range).**

Description and interpretation of the sequence stratigraphy identified in the Northwest Syria is based on a detailed biostratigraphic zonation of foraminiferal assemblages. Together with detailed lithostratigraphic descriptions (field observation) and high resolution carbon isotopes from the Late Albian - Early Turonian Coastal Range sections are used to highlight the global biotic and abiotic events in the shallow-marine limestones and hemipelagic marls in the Southeastern Tethyan realm.

Ghanem H., Mouty M., Kuss J. (subm.) Stratigraphic control of the Aptian - Early Turonian sequences of the Levant Platform (Northwest Syria - Coastal Range). GeoArabia.

The first manuscript

VII. SEQUENCES, FACIES AND LOG RESPONSE - A CASE STUDY FROM NW SYRIA

Hussam Ghanem[a] and Jochen Kuss[a]

[a] Department of Geoscience, Bremen University, PO Box330440, 28359 Bremen, Germany

To be submitted.

VII. SEQUENCES, FACIES AND LOG RESPONSE - A CASE STUDY FROM NW SYRIA

VII.1 Introduction

The objective of this manuscript is to contribute to sequence stratigraphic models that correlate outcrop records (e.g. from the Palmyrides and the Coastal Range) with borehole records of e.g. the Ad-Daww and Homs depression and the Latakia Basin. The study area forms part of the North Levant Platform (Aptian - Early Turonian) and the analyzed microfacies, lithofacies and sequence stratigraphic data are based on 10 outcrop sections and seven boreholes (including lithofacies, gamma ray, and one cored record) (Figure VII.1).

The aim is to identify comparable log patterns in different environmental settings and to combine biostratigraphic, lithostratigraphic and spectral gamma-ray data with respect to sequence stratigraphic and paleoenvironmental interpretations and to correlate surface and subsurface units.

The microfacies (MFTs) of the Aptian - Early Turonian deposits differ obviously, and were evaluated with respect to local and regional environmental changes. The MFTs interpretations present a sensitive parameter of the interplay between sea level fluctuations, accommodation, and siliciclastic input, confirming the correlation between lithofacies and biofacies within individual marine environments.

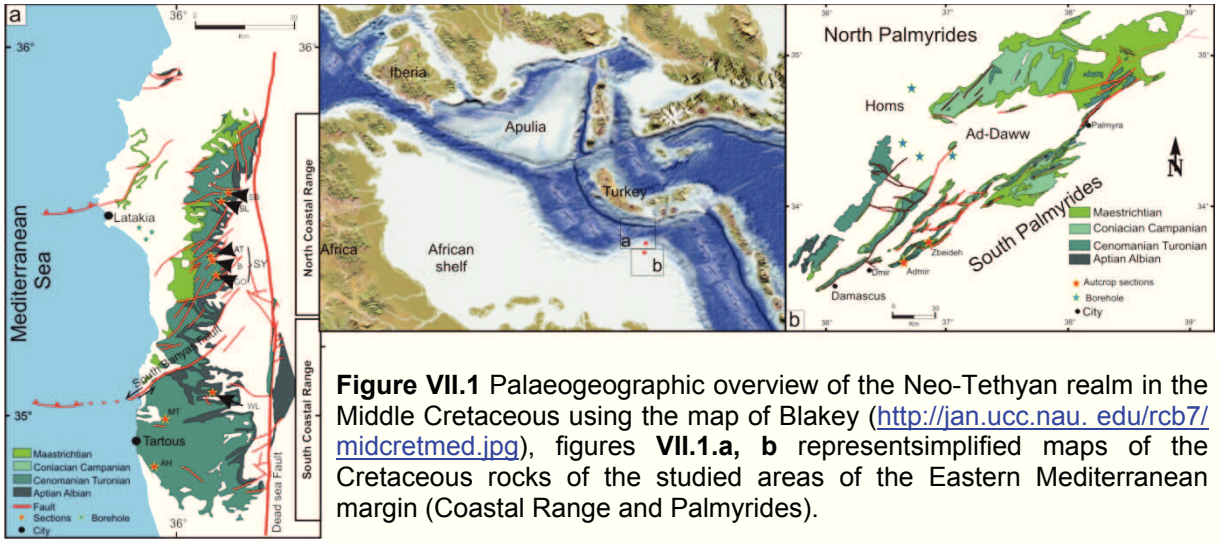

Figure VII.1 Palaeogeographic overview of the Neo-Tethyan realm in the Middle Cretaceous using the map of Blakey (http://jan.ucc.nau. edu/rcb7/ midcretmed.jpg), figures **VII.1.a, b** representsimplified maps of the Cretaceous rocks of the studied areas of the Eastern Mediterranean margin (Coastal Range and Palmyrides).

VII.2 Depositional setting

The lithostratigraphic subdivision of the here considered Aptian – Turonian succession allows to differentiate three subsurface formations that were correlated with the adjacent age-eqivalent formations from outcrops. The **Rutba Formation** is composed of Aptian siliciclastic deposits in the subsurface of Syria. It is composed of siltstone, shale and sandstone with some volcanic deposits that overly a Jurassic unconformity and are unconformably overlain by the Early to Mid Albian **Hayane Formation** and the Cenomanain – Turonian **Judea Formation** (Figure VII.2). The Lower Rutba Formation is equivalent to the Palmyra sandstone Formation in the South Palmyrides (Mouty and Al-Maleh, 1983). The marly lithologies in age-equivalent surface outcrops of the Coastal Range (Bab Janneh Formation, Ghanem and Kuss, subm.), indicate deeper water environments to the west (Brew et al, 2001).

The Hayane Formation (Albian) is well-developed in the Palmyra region of central Syria, passing from gypsum in the lower part upward into dolomite with intercalated anhydrite (Brew et al., 2001). It correlates with dolomites and limestones of the Zbeideh Formation in the South Palmyrides and the Ain Elbeida and Blaatah Formations in the Coastal Range (Figure VII.2).

The Judea Formation indicates shallow neritic waterdepths and shallow-marine conditions in the Ad-Daww and Homs depressions. It is equivalent in the South Palmyrides to Abou Zounar-, Abtar-, and Halabat Formations (Figure VII.2). The comparable Cenomanian - Turonian strata in the Coastal Range exhibit clearly deeper water environments (Brew et al., 2001), and less clastic contents (Slenfeh, Bab Abdallah, Hannafyah, and Aramo Formations).

Different lithologies can be distinguished for these formations which are typed into the following seven lithofacies-types:

1. Fluvial and marginal siliciclastics (quartz sandstone) are present at the base, marking the major Aptian deposits in the South Palmyrides (Caron and Mouty, 2007; Ghanem et al., 2012). It is forming fluvio-deltaic sands with clay, deposited in a continental to nearshore setting. In the Coastal Range, several parts of the Aptian and early Cenomanian strata are characterized by thin

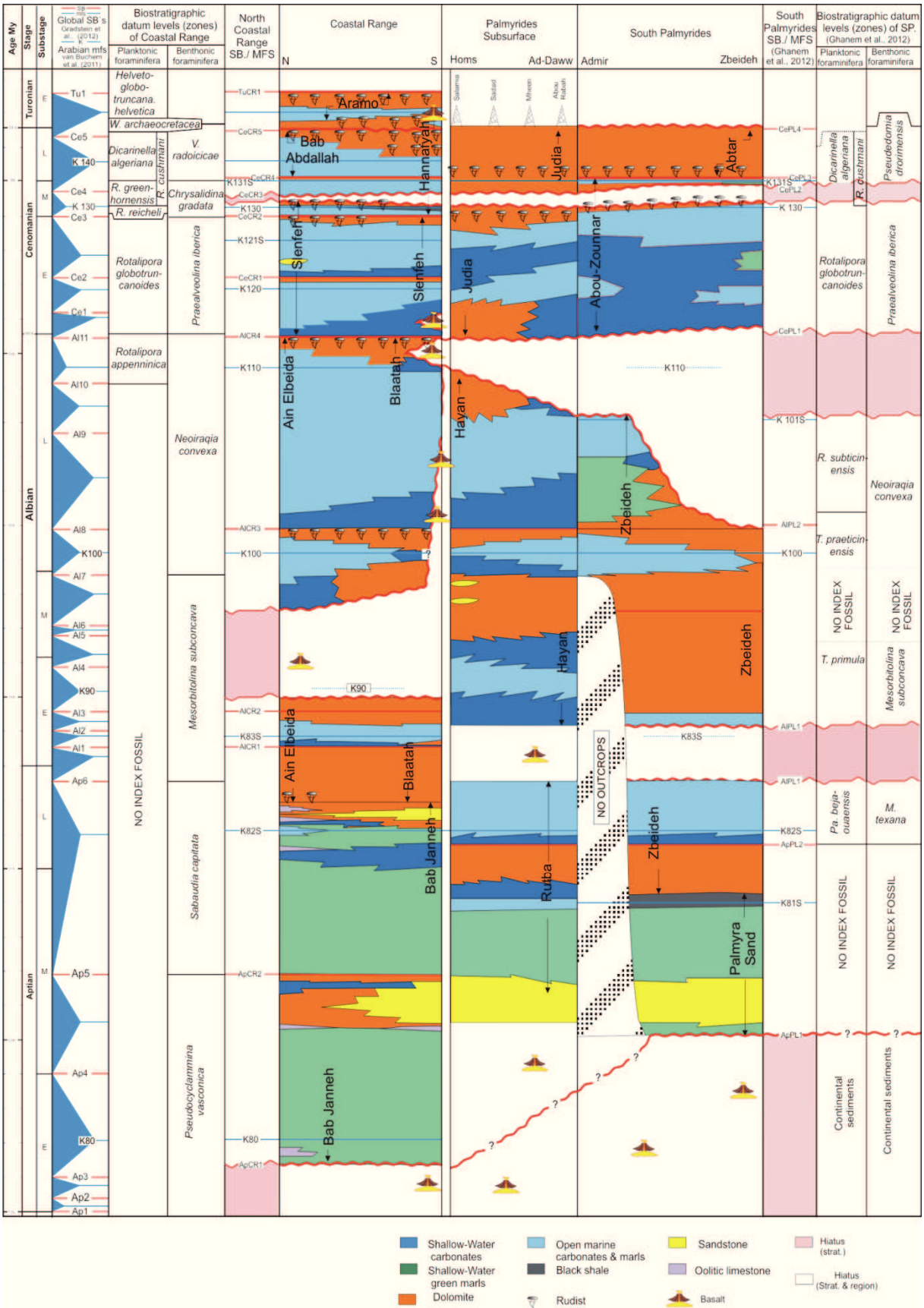
Age My
Stage
Substage
Global SB's Gradstein et al. (2012)
Arabian mfs van Buchem et al. (2011)
Biostratigraphic datum levels (zones) of Coastal Range
Planktonic foraminifera
Benthonic foraminifera
North Coastal Range SB./ MFS
Coastal Range
N
S
Palmyrides Subsurface
Homs
Ad-Daww
South Palmyrides
Admir
Zbeideh
South Palmyrides SB./ MFS (Ghanem et al., 2012)
Biostratigraphic datum levels (zones) of SP. (Ghanem et al., 2012)
Turonian
Cenomanian
Albian
Aptian
Helveto-globo-truncana. helvetica
W. archaeocretacea
Dicarinella algeriana
R. cushmani
R. green-hornensis
R. reicheli
V. radoicicae
Chrysalidina gradata
Praealveolina iberica
Rotalipora globotrun-canoides
Rotalipora appenninica
Neoiraqia convexa
Mesorbitolina subconcava
Sabaudia capitata
Pseudocyclammina vasconica
NO INDEX FOSSIL
Aramo
Bab Abdallah
Hannatiyan
Slenfeh
Ain Elbeida
Blaatah
Bab Janneh
Judia
Hayan
Abou-Zounnar
Abtar
Zbeideh
Rutba
Palmyra Sand
NO OUTCROPS
Continental sediments
Pseudedomia droimensis
T. praeticin-ensis
R. subticin-ensis
T. primula
Pa. beja-ouaensis
M. texana
Shallow-Water carbonates
Shallow-Water green marls
Dolomite
Open marine carbonates & marls
Black shale
Rudist
Sandstone
Oolitic limestone
Basalt
Hiatus (strat.)
Hiatus (Strat. & region)

Figure VII.2 (Previous page)- Correlation chart of the Aptian-Early Turonian succession based on integrated biostratigraphy, with depositional sequences in the Coastal Range (after Ghanem and Kuss, subm.), South Palmyrides (Ghanem et al., 2012) and the subsurface area in between (Ad-Daww and Homs Depressions). Comparison with regional and global sequence boundaries and maximum flooding surfaces on the left after Gradstein et al., (2012).

tongues of alluvial siliciclastics and peritidal dolomites (Ghanem and Kuss, subm., FigureVII.4).

2. Marls and marly limestones, green and gray marls, and marly limestones range between decimeters to several meters of fossiliferous intervals. The green marls characterize the Aptian strata of the Coastal Range (Bab Janneh Fm.) and different intervals of the Palmyrides (in the Late Albian of Zbeideh Fm. and Hayan Fm.) and in the Late Cenomanian of the Abou-Zonnar Fm. and Judea Fm (Ghanem et al., 2012, FigureVII.4).
3. Well bedded limestones comprise centimeter to decimeter thick beds alternating with dolostones and thin fossiliferous marls. The fossiliferous limestones are also containing peloids, ooids, rounded intraclste with a dominantly packstone and occasionally grainstone texture. This lithofacies is very common in the Aptian-Cenomanian succession of the Coastal Range and in the Albian-Cenomanian succession of the Palmyrides (FigureVII.4).
4. Massive limestones and dolostones (floatstones/rudstones) are dominated by rudists. The limestones exhibit massive cliff walls, while the massive dolostones are additionally characterized by silicified chert nodules, cauliflower and flint lenses. The latter occur in the Albian of the Zbeideh Formation and the late Cenomanian of the Abou-Zonnar Formation of the South Palmyrides, and in the latest Albian- Early Cenomanian of the Slenfeh Formation and several intervals of the Middle and Late Cenomanian of Bab Abdallah and Hannafyah Formations in the Coastal Range (FigureVII.4).
5. Nodular limestones exhibit a conspicuous fabric characterized by centimeter- and decimeter-sized, often 'rounded' nodules. This lithofacies appears in Zbeideh - and Abou-Zonnar Formations of the South Palmyrides and very frequent in the Bab Abdallah Formation of the Coastal Range (FigureVII.4).
6. The characteristic lithofacies of the Abtar Formation of the Palmyrides consists of distinctly bedded dolostones with *Thalassinoides*, lamination and bioturbation,

alternating with thin marls. This lithofacies marks shallowing-up deposits of the Late Cenomanian of the Palmyrides trough (surface and subsurface FigureVII.4).

7. Thinly bedded black shales rich in organic material, with variable amounts of clay minerals and quartz grains are found in the Aptian rocks of the Palmyrides (surface and subsurface). In the Coastal Range, this lithofacies is very common in the Latakia Basin (Fidio1, Latakia1) and appears very clear in outcrops of the middle Cenomanian Hannafyah Formation (FigureVII.4).

VII.3 Microfacies association and their geometries

VII.3. Microfacies:

The principal microfacies-types of the North Levant (Coastal Range and South Palmyrides) are described in detail to discuss the lithofacies association and sequence stratigraphic concepts. Based on nearly 1400 m of outcrop and 400m borehole records, the depositional system of Aptian – Early Turonian succession is summarized in 16 microfacies types (compare Figure V 3d):

VII.3.1.1 MFT 1: Caliche facies

Description: It includes two diagenetically different deposits, the weathering remains and the karstic sediments (vadose). The intensity of red colour and different microfabric types are related to the diagenetic processes forming this type of facies, based on dissolution, recrystallization and the remaining carbonate soil with abundant iron oxide (Flügel, 2004; Blomeier et al., 2008). This non-marine facies is characterized by fenstral fabrics and birdseyes, nodular or brecciated fabrics and other empty or filled solution seams with calcitic cement of different crystals sizes. The caliche facies consists of parautochthonous particles and poorly sorted lithoclasts, siliciclasts (silt), peloids, and skeletal fragments of ostracoda, foraminifera, calcareous algae etc. with different diversities (Figure VII.3.a.1).

Occurrence and association: This MFT is recorded in centimeter to meter thick beds and occurs frequentedly in sections Zbeideh, Admir, Sayno, Slenfeah, Bab Abdallah,

Wadi Alheddah, Wadi-Layoun and Al-Meten Sections. Caliche facies is recorded at the top of individual shallowing-up cycles (Figures VII.2, VII.3.d).

Interpretation: This facies is formed in terrestrial subaerially exposed settings and in submarine aquatic settings (Flügel, 2004). It records a regression on the carbonate platform and is often associated with erosional surfaces. The latter may form important unconformity surfaces indicating a hiatus within the sedimentary record. (Figure VII.3.d).

VII.3.1.2 MFT 2: Siliciclastic facies:

Description: This MFT represents a mixture of cemented or non-cemented grain-dominated textures. It is characterized by fine- to coarse grained quartz sand with low diverse components; among them are fragments of unkown skeletal grains, and benthic foraminifera (Figure VII.3.a.4). It represents high to low energy intertidal deposits of mixed bioclastic (carbonate) and siliciclastic (quartz) grains.

Occurrence and association: Much of the siliciclastic sediment occurs in the Aptian sections of both Coastal Range and South Palmyrides; moreover, it was found in thin beds of the Lower Cenomanian section SB (Figures VII.2, VII.3.d).

Interpretation: The siliciclastic material indicates fluvial transport in tropical humid environments. The mixture of those sands with marine components indicates depositional envrionments along clastic beaches, dunes or deltaic sedimentation. Many of the major sequence boundaries are marked by facies changes from fluvial to carbonate platform environments (Figure VII.3.d).

VII.3. 1.3 MFT 3: Laminated wacke-/packstone facies

Description: This MFT comprises two different types of micritic and grained laminae that occur with parallel wavy to planar lamination. The laminae are due to incrusted cyanobacteria (stromatolithic) with very small peloidal components, micrite, angular

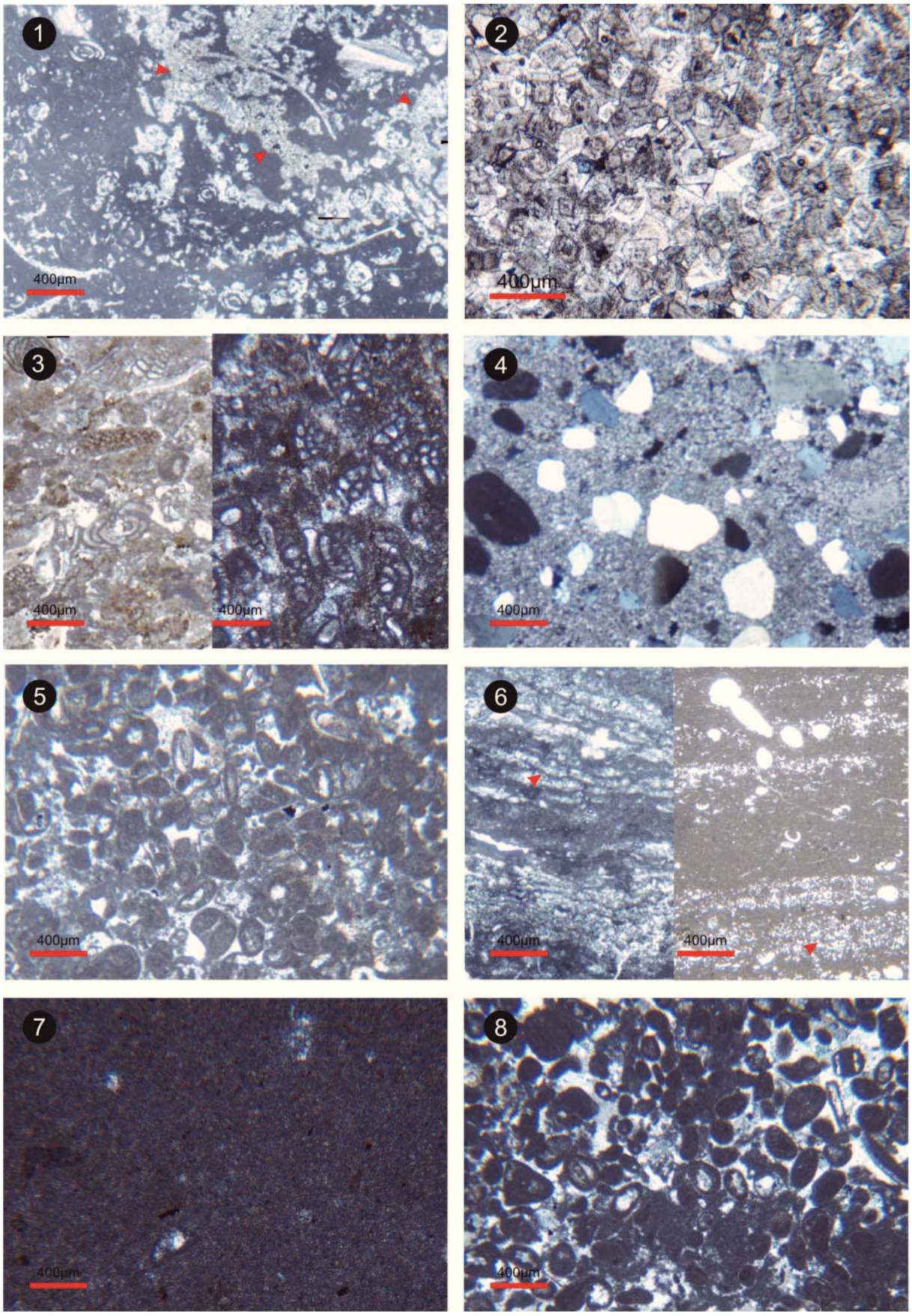
1
400µm
2
400µm
3
400µm
400µm
4
400µm
5
400µm
6
400µm
400µm
7
400µm
8
400µm

Figure VII.3.a (previous page)– Microfacies types (MFT) of the studied Aptian – Early Turonian strata: **1** Caliche (MFT1) wackestone to packstone, the asterisks exhibit fresh water cement (vadose sediments), 2 Dolostone (MFT4) with euhedral crystals, 3 Benthonic foraminifera packstone (MFT15) with Praealveolina sp. to the left and abundant Nezzazata sp. to the right, 4 Quartz sandstone (MFT2) with angular and subrounded quartz grain in a micrite matrix, 5 Miliolids and ostracods (MFT9) packstone to grainstone with peloids, 6 Laminated wackestone to packstone (MFT2), the asterisks to left show the stromatolitic bands and peloidal fabric to the right, 7 Mudstone facies (MFT5), 8 Peloids packstone to grainstone(MFT5).

quartz grains, and/or fine dolo-crystals. Occasionally, the laminae comprise alternating micritic and thicker grained laminae that are composed of coarse euhedral dolocrystals, well oriented ostracoda shells, and well sorted peloids (Flügel 2004). Small stromatolitic structures or evaporate pseudomorphs support this shallow water depositional environment. Primary sedimentary structures are generally characterized by fenestral fabrics of recrystallized open voids, associated with secundary structures like stylolithes (Figure VII.3.a.6).

Occurrence and associations: This MFT mainly occurs in the upper part at the very top of the individual cycles, belonging to the caliche facies. In addition, they are associated with peloids, ostracoda and foraminifera of individual cycles through the Aptian-Cenomanian succession of the Coastal Range and South Palmyrides (Figures VII.2, VII.3.d).

Interpretation: In accordance to different interpretations of laminated fabric (compare Flügel, 2004), this laminated carbonate microfacies is based on structural and textural criteria. Lamination is caused by changes in depositional and biological controls of irregular intercalation of micritic thin layers and peloidal fabric. This MFT occurs in very restricted shallow marine environments of supratidal zone (Flügel 2004, Figure VII.3.d).

VII.3. 1.4 MFT 4: Dolomite facies

Description: In the field this very distinctive facies is characterized by light grey to buff coloration and by moldic porosity, stylolites, different dissolution phenomena, and by the different degrees of dolomitization processes into the rock. Dolomites are very frequent in the northern Levant Platform, with two prinicipal types: 1- Primary dolomite and 2- Diagenetic dolomite. Dolomitic pseudomorphs after gypsum are common and are comparable to the descriptions of Preat and Carliez (1996), Mamet and Preat (2005). As with the facies described here, the dolomite crystals within the pseudomorphs are

coarser than those of the matrix (Mamet and Preat, 2005; Demicco and Hardie (1994) commented that intra-sediment growth of evaporate crystals (halite, gypsum or anhydrite) provides unequivocal evidence of post-depositional crystallisation in an evaporated environment.

The euhedral dolomite in this facies is associated with aggregates of subhedral dolomite that keep the ghost of structures of some organisms; the feature of remained fragments depends on the strength of dolomitization, which generally consists of some clastic material, ooids, peloids, in addition to echinoderms, mollusks, and foraminifera (Figure VII.3.a.2).

Occurrence and association: This facies occurs very frequent in the Aptian Albian and Cenomanian succession especially near the top of individual cycles in the area of the emerged platform surface (Figures VII.2, VII.3.d).

Interpretation: This facies therefore is interpreted as being deposited in a shallow, calm, highly restricted environment that was then subjected to evaporitic, subaerial conditions. More than 70% of dolomite was formed diagenetically after the dolomitization of limestones beds, where some of the synsedimentary features remain in the final dolomitized rock like fabrics and some parts of dolomitized components (Figure VII.3.d).

VII.3. 1.5 MFT 5: Mudstone facies

Description: Only few components occur in the fine grained micritic intervals with varying amounts of silt-sized quartz grains. Occassionally mudstone deposits show chert nodules or local flint intercalations. On the other hand, the mudstones exhibit massive nodular or wavy horizontal fabrics, similar to the laminated wackstone facies. Bioturbation and vertical or horizontal burrows are common with fenestral fabric. Also diagenetic or post-depositional features include secondary structures like cracks and Fe-staining and “horsetail” stylolites. Among the few components are gastropods, bivalves, echinoderms, ostracodes, miliolids, peloids or planktonic foraminifera and isolated euhedral dolomite crystals (Figure VII.3.a.7).

Occurrence and associations: This facies is normally present in the upper or lower part of individual cycles. The mudstone facies of the upper cycles are characterized by

multicolored massive rocks associated with very restricted benthic organisms, strongly dolomitzed with fenestral fabric. Whereas the mudstones of the lower cycles are mostly nodular or cm-bedded limestones mainly with chert nodules of flints, associated with wackestones rich in planktonic foraminifera and pelagic mollusks (Figures VII.2, VII.3.d).
Interpretation: The mudstone facies is interpreted as forming in low-energy, open marine and restricted shallow marine environments. The low faunal abundances and diversities of massive mudstones indicate a shallow-water, restricted intertidal setting. Mudstones are typically in the regressive parts of shoaling upward sequences and also observed in the basal portion of transgressive limestones. The deeper mudstone facies is interpreted as originating in a low-energy, open marine setting (hemipelagic) below the effective wave base, and consists of structureless micritic (sometimes peloidal fabric), mud matrix, chert with few planktonic foraminifera and calcispheres (Figure VII.3.d).

VII.3. 1.6 MFT 6: Echinoderm wacke-/packstone facies

Description: The depositional texture of this facies ranges from packstones to wackestones and is the most typical Aptian to Cenomanian facies of the North Levant Platform. It consists of primarily massive wacke- and packstones in which crinoid particles and echinoid plates make up the highest percentage of the components. Whereas the sediments are characterized by low-diverse components, they may consist of fragments of rudists, calcareous green algae, benthic foraminifera, peloids and few planktonic foraminifera. The components size ranges between small to coarse grained (Figure VII.3.d.4).
Occurrence and association: The echinoderm wacke-/packestone facies is thought to be representative of low- to moderate-energy; consequently the sedimentary environment was a calcareous shoal, but in case of planktonic crinoids the wackestone echinoderm facies can be deposits in very deep water environment (Flügel, 2004). The echinoderm fragments has wide range occurrence into microfacies types; caliche, peloids, ooids dolostone and foraminifera facies. Interpretation: The low diversity of echinoderms is caused by their sensitivity against salinity, oxygenation, and temperature (Flügel, 2004; Blomeier et al., 2008). The well preserved benthic

echinodermal wacke- to packstone occurs in different marine depositional environments, ranging from lagoonal to inner ramp to mid ramp, deposited below normal wave base or within storm wave base (Flügel 2004, Figure VII.3.d).

VII.3. 1.7 MFT 7: Oolitic grainstone facie**s**

Description: The oolitic grainstone facies is characterized by abundant micritic and radial ooids. The central nuclei of the ooids mainly consist of peloids, skeletal fragments and green algae. These well sorted arenitic grains are always associated with calcareous green algae, reworked bivalves and gastropods, intraclasts and *Lithocodium* sp. (Figure VII.3.b.3).

Occurrence and association: This microfacies occurs in thin bedded limestones of the Aptian part of the Coastal Range sections and rarely in the Albian. This MFT is commonly shown in the upper part of the individual cycle.

Interpretation: The oolitic grainstone facies reflects special environmental conditions, influencing water energy, salinity, water depth and transport processes

control the growth of centralized coatings. The oolitic grainstone facies is almost found with peloidal intraclasts, reworked green algae and *Lithocodium*. This MFT is considered as foreshore sediments of high energetic lagoonal areas (Flügel 2004, Figure VII.3.d).

VII.3. 1.8 MFT 8: Peloidal pack-/grainstone facies

Description: This microfacies comprises abundant sand-sized grains of 100- 500µm diameter, composed of microcrystalline carbonate components (rounded or subrounded, spherical to irregular peloids). This MFT is generally associated with low diversity of components, few benthic foraminifera (miliolids) and ostracods, green algae, echinoderms and gastropods. The moderate to massive peloidal beds characterized by texture ranged from grainstone to packestone (Figure VII.3.a.8).

Occurrence and association: The peloidal facies is an important constituent of shallow marine carbonates, occurring in thin- to intermediate bedded to laminated limestones of certain cycles in the uppermost part of the entire sedimentary successions. It was deposited in a gradual energetic position between mudstone facies and oolithic, echinodermal and benthic foraminifera facies (Flügel, 2004). It forms the

most frequent facies type within the Aptian to Cenomanian carbonates of the Coastal Range and South Palmyrides (Figures VII.2, VII.3.d).

Interpretation: Many peloids of this facies are thought to of be fecal origin, when contain more than 30% of fecal pellets, in addition to, some mictritized grains such as shell fragments and algae. This facies is a typical record of shallow, low energy and restricted marine environments. The packstone-/grainstone facies was commonly deposited in shallow marine tidal and subtidal shelf carbonates above the fair-weather wave base (FWWB) (Flügel 2004, Figure VII.3.d).

VII.3. 1.9 MFT 9: Miliolids and ostracods wacke-/packstone facies

Description: This facies exhibits abundant miliolid foraminifera, and ostracods of very low diversities; pellets are frequent too, while intraclasts are rare. Occasionally it can show few nonmarine features as fenestral fabrics or diagenetically leached cavities filled by sparite, either embedded in micrite or in pockets of calcite within the micrite matrix. Normally textures are inhomogenous as a consequence of bioturbation. The wacke- to packstone facies represents poorly sorted fragments, with miliolids, ostracods, and peloids as most freuquent components; the occurrence of Nezzazatidea and echinoderms is questionable (Figure VII.3.a.5).

Occurrence and association: This microfacies indicates very shallow restricted lagoonal environments with temporarily sub-aerial exposure. It occurs in the uppermost part of individual cycles in the Late Aptian to Early Albian of sections Sayno, Wadi-Layoun and in the uppermost Cenomanian of section Al-Meten (Coastal Range). In the South Palmyrides, this microfacies is present in the Albian - Cenomanian succession especially in the latest Cenomanian of the Abtar Formation (Figures VII.2, VII.3.d).

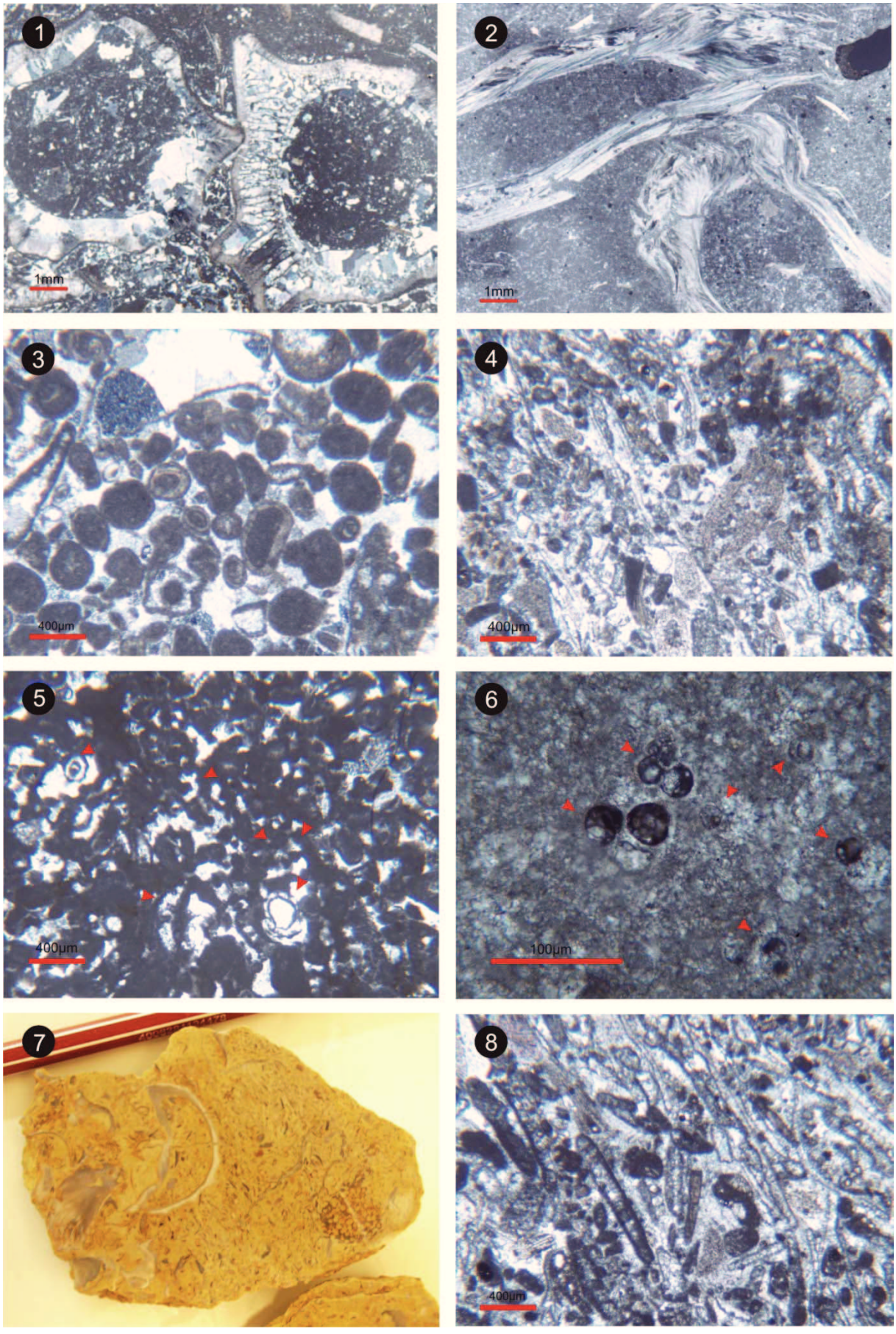
1
1mm
2
1mm
3
400µm
4
400µm
5
400µm
6
100µm
7
8
400µm

Figure VII.3.b (previous page)– Microfacies types (MFT) of the studied Aptian – Early Turonian strata: **1** and **2** Rudist facies (MFT12), **3** Ooids grainstone facies (MFT7), **4** Echinoderm facies (MFT7), **5** Alga debris packstone (MFT13), asterisks are alga fragments, **6** Planktonic foraminifera facies (MFT16) asterisks are *Hetrohelix* sps., **7** Bivalves-Gastropods packstones facies (MFT10), **7** Reworked skeletal grains of bivalves and echinoderm (MFT11).

Interpretation: This facies was interpreted as restricted marine, possibly representing quiet water lagoonal or tidal flat sediments in sub- to intertidal environments of the platform interior. The local concentrations of thin miliolids, ostracods and peloids within the micrite deposits argue for low energy and silent water environments (Figure Figure VII.3.d).

VII.3. 1.10 MFT 10: Bivalve-gastropod packstone facies

Description: The intervals forming this facies represent floatstones to rudstones with packstone matrix and are characterized by the dominance of gastropods and bivalves; occasionally oysters form a higher percentage of the rock components. Echinoderms, benthic foraminifera, green algae as well as other biogenic remains are present in various amounts and preservation beside the two facies markers. It is a poorly sorted facies between arenitic to ruditic grain size (Figure VII.3.b.7).

Occurrence and association: The bivalve-gastropod packstone facies is very frequent in the Aptian, Albian and Cenomanian succession of the North Levant Platform. It is present at the base of individual cycles (Flügel 2004). Here, the facies is associated mainly with the peloidal, mixed bioclastic, rudist facies (MFT 12) and rarely with benthic foraminifers' facies (MFT15). Also it shows gradual lateral and vertical transitions to the miliolid-ostracod wacke-/packstones (MFT9) and to the peliodal pack-/grainstone facies (MFT8).

Interpretation: Typically the bivalve-gastropod packstones characterize intertidal or shallow subtidal conditions. Sedimentary signature of bivalves-gastropods accumulations provide information to high-energy environments, such as fair weather and storm waves base (Flügel 2004, Figure VII.3.d).

VII.3. 1.11 MFT 11: Bioclastic pack-/grainstone facies

Description: The mixed–bioclastic wacke-/packstones correspond to decimeter-thick irregular beds with frequent bioturbation and parallel lamination. Dominant grains are poorly sorted and poorly rounded, ranging between millimeters to centimeters-size extraclasts, grading into poorly sorted peloids. A further attribute of that facies are highly diverse bioclastic fragments of echinoderms, bivalves (frequently accumulated in mm-thick laminae), gastropods, corals, orbitolids, textulariids, miliolids, serpulids, green algae, and intraclasts (Figure VII.3.b.8).

Occurrence and association: This microfacies occurs in different localities of the Coastal Range and the South Palmyrides during the Aptian-Cenomanian succession. The big variety of reworked components and the size of grains reflect wide depositional settings of moderate to high energetic environments. Thus MFT11 may be present in different positions within the individual cycles (Sari and Özer, 2001).

Interpretation: The reworked or fragmented skeletal grains of diverse organisms (e.g. foraminifera, mollusks) and lithoclasts are present within most of the facies types. In general, this shallow marine facies occurs above the mean fair-weather wave base (FWWB) e.g. in sand shoals of the inner ramp (Flügel 2004, Figure VII.3.d).

VII.3. 1.12 MFT 12: Rudist facies

Description: The composition of these poorly to moderately sorted wacke-/floatstones (and minor packstones) is characterized by the predominance of arenitic to ruditic fragments of rudist fragments; complete shells occur and indicate primary growth of rudists (biostromes). Additional bioclasts of abundant benthic foraminifers (miliolids and Orbitolina sp.), green algae and non-skeletal components (e.g. intraclasts and peloids) are present in the matrix of this facies (Figure VII.3.b.1, 2).

Occurrence and association: Rudist fragments occur mostly in the Aptian- Albian deposits of Coastal Range sections. Furthermore, rudists are concentrated in several biostromes of the Cenomanian interval in the Coastal Range and the South Palmyrides as well as in the upper Aramo Formation of Early Turonian age (Figures VII.2, VII.3.d).

Figure VII.3.c - Debris flow boulders within a layer of pelagic limestones (MFT16, unit 21 of Slenfeh Formation, SB section).

VII.3. 1.13 MFT 13: Algal debris wacke-/packstone facies

Description: This facies is characterized by algal debris with monospecific mass occurrences of dasycladalean alga. This wacke-/packestones are composed of fine debris of an unknown *Salpingoporella* sp. associated with extremely rare benthonic foraminifera. The resedimented thin calcareous algal skeletons show lutitic grainsize (Figure VII.3.b.5).

Occurrence and association: This MFT mainly occurs at the base of the individual cycles, above the maximum flooding surface. The depositional settings of this wacke-/packstones are quite water environments. Algae debris can be found in between the fair weather wave base and the storm wave base of the lagoonal and inner ramp environments. The algal debris facies represents limestones of the Late Aptian to Early Albian successions of sections SY and AH.

Interpretation: The algal debris facies was described as a characteristic limestone type of the Lower Cretaceous of the Middle East (Elliott, 1962). During that time, extended shallow shelf sea covered large continental areas by extremely low depositional gradient during periods of high global sea level. Consequently, reworking caused by storms transported the flora into most depositional areas of the platform, also in low energetic systems as (Elliott, 1962; Flügel 2004, Figure VII.3.d).

VII.3. 1.14 MFT 14: Resedimented pack-/grainstone facies

Description: The described facies represents a mixture of poorly sorted resedimented and reworked skeletal grains (rounded and subrounded); peloids, external organism-bearing encrustations (serpulids, *Lithocodium* and intraclasts like oncoids) and *Tubiphytes*, recrystallized gastropods, bivalves and shell fragments. The arenitic to ruditic biotic components also contain benthonic foraminifera, including *Orbitolina*, *Nezzazata*, *Peneroplis* and other miliolids. This facies comprises half meter thick, well bedded limestones of near shore environment. Furthermore, this MFT occurs in reworked debris flow boulders within a layer of pelagic fragments (Figure VII.3.c).

Occurrence and association: This MFT has a wide range distribution. It occurs within medium bedded limestones from the base to the top of individual cycles. The resedimented facies formed under low to high energy conditions, associated with benthonic foraminifera and peloidal facies (Flügel 2004, Figure VII.3.d). MFT 14 occurs in Aptian – Cenomanian sections of the Coastal Range and the South Palmyrides.

Interpretation: MFT 14 represents a mixture of reworked and transported bioclastic grains accumulated in the transition area between the more proximal (high-energy) tidal and the distal (low-energy) mid-ramp environments below or around the mean FWWB on submarine (Flügel 2004, Figure VII.3.d).

VII.3. 1.15 MFT 15: Benthic foraminifera wacke-/packstones facies

Description: This MFT consists of massive, moderate to poorly sorted, mainly arenitic, foraminiferal and bioclastic wacke-/packestones, which show strongly varying component composition of highly diverse benthonic foraminifera associations; miliolids, nezzazatinae, orbitolinids, praealveolinidae, chrysaldinids, *Dicyclina* spp., *Cuneolina* spp. etc. with other uniserial and biserial foraminifera. Rare to common mollusks are also present associated with other component such as echinoderms, green algae and peloids (Figures VII.3.a.3).

Occurrence and association: MFT 15 is represented by thick to intermediate bedded limestones in the upper part and on top of the individual cycles of all sections (Flügel

2004). This microfacies is occurring mainly with peliodal facies and less with green algae and rudist.

Interpretation: Cretaceous benthonic foraminifera are present in varying amounts within most MFT 15 sediments of peloidal, rudist, mixed bioclastic and resediment facies. It ranges from pure micrite with rare to abundant benthonic foraminifera, deposited from the restricted lagoonal environments to open lagoon low energetic environments. The generally well sorted wacke-/packstones were deposited above the FWWB within shallow-submarine to intertidal open lagoon areas (Figure VII.3.d).

VII.3. 1.16 MFT 16: Planktonic mud-/wackstones facies

Description: The MFT is characterized by a mudstone or wackestone matrix together with varying amounts of ammonites, calcispheres and planktonic foraminifera (*Heterohelix* spp., *Ticinella* spp., *Rotalipora* spp., *Whiteinella* spp., and some other Cretaceous genera), which float in a homogenous, microcrystalline matrix. Besides bivalves, gastropods, and echinoderms reworked *Orbitolina* spp. can be found together with planktonic organisms (Figures VII.3.a.6).

Occurrence and association: This microfacies type consists of marly, chalky, and nodular limestones, occasionally characterized by specific depositional structures such as microcross- laminae (turbidity limestones) with chert nodules and flints, deposited in low energy conditions of outer ramp environment at the base of the individual cycle. The planktonic facies is one of the most widespread facies, present in the Late Aptian - Cenomanian sections of Coastal Range and South Palmyrides and in the Early Turonian of the Aramo Formation.

Interpretation: MFT 16 is interpreted to have been formed in low-energy environments, associated mainly with mudstones of MFT5. The pelagic facies interpreted always deposits in open-marine setting (hemi-pelagic) below the effective wave base in the lower middle to outer ramp environments. The normal and microcross- laminae limestones were deposited in the deep water conditions by turbidity currents (Figure VII.3.d).

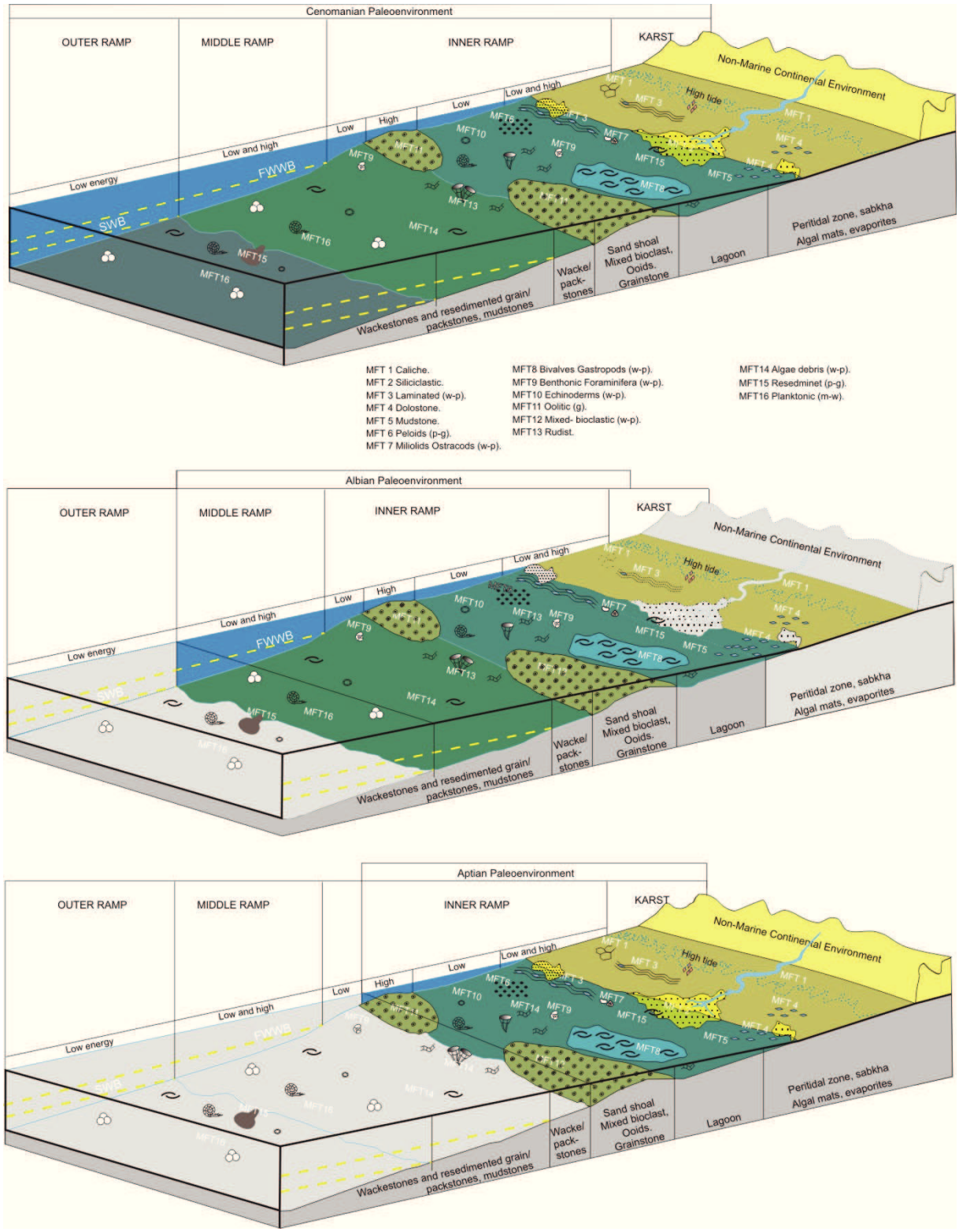

Figure VII.3.d – Schematic cartoon to illustrate the five major depositional environments of the Aptian – Cenomanian strata (coloured areas) of the Aptian, Albian, and Cenomanian platform of the North Levant margin, based on sixteen microfacies types identified in the study area.

VII.3. 2 Depositional environments

Combining outcrop information with the detailed microfacies investigation enables the modeling of different facies zones, in which the depositional area of the North Levant Platform can be arranged. These facies zones are marked by characteristic depositional environments and thus yield specific sediments and biotic associations.

The lateral trends recorded were most probably dependent on environmental change with various distances from the shore line, e.g. siliciclastic input, climatic changes, salinity, light, oxygenation, nutrient influx, and the sea level change, rather than on sedimentation rates and subsidence.

Litho- and biofacies characteristics of the Aptian - Turonian formations suggest deposition in a shallow to deep, low-gradient ramp with no apparent break in slope, summarized in deposition of diverse facies in a wide range of water depth from low-energy deep marine facies to tidal-flat facies with an intermediate high-energy inner ramp facies belt (Figure VII.3.d). Individual ramp depositional zones differ strongly in their facies compositions. Inner-ramp deposits consist mostly of oolitic or bioclastic components. These components build shoals, barriers, and back-barrier deposits and shoreface deposits in the Aptian - Early Albian of the Coastal Range. Lagoonal environments are characterized by mud-, wacke-, or packstone s. Shallow water depth may be reflected by biostromal buildups. Mid-ramp deposits, formed below the FWWB, and reflect storm depositional environments. During fairweather interval sediment is formed by reworked (terrigenous mud or lime) and becomes bioturbated.

Individual depositional zones of the ramp model differ strongly in their facies compositions. Inner-ramp deposits consist mostly of oolitic or bioclastic components. These components build shoals, barriers, and back-barrier deposits and shoreface deposits in the Aptian - Early Albian Coastal Range. Lagoonal environments are characterized by mud-, wacke-, or packstone sediments. Shallow water depths are reflected by biostromal biotas. Slight drowning of the platform during the Late Albian - Turonian resulted in a hemipelagic environment (shelf sea with open circulation) on the platform that gave rise to the appearance of planktonic foraminifera, marking the late transgressions and the maximum flooding surfaces.

VII.4 Lithofacies units, microfacies, and log response

The Aptian – Cenomanian lithofacies units are compared with the gamma ray log response of seven wells based on the comparison of characteristic log-signatures and facies. The before defined characteristic lithologies of the surface sections in the South Palmyrides and the Coastal Range (chapters VI, VII) as well as marker species formed distinctive stratigraphic intervals that allow to correlate the surface and subsurface sections with characteristic gamma ray logs (FiguresVII.4, VII.4.e and VII.4.d).

The green marls (Aptian) are clearly correlated with similar subsurface lithofacies units intercalated with few black shale intervals. The black shale intervals exhibit highest rates of gamma ray (70-150 API) during the maximum flooding surface (FigureVII.4).

The well bedded limestones of the early transgressive facies are characterized by a low irregular gamma ray log (10-20 API). The radioactivity of these rocks is related to the abundance of clayey material. Therefore, thin marl layers exhibit a rapid increase of gamma ray (50-80 API), which can be easily distinguished from pure limestones (FigureVII.4). Normally the limestones rich in particles (grainstone packestones) have lower impulse rates of gamma ray. The nodular limestones succession of (FigureVII.4) becomes more marly upwards. Thus, the gammy ray log is marked by an increase of impulse rate.

In our analysis of litho- and biofacies change and their gamma ray expression, three examples were used to interpret lithology, subject to borehole logs during sea level changes of different cycles (FigureVII.4). More details were strengthened when the outcrop sections were correlated with the subsurface interpretations.

The Aptian period of the Levant Platform is characterized by volcanic activity (Kazmin, 2002; Segev and Rybakov, 2010) and humid climatic conditions (Stampli and Borel, 2002), supporting the platform changes from carbonate to siliciclastic environments, e.g. the Rutba Fm. of the North Levant (Figure VII.6.a). The deepening-up facies change of the Aptian sequences exhibits an upward increase in the gamma reading (the early tst of FigureVII.4.1) that is related to a gradual upward change to a clay-mineral rich matrix (micrite).Similar facies changes occur, for example from peloidal or oolitic grainstone to foraminiferal wacke/packstone facies or from sand to shale. In the shallow marine (Aptian) succession, an increase of water energy is related to decreasing water

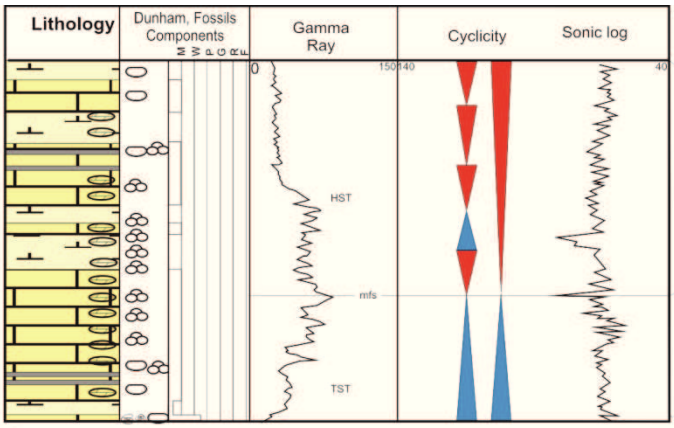

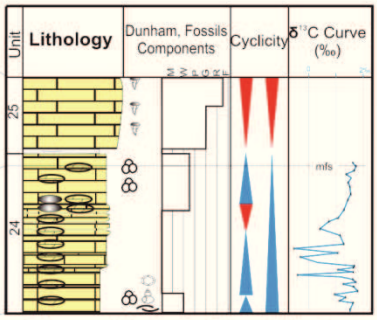

The correlated units of the nighbouring outcrops of Bab Abdellah section.

3 Nodular limestones with planktonic foraminifera from the Fidio1 cored well.

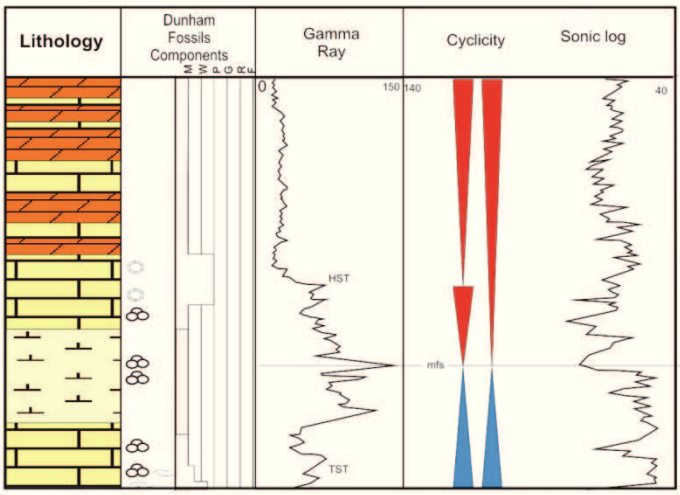

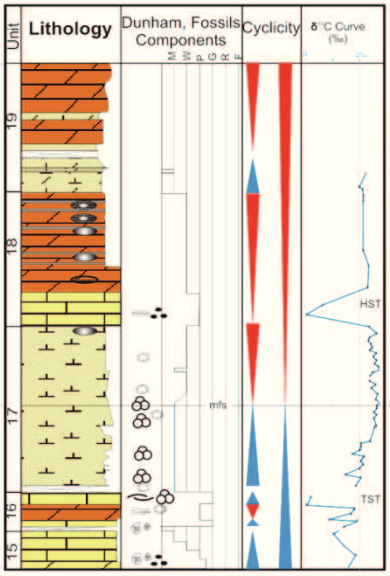

2 GR. and sonic log of the deep water limestones, marls and dolostones from the Fidio1 cored well.

The correlated depositional sequence of the neighboring outcrops of Slenfeh section.

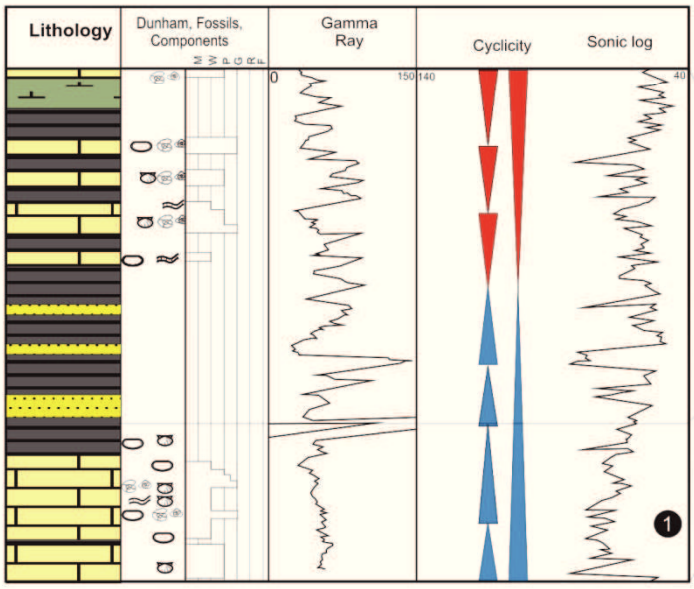

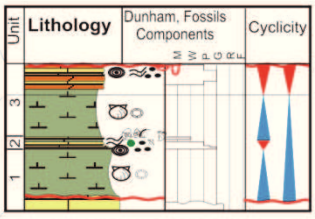

The comparable green marl formation (Bab Janneh Fm., Sayno section).

1 Gamma ray (GR) and sonic records of green marls, black shale, and lagoonal limestones (Fidio1 well).

Figure VII.4 (previous page)– Some examples of characteristic gamma ray and sonic log shapes (including lithology and Dunham-classification) of different intervals of Fidlio1 well, correlated with neighbouring outcrop units of the Coastal Range. Special emphasis was given on the cyclicity patterns of both, subsurface and surface sections.

depths and clay minerals, indicated byminimum gamma ray values. Therefore, shallowing up trends are usually reflected by a transition from micrit-rich matrix (mudstone facies) to coarse crystallized (cement) facies in the carbonates; it can also be marked by upward changes from shale-rich to coarse sand-rich lithologies (free of shale lithofacies) (FigureVII.4.1). The sand is marking minimum GR-values, while the shale is marking maximum gammy ray readings that are correlating to the mfs.

The second example FigureVII.4.2) is carried out at the AlS4 Syrian sequence of the Albian- Cenomanian boundary (Ghanem and Kuss, submit). The variety of gamma ray values of the early transgressive systems tract are comparable to the facies change from bivalves packstone to planktonic wackestone facies, followed by deeper ramp marls (rich in planktonic foraminfera). These values show an increase maybe a result of the gradual increase in anoxicity during the AOEd1 (Ghanem and Kuss, subm.). The interbedded overlying limestones and dolomites of this sequence reflect an upward shallowing during the highstand (HST). While the early highstand is marked by a gradual decrease of clay-minerals and the gamma ray response, the late HST is more dolomitized with lower gamma ray rates.

The pelagic sediments of the sequence CeS3 (FigureVII.4.3) reflect a gradual increase of the gamma ray record during sea level rise and show maximum values during the maximum flooding surface, associated with abundant planktonic foraminifera. These units are well comparable with the adjacent outcrops.

VII.5 Sequences, Facies and log response arrangement

The regional correlation of the North Levant platform is based on the litho- and biostratigraphic subdivision of the outcrops compared with the log response of

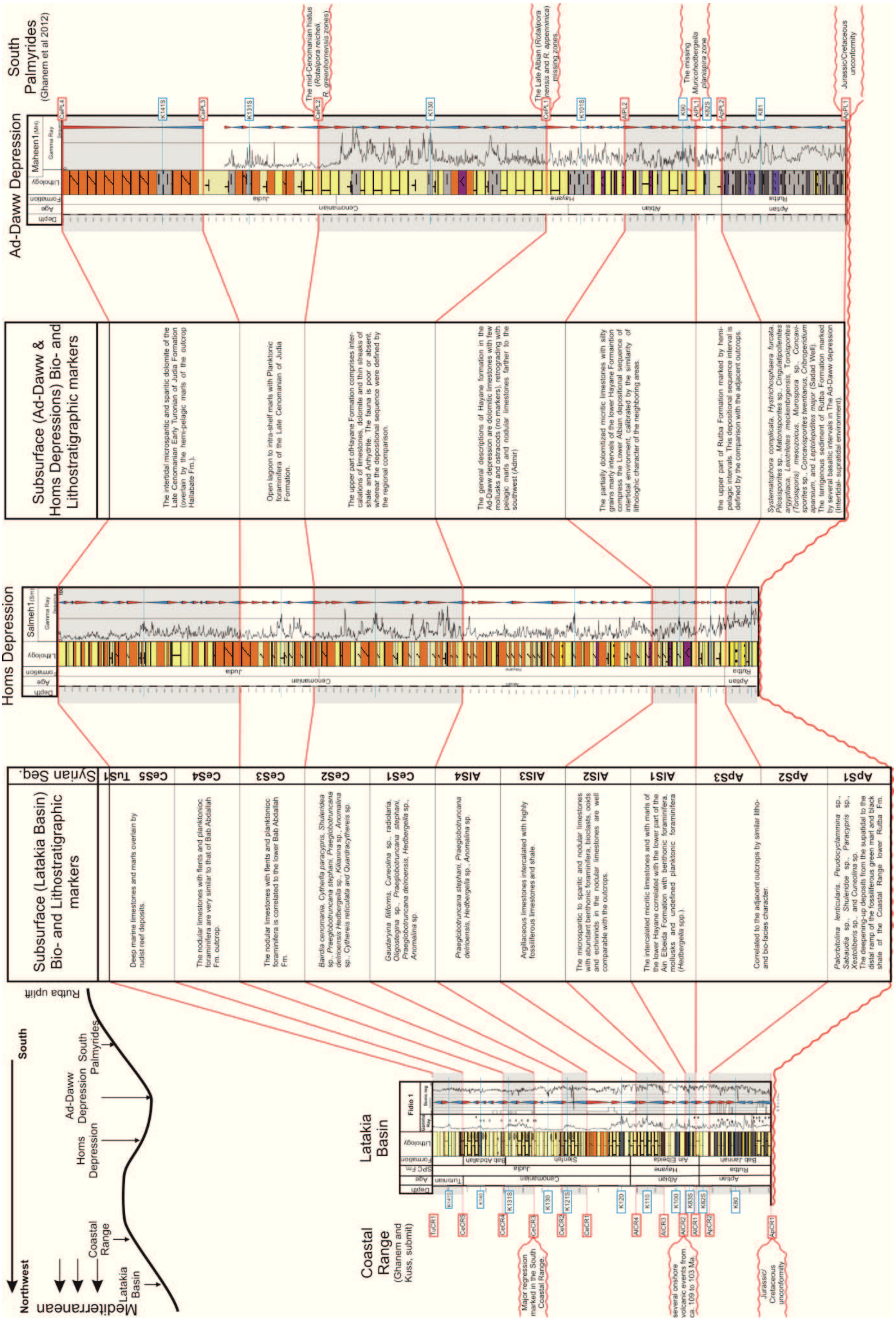
Northwest
South
Mediterranean
Latakia Basin
Coastal Range
Homs Depression
Ad-Daww Depression
South Palmyrides
Rutba uplift
Coastal Range (Ghanem and Kuss, submit)
Latakia Basin
Fidio 1
Major regression marked in the South Coastal Range.
several onshore volcanic events from ca. 109 to 103 Ma.
Jurassic/ Cretaceous unconformity
Subsurface (Latakia Basin) Bio- and Lithostratigraphic markers
Syrian Seq.
TuS1
CeS5
Deep marine limestones and marls overlain by rudist reef deposits.
CeS4
The nodular limestones with flents and planktonioc foraminifera are very similar to that of Bab Abdallah Fm. outcrop.
CeS3
The nodular limestones with flents and planktonioc foraminifera is correlated to the lower Bab Abdallah Fm.
CeS2
Bairdia cenomania, Cytherlla paracypris, Shulerldea sp., Praeglobotruncana stephani, Praeglobotruncana delrioensis Hedbergella sp., Kilianina sp., Anomalina sp., Cythereis reticulata and Quardracythereis sp.
CeS1
Gaudaryina filiforms, Cuneolina sp., radiolaria, Oligostegina sp., Praeglobotruncana stephani, Praeglobotruncana delrioensis, Hedbergella sp., Anomalina sp.
AlS4
Praeglobotruncana stephani, Praeglobotruncana delrioensis, Hedbergella sp., Anomalina sp.
AlS3
Argillaceous limestones intercalated with highly fossiliferous limestones and shale.
AlS2
The microsparitic to sparitic and nodular limestones with abundant benthonic foraminifera, bioclasts, ooids and echininids in the nodular limestones are well comparable with the outcrops.
AlS1
The intercalated micritic limestones and with marls of the lower Hayane correlated with the lower part of the Ain Elbeida Formation with benthonic foraminifera, mollusks and undefined planktonic foraminifera (Hedbergella spp.).
ApS3
Correlated to the adjacent outcrops by similar litho- and bio-facies character.
ApS2
ApS1
Palorbitolina lenticularis, Peudocyclammina sp., Sabaudia sp., Shuleridoe sp., Paracypris sp., Xestoliberis sp., and Cuneolina sp. The deepening-up deposits from the supatidal to the distal ramp of the fossiliferous green marl and black shale of the Coastal Range lower Rutba Fm.
Homs Depression
Salmeh1(Sm)
Subsurface (Ad-Daww & Homs Depressions) Bio- and Lithostratigraphic markers
The intertidal microsparitic and sparitic dolomite of the Late Cenomanian Early Turonian of Judia Formation (overlain by the hemi-pelagic marls of the outcrop Hallabate Fm.).
Open lagoon to intra-shelf marls with Planktonic foraminifera of the Late Cenomanian of Judia Formation.
The upper part ofHayane Formation comprises inter-calations of limestones, dolomite and thin streaks of shale and Anhydrite. The fauna is poor or absent, wherear the depositional sequence were defined by the regional comparison.
The general descriptions of Hayane formation in the Ad-Daww depression are dolomitic limestones with few mollusks and ostracods (no markers), retrograding with pelagic marls and nodular limestones farther to the southwest (Admir)
The partially dolomitized micritic limestones with silty grains marly intervals of the lower Hayane Formaintion compress the Lower Albian depositional sequence of intertidal environment, calibrated by the similarity of lithologic character of the neighboring areas.
the upper part of Rutba Formation marked by hemi-pelagic intervals. This depositional sequence interval is defined by the comparison with the adjacent outcrops.
Systematophora complicata, Hystrichosphaera furcata, Pilosisporites sp., Matonisporites sp., Cingulatipollenites argyptiaca, Leiotriletes meckenbrgensis, Toroisporites (Toroisporis) mesozoicus, Murospora sp., Concavi-sporites sp., Concavisporites twentianus, Cribroperidium aparsium, and Leptolepidites major (Sadad Well). The terrigenous sediment of Rutba Formation marked by several basaltic intervals in The Ad-Daww depression (Intertidal- supratidal environment).
Ad-Daww Depression
Maheen1(MH)
South Palmyrides (Ghanem et al 2012)
The mid-Cenomanian hiatus (Rotalipora reicheli, R. greenhornensis zones)
The Late Albian (Rotalipora ...nensis and R. appenninica) missing zones.
The missing Muricohedbergella planispira zone
Jurassic/Cretaceous unconformity

Figure **VII.5** (previous page)– Correlation of the Syrian sequence boundaries (2. column), with those described form outcrops in South Palmyrides (right column: Ghanem et al., 2012) and the Coastal Range (left column: Ghanem and Kuss, subm.) with subsurface data ofthe Ad-Daww and Homs Depression and the Latakia Edge Basin. Red and blue lines mark sequence boundaries and maximum flooding surfaces (more details of the three profiles are visible in figures VII.6a, b).

borehole sections of the Aptian-Cenomanian succession (FiguresVII.4,VII.5, VII.6.a and VII.6.b).

Sea level fluctuations reflect various facies types in the unique depositional environments. The Aptian - EarlyTuronian strata are represented by deepening/ shallwing-up cycles. The deepening-up of the depositional environments is recorded by transgressive facies sets at the basal half of the single cycle. Shallow subtidal (lagoonal) environments represent the basal part of each deepening-up (half)cycle. It is characterized by a muddy facies (wacke- to packstones), which subsequently exhibits a transition from nearshore to shallow water platform/ramp settings. The overlying open marine facies consists of siltstones or grain-/packstones, extending into deeper ramp settings (Figure VII.2). These deposits have high gamma-ray values at their base and lower rates at their tops. Here, it is characterized by pelagic marls and limestones. The upper overlapping transgressive sediments are thinner, composed of low energetic packstones and deeper ramp facies (interbedded skeletal packstones, pelagic wackestones and marls; the shale content increases upward, well comparable to increasing gamma-ray values near the maximum flooding surfaces (FiguresVII.4,VII.5 VII.6.a and VII.6.b).

Maximum flooding surfaces (mfs) are present within wackestone (with abundant planktonics) and/or within shales, both in outcrop and cores. The mfs are evident on gamma-ray logs as abrupt peaks between increasing (below) and decreasing (above) gamma-ray values. The shallowing-up (half) cycles are thick and consist of aggradational facies (rudist rud-floatstone) or progradational peritidal facies (laminated, peloidal and restricted skeletal wacke-/packstone with fenestral mudstones or silty dolomites).

Sequence boundaries are represented by sabkha and peritidal facies (including caliche conditions). They reflect subaerial exposure, marked by paleoweathering surfaces and/or sharp changes between the underlying and overlying facies of the next cycle.

VII.6 Outline of Paleogeographic Model and sequence stratigraphy of Northern Levant

The paleogeographic model of the Northern Levant Platform during Aptian – Early Turonian discussed in the present paper is based on thirteen $2^{nd}/3^{rd}$ order sequences of Syria (defined in the Palmyrides and Coastal Range) and compared with adjacent areas. The stratigraphic model of correlating the surfaces and subsurfaces in the Palmyrides Basin and the Coastal Range (the latter forms the passive marginal edge of Eastern Mediterranean) is basd on detailed biostratigraphic data of the Palmyrides and Coastal Range as well as on lithostratigraphic correlations of the Aptian – Early Turonian formations (FigureVII.5).

In the South Palmyrides, a Cretaceous lithostratigraphic subdivision was established by Ponikarov et al. (1967) and modified by Mouty et al. (2003) and Ghanem et al. (2012). The bio- and sequence stratigraphic investigation of the Aptian-Cenomanian succession of Ghanem et al. (2012) resulted in four depositional periods (comparing to the seven 2^{nd} order sequences, FigureVII.5), separated by five hiatusses; Neocomian-early Aptian?, earliest Albian (*Muricohedbergella planispira*), latest Albian (*Rotalipora ticinensis* and *R. appenninica*), mid Cenomanian (*Rotalipora reicheli*) and late Cenomanian-early Turonian (FigureVII.5).

In the Coastal Range, we follow the lithostratigraphy subdivision of mid-Cretaceous strata of Mouty and Saint-Marc (1982), modified by revised biostratigraphic data of Ghanem and Kuss (subm.); the latter authors discribed three major unconformities: the Jurassic - Cretaceous boundary, the late Albian (South Coastal Range) and the late mid-Cenomanian paleokarstic surface (early *R. globotuncanoides* zone) (FigureVII.5).

VII.6.1 The Aptian depositional sequences of Syria

The Aptian strata are unconformably overlying Jurrassic rocks in most parts of the Coastal Range and the Palmyrides, except few localities of the South Coastal Range (NE Safita, Qadmous), where eroded “Neocomian” limestones occur, including

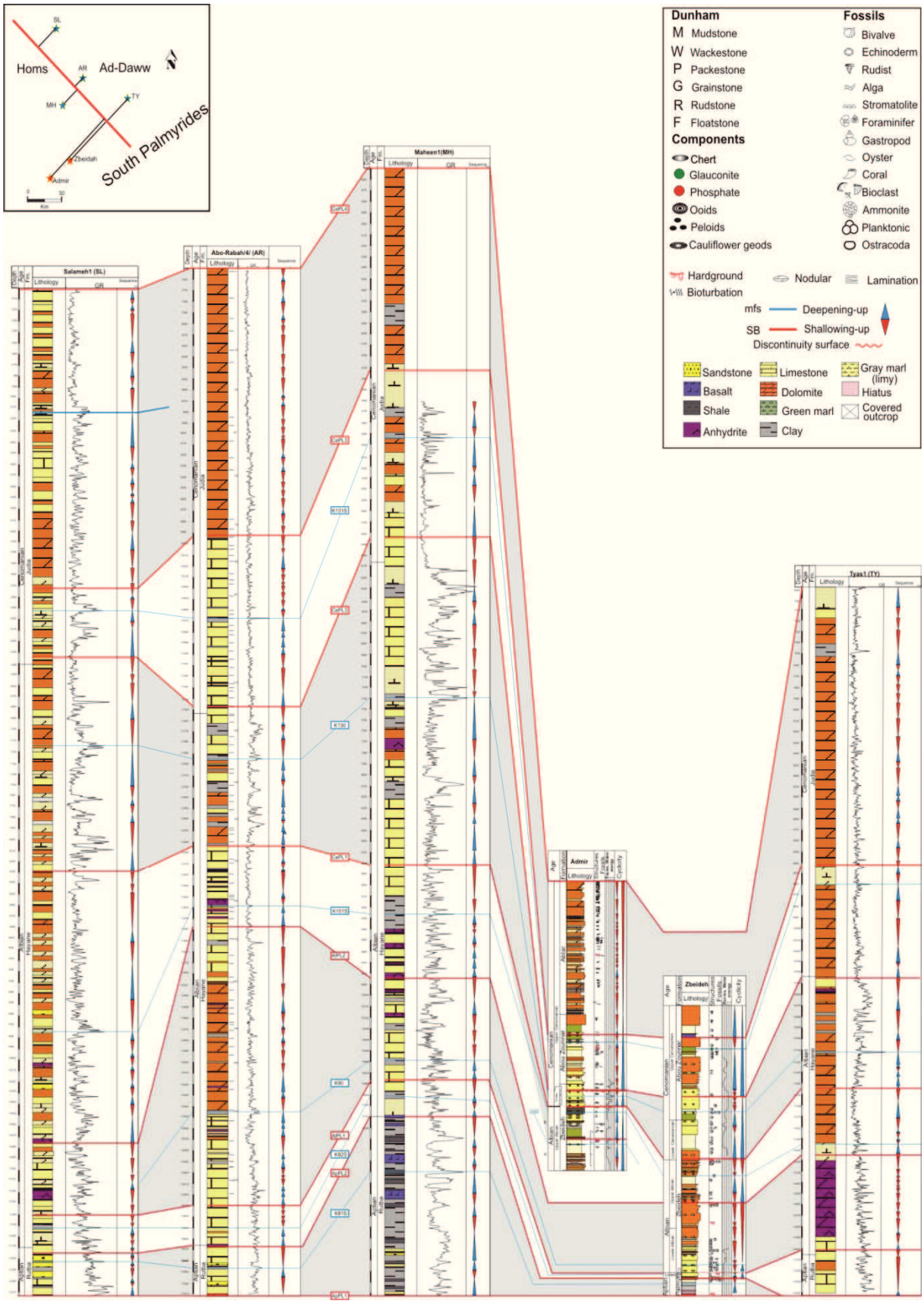
Homs
Ad-Daww
South Palmyrides
SL
AR
MH
TY
Zbeidah
Admir
Dunham
M Mudstone
W Wackestone
P Packestone
G Grainstone
R Rudstone
F Floatstone
Components
Chert
Glauconite
Phosphate
Ooids
Peloids
Cauliflower geods
Fossils
Bivalve
Echinoderm
Rudist
Alga
Stromatolite
Foraminifer
Gastropod
Oyster
Coral
Bioclast
Ammonite
Planktonic
Ostracoda
Hardground
Bioturbation
Nodular
Lamination
mfs
Deepening-up
SB
Shallowing-up
Discontinuity surface
Sandstone
Limestone
Gray marl (limy)
Basalt
Dolomite
Hiatus
Shale
Green marl
Covered outcrop
Anhydrite
Clay
Salameh1 (SL)
Abo-Rabah/4/ (AR)
Maheen1(MH)
Tyas1 (TY)
Admir
Zbeideh

Figure VII.6.a (previous page)– Sequence stratigraphic correlation between the South Palmyrides outcrops and the four boreholes of Ad-Daww and Homs depressions, based on lithofacies, microfacies, biostratigraphy, sonic logs and gamma ray. The South Palmyrides sequences are after Ghanem et al., (2012).

Barremian sediments of the lower "Gras de base" Fm. of Lebanon (Dubertret, 1955; Ponikarov et al., 1967; Krasheninnikov et al., 2005). The upper boundary of the Aptian strata is confirmed by a hardground of the lower hiatal surface of the missing *Muricohedbergella planispira* biozone in the South Palmyrides (Ghanem et al., 2012) and the ApCR1 sequence boundary of the Coastal Range (Ghanem and Kuss, subm.). The missing *Muricohedbergella planispira* zone in the South Palmyrides (Ghanem et al., 2012) may be comparable with part of the "Falaise de Blanche" (limestone Fm.) and the upper unnamed terrigenous formation of the Anti-Lebanon (Dubertret, 1955), and with the overlying shallowing-up subcycles of the Costal Range (Figures VII.6.a, VII.6.b). This hiatus coincides with the basalt of upper Rutba Fm. of Mahen borehole (Palmyrides subsurface) (Figures VII.6.a, VII.6.b). Humid climates are assumed for most of the Aptian (compare Bachmann et al., 2010), as indicated by the combined effects of regional volcanism and of increased clastic input that was transported from the neighbouring hinterlands of the Arabian Shield, Hamad Arch (Rutba uplift), and Mardin uplift (Caron and Mouty, 2007, Figures VII.6.a, VII.6.b).

The siliciclastic input influenced the carbonate deposition and characterized nearshore environments, rich in autochthonous ooids, bioclasts and quartz. Moreover, the Aptian deposits of the Coastal Range contain extensive green-marls alternating with shallow marine limestones and sandstones, limited to the shallowing-up cycles of the first Early Aptian sequence (ApCR1) of Bab Janneh Fm. of North West Syria.The Latakia Basin is in contrast marked by thick black shale accumulations (onshore boreholes, Figures VII.6.a, VII.6.b). The ApCR2 sequence of the Coastal Range is correlated with the Palmyra Sandstone Formation (and the subsurface equivalent Rutba Formation) of the Palmyrides trough and with the "Gras de base" Formation of Anti-Lebanon and the upper "Gras de base" Formation of Lebanon (Ponikarov et al., 1967; Krasheninnikov et al., 2005). The Palmyra Sandstone Formation is characterized by gradually changing lateral transitions from continental fluvial systems (Boggs, 1987; Miall, 1996) to shallow

marine sand beds and subtidal clays and shales (rich in bivalves) to the latest Aptian pelagic carbonates of the Zbeideh Formation (mfs ApS3 of Ghanem et al., 2012). This interval is correlated with the mfs of sequence ApCR2 (Figures VII.2, VII.6.a).

The Late Aptian strata of the Coastal Range show similarities to the Early Aptian lithofacies. Again, the carbonate sediments (limestones, dolostones) dominate the shallowing-up subcycles. The limestones are characterized by high energetic microfacies (ooilitic grainstones and bioclastic pack-/grainstones), alternate with sandstones, dolostones and green marls containing few autochthonous benthic foraminifera (Mouty and Saint-Marc, 1982). The mfs of the Late Aptian 2nd order sequence of the Costal Range is mainly deeper than the mfs ApCR1, including the planktonic mud-/wackestones and black shale in the Coastal Range (onshore boreholes, Figures VII.6.a, VII.6.b). This interval is correlated with a similar planktonic wackestone interval (mfs K82S Ticinella bejaouaensis zone) of the lower Zbeideh Fm. (South Palmyrides) and with the thin marly interbeds of the “Falaise de Blanche” Fm. of Lebanon and Anti-Lebanon.

Several areas of northwestern Syria are marked by volcanic activity, visible e.g. in the unconformable pre-Aptian suface. The first Early Cretaceous sequence started after the Late Neocomian volcanic event at 126my (±2 7) of Machta pres de Kafroun and 125 my (± 3.1) Massiaf (South Coastal Range, Mouty et al., 1992), also present in the South Palmyrides (Zbeideh, Abou-Zonnar) and Anti-Lebanon (Jabal Ash-Sheikh). The upper part of the terrigenous formation “Gras de base” of Shaqif El-Kharn of Anti-Lebanon includes the second Aptian volcanic event (Ponikarov et al., 1967; Krasheninnikov et al., 2005; Ghanem et al., 2012).

VII.6.2 Albian-Turonian Paleogeography of the northern Levant area

VII.6.2.1 The Albian depositional sequence of the Syria

The Albian time period spanned the deposition of the Ain Elbeida, the lower part of Slenfeh (North CR), Blaatah, and the lower part of Slenfeh (Sourth CR), Zbeideh (South Palmyrides), Hayane (Palmyrides, Latakia subsurface) formations. The albian

sediments are sandwiched between the late Aptian siliciclastics and green marls and carbonates of the Albian-Cenomanian Oceanic Anoxic Event (OAE1d). The Albian period of Syria was subdivided into four sequences (AlS1-AlS4), coincideingwith four Coastal Range sequences (AlCR1-AlCR4) and two South Palmyrides sequences (AlPL1, AlPL13) (Ghanem et al., 2012; Ghanem and Kuss, subm.). The Albian succession of South Palmyrides is bounded by two hiatal surfaces in the earliest Albian (Muricohedbergella planispira zone), and in the latest Albian (Ticinella praeticinensis, Rotalipora subticinensis zones) (Ghanem et al., 2012, Figures VII.6.a, VII.6.b).

Chronostsratigraphic and cyclic similarities of the Albian formations of the Coastal Range and the South Palmyrides (subsurface, outcrops) led to conclude that the shallow marine Albian succession is represented by the platform carbonates, predominantly alternating of marls, dolostones, and limestones. The limestones are composed of fine grained peloidal (laminated), bioclastic packestones, and several rudist banks. Deep marine limestones occurred especially in the Late Albian, formed the mfs of the second South Palmyrides sequence (AlPL2) and the third Albian sequence of Coastal Range (AlCR3). Farther to the east of South CR (Blaatah Fm.) coeval strata are characterized by restricted lagoonal limestones, intercalated with dolostones and marly dolostone intervals. In the Latakia Basin all mfs of the four Syrian sequences (AlS1-4) are marked by deep marine black shales and controlled by *Praeglobotruncana stephani, Praeglobotruncana delrioensis, Hedbergella* sp., and *Anomalina* sp. in the Late Albian. A similar lithology occurs in neighbouring areas of the Ad-Daww depression (Figures VII.6.a, VII.6.b).

The missing Muricohedbergella planispira zone of The South Palmyridesis probably due to the tectono-magmatic event of the adjacent Levant area that straddles the Aptian-Albian boundary (Segev and Rybakov, 2009) that are part of the major rifting episode which formed the Palmyrides aulacogene (Brew et al., 2001; Kazmin, 2002). This hiatus may be correlated with the basalts of the upper Rutba Fm. (Mahen borehole, Figure VII.6.a). The AlCR2 is represented by an intra-sequence hiatus and a volcanic interval

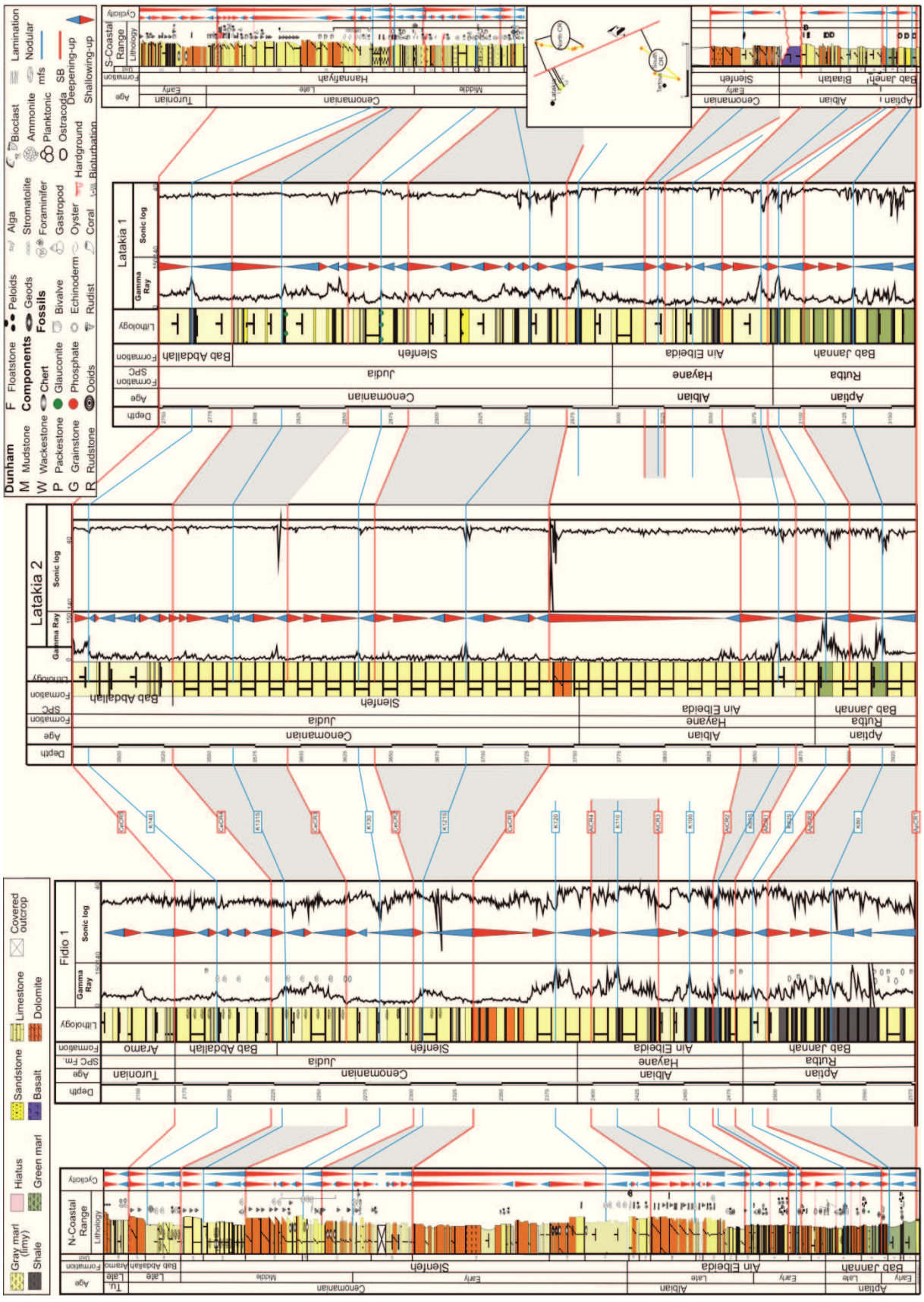
Dunham
Mudstone
Wackestone
Packestone
Grainstone
Rudstone
Floatstone
Components
Peloids
Geods
Fossils
Chert
Glauconite
Phosphate
Ooids
Alga
Stromatolite
Foraminifer
Bivalve
Echinoderm
Rudist
Bioclast
Ammonite
Planktonic
Ostracods
Lamination
Nodular
mfs
SB
Deepening-up
Shallowing-up
Hardground
Bioturbation
Coral
Oyster
Gastropod
Cyclicity
S-Coastal Range
Lithology
Formation
Age
Cenomanian
Turonian
Early
Late
Middle
Hannafiyah
Aptian
Albian
Bab Janah
Sienfeh
Bab Abdallah
Latakia 1
Sonic log
Gamma Ray
Depth
SPC Formation
Judia
Hayane
Ain Eldeida
Rutba
Latakia 2
Fidio 1
N-Coastal Range
Gray marl (limy)
Shale
Sandstone
Limestone
Dolomite
Hiatus
Green marl
Basalt
Covered outcrop
Aramo
Tu.

Figure VII.6.b (previous page)– Sequence stratigraphic correlation of Aptian – Early Turonian strata between outcrop-sections of the N-Coastal Range (left) and the S-Coastal Range (right - after Ghanem and Kuss (subm.), and three onshore wells of the Latakia Basin between. The correlation is based on lithofacies, microfacies, biostratigraphy, sonic, and gamma ray logs.

in the North Coastal Range (Joubet Barghal) that was dated 108.9±2.6 My by Mouty et al. (1992). In the South Coastal Range (Wadi-Layoun), another intra-sequence hiatus is marked by two volcanic intervals (106.3± 0.2, 103.4± 0.3 My, Ma et al., 2011) above the AlCR2 sequence boundary (Figures VII.6.a, VII.6.b), included the rest of AlCR2 and AlCR3.

The Albian-Cenomanian boundary of the South Palmyrides is evidenced by missing of the *R. ticinensis* and *R. appenninica* biozones directly above the mfs of AlPL2 (Ghanem et al., 2012). This hiatus is correlated with the shallowing-up (half)cycle of the AlCR3 of the North Coastal Range (the rudists banks of Slenfeh wall) and with basaltic intervals in the South Coastal Range (Wadi-Layoun, E Safita etc..) (Shatsky et al., 1966; Kozlov, 1966; Ponikarov et al., 1967; Ghanem and Kuss, submit). Segev and Rybakov (2009) mentioned a volcanic event, followed by thermal uplift in response to mantle plume activity in the north western Arabian platform during Upper Albian-Middle Cenomanian. This event may be correlated with the stratigraphic gap of *R. ticinensis* and *R. appenninica* biozones of the South Palmyrides (see above, Figures VII.2) and is confirmed by an erosion surface at this time described in the Anti Lebanon and in different localities to the west of the Dead Sea fault (Ferry et al., 2007).

VII.6.2.2 The Cenomanian depositional sequence of the Syria

The Cenomanian time period spanned the deposition of Slenfeh, and Bab-Abdalah (North Coastal Range), Slenfeh, and Hannafiyah (Sourth Coastal Range), Abo-Zonnar, and Abtar (South Palmyrides), Hayane, and Judia (Palmyrides and Latakia subsurface) Formations. It is delineated by two major 3rd order sequence boundaries (AlS4 and CeS5) of the Coastal Range that correlate with the Albian-Cenomanian hiatus in the South Palmyrides (Ghanem et al., 2012) and with the Cenomanian-Turonian disconformity between Abtar and Hallabate Formations after Mouty et al. (2003). A

regional middle Cenomanian hiatus allows to subdivide the Cenomanian succession into a Lower-Middle Cenomanian and a Late Cenomanian depositional unit: (Figures VII.6.a, VII.6.b).

In the North Coastal Range, the Lower-Middle Cenomanian period is clearly defined by an abrupt facies change from the restricted latest Albian deposits to the open marine Early Cenomanian environment (the first occurance of *Rotalipora globotruncanoides*) (Ghanem and Kuss, subm.) and by the basaltic contact with the deep marine marly limestones (rich of planktonic foraminifera) in the eastern South Coastal Range (Ponikarov et al., 1967; Krasheninnikov et al., 2005). Whereas, in the South Palmyrides the carbonates of the Lower-Middle Cenomanian period are marked by the upper hiatal surface, as indicated by missing latest Albian biozones (Figures VII.6.a, VII.6.b). In both areas, the Coastal Range and the South Palmyrides, a similar mid-Cenomanian regional disconformity surface was evidenced by a stratigraphic gap spanning the *Rotalipora reicheli* and the lower *R. greenhornensis* zones in South Palmyrides is marked by (Ghanem et al., 2012). This hiatus was correlated with a prominent paleokarstic surface within the lower *Rotalipora globotruncanoides* subzone of the South Coastal Range (Figures VII.6.a, VII.6.b).

The Lower Cenomanian strata of the Coastal Range comprise two 3rd order sequences AlCR4, CeCR2 that were correlated with sequence CePL1 of the South Palmyrides. Marls above, alternating with dolostones and limestones, mark a shallow marine depositional setting of the Early-Middle Cenomanian, They are superposed by marls and marly limestones of mainly low energy, deep marine environments. Pure dolostones and limestones above reflect protected lagoonal and tidal deposition with rudist beds. However, siliciclastic input of quartz occurs in sequence CeCR1 of the North Coastal Range, both in surface and subsurface sections (Figures VII.6.a, VII.6.b).

The Lower Cenomanian succession of the South Coastal Range includes an interval of basalt, observed to the east of Safita by Shatsky et al. (1966). The mid-Cenomanian hiatus was accompanied by volcanic activity of four local cyclical eruptions and emersion episodes in the Lebanon and the Carmel region (Ferry et al., 2007; Segev and Rybakov, 2009).

The Late Cenomanian time period comprises the Bab-Abdalah (North Coastal Range), upper Hannafiyah (Sourth Coastal Range), uppermost Abo-Zonnar, and Abtar (South Palmyrides), Judia (Palmyrides subsurface) formations. The Late Cenomanian sequences of the Coastal Range (CeCR3, CeCR4) coincide with CeP2 of South Palmyrides (Ghanem et al., 2012; and Kuss, subm., Figures VII.6.a, VII.6.b).

The Late Cenomanian facies characteristics are very similar to those observed within the Early-Middle Cenomanian deposits. Slightly higher ratios of planktonic and benthic foraminifera (Ghanem et al., 2012; Ghanem and Kuss, subm.) in the transgressive deposits, indicate slightly deeper water conditions especially in the Latakia Basin (Figures VII.6.a, VII.6.b). While, the regressive sediments form rudist banks as well as the platy limestone beds of the Cenomanian Turonian Event of South Coastal Range and the Abtar formation of South Palmyrides (Mouty et al., 2003).

VII.6.2.3 The Early Turonian depositional sequence of Syria

The Early Turonian time spanned the deposition of the Aramo Formation in Coastal Range, Hallabate Formation in the South Palmyrides and the upper most Judea Formation in the subsurface (Ad-Daww, Homs Depressions and Latakia Basin). These deposits comprise a 3rd order sequence (CeS5), comprsing latest Cenomanian to Early Turonian deposits. Sequence CeCR5 of the Range was correlated with CePL3 of the South Palmyrides foraminifera (Ghanem et al., 2012; Ghanem and Kuss, subm., Figures VII.6.a, VII.6.b) This sequence is defined by the Cenomanian-Turonian conglomeratic interval in the South Palmyrides (Mouty et al., 2003) and the basaltic interval (Bremant Almashaykh 93± 2My). The transgressive deposits are marked by a rapidly deepening depositional environments, represented by pelagic black shale, marls and marly limestones of the Judea, Hallabate, and Aramo Formations (Figures VII.6.a, VII.6.b); this is confirmed by the fossil record (increasing planktonic foraminifera) and the gradual to abrupt increase of the gamma ray values. The overlain dolostones and limestones reflect protected lagoon and tidal deposition and rudist banks overlain the deep marine deposits during the upward shallowing.

VII.7 Conclusions

Thirteen depositional cycles have been defined for the Aptian – Turonian seccession of west Syria. Variations of the accommodation space favoured progradation/ retrogradation and the establishment of 16 microfacis belts of different deepening-up and shallowing up sequences. A combination of global sea level fluctuations and regional tectonic activity associated with volcanic events controlled the litho- and biofacies and the palaeogeographic settings of the Eastern Mediterranean platforms. The palaeo- environmental positions extended from inner-platform carbonates to open lagoonal (including high energy) sediments that occured during the early transgressions; the late transgressions and maximum flooding surfaces are marked by marls and marly limestones (with abundant plankton) of the deeper ramp (e.g. in the Latakia Basin).Rudist-bearing and dolomitic inner-platform deposits characterized the shallowing-up sequences.

The correlation along a S-N transect of West Syria allows to reconstruct the platform configuration and to estimate the palaeogeographic evolution of the Palmyrides and Coastal Range Basins during the Aptian – Early Turonian. Several key episodes of the platform development that point to different Aptian, Albian, Cenomanin and Turonian platform stages of the North Levant have been distinguished; the correlation with major tectono-volcanic events and marginal progradation/ retrogradation was discussed.

The second manuscript

VIII. BIOSTRATIGRAPHY AND CARBON-ISOTOPE STRATIGRAPHY OF THE UPPERMOST APTIAN TO UPPER CENOMANIAN STRATA OF THE SOUTH PALMYRIDES, SYRIA

Hussam Ghanem[a], Mikhail Mouty[b] and Jochen Kuss[a]

[a] Department of Geoscience, Bremen University, PO Box 330440, 28359 Bremen, Germany
[b] Department of Geoscience, Damascus University, PO. Box 9487, Damascus, Syria

Published 2012
in GeoArabia
v. 17, p. 155-184

VIII. BIOSTRATIGRAPHY AND CARBON-ISOTOPE STRATIGRAPHY OF THE UPPERMOST APTIAN TO UPPER CENOMANIAN STRATA OF THE SOUTH PALMYRIDES, SYRIA

ABSTRACT Biostratigraphic and carbon-isotope data were used to introduce a highresolution stratigraphic reference section of the Upper Aptian to Upper Cenomanian platform carbonates of the South Palmyrides in Syria. We studied the biostratigraphic evolution of the Zbeideh to Abou-Zounnar formations in two sections, based on 42 species of benthonic foraminifera and 38 species of planktonic foraminifera. Comparisons with other Tethyan assemblages allowed determining 11 biozones; six are based on planktonic foraminifera, and five on benthonic foraminifera. Four hiatuses (earliest Albian, Middle–Late Albian, Late Albian–Early Cenomanian, and Mid Cenomanian) are marked by hardgrounds or dolomitic intervals. The planktic biozones *Ticinella bejaouaensis, T. primula, T. praeticinensis*, *Rotalipora subticinensis, R. globotruncanoides* and *R. cushmani* co-occur with the following benthonic biozones: *Mesorbitolina texana* partial range zone, *M. subconcava range zone, Neoiraqia convexa* taxon-range zone, *Praealveolina iberica* interval zone and *Pseudedomia drorimensis* range zone. Within this biostratigraphic framework, a new carbon-isotope curve from the South Palmyrides was compared with δ13C records of the Tethyan Realm and England that allows identifying several biotic events and Oceanic Anoxic Events (OAE), recorded in the Upper Albian to Upper Cenomanian succession. The combination of sequence-stratigraphic interpretations and comparisons, with our results have led to an improved understanding of the Cretaceous platform architecture of the South Palmyrides that links the Arabian Platform to the east with the Levant Platform to the southwest.

VIII.1 INTRODUCTION

Much progress has been made in the understanding of the Cretaceous sequence stratigraphy of the Arabian Plate (Sharland et al., 2001, 2004) and Levant Platform (Kuss et al., 2003; Homberg and Bachmann, 2010). In contrast, the Cretaceous stratigraphy of the Palmyrides in Syria, which lies between these two regions, is less well studied. The Palmyrides formed at the southwestern edge of the Neo-Tethys Ocean, which was isolated from the rest of the Arabian Platform by the Al-Hamad Uplift (Mouty, 1997). During the Late Aptian and Cenomanian they were characterized by the deposition of shallow-water carbonates, in addition to some Albian pelagic sediment. Surface exposures of Cretaceous sediments are located in the cores of anticlinal folds and domelike structures of the South Palmyrides Chain (Krasheninnikov et al., 2005;

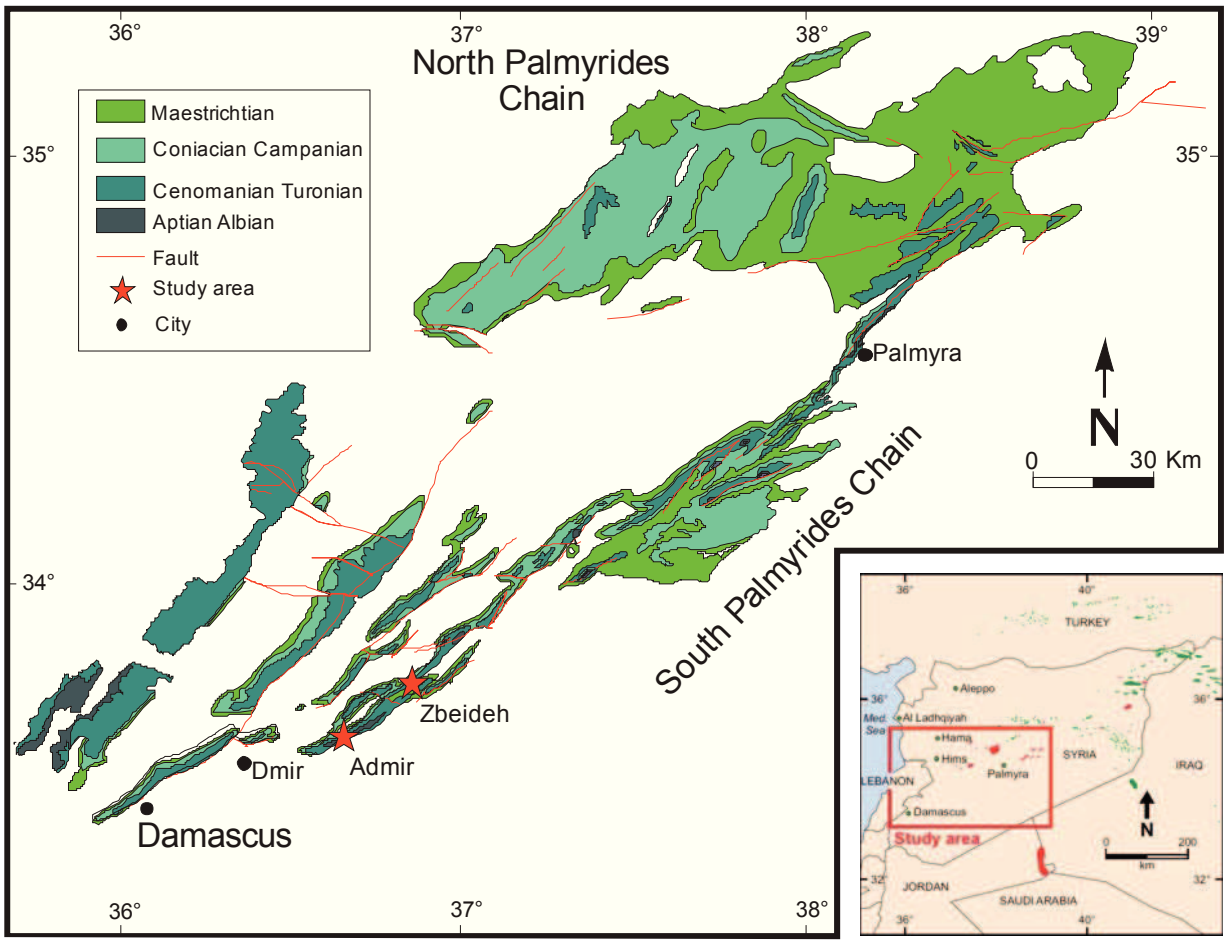

Figure VIII.1.a The Cretaceous outcrops of the Palmyrides, showing the locations of the Admir Section at latitudes 33°69'45"N and longitudes 36°86'55"E, and the Zbeideh Section at latitudes 33°78'36"N and longitudes 36°98'73"E.

Mouty et al., 1983; Ponikarov et al., 1966; Figure VIII.1.a). These folds were cut by large faults that produce a scarp-and-cliff ridge landscape (Al-Maleh et al., 2000). The investigated area is located northeast of Damascus and extends approximately 15–17 km between the Admir and Zbeideh sections in the southwestern part of the South Palmyrides (Figures VIII.1.a and VIII.3.a). In most localities of the South Palmyrides, the Cretaceous units are formed by shallow-water carbonates including limestone or dolomites with intercalated marly beds (Krasheninnikov et al., 2005; Mouty et al., 1983; Ponikarov et al., 1966). These sediments accumulated in peritidal, tropical water platform environments (Stampfli et al., 2001) with molluscs, foraminifera, echinoderms, ostracods and some green/red algae as major carbonate producers. We concentrated sampling to limestones (including marly and dolomitic limestone units). However, some intervals are strongly dolomitized and therefore lack biostratigraphically indicative fossils (Figure VIII.3.b). The abundant and varied planktonic and benthonic foraminifera permit high-resolution biostratigraphic subdivision of the Aptian to Cenomanian strata from the South Palmyrides, supplemented by a detailed Late Albian to Middle Cenomanian carbon-isotope record.

VIII.2 METHODS

We analyzed microfacies and biostratigraphy based on 65 thin sections from the Admir Section, and 78 from the Zbeideh Section. However, not all thin sections could be used for biostratigraphic zonation because of dolomitization (Figure VIII.3.b). The systematic identification of foraminifera is based on the schemes of various authors (Schroeder and Neumann, 1985; Caron, 1985; Loeblich and Tappan, 1988; Premoli Silva and Verga, 2004; Velić, 2007; Boudagher-Fadel, 2008). The biozone concepts used for the Palmyrides were correlated with those from other Tethyan areas proposed by the above-mentioned authors, as well as Ogg (2004a, b). Bulk rock samples (n = 103) for carbonisotope analysis have been collected from the Admir Section (Figures VIII.1.a and VIII.3.b). The curve of carbonisotopedata versus depth has been compared with trends derived from published carbon-isotope curves (Friedrich, 2010; Jarvis et al., 2006; Kennedy et al., 2004; Gale et al., 1996).

VIII.3 LITHOSTRATIGRAPHY

The lithostratigraphic subdivision of the here-considered siliciclastic Palmyra Sandstone Formation, the Zbeideh and Abou-Zounnar carbonate formations follows Mouty et al. (1983).

VIII.3.1 Palmyra Sandstone Formation

The Palmyra Sandstone Formation (12 m thick) is composed of grayish claystones with thin sandstone intercalations and thin dolomitic marls at the top (Figure VIII.3.b).

Age: Most authors attributed an (?Barremian– Aptian) age for the Palmyra Sandstone Formation (e.g. Mouty et al., 2002).

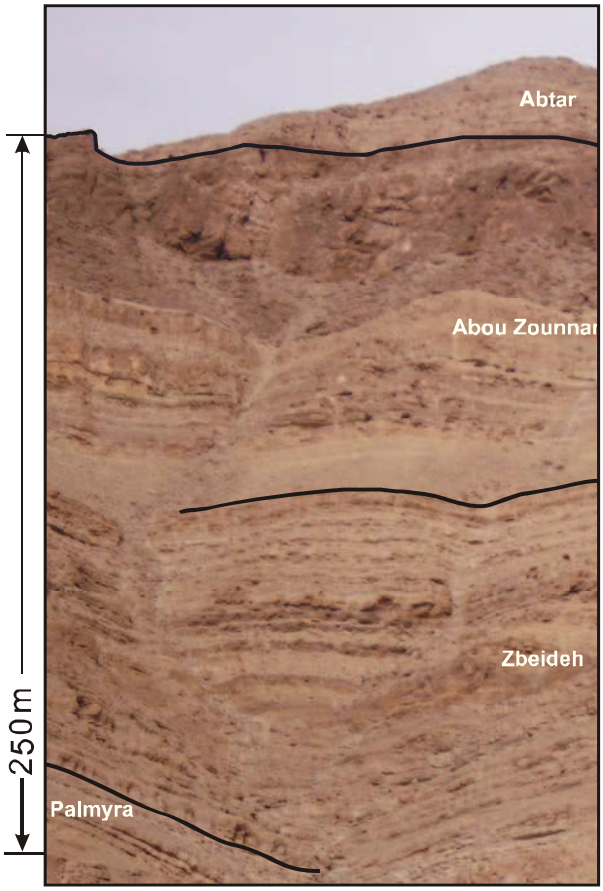

Figure VIII.3.a The studied succession of the Zbeideh Section with formation names.

VIII.3.2 Zbeideh Formation

Unit 1 is composed of massive limestones (packstones and wackestones with green algae, benthonic and planktonic foraminifera, and molluscs), intercalated with some marly limestones (rich in bivalves).

Unit 2 is composed of fossiliferous marly limestones (often rhythmic), intercalated with dolomitic limestones and dolomites.

Unit 3 is composed of unfossiliferous marly and massive dolomites, partly with moldic porosity and some quartz nodules.

Unit 4 consists of alternating dolomites and grayish dolomitic marls and intercalated with thin dolomitic limestones and soft green marls (with abundant bivalves). The upper part of

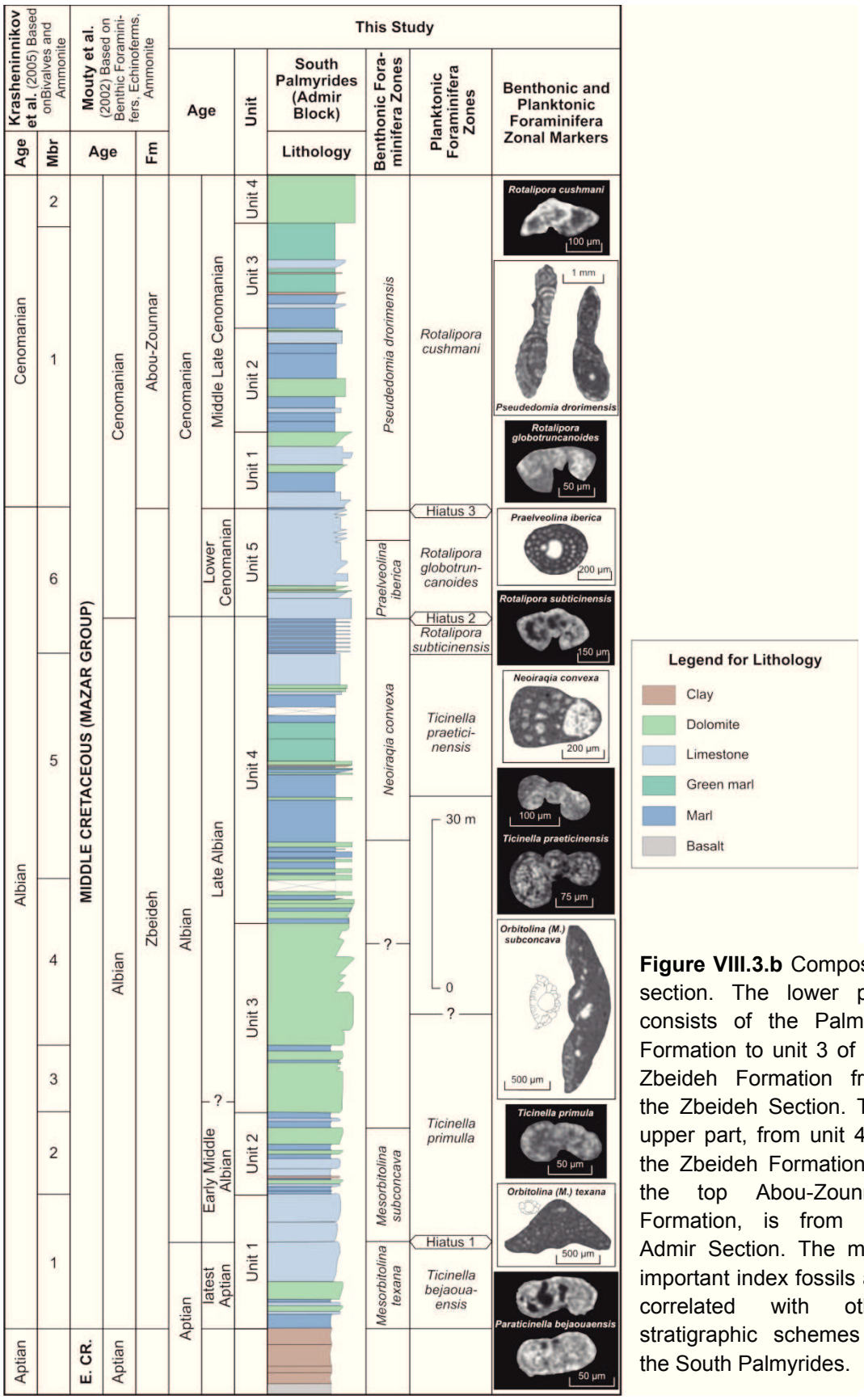

Figure VIII.3.b Composite section. The lower part consists of the Palmyra Formation to unit 3 of the Zbeideh Formation from the Zbeideh Section. The upper part, from unit 4 of the Zbeideh Formation to the top Abou-Zounnar Formation, is from the Admir Section. The most important index fossils are correlated with other stratigraphic schemes of the South Palmyrides.

unit 4 is restricted to the Admir Section and consists of fossiliferous white limestones (often nodular) with planktonic foraminifera, and intercalated nodular limestones (well-bedded) with marls rich in oysters.

Unit 5 is composed of fossiliferous massive limestones (packstones and wackestones with benthonic and planktonic foraminifera, and molluscs).

Age: Most previous authors attributed an Albian to Early Cenomanian age for the Zbeideh Formation (e.g. Mouty et al., 1983). Benthonic foraminifera of the lowermost limestones of unit 1, however, indicate a Late Aptian age (Figure VIII.3.b).

VIII.3.3 Abou-Zounnar Formation

The Abou-Zounnar Formation above is up to 115 m thick and was subdivided into four units (Figure VIII.3.b):

Unit 1 is represented by white limestones (mudstones and wackestones with benthonic foraminifera and red algae) and brownish dolomite with intercalations of fossiliferous grayish dolomarls and marly limestones.

Unit 2 is composed of green and gray marls with abundant oysters, intercalated with nodular thin to massive white dolomites and limestones (packstones and wackestones) with bivalves, gastropods, ostracods and some planktonic foraminifera.

Unit 3 is represented by green and gray marls with oysters, intercalated with foraminiferal limestone beds (the upper part of this unit marly gypsum).

Unit 4 forms cliff walls of massive dark brownish dolomite. Massive dolomites of the Abtar Formation overly this unit 5 (Figure VIII.3.a).

Age: Mouty et al. (1983) suggested Middle to Late Cenomanian age of the Abou-Zounnar Formation, which is confirmed by our data. The Cenomanian/Turonian boundary lies in the dolomites of the Abtar Formation above (based on interpretations of δ13C values).

VIII.4 BIOSTRATIGRAPHY

Our biostratigraphic subdivision is based on planktonic foraminifera and benthonic foraminifera (Late Aptian–Late Cenomanian) of both the Admir and Zbeideh sections

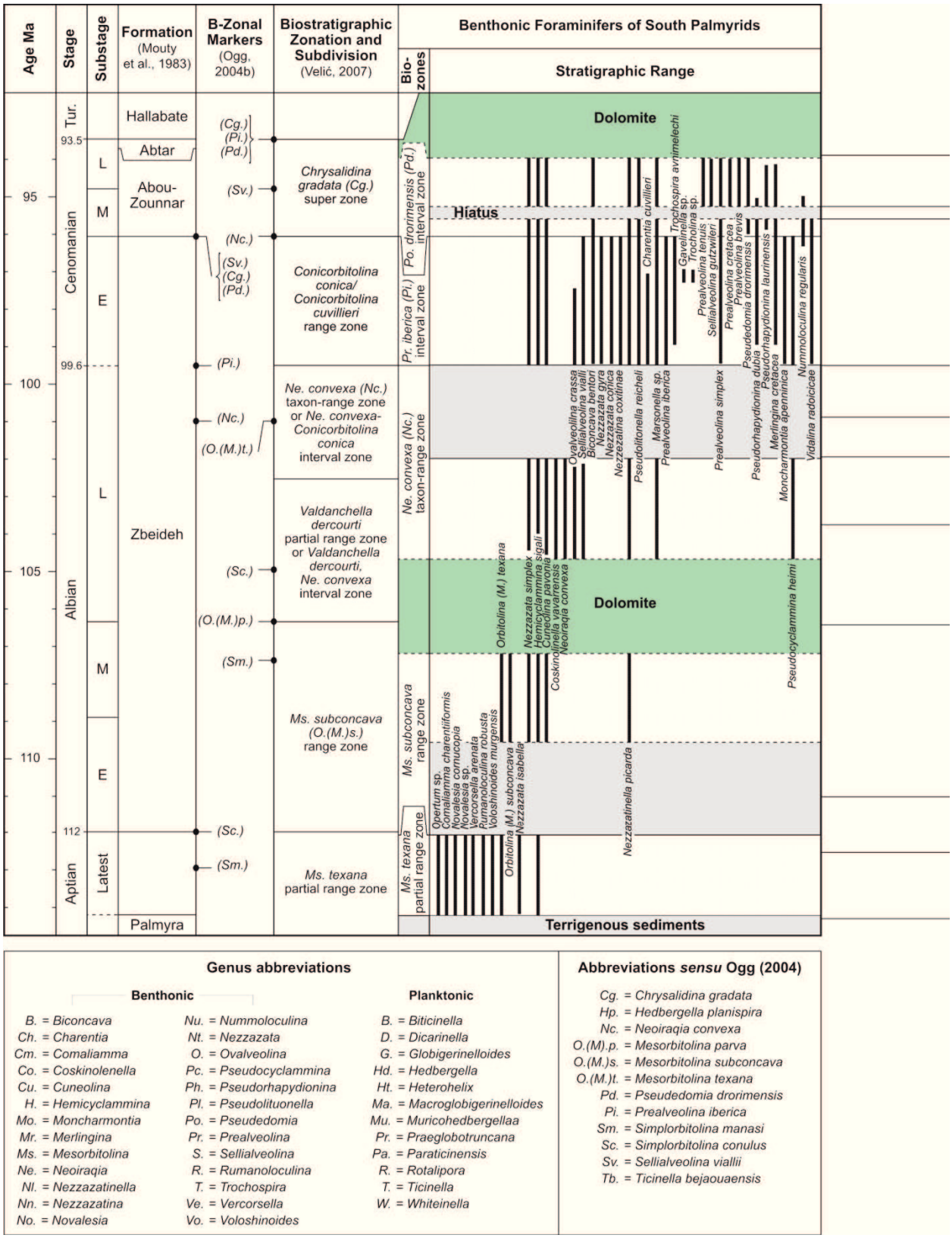

Figure VIII.4.1.a *See facing page for contination.*

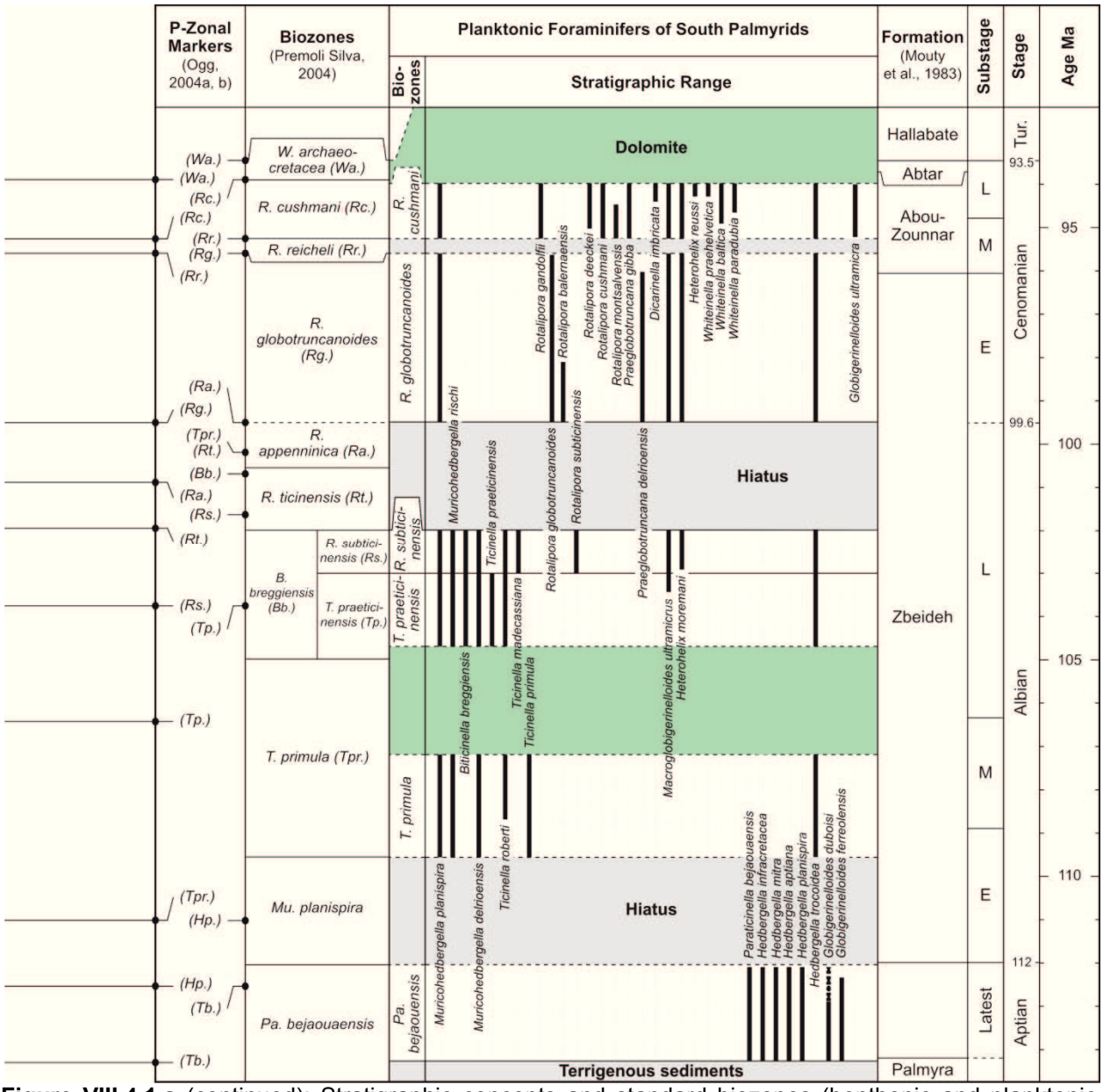

Figure VIII.4.1.a (continued): Stratigraphic concepts and standard biozones (benthonic and planktonic foraminifera) in the South Palmyrides. Shaded areas indicate hiatuses or dolomitized intervals.

from the South Palmyrides. Four major hiatuses are delimited, one around the Aptian/Albian boundary, the second around Middle/Late Albian, the third around the Albian/Cenomanian boundary and the fourth in the Middle Cenomanian (Figure VIII.4.1.a).

VIII.4.1 Planktonic Foraminifera Biostratigraphy

The high variety of planktonic foraminifera allows defining six biozones, based on the first (FO) and last occurrence (LO) of several index taxa. They range from Late Aptian to Late Cenomanian and are well comparable to assemblages from the Tethyan Realm (Ogg, 2004a, b; Premoli Silva and Verga, 2004).

VIII.4.1.1 Paraticinella bejaouaensis zone

Diagnosis: Total range zone of *Paraticinella bejaouaensis* (Sigal, 1966).

Description: The limestones of that biozone are characterized by *Paraticinella bejaouaensis*, an Upper Aptian trochospiral index species (Premoli Silva and Verga, 2004, Premoli Silva, et al. 2009) associated with *Hedbergella mitra, H. trochoidea, H. infracretacea, H. gorbachikae* (Figures VIII.4.1.a and VIII.4.1.b).

Correlation: The described assemblage holds several index species of the *Ticinella bejaouaensis* zone (Ogg, 2004a; Premoli Silva and Verga, 2004).

Age and Occurrence: Premoli Silva and Verga (2004) and Ogg (2004b) attributed a latest Aptian age for that biozone. In the present study, the *T. bejaouaensis* biozone occurs in a 15-m-thick succession of marly limestones and limestones, corresponding with the lower part of unit 1 of the Zbeideh Formation in the Zbeideh Section. This succession is uncomfortably overlain by limestones with *Ticinella primula* (Lower Albian, according to Caron, 1985).

VIII.4.1.2 Hedbergella planispira zone

This biozone is missing and may be represented by two hardgrounds (Figures VIII.3.b and VIII.4.1.a). We correlate this hiatus with a local unconformity described in the Palmyrid Aulacogene (Krasheninnikov et al., 2005), and regionally in the Levant Basin (Ferry et al., 2007; Segev and Rybakov, 2009).

VIII.3.1.3 Ticinella primula zone

Diagnosis: Total range zone of *Ticinella primula*.

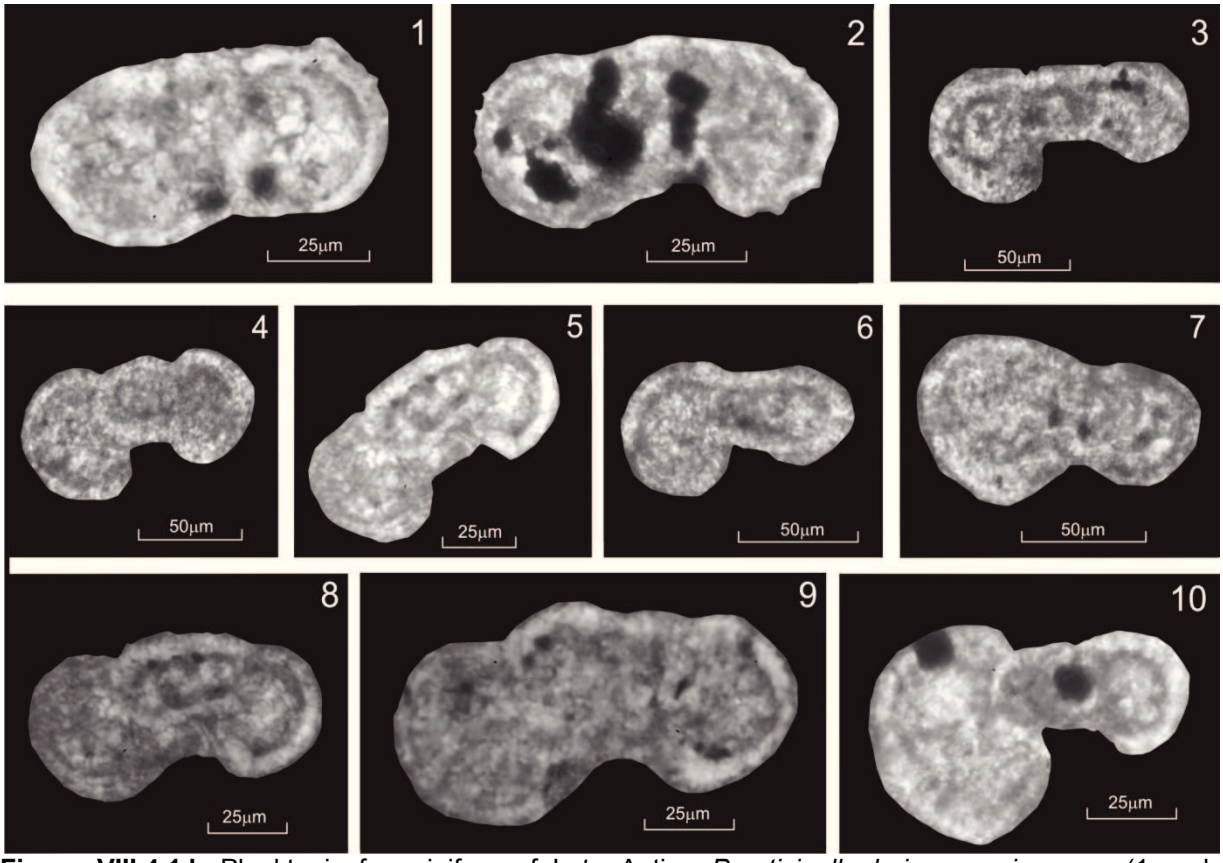

Figure VIII.4.1.b Planktonic foraminifera of Late Aptian *Paraticinella bejaouaensis* zone: (1 and 2) *Paraticinella bejaouaensis* (Zbeideh); (3 to 9) *Hedbergella* cf. *aptiana* (Zbeideh); (4) *Hedbergella mitra* (Zbeideh); (5) *edbergella trochoidea* (Zbeideh); (6 and 7) *Hedbergella infracretacea* (Zbeideh); (8) *Hedbergella* sp. (Zbeideh); (10) *Hedbergella gorbachikae* (Zbeideh). Note: 1 to 5, and 7 to 10 are axial sections, 6 is a subaxial section.

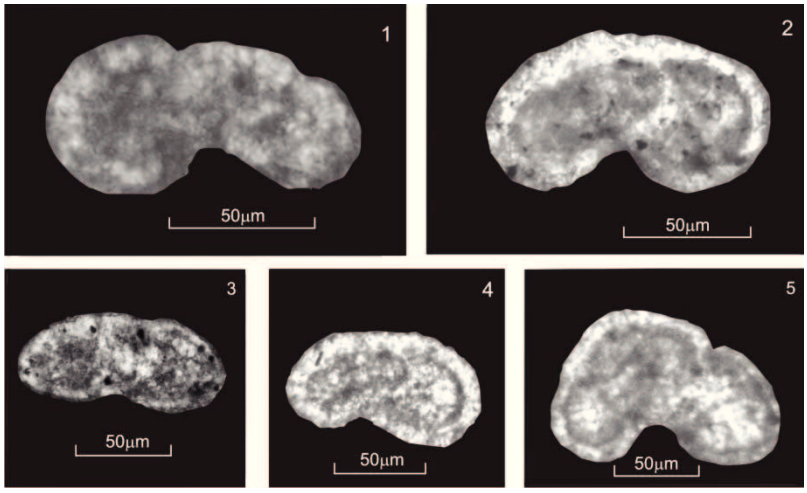

Figure VIII.4.1.c Planktonic foraminifera of of Early Albian *Ticinella primula* zone: (1, 2 and 4) *Ticinella primula* (Zbeideh); (3) *Muricohedbergella delrioensis* (Zbeideh); (5) *Ticinella roberti* (Zbeideh). Note: 1 and 4 are axial sections. 2, 3 and 5 are subaxial sections.

Description: This zone is delineated by *Ticinella primula*, associated with *T. roberti* (Gandolfi, 1942), *Hedbergella planispira* and *Muricohedbergella delrioensis*. The microfauna of this interval are badly preserved due to dolomitization processes (Figures VIII.3.b and VIII.4.1.a).

Correlation: The described planktonic assemblage correlates with the *Ticinella primula* zone according to Premoli Silva and Verga (2004) and Ogg (2004a).

Age and Occurrence: This biozone was attributed to the Early and Middle Albian according to Premoli Silva and Verga (2004) and Ogg (2004a). *T. primula* (Figure VIII.4.1.c) appears in the Zbeideh Section in two massive limestone beds (9 m) of the upper part of unit 1 (Zbeideh Formation), directly above two hardgrounds that overlie limestones with *Paraticinella bejaouaensis* (Figure VIII.4.1.a). The upper part of the *T. primula* biozone is missing because of dolomitization processes. The total thickness of this biozone may reach about 60 m (upper part of unit 1, units 2 and 3).

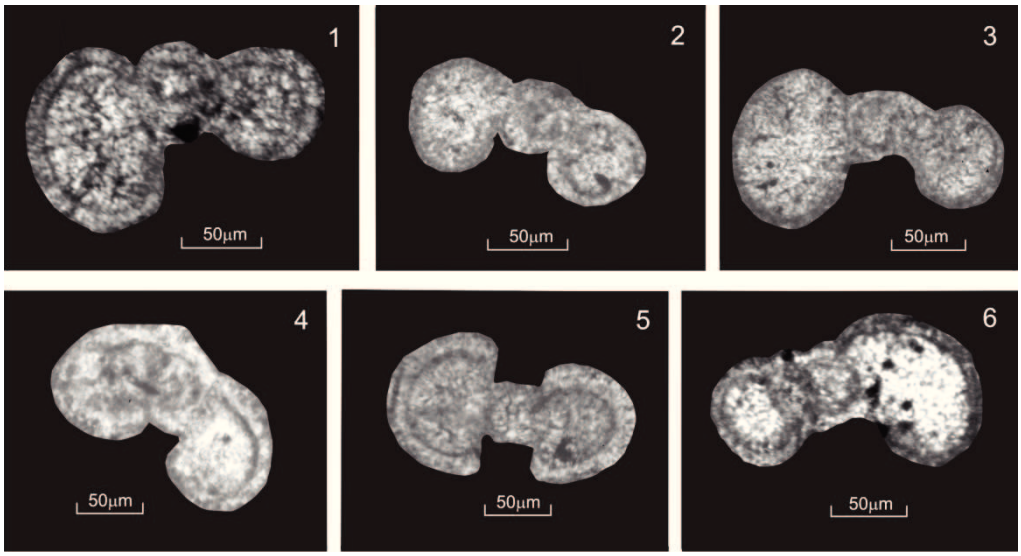

Figure VIII.4.1.d Planktonic foraminifera of Late Albian *Ticinella praeticinensis* zone: (1 and 2) *Ticinella praeticinensis* (Admir); (3) *Muricohedbergella planispira* (Admir); (4 to 6) *Ticinella roberti* (Admir); (5) *Biticinella breggiensis* (Admir). Note: 1 to 6 are axial sections.

VIII.4.1.4 Ticinella praeticinensis zone

Diagnosis*:* Interval zone comprising the range between the FO of the zonal marker to the FO of *Rotalipora subticinensis* (Ogg, 2004a).

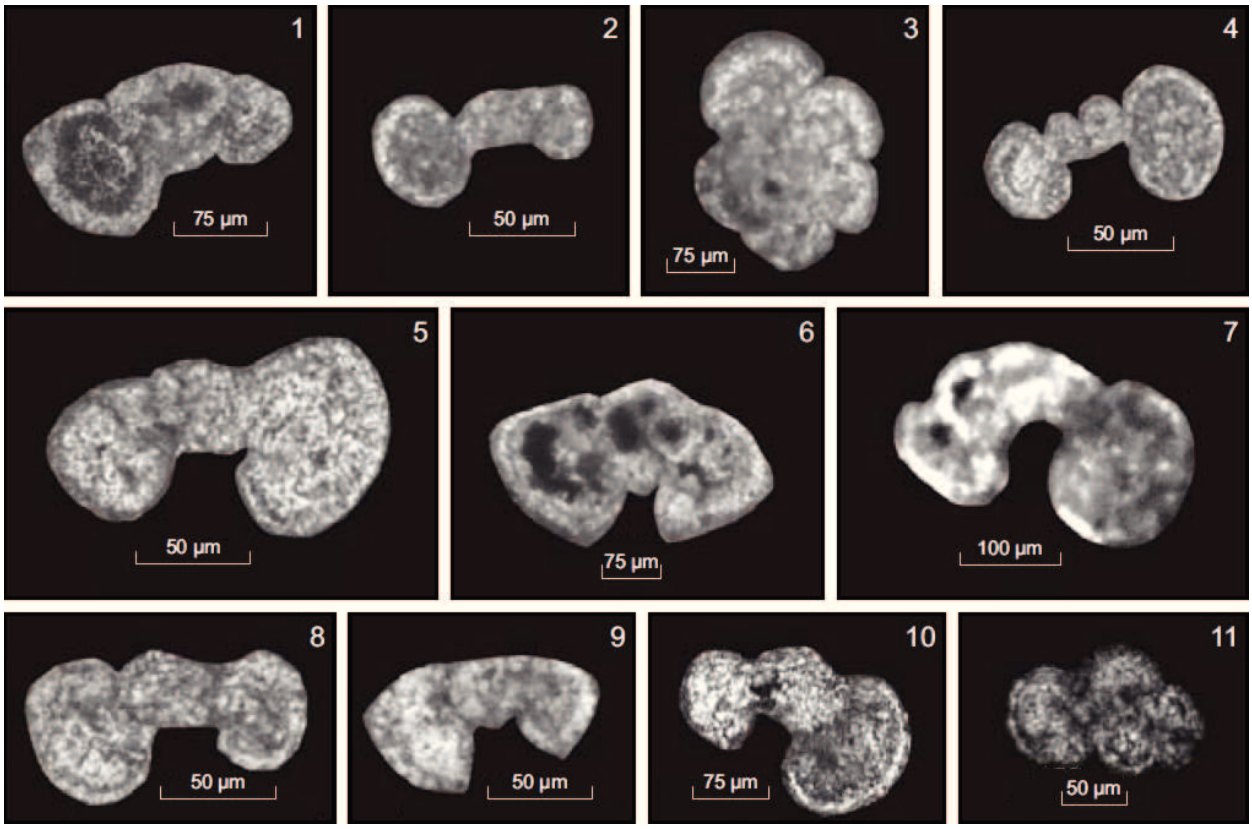

Figure VIII.4.1.e Planktonic foraminifera of Late Albian to Early Cenomanian *Rotalipora subticinensis* zone and *Rotalipora globotruncanoides* zone: (1 and 6) *Rotalipora subticinensis* (Admir);(2) *Muricohedbergella planispira* (Zbeideh); (3) *Ticinella madecassiana* (Admir); (4) *Foraminifera* sp. (Admir); (5) *Muricohedbergella rischi* (Admir); (7) *Muricohedbergella rischi* (Zbeideh); (8) *Muricohedbergella delrioensis* (Admir); (9) *Rotalipora* cf. *globotruncanoides* (Admir); (10) *Muricohedbergella delrioensis*; (11) *Heterohelix* cf. *moremani* (Admir); Note: 1, 4 to 6, and 8 are axial sections. 2, 7, and 9 to 11 are subaxial sections. 3 is a subequatorial section.

Description: Besides the zonal marker species, the following taxa characterize the *T. praeticinensis* interval zone: *T. roberti, Biticinella breggiensis, Muricohedbergella planispira, M. rischi* and *M. delrioensis.* The conspicuous increase in diversity and abundance is a further characteristic of that zone (Premoli Silva and Verga, 2004) (Figures VIII.4.1.a and VIII.4.1.d).

Correlation: Both, the marker species and the plankonic assemblage correlate with the *Ticinella praeticinensis* zone, defined by Ogg (2004a).

Age and Occurrence: This biozone corresponds to the Late Albian (Caron, 1985; Premoli Silva and Verga, 2004; Ogg, 2004a). It was defined in nodular limestones of unit 4 (Zbeideh Formation) of the Admir and Zbeideh sections (Figure VIII.3.b), with the FO of *Ticinella praeticinensis* and *Biticinella*

breggiensis at the base and the FO of *Rotalipora subticinensis* at the top (Ogg, 2004a).

VIII.4.1.5 Rotalipora subticinensis zone

Diagnosis*:* Total range zone of the zonal marker (Ogg, 2004a).

Description: The following planktonic foraminifera co-occur together with the zonal marker: *Biticinella breggiensis, Muricohedbergella delrioensis*, *M. rischi, M. planispira, Ticinella roberti* and *T. madecassiana* (Figure VIII.4.1.a). This biozone marks the onset of species with keeled peripheries (Premoli Silva and Verga, 2004) (Figure VIII.4.1.e).

Correlation: The *Rotalipora subticinensis* zone (Ogg, 2004a) may be correlated with the upper part of the *Ticinella praeticinensis* and *Rotalipora subticinensis* subzone (Premoli Silva and Verga, 2004).

Age and Occurrence: The *R. subticinesis* zone was attributed a Late Albian age according to Ogg (2004a) and Premoli Silva and Verga (2004). It was determined in (6.2 m) thick nodular limestones of unit 4 of the Zbeideh Formation (Admir Section), based on the FO of *R. subticinensis* (Figures VIII.3. b, VIII.4.1.a and VIII.4.1.f).

VIII.4.1.6 Rotalipora ticinensis and *Rotalipora appenninica* biozones

There is no evidence for these two biozones in the studied sections. We therefore assume a major hiatus at the Albian/Cenomanian boundary, confirmed by a major hardground at the base of unit 5 of the Zbeideh Section (Figure VIII.3. b). The LO of *R. subticinensis* (at the top of unit 4) is followed by the FO of *R. globotruncanoides* (limestones of unit 5) and thus account for a hiatus between both biozones, comprising the *R. ticinensis* and *R. appenninica*. Based on age estimates given by Ogg (2004a), this hiatus spans ca. 2.4 million years (Figure VIII.4.1.a).

VIII.4.1.7 Rotalipora globotruncanoides zone

Diagnosis*:* Total range zone of the zonal marker (Ogg, 2004a).

Description: The following planktonic foraminifera co-occur together with the zonal marker: *Ticinella madecassiana*, *Praeglobotruncana delrioensis, Muricohedbergella delrioensis* and *Heterohelix moremani.* Benthonic foraminifera are more frequent during that interval (Figures VIII.3.b, VIII.4.1.a and VIII.4.1.e).

Correlation: The described planktonic assemblage equals with the zonal marker of the standard global planktonic event (Ogg, 2004a, b) (compare Figures VIII.3.b and VIII.4.1.a).

Age and Occurrence: The *R. globotruncanoides* biozone correlates with the Early Cenomanian (Premoli Silva and Verga, 2004; Ogg, 2004a). It occurs in thick-bedded

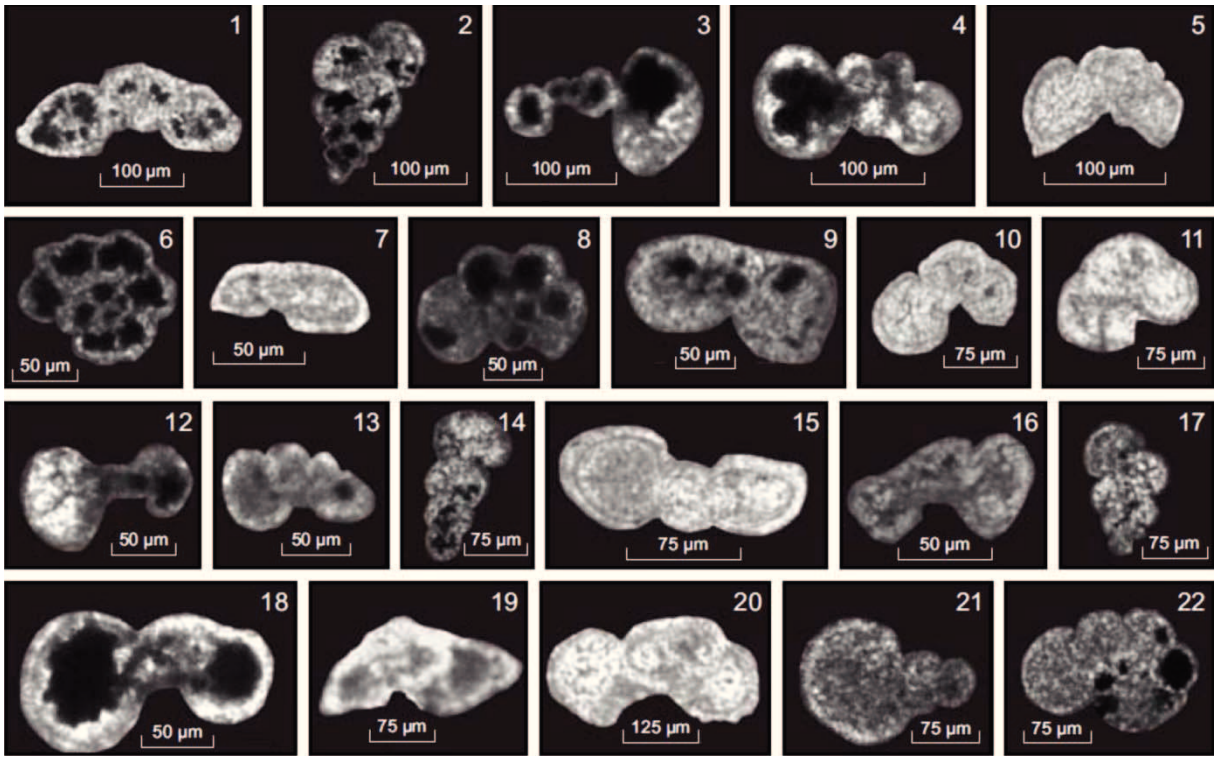

Figure VIII.4.1.f Planktonic foraminifera of Late Cenomanian *Rotalipora cushmani* zone: (1) *Dicarinella imbricata* (Admir); (3 and 15) *foraminifera* sp. (Admir); (2 and 14) *Heterohelix reussi* (Zbeideh); (4 and 20) *Whiteinella baltica* (Zbeideh); (5) *Praeglobotruncana gibba* (Admir); (6) *Macroglobigerinelloides ultramicra* (Zbeideh); (7) *Rotalipora* cf. *montsalvensis* (Admir); (8) *Hedbergella planispira* (Zbeideh); (9) *Hedbergella simplex* (Admir); (10 and 11) *Whiteinella* cf. *paradubia* (Admir); (12) *Macroglobigerinelloides* sp. (Zbeideh); (13 and 16) *Hedbergella* sp. (Zbeideh); (17) *Heterohelix moremani* (Zbeideh); (18) *Whiteinella praehelvetica* (Zbeideh); (19) *Rotalipora* cf. *cushmani* (Admir); (21 and 22) *Globigerinelloides ultramicra* (Zbeideh); Note: 1 to 4, 10, 17, 18 and 20 are axial sections. 5, 7, 9, 11 to 16, 19, 21 are subaxial sections. 6 and 22 are equatorial sections. 8 is a subequatorial section.

limestone of the uppermost part of the Zbeideh Formation. The base of this biozone is delineated by the FO of *R. globotruncanoides* – its top by the FO of *R. gandolfii*. (Figures VIII.3.b and VIII.4.1.a).

VIII.4.1.8 Rotalipora reicheli zone

A hardground surface between the LO of *Rotalipora globotruncanoides* and the FO of *R. cushmani* coincides with a stratigraphical gap that represents the *Rotalipora reicheli* zone of the Middle Cenomanian (between 97 to 96.6 Ma, Ogg, 2004a).

VIII.3.1.9 Rotalipora cushmani zone

Diagnosis*:* Total range zone of the zonal marker (Ogg, 2004a).

Description: Numerous keeled taxa occur in this biozone, which is characterized by *R. cushmani* associated with *Globigerinelloides ultramicra, Dicarinella algeriana, D. imbricata, Praeglobotruncana gibba, Whiteinella paradubia, W. praehelvetica, W. baltica, W. aumalensis, Heterohelix moremani, H. reussi, Rotalipora gandolfii, R. deeckei* and *R. montsalvensis.* Keeled taxa become more abundant and slightly bigger towards the middle part of this biozone and gradually disappear towards the upper part. The genus *Whiteinella* is more common in the upper part of this zone (Figures VIII.4.1.a and VIII.4.1.f).

Correlation: The described planktonic assemblage correlates with the *Rotalipora cushmani* zone according to Premoli Silva and Verga (2004) and Ogg (2004a) (Figure VIII.4.1.a).

Age and Occurrence: The *R. cushmani* biozone corresponds to the Late Cenomanian (Premoli Silva and Verga, 2004; Ogg, 2004a) (Figure VIII.4.1.a). It is determined in the Zbeideh Section based on the FO of *R. cushmani* and *R. deeckei* (Figure VIII.4.1.f) and in the Admir Section, based on the LO of *R. gandolfii* and the FO of *R. cushmani* (Figures VIII.3.b and VIII.4.1.a). The *R. cushmani* zone is evident in marly limestones, alternating with limestones and dolomites (ca. 40 m thick) of units 1, 2 and 3 of the Abou-Zounnar Formation of the Admir Section, corresponding to units 2 and 3 of Abou-Zounnar Formation of the Zbeideh Section (ca. 75 m thick).

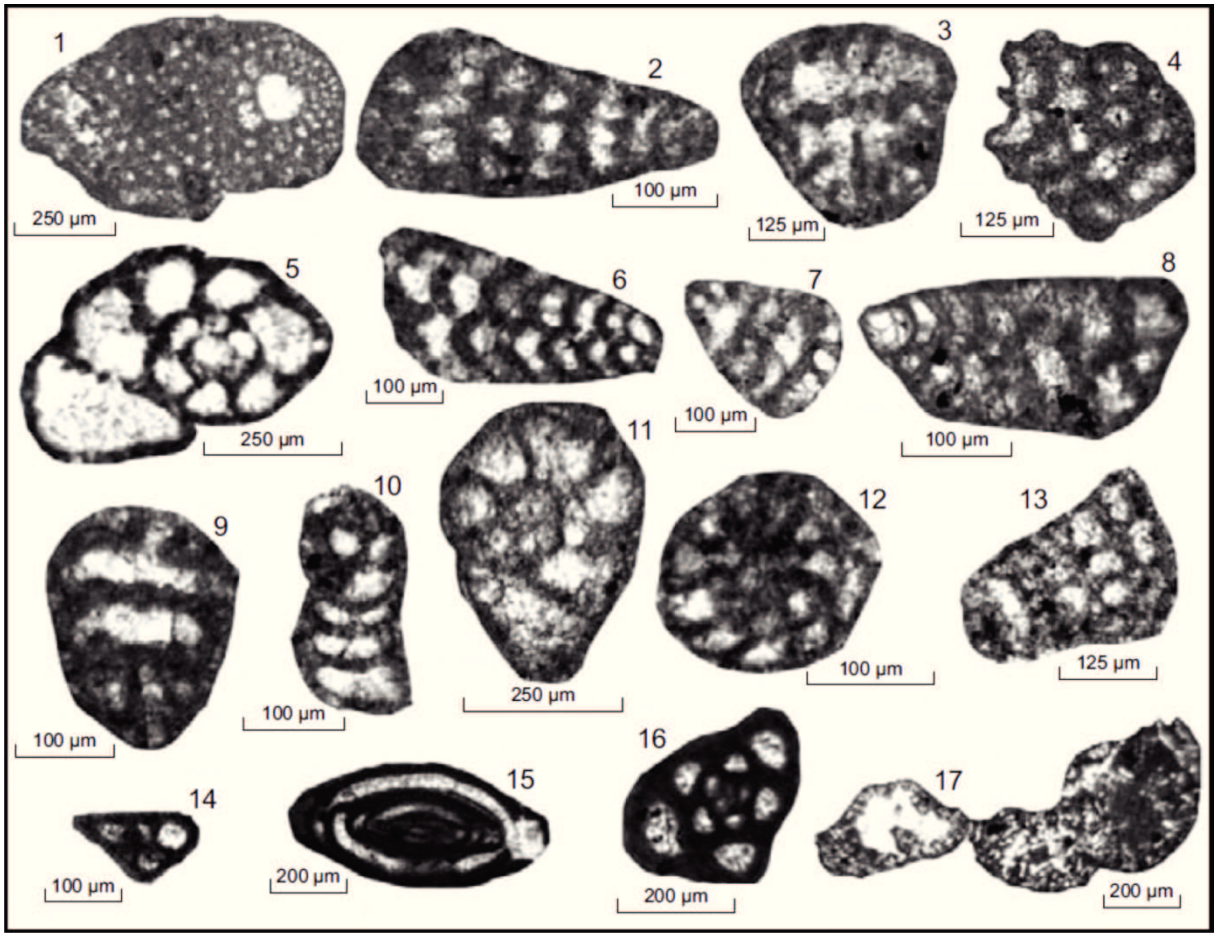

Figure VIII.4.2.a Benthonic foraminifera of the Late Aptian *Mesorbitolina texana* partial range zone: (1 and 4) *Mesorbitolina texana*, (1) [ob] through a young megalospheric form, (4) [sas]. (2, 3, 7 and 13) *Vercorsella arenata*, (2 and 13) [sas], (3 and 7) [ts] (4, 14 and 17) foraminifera sp. (Zbeideh). (5 and 11) *Comaliamma charentiiformis*, (5) [sas], (11) [es] (Zbeideh). (9) *Opertum* sp. [ts] (Zbeideh). (6 and 8)*Novalesia cornucopia*, [sas] (Zbeideh). (10) *Novalesia* sp., [sas] (Zbeideh). (12) *Nezzazata Isabella* [ses] (Zbeideh). (16) *Rumanoloculina robusta*, [sas] (Zbeideh). (15) miliolid indet. (Zbeideh), (Admir). Abbreviations: as = axial section; sas = subaxial section; es = equatorial section; ses = subequatorial section; ob = oblique section; ts = transversal section; ls = longitudinal section.

VIII.4.2 Benthonic Foraminifera Biostratigraphy

Numerous benthonic foraminifera are useful index fossils of the Cretaceous carbonate platforms (Boudagher-Fadel, 2008). They show a widespread distribution, high diversity and abundance in the studied sections of the South Palmyrides (Figures VIII.4.2.a to VIII.4.2.e), and thus are important for the biostratigraphic subdivision. Based on the concepts of Mouty et al. (2002), Velić (2007), Ogg (2004b), and Schroeder et al. (2010), the following five biozones (overlapping most planktonic zonal boundaries; Figure VIII.4.1.a) were defined.

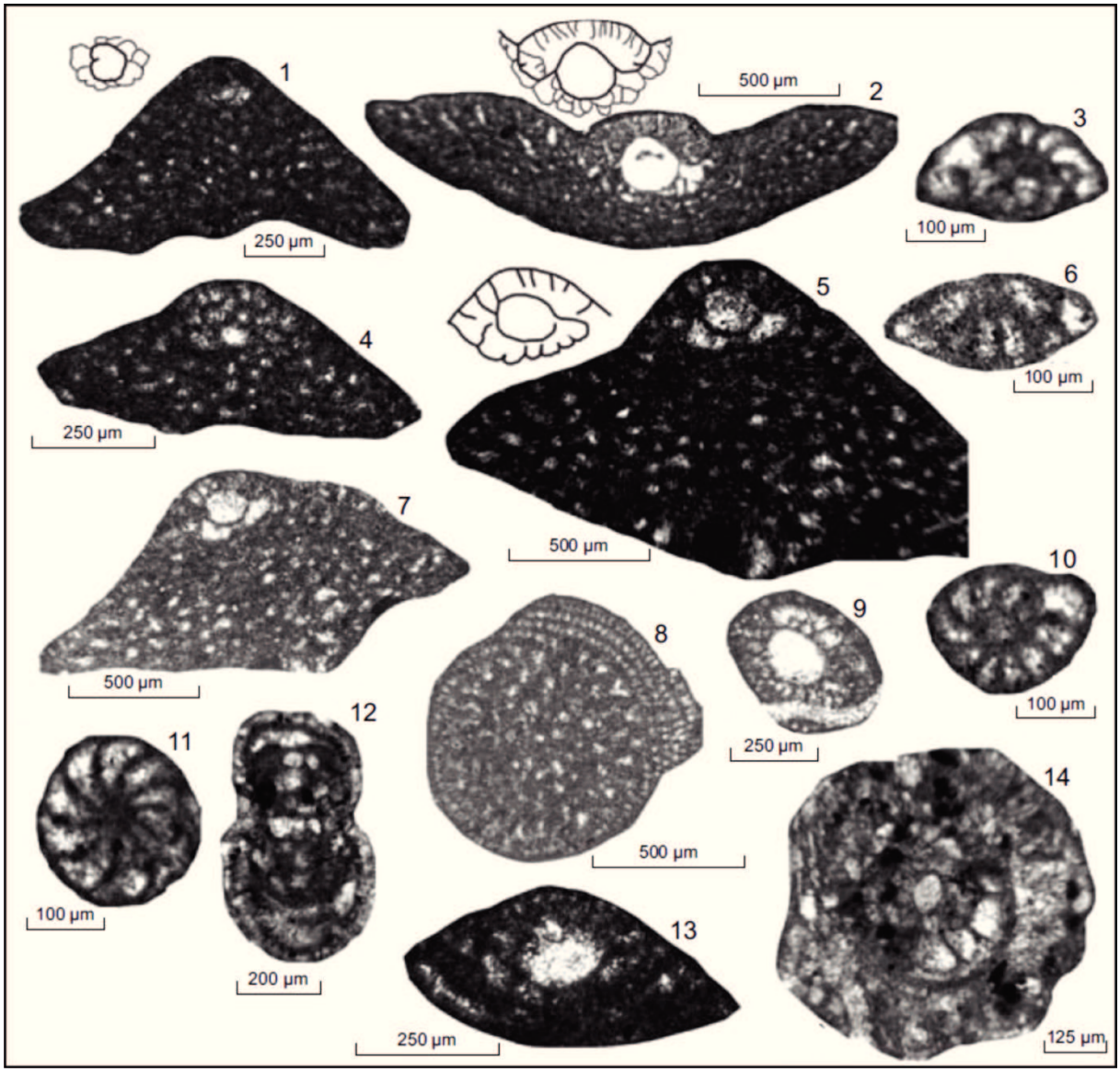

Figure VIII.4.2.b Benthonic foraminifera of Early Albian *Mesorbitolina subconcava* zone: (1 and 4) *Mesorbitolina texana*, [as] (Zbeideh). (6, 10 and 11) *Nezzazata isabella*, (6) [sas], [ses] (Zbeideh). (8) *Orbitolina* sp. [ts] (Zbeideh). (3) *Nezzazata simplex* [sas] (Zbeideh). (2, 5, 7, 9 and 13) *Mesorbitolina subconcava*, [as] (Zbeideh). (12 and 14) *Hemicyclammina sigali*, (12) [as] (Admir), (14) [es] (Zbeideh). Abbreviations: as = axial section; sas = subaxial section; es = equatorial section; ses = subequatorial section; ob = oblique section; ts = transversal section; ls = longitudinal section.

VIII.4.2.1 *Mesorbitolina texana* zone (Velić, 2007)

Diagnosis*:* The base of this partial range zone has been determined by the FO of the zonal marker. The top corresponds to the FO of *Mesorbitolina subconcava.*

Description: *M. texana* spans a long stratigraphic interval, ranging from the mid Late Aptian to the Middle Albian (Loeblich and Tappan, 1988; Velić, 2007). In addition to the zonal marker species, the following taxa occur within the *M. texana* biozone of the

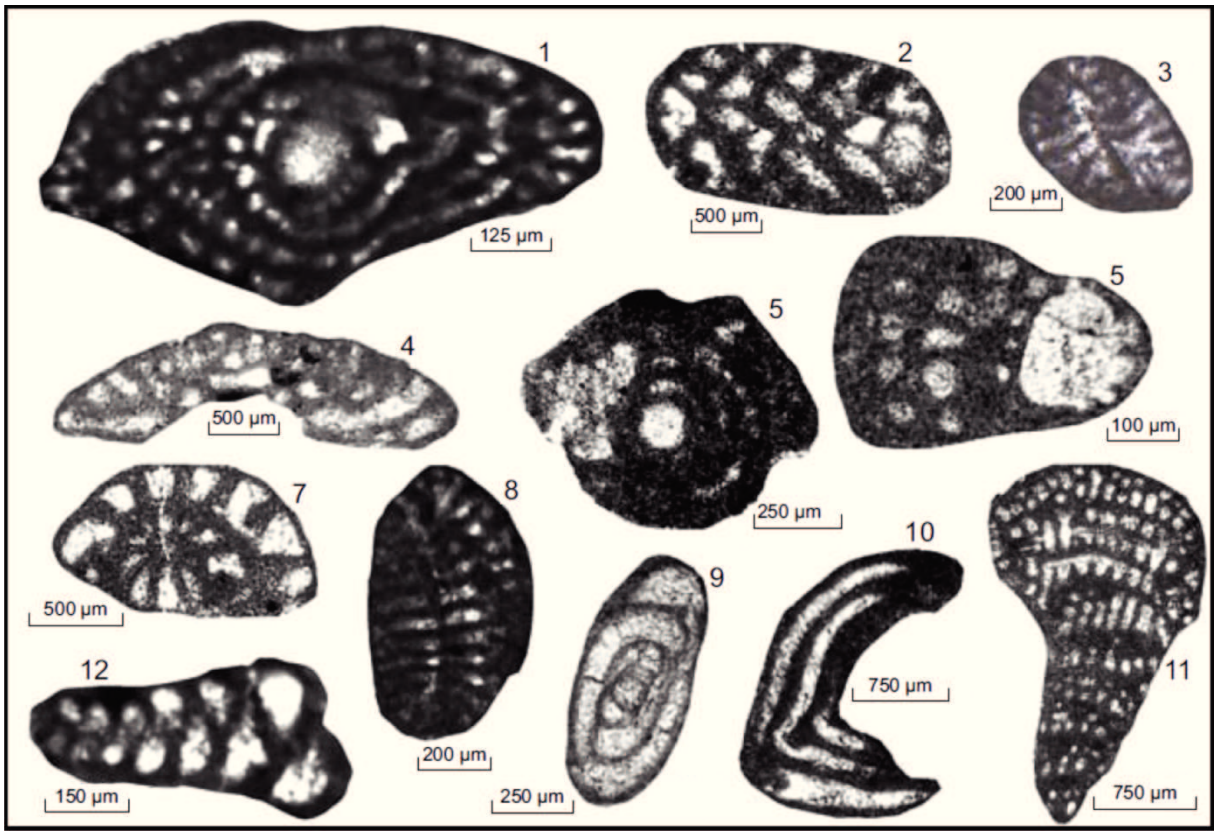

Figure VIII.4.2.c Benthonic foraminifera of Late Albian *Neoiraqia convexa* taxon-range zone: (1) *Sellialveolina viallii*, [as] (Admir). (2) *Coskinolinella* sp.,? [ts], microspheric form (Admir). (3, 8 and 11) *Cuneolina pavonia*, (3) [ts], (8 and 11) [sas] (Admir). (4) *Coskinolinella navarrensis*, [os] (Admir). (5) *Ovalveolina crassa*, [es] (Admir). (6) *Neoiraqia convexa*, [os] young megalospheric form (Admir). (7) *Nezzazata simplex* [ses] (Admir). (9) miliolid indet. (Admir). (10) *Pseudonummoloculina heimi* (Admir). (12) *Novalesia* sp. [sas] (Admir). Abbreviations: as = axial section; sas = subaxial section; es = equatorial section; ses = subequatorial section; ob = oblique section; ts = transversal section; ls = longitudinal section.

present study**:** *Voloshinoides murgensis*, *Opertum* sp., *Novalesia cornucopia, Comaliamma charentiiformis, Vercorsella arenata, Novalesia* sp*., Rumanoloculina robusta, Nezzazata isabellae,* including few miliolids and agglutinated foraminifera (Figures VIII.4.1.a and VIII.4.2.a).

Correlation: The described benthonic assemblage correlates with the *Mesorbitolina texana* partial range zone of the Adriatic platform, described by Loeblich and Tappan (1988) and Velić (2007).

Age and Occurrence*:* The *M. texana* zone indicates a latest Aptian age (Figures VIII.3.b and VIII.4.1.a), documenting the first benthonic foraminifera in the Cretaceous succession of the South Palmyrides.

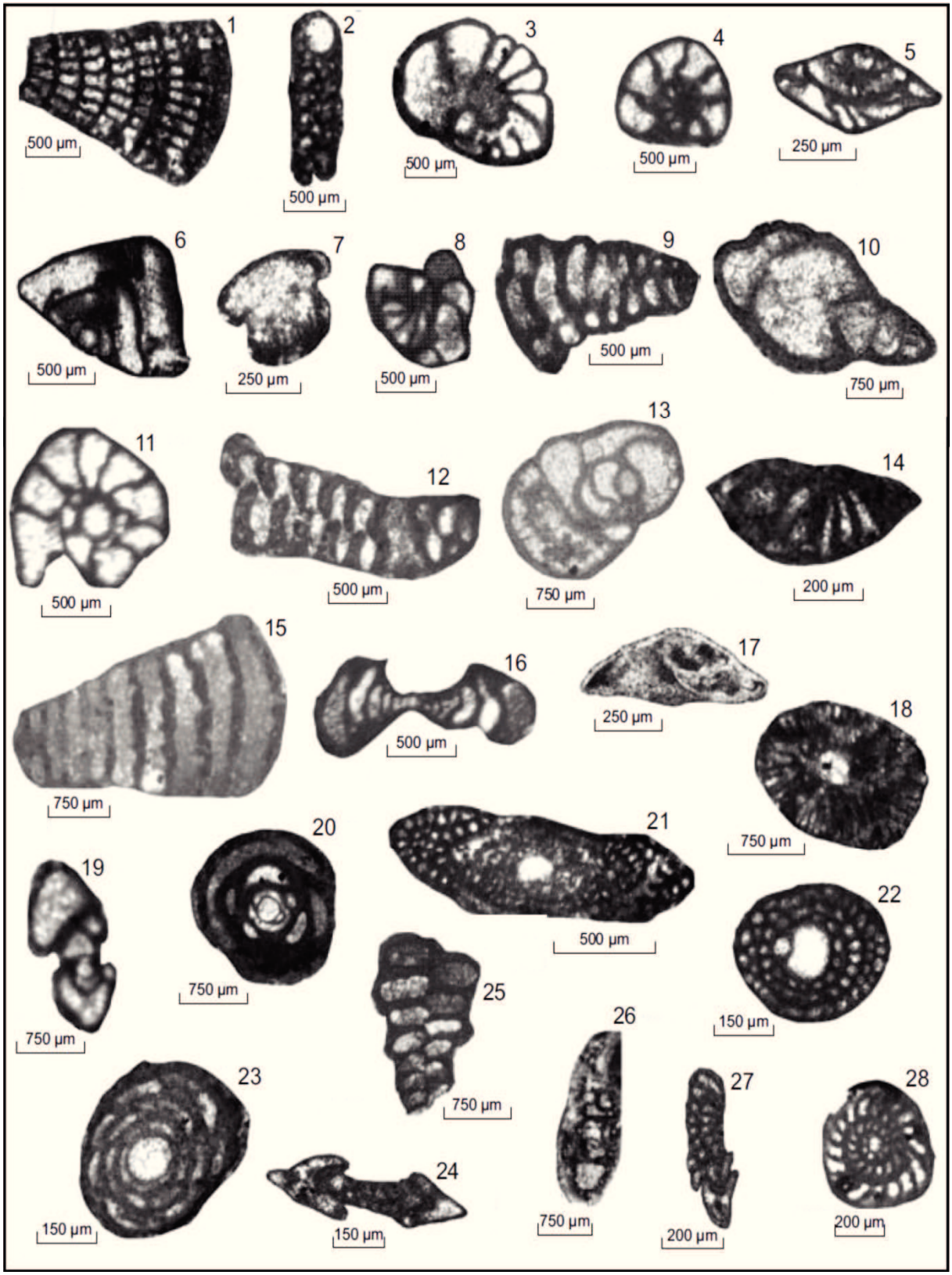
1
500 µm
2
500 µm
3
500 µm
4
500 µm
5
250 µm
6
500 µm
7
250 µm
8
500 µm
9
500 µm
10
750 µm
11
500 µm
12
500 µm
13
750 µm
14
200 µm
15
750 µm
16
500 µm
17
250 µm
18
750 µm
19
750 µm
20
750 µm
21
500 µm
22
150 µm
23
150 µm
24
150 µm
25
750 µm
26
750 µm
27
200 µm
28
200 µm

Figure VIII.4.2.d (previous page)- Benthonic foraminifera of Early Cenomanian *Praealveolina iberica* interval zone: (1 and 2) *Cuneolina pavonia*, [os] through a young megalospheric form, (3) *Nezzazatinella picardi* [sas] (Zbeideh), (4 and 8) *Nezzazata simplex*, [ses] (Admir), (25) [sas] (Zbeideh). (5) *Nezzezata gyra*, [as] (Zbeideh). (6) *Nezzazata conica*, [as] (Admir). (7) *Trocholina* sp. (Admir). (9 and 15) *Pseudolituonella reicheli*, [ls] (Admir). (10 and 13) *Peneroplis* sp., (Admir). (11) *Moncharmontia apenninica*, [es] (Admir). (12) *Novalesia* cf. [as] (Admir). (14) *Trochospira avnimelechi*, [sas] (Zbeideh). (16) *Nummoloculina regularis*, [sas] (Admir). (17) *Gavelinella* sp. (Admir). (18) *Dictyopsella* sp.,? [ts] (Admir). (19) *Moncharmontia apenninica*, [as] (Admir). (20) *Miliolid* sp. [as] (Admir). (21) S*ellialveolina viallii*, [as] (Admir). (22 and 23) *Praealveolina iberica*, (22) [os] of megalospheric form (Admir), (23) Slightly [os] (Z). (24, 27 and 28) *Biconcave bentori*, (27) [sas] (Admir), (28) [es] (Zbeideh), (25) *Marssonella* sp. [sas] (Admir). (26) *Charentia cuvillieri*, slightly [as] (Admir). Abbreviations: as = axial section; sas = subaxial section; es = equatorial section; ses = subequatorial section; ob = oblique section; ts = transversal section; ls = longitudinal section.

It is recorded from 15-m-thick marly limestones and limestones, representing the lower part of unit 1 (Zbeideh Formation) in the Zbeideh Section (Figures VIII.3.b and VIII.4.1.a). According to Velić (2007) the *M. texana* zone is defined by the total range of *Voloshinoides murgensis* or by the interval between the FO of *V. murgensis* and *Novalesia* sp. to the FO of *Mesorbitolina subconcava*.

VIII.4.2.2 *Mesorbitolina subconcava* zone

Diagnosis*:* Total range zone of the zonal marker (Velić, 2007).

Description: Besides the zonal marker, additional foraminifera (known as Albian index taxa) occur, such as *Nezzazata*, *N. simplex*, *Hemicyclammina sigali,* and *Nezzazatinella picardi* plus some miliolids and *M. texana* (Figures VIII.4.1.a and VIII.4.2.b).

Correlation: The benthonic foraminifera assemblage described coincides with *Mesorbitolina subconcava* zone of Velić (2007) (Figure VIII.4.1.a).

Age and Occurrence: The *M. subconcava* zone comprises the Early to Middle Albian (Velić, 2007). Our planktonic biozonation confirms the FO of *M. subconcava* in the Lower Albian (Figure VIII.4.1.a) in contrast to Schroeder et al. (2010), who discuss an earlier appearance of the zonal marker. The M. subconcava biozone was evidenced in 12-m-thick limestones of the Zbeideh Formation (Zbeideh Section, Figure VIII.5.a), spanning the upper part of unit 1 and nearly all of unit 2. Its base is defined by the FO of M. subconcava, while the upper boundary of this biozone is missing due to strong dolomitization processes. The dolomitization also affected the lower part of Neoiraqia convexa biozone (Figures VIII.3.b and VIII.4.1.a).

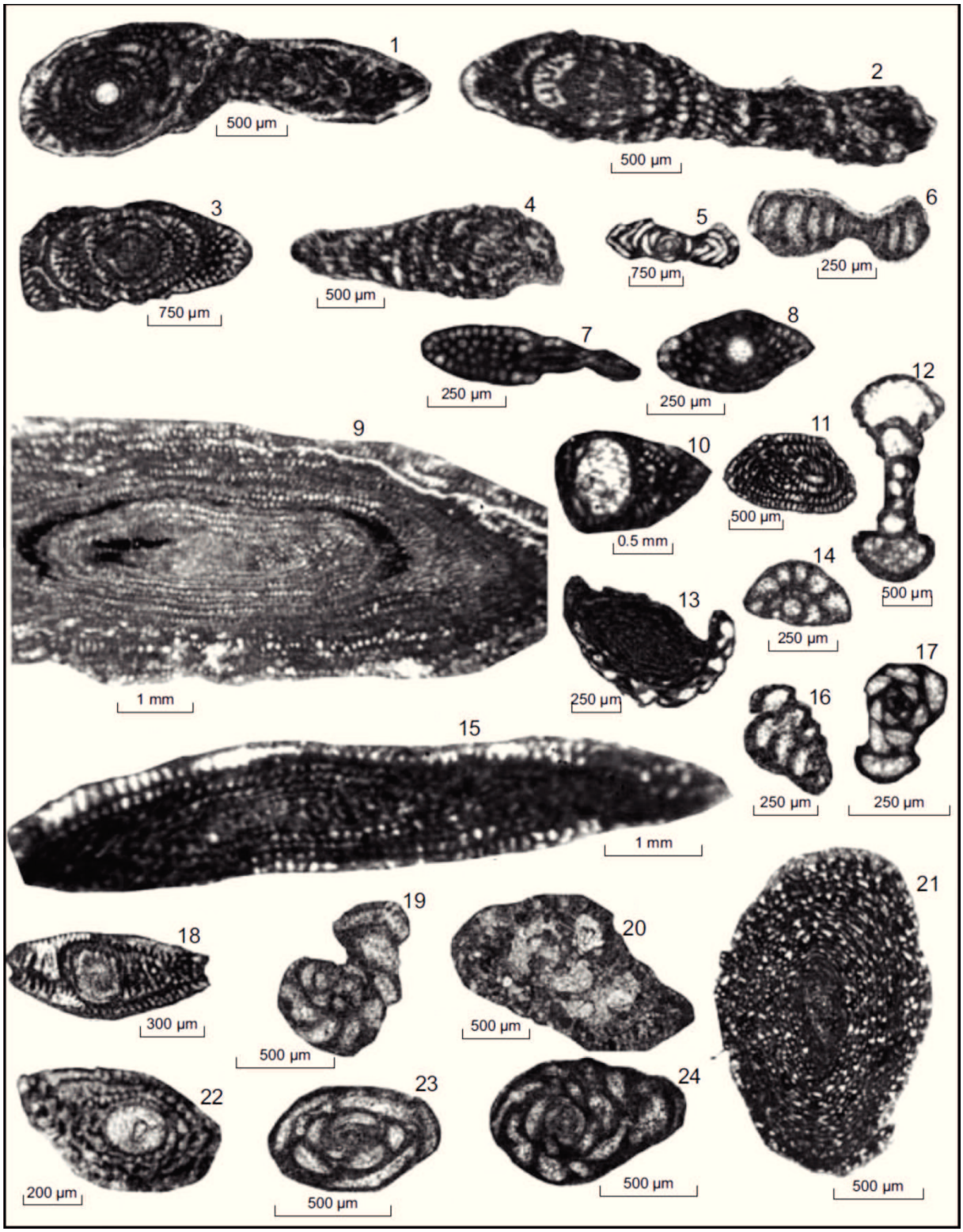
1
500 µm
2
500 µm
3
750 µm
4
500 µm
5
750 µm
6
250 µm
7
250 µm
8
250 µm
9
1 mm
10
0.5 mm
11
500 µm
12
500 µm
13
250 µm
14
250 µm
15
1 mm
16
250 µm
17
250 µm
18
300 µm
19
500 µm
20
500 µm
21
500 µm
22
200 µm
23
500 µm
24
500 µm

Figure VIII.4.2.e (previous page)- Benthonic foraminifera of Late Cenomanian *Pseudedomia drorimensis* range zone: (1 to 4) *Pseudedomia drorimensis*, (1) [as], (2 to 4) [sas] (Admir). (5) *Pseudocyclammina heimi*, [as] (Admir). (6) *Nummoloculina regularis*, [sas] (Zbeideh). (7 and 8) *Sellialveolina* sp., (7) [sas], (8) [as] (Admir). (9, 10, 15, 18, 21 and 25) *Praealveolina tenuis*, (9, 21 and 25) [sas], (9) (Admir), (21 and 25) (Zbeideh), (10 and 18) [as] (Zbeideh). (11) *Praealveolina simplex*, [sas] (Zbeideh). (12 and 20) *Hemicyclammina* sp., (12) [as], (20) [ses] (Admir). (13 and 22) *Praealveolina cretacea*, 13 [sas] (Zbeideh), (22) [as] (Admir). (14) *Nezzazata simplex* [sas] (Zbeideh). (16) foraminifera sp., (19 to 24) *Pseudorhapydionina dubia*, [as] (Admir). (17 and 23) miliolid indet. (Admir). Abbreviations: as = axial section; sas = subaxial section; es = equatorial section; ses = subequatorial section; ob = oblique section; ts = transversal section; ls = longitudinal section.

VIII.4.2.3 *Neoiraqia convexa* taxon-range zone

Diagnosis*:* Total range zone of zonal marker (Velić, 2007).

Description: This biozone is defined by the index fossil *Neoiraqia convexa,* associated with *Coskinolinella navarrensis*, *Ovalveolina crassa* and *Sellialveolina viallii* (Mouty et al., 2002). Moreover, further taxa of wide stratigraphic range like *Cuneolina pavonia, Nezzazata simplex, Pseudocyclammina heimi, Novalesia* sp. and some miliolids occur in that biozone (Figures VIII.4.1.a and VIII.4.2.c).

Correlation: The *Neoiraqia* biozone correlates with the upper part of *Valdanchella dercourti* partial range zone and *Neoiraqia convexa* taxon-range zone proposed by Velić (2007). Moreover, it is characterized by the uppermost occurrence of the *M. texana* zonal marker (Ogg, 2004b) (Figure VIII.4.1.a).

Age and Occurrence: This biozone is delineated by the total range of *N. convexa* (Velić, 2007) and is attributed to the Late Albian (Ogg, 2004b). It occurs in marly limestones and limestones (28 m) of the Admir and Zbeideh sections. Here, the top of the biozone is determined by the FO of *Praealveolina iberica, Pseudolituonella reicheli, Nezzazata gyra* and *Nezzazata conica* (Figures VIII.3.b and VIII.4.1.a).

VIII.4.2.4 *Praealveolina iberica* interval zone (Ogg, 2004b), (*Conicorbitolina conica/ Conicorbitolina cuvillieri* range zone, Velić, 2007)

Diagnosis: Interval zone ranging from the FO of *Praealveolina iberica* to the FO of *Pseudedomia drorimensis.*

Description: The index fossils of Velić (2007) are not present in the studied section. We therefore introduced the *Praealveolina iberica* interval zone based on the FO of the marker species (compare Ogg, 2004b). The *Praealveolina iberica* biozone is

additionally characterized by the FO of the following three Cenomanian species: *P. iberica, Pseudolituonella reicheli* and *Charentia cuvillieri* (Mouty et al., 2002) that are associated with a rich assemblage of further Cenomanian benthonic foraminifera like *Trochospira avnimelechi, Nezzazata gyra, N. conica, Biconcava bentori, Moncharmontia apenninica, Pseudorhapydionina dubia, Merlingina cretacea, Vidalina radoicicae, Trocholina* sp. and *Gavelinella* sp.. They co-occur with some wide range species: *Ovalveolina crassa, Sellialveolina viallii, Cuneolina pavonia,* miliolids div. sp., *Nezzazata simplex, Nezzazatinella picardi, Pseudonummoloculina heimi, Nummoloculina* sp., *Peneroplis* sp., *Dictyopsella* sp.?, *Novalesia* cf. and *Marssonella* sp. (Figures VIII.4.1.a and VIII.4.2.d)**.**

Correlation: The *Praealveolina iberica* interval zone is equivalent to the *Conicorbitolina conica/ Conicorbitolina cuvillieri* range zone (Velić, 2007), delineated by the range between the FO of *Praealveolina iberica* and the FO of *Pseudedomia drorimensis* (Ogg, 2004b) (Figure VIII.4.1.a).

Age and Occurrence: The *P. iberica* interval zone represents the early Cenomanian and comprises the interval between the FO of *P. iberica, Pseudolituonella reicheli, Nezzazata gyra* and *Nezzazata conica* and the FO of *Pd. drorimensis, P. cretacea, P. brevis* and *P. tenuis* (Ogg, 2004b; Velić, 2007). In the South Palmyrides, this biozone represents early Cenomanian shallow marine limestones with high foraminiferal diversities (Figure VIII.4.1.a). It occurs in unit 5 of the uppermost Zbeideh Formation, composed of (18 m) thick limestones in the Admir Section (Figure VIII.5.a).

VIII.4.2.5 *Pseudedomia drorimensis* range zone (Ogg, 2004b)

Diagnosis*:* Total range zone of zonal marker.

Description: The *P. drorimensis* biozone is delineated by the total range of the zonal marker together with *Praealveolina tenuis* and *P. brevis* (Mouty et al., 2002), originally defined on the Adriatic Carbonate Platform (Velić, 2007). Several benthonic taxa were found that are well comparable with that biozone. Among those, *Sellialveolina* sp., *Hemicyclammina sigali, Nezzazatinella picardi, Praealveolina simplex, Pseudonummoloculina heimi, Pseudorhapydionina dubia, Nezzazata simplex,*

Nummoloculina regularis, Cuneolina pavonia and miliolids div. sp. occur (Figures VIII.4.1.a and VIII.4.2.e).

Correlation: The *P. drorimensis* range zone according to the FO of the marker species (compare Ogg, 2004b). The latter author mentioned the co-occurrence with *Praealveolina iberica,* which, however, is restricted to the biozone below in the South Palmyrides (Figure VIII.4.1.a).

Age and Occurrence: According to Ogg (2004b), the *P. drorimensis* biozone comprises the Middle to Upper Cenomanian (VIII.3.b and VIII.4.1.a). It is identified within a 45-m-thick succession of limestones, intercalated with marls and dolostones of the Abou-Zounnar Formation (Admir Section, VIII.5.a), equivalent to 75 m of marly limestones and limestones of the Zbeideh Section.

VIII.5 SEQUENCE STRATIGRAPHY

Within the integrated high-resolution stratigraphic framework of the latest Aptian to Late Cenomanian strata of the South Palmyrides, a sequence-stratigraphic model is here proposed. It is based on lithofacies characteristics, the geometric relationship of the strata, and their stacking pattern (i.e. the hierarchy of subcycles), microfacies interpretations, and stratigraphic attributions (Figure VIII.5.a). Five depositional sequences, named South Palmyrides Sequence 1 to South Palmyrides Sequence 5, are here tentatively identified. Where possible the sequences are tied by biostratigraphic criteria to the maximum flooding surfaces (MFS) of Sharland et al. (2001, 2004) and sequences of Ogg (2004a).

VIII.5.1 South Palmyrides Sequence 1

In Syria a regional Lower Cretaceous unconformity separates the Jurassic Satih Formation from Lower Cretaceous basalt ((Mouty, 1997; Mouty et al., 2002; Krasheninnikov et al., 2005). Intensive uplift, rifting, and volcanism correspond in the Palmyrides to the Tayasir basaltic volcanics of the Negev, Galilee High (Mouty et al., 1992; Segev and Rybakov, 2009) and Mount Lebanon area (Ferry et al., 2007). In the region of the Zbeideh Section, the volcanism was followed by the deposition of the

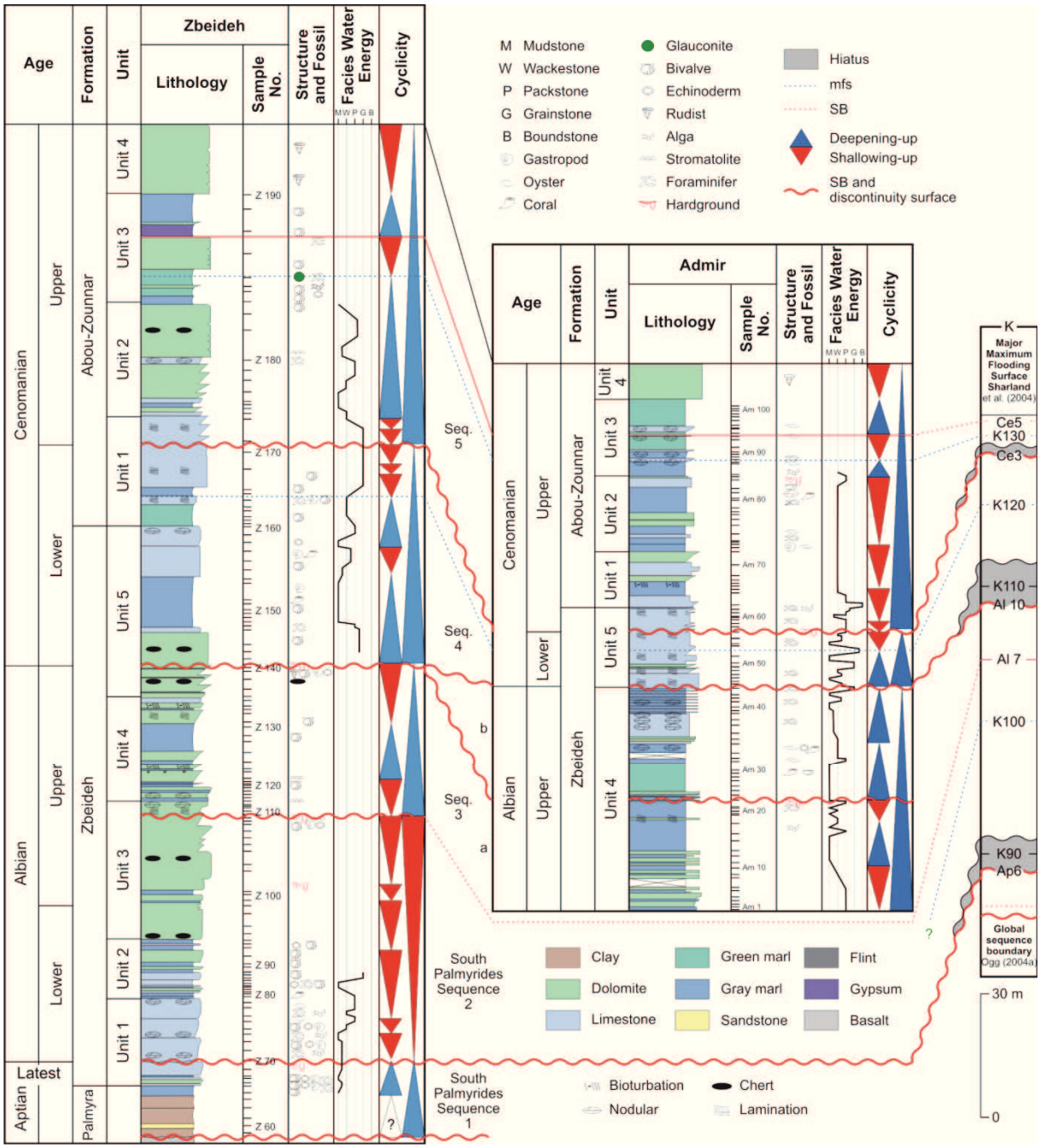

Figure VIII.5.a Correlation of the South Palmyrides sequences 1 to 5 in the Zbeideh and Admir sections with the maximum flooding surfaces of the Arabian Plate (right column, after Sharland et al., 2001; Ogg, 2004a; Haq and Al-Qahtani, 2005).

Palmyra Formation in a fluvial setting, and then the Zbeideh Formation in a marginal-marine environment. South Palmyrides Sequence 1 consists of the Palmyra Formation and the lowermost Zbeideh Formation, which contains thin marly limestones with planktonic and benthonic foraminifera of latest Aptian age. Early Albian MFS K90

(Sharland et al., 2004) was not confirmed in the South Palmyrides because of the absence of the *Hedbergella planispira* zone (Figures VIII.4.1.a and VIII.5.a).

VIII.5.2 South Palmyrides Sequence 2 (around MFS K100)

The sequence boundary between sequences 1 and 2 is a hardground and unconformity/hiatus as evident by the missing *Hedbergella planispira* zone (Figures VIII.4.1.a and VIII.5.a). South Palmyrides Sequence 2 represents the lower part of the Zbeideh Formation in the Zbeideh Section. It is composed of six shallowing-up subcycles (Figure VIII.5.a). The basal two subcycles are nodular mudstones/ wackestones with green algae, orbitolinids and planktonic foraminifera. The third subcycle consists of packstones with echinoderms, bivalves and gastropoda. The upper three subcycles are characterized by thinning-up stacking patterns from massive to laminated dolomite with chert nodules at the base (Figure VIII.5.a).

Two shallow-water depositional settings are interpreted for the six shallowing-up subcycles of Sequence 2: the first three subcycles represent peritidal sediments, while the upper three subcycles are formed in shallow subtidal to supratidal environments.

The lower sequence boundary of Sequence 2 may correlate with the Late Aptian global sequence boundary SB AP6 of Ogg (2004a). A clear correlation of the Middle Albian MFS K100 of Sharland et al. (2004) with the shallow shelf limestones and dolomites of the Zbeideh Formation is hampered by their gross stratigraphic attribution within the *Mesorbitolina subconcava* zone.

VIII.5.3 South Palmyrides Sequence 3 (below MFS K110)

The sequence boundary between sequences 2 and 3 is a hardground within dolomites of the Zbeideh Formation of the Zbeideh Section. A similar hardground is missing in the Admir Section. However, the lower part of Sequence 3 is evidenced here by Upper Albian foraminifera (*Neoiraqia convexa*, *T. praeticinensis*). Therefore, we assume the lower boundary of Sequence 3 directly below the exposed part of the Admir Section (Figure VIII.5.a).

The Upper Albian South Palmyrides Sequence 3 (divided into 3a and 3b) corresponds to the middle part of the Zbeideh Formation. It reflects a deepening-upwards cycle

composed of three subcycles in both the Admir and Zbeideh sections (Figure VIII.5.a). The basal subcycle shows a shallowing-up trend from restricted subtidal facies (bioclastic wackestone, peloidal pack-grainstone) to intertidal facies (laminated, stromatolites, dolo-mudstone). It is overlain by a deepening-up subcycle characterized by increasing diversity that reflects a local subcylic flooding surface on top of algal mound facies of the Admir Section. At the top of Sequence 3 a conspicuous fall of the sea level is evidenced by a hardground surface in both sections (Figure VIII.5.a).

The middle part of the Zbeideh Formation of the Admir Section is composed of marly limestones with oysters, corals, echinoderms and of nodular limestones with planktonic foraminifera (Sequence 3b). Equivalent deposits are missing in the neighbouring Zbeideh Section. We therefore assume that the top of Sequence 3a (Zbeideh Section) was accompanied by erosion and/or amalgamation of synchronous Admir deposits of Sequence 3b (Figure VIII.5.a).

The Upper Albian global sequence boundary Al7 of Ogg (2004a) is comparable to the lower boundary of Sequence 3. The Late Albian MFS K110 (Sharland et al., 2004) could not be identified in the South Palmyrides because of a major hiatus that spans the *Rotalipora appenninica* zone (Figures VIII.4.1.a and VIII.5.a).

VIII.5.4 South Palmyrides Sequence 4 (including MFS K120)

Sequence 4 corresponds to the uppermost Zbeideh Formation and the lowermost Abou-Zounnar Formation in the Zbeideh Section, and to the uppermost Zbeideh Formation of the Admir Section.

The base of the Lower Cenomanian South Palmyrides Sequence 4 coincides with the Albian/ Cenomanian hiatus (Figure VIII.4.1.a). It may correlate with the Late Albian SB Al10 of Ogg (2004a) (Figure VIII.5.a). The sequence is composed of two deepening-upwards subcycles overlain by three shallowing-upwards subcycles in the Zbeideh Section. In the Admir Section, the sequence consists of only one deepening-upwards and one shallowing-upwards subcycle (Figure VIII.5.a).

The deepening-upwards subcycles of both sections are composed of well-bedded to laminated, fine-grained limestones (wackestone to packstone, rich in heavily micritized large benthonic foraminifera), serpulids and large bivalves. The overlying shallowing-

upwards subcycle(s) contain mainly wackestones with trocholinids and boundstones (red algae). In addition, bioturbated mudstones and wackestones occur, with shallow water benthonic foraminifera (praealveolinids, *Cuneolina*, nezazzatids), rare gastropods and bivalves.

The deepening-upwards cycle(s) are interpreted to represent mainly open-marine shallow subtidal environments, the shallowing-upwards cycle(s) are attributed to open lagoonal environments. The lower number of subcycles in the Admir Section is possibly due to lower sedimentation rates.

The Lower Cenomanian MFS K120 of Sharland et al. (2004) corresponds to laminated fossiliferous limestones of the upper *R. globotruncanoides* zone of the Admir Section (Figures VIII.4.1.a and VIII.5.a). A correlation with laminated limestones of the Zbeideh Section is mainly based on comparisons of the stacking patterns.

VIII.5.5 South Palmyrides Sequence 5 (including MFS K130)

The lower boundary of the Upper Cenomanian South Palmyrides Sequence 5 in the Admir Section is represented by a hardground surface (Figure VIII.6.b), associated with a hiatus spanning the *Rotalipora reicheli* zone. This boundary is comparable to the Middle Cenomanian SB Ce3 of Ogg (2004a).

Sequence 5 corresponds to the uppermost Zbeideh to Abou-Zounnar formations of the Admir Section, and to the Abou-Zounnar Formation in the Zbeideh Section. Sequence 5 is composed of thin to massive nodular white dolomites and limestones with few corals, bivalves, gastropods and ostracods. Green and gray marls above with abundant oysters and intercalated thin pelagic limestones are overlain by gypsum-rich marls in the Zbeideh Section. Massive dolomites (unit 4) of both sections contain disarticulated, complete or dissolved rudists (dolomitized bioturbated floatto wackestones) (Figure VIII.5.a).

The general deepening-upwards trend of both the Zbeideh and Admir sections exhibits subcyclic stacking patterns (Figure VIII.5.a): four shallowing-upwards subcycles in the Admir Section correspond to two minor shallowing-upwards subcycles in the Zbeideh Section. Synchronous stacking patterns of two deepening-upwards and two shallowing-upwards subcycles follow above in both sections.

The rapid increase of planktonic foraminifera and glauconite of unit 3 of both sections (*Pseudedomia drorimensis* and *Rotalipora cushmani* biozones) corresponds to MFS K130 (Sharland et al., 2004; Haq and Al-Qahtani, 2005). It coincides in both sections with the boundary between a shallowingupwards and a deepening-upwards subcycle (Figure VIII.5.a). The evaporitic marly interval above (unit 3 of Zbeideh Section) may correspond with the uppermost Cenomanian SB Ce5 of Ogg (2004a), which is represented by another subcyclic boundary in both the Zbeideh and Admir sections (Figure VIII.5.a).

VIII.6 CARBON ISOTOPES

Carbon-isotope records of shallow-water limestones are sensitive to early diagenetic alteration due to subaerial exposure of the seafloor (Joachimski, 1994) and to burial diagenesis. Moreover, the δ13C ratios may be influenced by isotopically light carbon from soil zone CO2 (Allan and Matthews, 1982). Our microfacies interpretations of pure limestones and marls indicate that most isotope data are not influenced by syn-sedimentary soil zone or karstic processes. However, the interaction with diagenetic fluids may have converted the original stable-isotope signature of marine carbonates (compare Parente et al., 2007), as indicated by diagenetic processes of the mixing-zone in both

intervals D1 and D2 of the Admir Section (Figure VIII.6.d). Consequently we excluded ten samples of the D1-interval (negative δ13C values) and 10 samples of the D2-interval (wide fluctuations of δ18O values coinciding with dolomitic intercalations) for further considerations. The adjusted curve (Figure VIII.6.d,b) was used for the comparison of the Late Albian–Late Cenomanian isotopic record of the Palmyrides with age-equivalent strata (Luiciani et al., 2006; Kennedy et al., 2004; Jarvis et al., 2006) (Figures VIII.6.a, VIII.6.c and VIII.6.d).

VIII.6.1 Major Trends of the Carbon-isotope Signature

The carbon-isotope variations of the studied Late Albian–Late Cenomanian interval of the Admir Section (Figures VIII.6.a and VIII.6.c) allows for the biostratigraphic

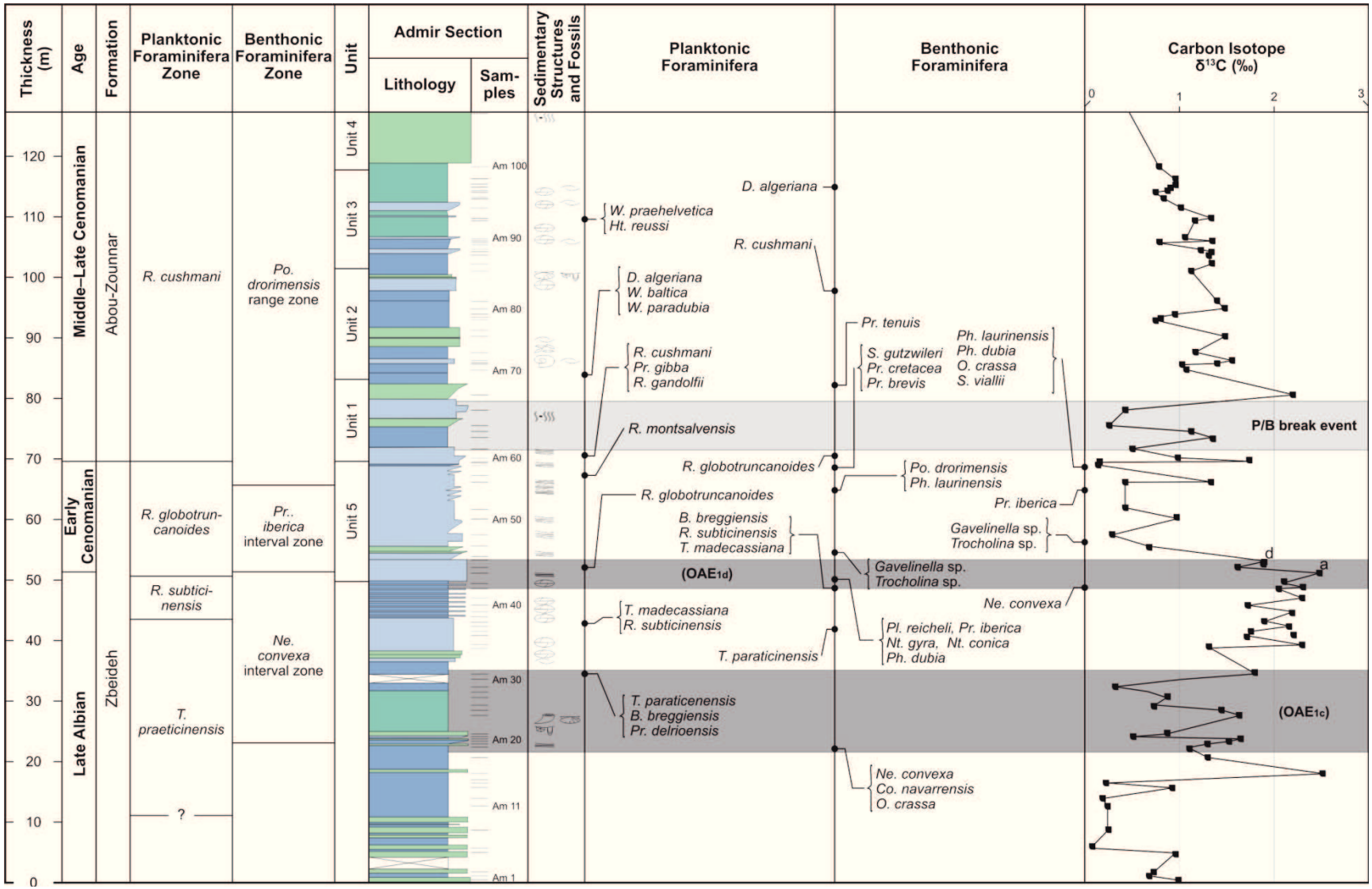

Figure VIII.6.a Biostratigraphy of the Admir Section compared with $\delta^{13}C$ fluctuations (stippled line indicates third average values). Several $\delta^{13}C$ events allow for comparison with those defined by Friedrich (2010), Jarvis et al. (2006), Luiciani et al. (2006), and Kennedy et al. (2004). Compare to Figure 10 for a detailed correlation around the Albian/Cenomanian boundary. For lithological colors see Figure VII.5.a.

Figure VIII.6.b Hardground surface with vertical burrows indicates the Lower Cenomanian discontinuity discontinuity surface Ce3 (section Admir, Figure VIII.5.a).

comparison and calibration of the planktonic and benthonic foraminifera biozonation, and the determination of organic-matter-rich intervals that are correlated with oceanic anoxic events (OAEs). Based on our sequence-stratigraphic interpretations, the δ13C curve was split into three segments South Palmyrides sequences 3, 4, 5, separated by hiatuses (Figure VIII.6.c), and compared with age-equivalent δ13C records documented by Luiciani et al. (2006), Kennedy et al. (2004) and Jarvis et al. (2006).

The early Late Albian record of the Admir Section starts with positive δ13C values and reaches a short maximum of 2.9‰. The following δ13C values of an overlying 12-m-thick unit (Figure VIII.6.c) are well comparable to the age-equivalent OAE1c-interval of the δ13C-curve of Coppa della Nuvola (Luiciani et al., 2006). The similar trend of both early Late Albian curves is evident (Figure VIII.6.c).

During the latest Albian, carbon-isotope values increased and reached nearly constant values of ca. 2.6‰ at the Admir Section. A short decline of δ13C values directly above the LO of *R. subticinensis* was compared with the Breistroffer-Event of the Mount Risou

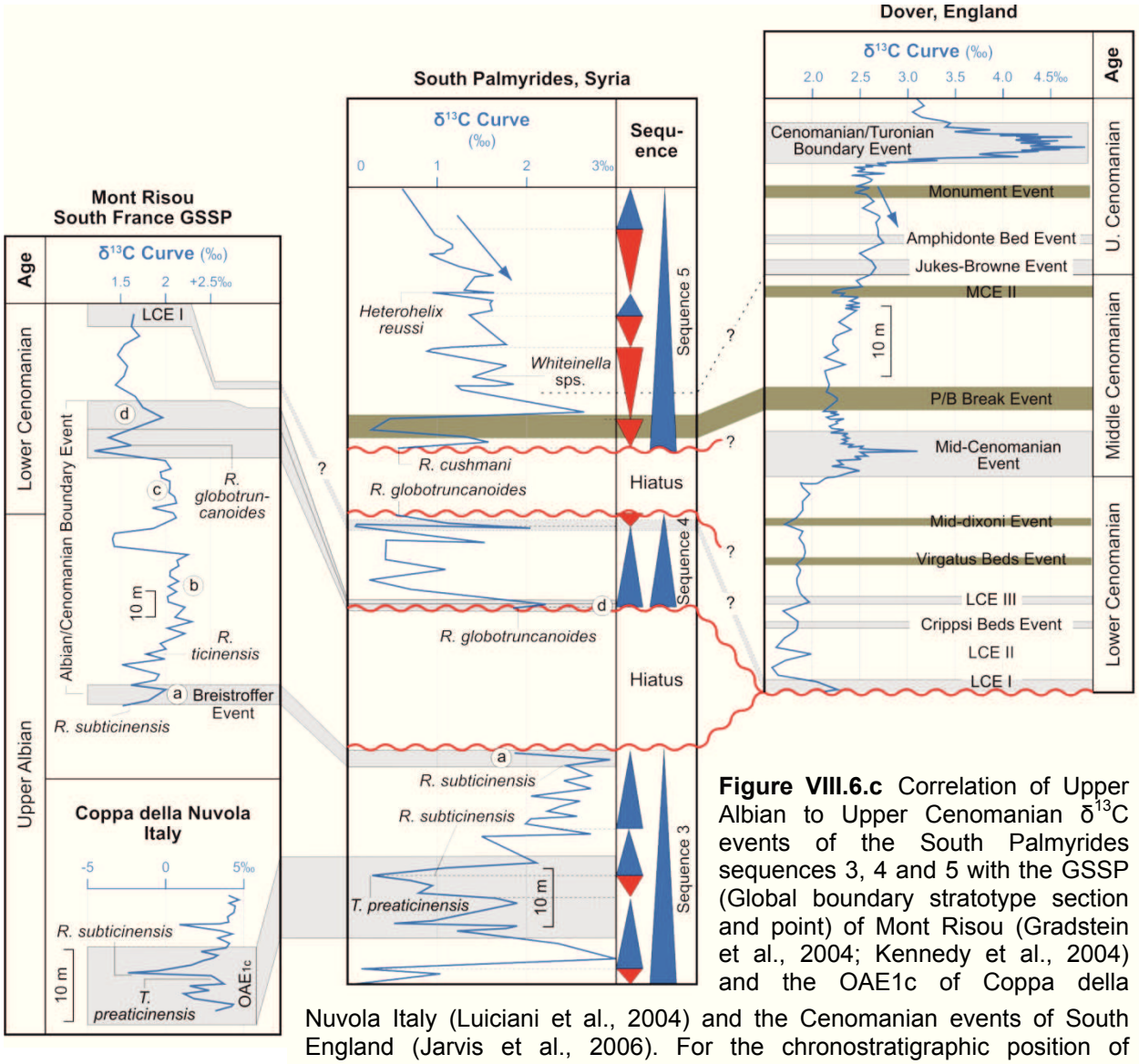

Figure VIII.6.c Correlation of Upper Albian to Upper Cenomanian $\delta^{13}C$ events of the South Palmyrides sequences 3, 4 and 5 with the GSSP (Global boundary stratotype section and point) of Mont Risou (Gradstein et al., 2004; Kennedy et al., 2004) and the OAE1c of Coppa della Nuvola Italy (Luiciani et al., 2004) and the Cenomanian events of South England (Jarvis et al., 2006). For the chronostratigraphic position of Palmyrides section Am, compare Figures 4, 7 and 8.

Section (Kennedy at al., 2004), corresponding to peak a (Figure VIII.6.c). The Albian/Cenomanian boundary at Mount Risou spans a broad positive excursion (subdivided into four discrete peaks a to d). Comparable strata are nearly completely missing at the Admir Section, due to a major hiatus. Here, the Lower Cenomanian strata record δ13C values that may correlate with peak d of Kennedy et al. (2004), confirmed by *R. globotruncanoides* (Figure VIII.4.1.a). The overlying sediments of South Palmyrides Sequence 4 correlate with a thin Lower Cenomanian interval that is topped by a thin positive excursion of δ13C-values, probably equivalent to LCE I of Jarvis et al.

(2006) (Figure VIII.6.c).Following a major hiatus (*R. reicheli* biozone) the third segment of the δ13C curve of the Admir Section spans Middle to Upper Cenomanian interval (South Palmyrides Sequence 5 – Figure VIII.6.c). Compared to Jarvis et al. (2006), the δ13C-values of the Palmyrides show several discrepancies, probably due to diagenetic overprint (Figure VIII.6.c).

VIII.6.2 Oceanic Anoxic Event 1c, Albian/Cenomanian Boundary and Planktonic/Benthonic Break Event

The δ13C curve of the Admir Section was calibrated with biostratigraphic results (based on benthonic and planktonic foraminifera) of the Late Albian to Late Cenomanian succession. Significant perturbations of the foraminiferal diversity, abundance or their total absence are compared with δ13C-values to highlight the Late Abian to Late Cenomanian biotic events and possible equivalents of Oceanic Anoxic Events (OAE) (Jarvis et al., 1988, 2006; Luciani et al., 2004, 2006; Friedrich, 2010).

VIII.6.2.1 OAE1c Event

The lower Upper Albian δ13C values of the Admir Section are generally comparable to those of the Nuvola in Italy (Luciani et al., 2004, 2006). The lower Upper Albian δ13C values of South Italy fall to -2.6‰ and rise to values between 0.8‰ to 2‰ in the upper *T. praeticinensis* to the lowermost *R. subticinensis* zones (Luciani et al., 2006). In the Admir Section the δ13C values remain within the range 0.1‰ to 2.3‰ in the same biostratigraphic interval. The OAE1c Event is marked by the LO of *T. praeticinensis* and the FO of *R. subticinensis*, and the associated planktonic foraminifera of this biozone (Figure VIII.6.c).

VIII.6.2.2 Albian/Cenomanian Boundary Event (Wilson and Norris, 2001; Kennedy et al., 2004; Friedrich, 2010)

Although most parts of the Albian/Cenomanian Boundary Event are missing in the South Palmyrides (hiatus), its lower boundary (Peak a: Breistroffer event, Figure VIII.6.c)

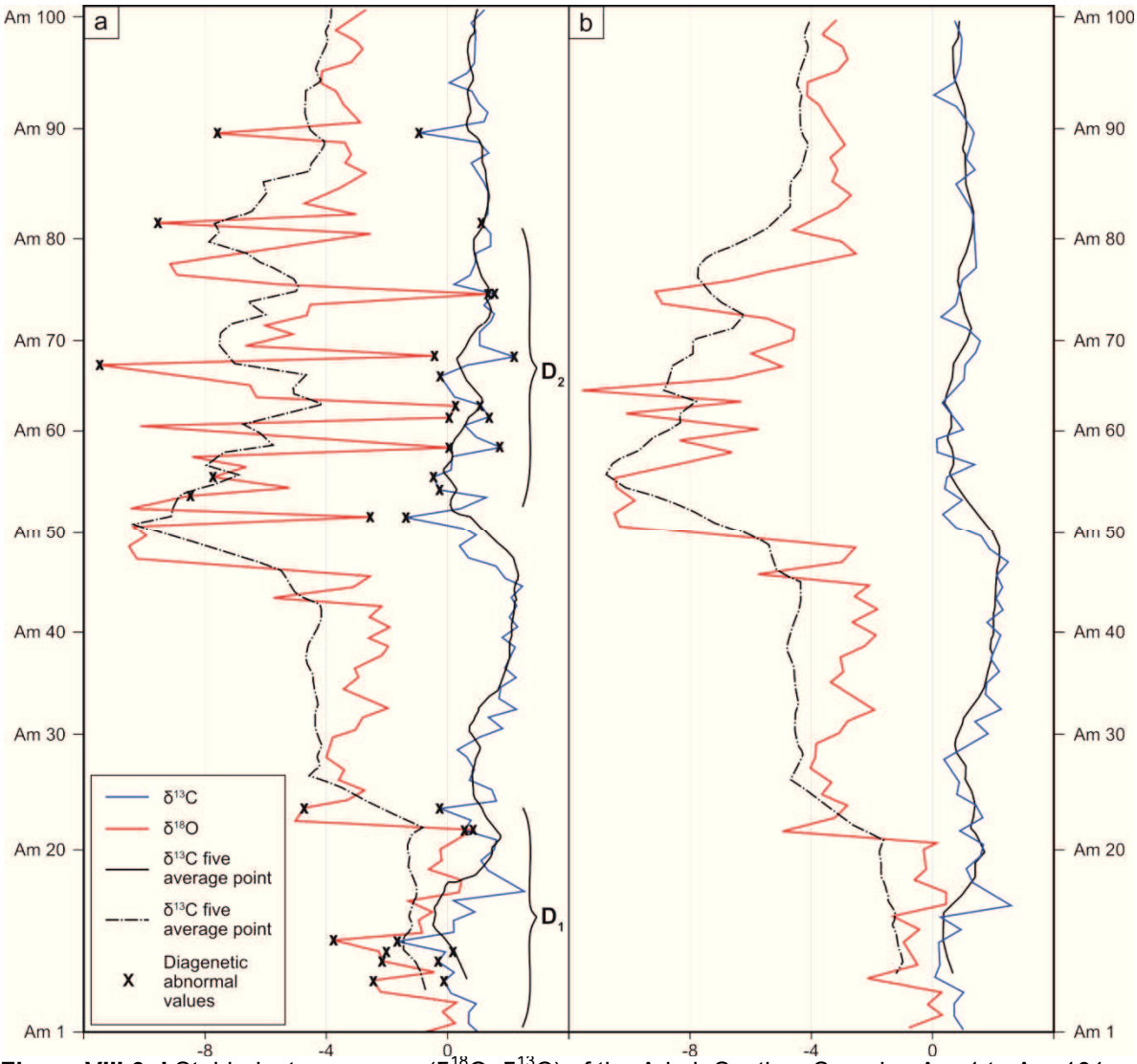

Figure VIII.6.d Stable-isotope curves ($\delta^{18}O$, $\delta^{13}C$) of the Admir Section. Samples Am-1 to Am-101 refer to Figure VIII.5.a.
(a) Measured δ18O between (1‰ and -10‰) and $\delta^{13}C$ (between ca. 3‰ and -2.7‰). D1 and D2 correspond to meteoric and subaerial diagenetic intervals.
(b) $\delta^{18}O$ and $\delta^{13}C$ curves after excluding 10 high negative $\delta^{13}C$ values and 10 extreme widely fluctuating $\delta^{18}O$ values, marked with X in (a). The curve $\delta^{13}C$ of (b) was used in Figures 5 and 10.

and its upper boundary (Peak d, Figure VIII.6.c) are biostratigraphically confirmed. Therefore it is possible to discuss the correlation of carbon-isotope values.

The carbon-isotope curve shows maximum values of 2.3‰ to 2.7‰ within a 5-m-thick interval near the Albian/Cenomanian boundary (Admir Section, Figures VIII.4.1.a and VIII.6.c). These values demonstrate two peaks (lettered a and d, Figure VIII.6.c) that occur within marly limestones intercalating with nodular limestones (Peak a),

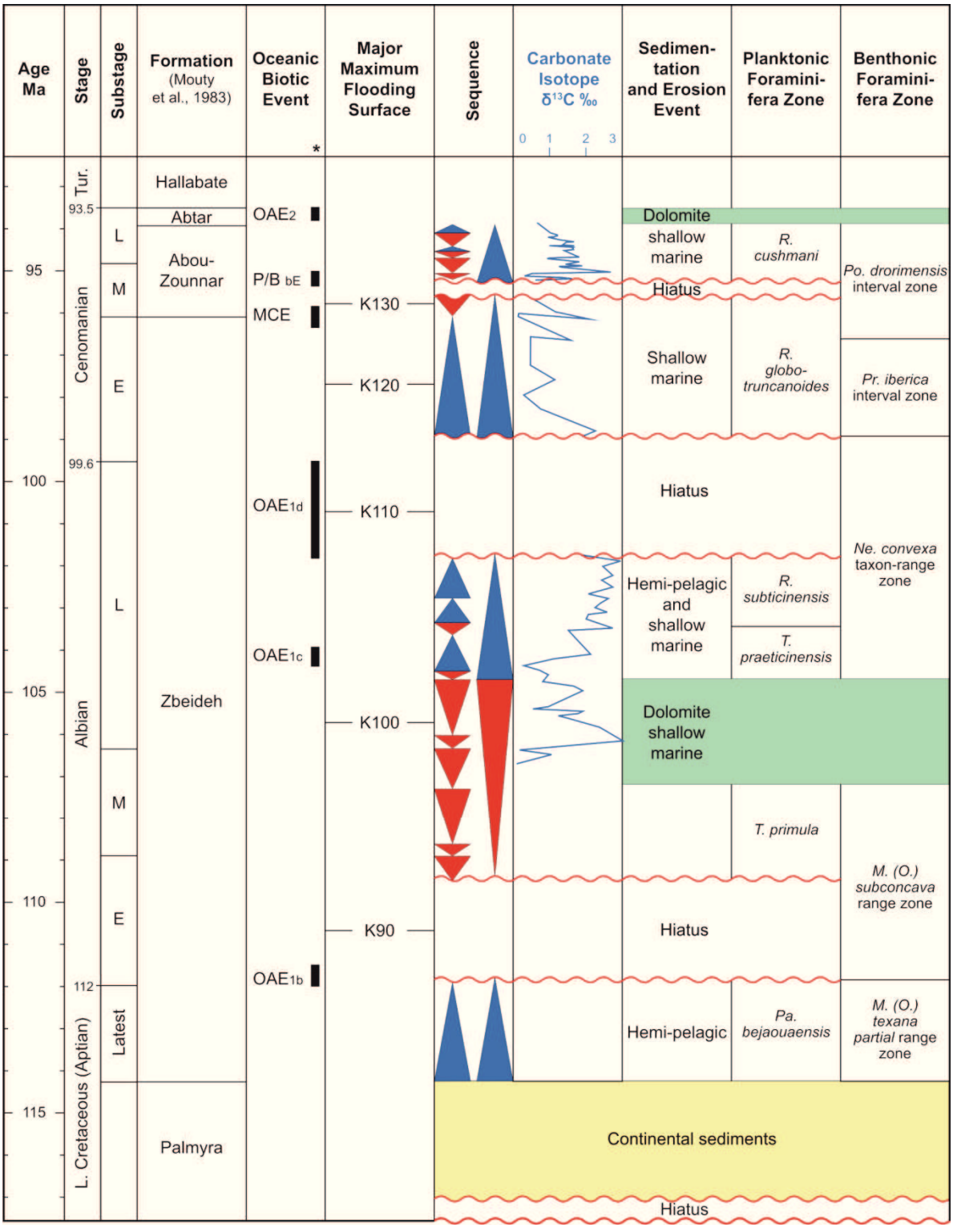

Figure VIII.6.e Summary of major stratigraphic events, including sequence-stratigraphic interpretation, of the Lower to middle Cretaceous succession in the South Palmyrides. * = Friedrich, 2010; Jarvis et al., 2006; Lucia et al., 2004.

unconformably overlain by massive limestones (Peak d) of the Admir Section (Figures VIII.4.1.a and VIII.6.c). Peaks a and d are comparable with two of the four minor peaks (a
to d) defined around the Albian/Cenomanian boundary of Mont Risou (GSSP section; Kennedy et al., 2004, compare Figure VIII.6.c). The correlation between the South Palmyrides δ13C curve and that from Mont Risou (with respect to the Albian/Cenomanian boundary, Figure VIII.6.c) is based on our new biostratigraphic data around the Late Albian hiatus (Figure VIII.3. b) combined with the new δ13C variations of the Admir Section. The following arguments favor the correlation: Peak d coincides with the first event (Breistroffer event), determined by the LO of *R. subticinensis*. In the Admir Section, however, a gap is registered between LO of *R. subticinensis* and the FO of *R. globotruncanoides* (based on the missing of both biozones *R. ticinensis* and *R. appenninica*), equivalent to the postulated hiatus in the South Palmyrides carbonate platform.

VIII.6.2.3 Planktonic/Benthonic (P/B) Break Event

This event is explained by a dramatic increase of both diversity and abundance of the planktonic foraminifera (see description of the *Rotalipora cushmani* zone above; Figures VIII.3.b and VIII.4.1.a). The δ13C signature of this bio-event is represented by falling δ13C values (0.3‰), contrasting to a slight increase recorded by Jarvis et al. (2006; Figures VIII.4.1.a and VIII.6.c). At this level the abundance of the planktonic foraminifera has been used as a marker; moreover, this interval is characterized by the FO of *R. cushmani* (compare Jarvis et al., 2006).

VIII.6.2.4 The characteristic of Upper Cenomanian δ13Ccarb

The Upper Cenomanian δ13C curve of the Admir Section ranges between 1.2‰ and 1.5‰. The correlation with Jarvis et al. (2006) suggests that the base of the Upper Cenomanian of the South Palmyrides is defined very close to the FO of the genus *Whiteinella.* In addition, the Amphidonte Bed Event is stratigraphically comparable with the FO of *Heterohelix reussi* (Ogg, 2004a) (Figure VIII.6.c). The carbon-isotope excursion of the Tethys realm of Jarvis et al. (2006) and the South Palmyrides has

similar decreasing of δ13C above the Amphidonte Bed Event (Ogg, 2004a; Jarvis et al., 2006) (Figure VIII.6.c).

VIII.7 CONCLUSIONS

Detailed stratigraphic studies on limestones were conducted in two sections from the shallow carbonate platform of the South Palmyrides, Syria. They allowed us to reconstruct the uppermost Aptian to Upper Cenomanian framework, based on planktonic foraminiferal biostratigraphy (Ogg, 2004a, b; Premoli Silva and Verga, 2004), benthonic foraminiferal biostratigraphy (Velić,2007; Schroeder et al., 2010), and δ13C fluctuations (Kennedy et al., 2004; Jarvis et al., 2006). New biostratigraphic data was used to correlate global biotic and abiotic events with local events of the South Palmyrides: OAE1c, Albian/Cenomanian boundary, and Planktonic/Benthonic break.

Missing planktonic and benthonic biozones and thick dolomitic intervals were used to define four major stratigraphic hiatuses: The Early Albian hiatus of the *Mucrohedbergella planispria* biozone; the Late/Middle Albian dolomitic hiatus, the Late Albian/Early Cenomanian hiatus spanning the *Rotalipora ticinensis* and *R. appenninca* biozones, and the Mid Cenomanian hiatus of the *Rotalipora reicheli* biozone.

With the recovery of hemipelagic conditions in the South Palmyrides Basin during latest Aptian, the continuous marine succession (latest Aptian to Late Cenomanian) reflects two main episodes of maximum sea-level rise comparable with the maximum flooding surfaces MFS K120 and MFS K130 of the Arabian Plate (Sharland et al., 2004). Major hiatuses and hardgrounds were interpreted as sequence boundaries of five local sequences, South Palmyrides sequences 1 to 5, which stratigraphically correspond with some of the third-order global sequences of Ogg (2004a).

VIII.8 ACKNOWLEDGEMENTS

We are indebted to Ahmed A.M. Abd El-Naby, Geology Department, Ain Shams University (Egypt) for his help and Christian Scheibner, Geochronology Department, Bremen University (Germany) for his support. We would like to extend our special thanks to our colleagues of the Geochronology working group in Bremen University for various help. We thank GeoArabia's three anonymous reviewers for their helpful comments, Arnold Egdane for designing the paper for press, and Kathy Breining for proof-reading it.

VIII.9 REFERENCES

Allan, J.R. and R.K. Matthews 1982. Isotope signatures associated with early meteoric diagenesis. Sedimentology, v. 29, p. 797-817.

Al-Maleh, A.KH. M. Mouty, T. Sawaf, G. Brew and M. Barazangi 2000. Mesozoic depositional trends in the northern Arabian Platform in Syria; regional and tectonic implications. GeoArabia, v. 5, no. 1, p. 30-31.

Boudagher-Fadel, M.K. 2008. Evolution and Geological Significant of Lager Benthic Foraminifera, Developments in Paleontology and Stratigraphy. Elsevier, Amsterdam, 544 p.

Caron, M. 1985. Cretaceous planktic foraminifera. In H.M. Bolli, J.B. Saunders and K. Perch-Nielsen (Eds.), Plankton Stratigraphy. Cambridge University Press, p. 17-86.

Ferry, S., Y. Merran, D. Grosheny and M. Mroueh 2007. The Cretaceous of Lebanon in the Middle East (Levant) context [Le Crétacé du Liban dans le cadre du Moyen-Orient (Levant)]. Carnets de Géologie, p. 38-42.

Friedrich, O. 2010. Benthic foraminifera and their role to decipher paleoenvironment during mid-Cretaceous Oceanic Anoxic Events – the “anoxic benthic foraminifera” paradox. Revue de Micropaleontologie, v. 53, p. 175-192.

Gale, A.S., W.J. Kennedy, J.A. Burett, M. Caron and B.E. Kidd 1996. The Late Albian to Early Cenomanian succession at Mont Risou near Rosans (Drome, SE France): An integrated study (ammonites, inoceramids, planktonic foraminifera, nannofossils, oxygen and carbon isotopes).Cretaceous Research, v. 17, p. 515-606.

Gradstein, F.M., J.G. Ogg and A.G. Smith 2004. A Geologic Time Scale 2004. Cambridge UniversityPress, 589 p.

Haq, B.U. and A.M. Al-Qahtani 2005. Phanerozoic cycles of sea-level change on the Arabian Platform. GeoArabia, v. 10, no. 2, p.127-160.

Homberg, C. and M. Bachmann 2010. Evolution of the Levant margin and western Arabian Platform since the Mesozoic: Introduction. Geological Society, London, v. 341, p. 1-8.

Jarvis, I., G.A. Carson, M.K. Cooper, M.B. Hart, P.N. Leary, B.A. Tocher, D. Horne and A. Rosenfeld 1988. Microfossil assemblages and the Cenomanian-Turonian (late Cretaceous) oceanic anoxic event. Cretaceous Research, v. 9, p. 3-103.

Jarvis, I., A.S. Gale, H.C. Jenkyns and M.A. Pearce 2006. Secular variation in Late Cretaceous carbon isotopes: A new δ13C carbonate reference curve for the Cenomanian–Campanian (99.6–70.6 Ma). Geological Magazine, v. 143, p. 561-608.

Joachimski, M.M. 1994. Subaerial exposure and deposition of shallowing upward sequences: Evidence from stable isotopes of Purbeckian peritidal carbonates (basal Cretaceous), Swiss and French Jura Mountains. Sedimentology, v. 41, p. 805-824.

Kennedy, W.J., A.S. Gale, J.A. Lees and M. Caron 2004. The global boundary stratotype section and point (GSSP) for the base of the Cenomanian Stage, Mont Risou, Hautes-Alpes, France. Episodes, v. 27, no.1, p. 21-32.

Krasheninnikov, V.A., J.K. Hall, F. Hirsch, C. Benjamini and A. Flexer (Eds.) 2005. Geological framework of the Levant, Volume I: Cyprus and Syria, p. 165-416.

Kuss, J., A. Bassiouni, J. Bauer, M. Bachmann, A. Marzouk, C. Scheibner and F. Schulze 2003. Cretaceous – Paleogene Sequence Stratigraphy of the Levant Platform (Egypt, Sinai, Jordan). In E. Gili, H. Negra and P. Skelton (Eds.), North African Cretaceous Carbonate Platform Systems. Nato Science Series, p. 171-187.

Loeblich, A.R. and H. Tappan 1988. Foraminiferal genera and their classification. Van Nostrand Reinhold Co., New York, 970 p.

Luiciani, V., M. Cobianchi and H.C. Jenkyns 2004. Albian high-resolution biostratigraphy and isotope stratigraphy: The Coppa della Nuvola pelagic succession of the Gargano Promontory (Southern Italy). Eclogae Geologicae Helvetiaev, 97, p. 77-92.

Luiciani, V., M. Cobianchi and C. Lupi 2006. Regional record of a global oceanic anoxic event: OAE1a on the Apulia Platform margin, Gargano Promontory, southern Italy. Cretaceous research, v. 27, p. 754-772.

Mouty, M. 1997. Le Jurassique de la chaîne des Palmyrides, Syrie centrale. Bulletin of the French Geological Society, France, v. 168, no. 2, p. 181-186.

Mouty, M., A.KH. Al-Maleh, H. Abou-Laban and Y. Al-Joubeli 1983. The geological study of the Palmyridean chain through typical geological sections. The General Establishment of Geology and Mineral Resources. C No. 140/NA.

Mouty, M., M. Delaloye, D. Fontignie O. Piskin and J.-J. Wagner 1992. The volcanic activity in Syria and Lebanon between Jurassic and Actual. Schweizerische Mineralogsche und Petrographische Mitteilungen, v. 72, no. 1, p. 91-105.

Mouty, M., A.KH. Al-Maleh and H. Abou-Laban 2002. Le Crétacé moyen la chaîne des Palmyrides (Syrie centrale). Geodiversitas, Paris, v. 25, p. 429-443.

Ogg, J.G. 2004a. Mid- Late Cretaceous Charts. http://norges.uio.no/timescale/Late_Cretaceous.pdf and, http://norges.uio.no/timescale/Early_Cretaceous.pdf.

Ogg, J.G. 2004b. Mid- Late Cretaceous Charts. In F.M. Gradstein, J.G. Ogg and A.G. Smith (Eds.), A Geologic Time Scale 2004. Cambridge University Press, p.589

Parente, M., G. Frijia and M. Dilucia 2007. Carbon-isotope stratigraphy of Cenomanian–Turonian platform carbonates from the southern Apennines (Italy): A chemostratigraphic approach to the problem of correlation between shallow-water and deep-water successions. Journal of the Geological Society, London, v. 164, p. 609-620.

Ponikarov, V.P., V.G. Kazmin, I.A. Mikhailov, A.V. Razvaliayev, V.A. Krasheninnikov, V.V. Kozlov, E.D. Soulidi-Kondtatiyev and V.A. Faradzhev 1966. The Geological map of Syria. 1:1,000,000. Explanatory Notes. Technoexport, USSR, 111 p.

Premoli Silva, I. and D. Verga 2004. Practical manual of Cretaceous planktonic foraminifera. In D. Verga, R. Rettori (Eds.), International School on Planktonic Foraminifera: Perugia, Italy, Tipografia Ponte Felcino, Universities of Perugia and Milan, 3rd Course, 283 p.

Premoli Silva, I., M. Le Caron, R.M. Leckie, M.R. Petrizzo, D. Soldan and D. Verga 2009. Paraticinella Gen and Taxonomic Revision of Ticinella Bejaouaensis Sigal 1966. Journal of Foraminiferal Research, v. 39, no. 2, p.126-137.

Schroeder, R. and M. Neumann 1985. Les grands foraminifères du Crétacé moyen de la region Méditerranéenne. Geobios, Mémoire Spécial 7, p. 1-160.

Schroeder, R., F.S.P. van Buchem, A. Cherchi, D. Baghbani, B. Vincent, A. Immenhauser and B. Granier 2010. Revised orbitolinid biostratigraphic zonation for the Barremian – Aptian of the eastern Arabian Plate and implications for regional stratigraphic correlations. In F.S.P. van Buchem, M.I. Al-Husseini, F. Maurer and H.J. Droste. Barremian – Aptian Stratigraphy and Hydrocarbon Habitat of the Eastern Arabian Plate. GeoArabia Special Publication 4, Gulf PetroLink, Bahrain, v. 1, p. 49-96.

Sharland, P.R., R. Archer D.M. Casey, R.B. Davies, S.H. Hall, A.P. Heward, A.D. Horbury and M.D. Simmons 2001. Arabian Plate sequence stratigraphy. GeoArabia Special Publication 2, Gulf PetroLink, Bahrain, 371 p., with 3 charts. Sharland, P.R., D.M. Casey, R.B. Davies, M.D. Simmons and O.E. Sutcliffe 2004. Arabian Plate Sequence Stratigraphy. GeoArabia, v. 9, no. 1, p. 199-214.

Sigal, J. 1966. Contribution a` une monographie des Rosalines. 1. Le genre Ticinella Reichel, souche des Rotalipores. Eclogae Geologicae Helvetiae, v. 59, p. 186-217.

Stampfli, G.M., J. Mosar, P. Favre, A. Pillevuit and J.-C. Vannay 2001. Permo-Mesozoic evolution of the western Tethyan realm: The Neotethys/East-Mediterranean connection. In P.A. Ziegler, W. Cavazza, A.H.F. Robertson and S. Crasquin-Soleau (Eds.), Peritethys, Memoir 6: Peritethyan Rift/Wrench Basins and Passive Margins, IGCP 369. Memorial Museum of Natural History, v. 186, p. 51-108.

Velić, I. 2007. Stratigraphy and palaeobiogeography of Mesozoic benthic foraminifera of the karst dinarides (SE Europe). Geologia Croatica, v. 60, no. 1, p. 1-113.

Wilson, P.A. and R.D. Norris 2001. Warm tropical ocean surface and global anoxic during the mid- Cretaceous period. Nature, v. 412, p. 425-429.

The third manuscript

IX. STRATIGRAPHIC CONTROL OF THE APTIAN - EARLY TURONIAN SEQUENCES OF THE LEVANT PLATFORM (NORTHWEST SYRIA - COASTAL RANGE)

Hussam Ghanem[1], Jochen Kuss[1]

[1]Department of Geosciences, University of Bremen – FB 5, Bibliothekstrasse 1, D-28344 Bremen

Submitted to GeoArabia (June, 2012)

IX STRATIGRAPHIC CONTROL OF THE APTIAN - EARLY TURONIAN SEQUENCES OF THE LEVANT PLATFORM (NORTHWEST SYRIA - COASTAL RANGE)

ABSTRACT The predominant carbonatic Aptian – Early Turonian succession of the Costal Range (northwest Syria) represents the Northern edge of the Levant Platform and was subdivided into 28 lithostratigraphic units, mainly reflecting shallowing-up and deepening-up intervals. We applied a combined approach of litho-, bio-, and carbon-isotope stratigraphy with facies interpretations to establish a sequence stratigraphic framework, adapted from outcrop data along two transects. The sequence stratigraphic evolution records major transgressions/regressions and hiati that are compared with regional sequences of the Arabian and Levant platforms and of the Tethyan realm. The age control based on planktonic/benthonic foraminifera and ammonite biostratigraphies is relatively good, despite changing diversities and occurrences. It builds on eight benthonic foraminiferal biozones (Aptian to Early Turonian) and seven planktonic foraminiferal biozones (latest Albian to Cenomanian). The studied carbon isotope fluctuations record significant perturbations that are well comparable with several global changes of the carbon cycle: OAE1d, LCE I-III, MCE, and OAE2. A combined chemostratigraphic and biostratigraphic approach allows for correlating the carbon isotope curve of the Coastal Range with those from the Tethyan Realm, England, and South Palmyrides.

IX.1 INTRODUCTION

In this study we present sequence stratigraphic interpretations of a relatively monotonous succession of limestones, marls, and dolostones of Aptian-Early Turonian age in northwest Syria, representing the northwestern edge of the Levant Platform. We analyzed the stratigraphic evolution and different depositional settings with respect to regional comparisons of neighboring surface data.

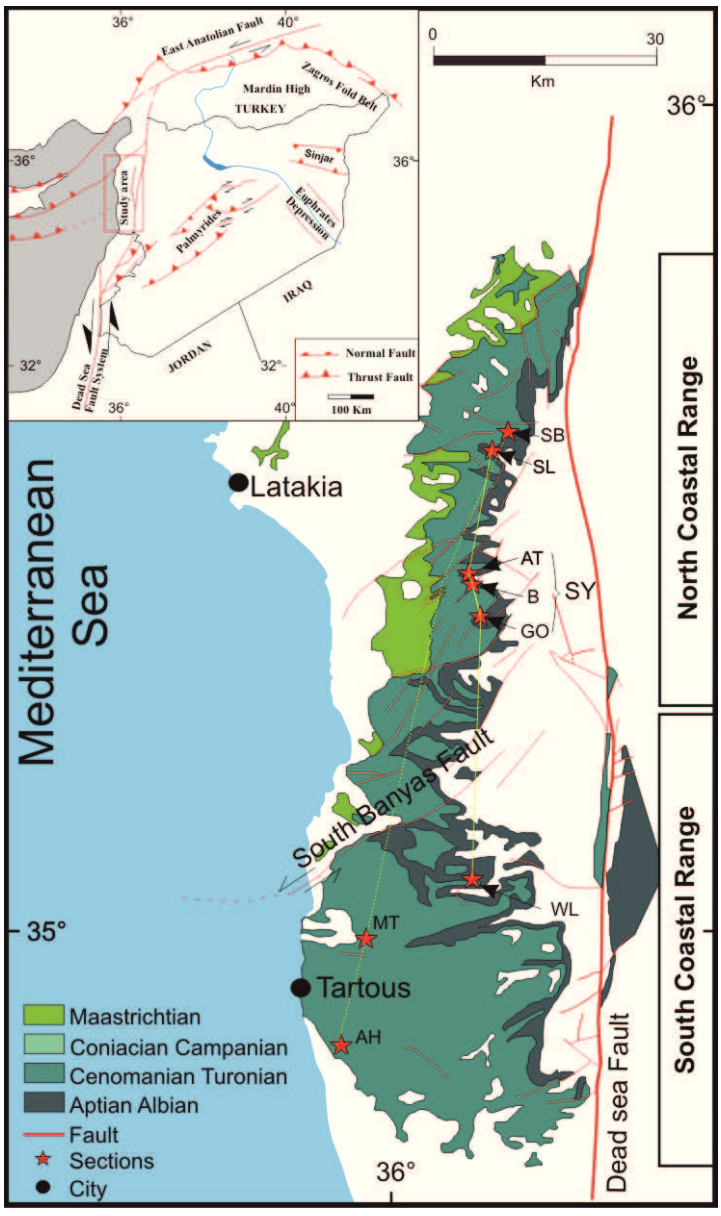

The stratigraphic evolution of the Aptian to Early Turonian carbonate succession of the Coastal Range (CR) of northwest Syria was investigated in six outcrop sections, slopes are cut by the Dead Sea Fault (Mouty and Saint-Marc, 1982; Krasheninnikov et al., 2005). The along two N-S trending transects (Figure IX.1). The western slopes of the CR gradually dip to the west

Figure IX.1: The Cretaceous outcrops of the Coastal Range, showing the locations of the Slenfeh Section (SL) 35°35'74"N 36°12'05"E, the Bab Abdallah Section (SB) 35°37'11"N 36°10'25" E, the Sayno Section (SY) is composed of three subsections; Gobet Al-Berghal (GO) 35°29'23"N and 36°09'50"E, Ain Tina (AT) 35°59'92"N 36°11'62"E Al-Bragh Section (B) 35°32'39"N 36°10'34"E, the Wadi-Layoun Section (WL) 34°59'53"N 36°11'57"E, the Al-Meten Section (MT) 34°59'27"N 35°55'23"E and Wadi Al-Haddah section (AH) 34°49'18"N 35°59'23"E. The yellow line marks transect 1 along sections SL- AT- B- GO- WL (see Figure IX.3.a). The stippled yellow line marks transect 2 along sections SB- MT- AH (see Figure IX.3.b).

in the Mediterranean Sea direction, while its eastern Aptian to Early Turonian succession is characterized by passive continental margin depositional sequences, commonly passing upward into alluvial to carbonate shelf or pelagic ramp settings (Mouty and Saint-Marc, 1982; Alsharhan and Nairn, 1997; Sharland, 2001; Gerdes et al., 2010). The depositional record of the Cretaceous succession of the CR reflects fluctuating environmental conditions regardless of duration and genesis (Immenhauser & Scott 1999). Therefore, the relation between organism's variation and the environmental changes during sedimentation reflect the importance of the geological time control. This is assumed from determining the stratigraphic relationships of the described organisms to establish the biostratigraphic zones (Schroeder et al. 2010). Moreover, the development and understanding of sequence stratigraphy and chemostratigraphyis defined by a rigorous biostratigraphic framework that led to the definition of a new stratigraphic scheme of the CR.

IX.2 METHODS

The study is based on detailed bed-by-bed measuring and sampling of six sections, which crop out along road cuts and two quarries of the CR. The Aptian-Early Turonian deposits comprise a maximum thickness of 360m (Figures 2, 3). In the North CR (north of the South Banyas Fault - Figure IX.1) three sections were measured, spanning an Aptian to Early Turonian succession: Slenfeh (SL), Bab Abdallah (SB) and Sayno (SY); the latter represents a composite section, comprising three subsections: Ain-Tina, Al-Bragh, and Gobet Al-Berghal (Figure IX.1). In the South CR (south of the South Banyas Fault) three sections covered the Aptian to Early Turonian: Wadi Layoun (WL), Al-Meten (MT) and Wadi Al-Haddah (AH, Figure IX.1). Approximately 600 rock samples were collected. Benthonic/planktonic foraminiferal biostratigraphy and microfacies were identified in ca. 400 thinsections, using a standard transmitted light/polarized microscope. The microfacies analysis followed the classification of Dunham (1962) and the standerd microfacies types of Flügel (2004). The biostratigraphic investigations are based on various descriptions of larger benthonic foraminifera: Loeblich and Tappan

(1988), Velić (2007), Boudagher-Fadel (2009), and Schroeder et al. (2010) and of planktonic foramnifera: Verga and Premoli Silva (2002), Premoli Silva and Verga (2004). The biozone concepts used for the Coastal Range were correlated with those from other Tethyan areas proposed by the above-mentioned authors, as well as Ogg et al. (2008). Bulk rock samples (n = 340) for carbon isotope analysis have been collected from sections SL, SB, AH and MT (Late Albian to Turonian). The carbon isotope versus depth plots have been compared with trends derived from published carbon-isotope curves (Paul et al., 1994; Gale et al., 1996; Kennedy et al., 2004; Jarvis et al., 2006; Gertsch et al., 2010).

IX.3 LITHOSTRATIGRAPHY

The Cretaceous succession of the Coastal Range of Syria disconformably overlies Upper Jurassic limestones. In the North CR the following Aptian to Turonian formations were defined by Mouty and Saint-Marc (1982) in ascending order Bab Janneh, Ain-Elbeida, Slenfeh, Bab Abdallah and Aramo Formations and in the South CR Bab Janneh, Blaatah, Slenfeh and Hannafiyah Formations. 28 lithostratigraphic units are proposed for the Aptian- Early Turonian succession of the CR, the reference section for the first 11 units is SY section, for units 12- 19 is SL section and for units 20 to 28 SB section (Figures 2, 3). In the South CR, 17 subunits were defined in the fresh quarries of sections MT and AH (Hannafiyah Fm.), comparable to the upper Slenfeh and Bab Abdallah Formations (units 21- 27 of North CR).

IX.3.1 Bab Janneh Formation (North & South CR)

The Bab Janneh Formation (Aptian) attains a thickness of ca. 65m in the northern part of CR and thins to ca. 20m to the south. Bab Jannah Formation was described by several authors as greenish gray fossiliferous marls with thin limestones and dolomitic interbeds, alternating with grained sandstones (Mouty and Saint-Marc, 1982;

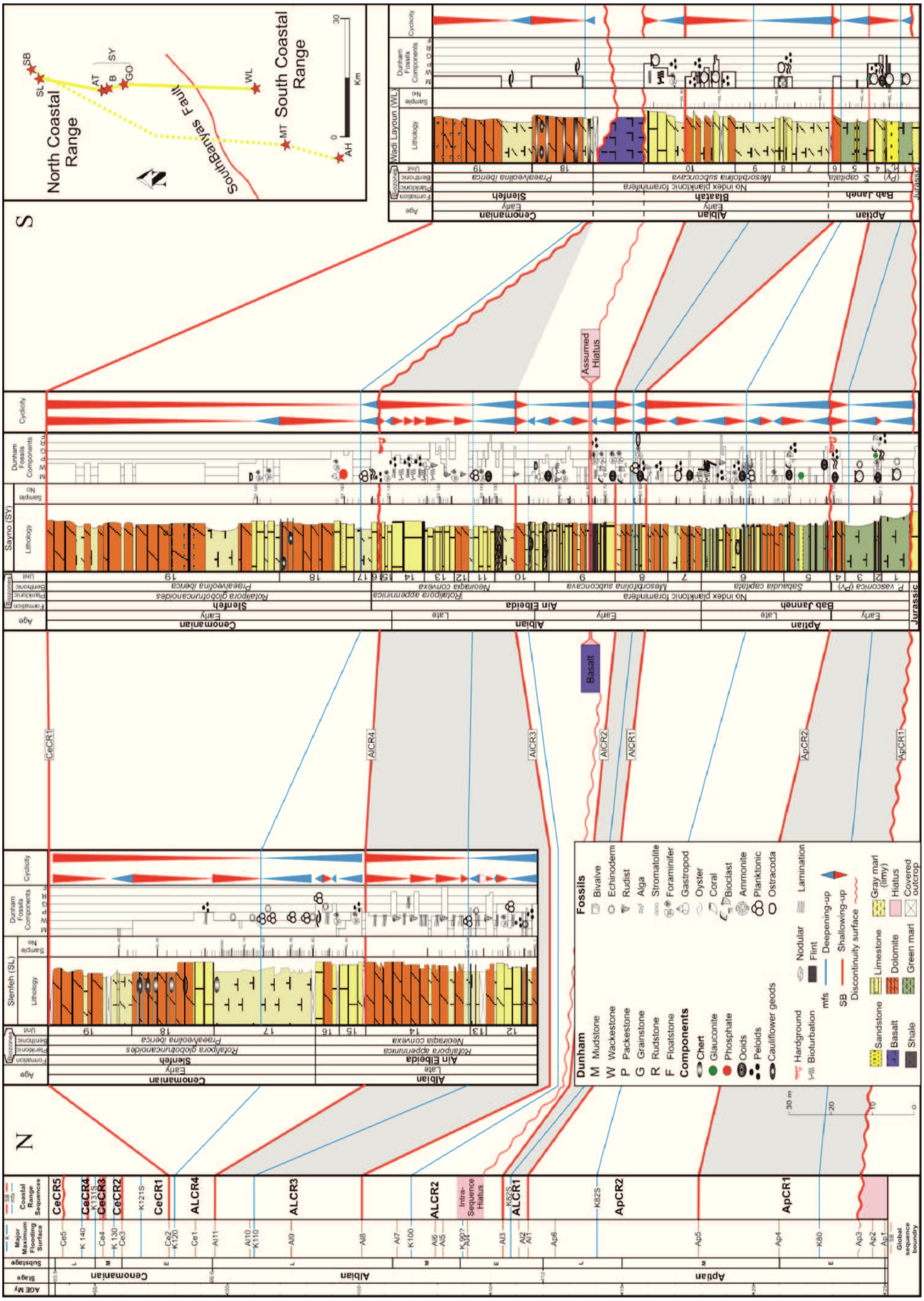
North Coastal Range
South Coastal Range
SouthBanyas Fault
Sayno (SY)
Slenfeh (SL)
Wadi Layoun (WL)
Assumed Hiatus
Basalt
Intra-Sequence Hiatus
N
S

Figure IX.3.a (previous page)- N-S running correlation of the Coastal Range sequences ApCR1 to CeCR4 (red lines) in the Slenfeh, Sayno and Wadi-Layoun sections and maximum flooding surfaces of the Arabian Plate (blue lines); 3rd order global sequence boundaries (Ap1-Ce 5 brown lines) after Hardenbol et al., 1998 harland et al., 2001, 2004; Ogg, 2004a; Haq and Al-Qahtani, 2005).

Krasheninnikov et al., 2005). In this study six lithostratigraphic units were defined from base to top (Figure IX.3.a):

Unit 1 comprises an approximately 7-8m thick succession of greenish-grey marls with rare intercalations of sandstones in the north (SY section) and predominantly thick intercalations of fluvial quartz sandstone in the south (WL section Figure IX.3.c.d). The marls are very rich in bivalves and echinoderms.

Unit 2 This approximately 1-3m thick unit is mainly composed of thin-bedded bioclastic ooidal/peloidal limestones (green algae, benthonic foraminifera, *Lithocodium* sp., ostracods and mollusks) with grain-supported texture in the SY section and intercalated with dolomitic limestones in WL section (Figure IX.3.c.d).

Unit 3 is very similar to unit 1 and composed in SY (North CR) section of 8 m-thick greenish-grey marls rich in mollusks. Thin intercalations of (alluvial) sandstones are present in the WL (South CR) section.

Unit 4 The 3.5m thick unit consists of 20-60cm thick beds of alternating dolomites and limestones. The lower- middle part of unit 4 is composed of algal-, miliolid-, peloidal-, wackestones or packstones, while the upper part is characterized by distinctive fenestral mudstones/wackestones and topped by a hardground. This unit of the North CR is correlated to 4 m of dolomitized limestones (wackestones and packstones with bivalves, green algae, peloids and ooids) in WL section.

Unit 5 is composed of an 11m thick bed of green and gray marls with abundant bivalves, intercalated with thin beds of limestones (mudstones and wackestones with bivalves, gastropods, ostracods and miliolids) and a 70cm thick glouconitic bed in the upper part of SY section (partly similar to the south: WL section).

Unit 6 This 19m thick unit of the SY section is arranged in 30-100cm (average 90cm) thick beds. It comprises lower alternating dolomites and green marls with rare limestones and upper alternating limestones (occasionally nodular) and green marls with benthonic and planktonic foraminifera, ammonites, mollusks, green algae, peloids

and ooids. In section WL section, unit 6 is either amalgamated in the dolostones or partly missing due to late tectonic processes (Figures 2, 4d).

Age: Most previous authors attributed an Aptian age for the Bab Jannah Formation (eg. Mouty and Saint-Marc, 1982; Krasheninnikov et al., 2005) that is confirmed by our data (the Early Aptian *Pseudocyclammina vasconica* range zone and the Late Aptian *Sabaudia capitata* interval zone).

IX.3.2 Ain Elbeida Formation (North CR) and Blaata Formation (South CR)

The Bab Jannah Fm. is conformably overlain by a ca. 75 m-thick succession of limestones, marls and dolostones of the Ain Elbeida Fm. (North CR) and by a ca. 56 m-thick succession of dolomitic marls, dolostones and limestones of the Blaata Fm. (South CR Figure IX.3.a). Previous studies of these formations characterized them as unfossiliferous dolostones, marls and subordinate limestones. Here, both formations were subdivided into 10 units (7- 16 of SY section) and 4 units (7 to 10 of WL section):

Unit 7 of the Ain Elbeida Fm. comprises approximately 8.5m thick brownish-grey bedded dolostones and dolomitized limestones with few intercalations of pure limestones. The latter holds ostracods and ooids. Beds are 10- 140 cm (average 50 cm) thick; only in the lower two beds 8-10cm long burrows occur. This unit correlates with 9m thick dolo-marls of WL section in the eastern edge of South CR.

Unit 8 has **a** total thickness of 13.5m in section SY. It includes several 40-210cm (average 80cm) thick beds of alternating dolostones, marls and fossiliferous white limestones with benthic foraminifera, echinoderms, mollusks, green algae, ooids, peloids, bioclast and algae debris. Packstone/grainstone textures prevail and occur within thicker limestone beds in the middle part of this unit. In section (WL) a 4.5m thick alternation of limestones and dolo-limestones with ostracods, miliolids and green algae occur which are comparable with unit 8 of section SY.

Unit 9 in the North CR is represented by an approximately 15m thick unit that comprises predominantly sparitic limestones (packstones- grainstones). Bed thickness ranges from 10 to 85 cm (average 20cm) of alternating limestones and subordinate marls and dolostones in the middle parts. Bioclasts and benthonic foraminifera are the

most frequent fossils, while peloids are the most important non-skeletal grains. In the South CR a corresponding unit of 9.5m thick dolomarls is defined in WL section.

Unit 10 is represented in section SY by white limestones and nodular limestones with intercalated marly dolostones and massive dolomites. At the top benthonic foraminifera are frequent. Peloids are the most common non-skeletal grains. This 13m unit in the middle of the Ain Elbeida Fm. shows average bed thickness of ca. 2m was correlated with a 22m thick unit of massive dolostones and limestones in Blaatah Fm. of the South CR.

Unit 11 is an approximately 6m-thick unit in section SY (North CR). It is mainly composed of wackestones- packstones. The lower 2m are composed of 10-70cm (average 25cm) thick beds, while the upper 110cm are marly limestones with planktonic foraminifera. No corresponding lithofacies of unit 11 and the overlying units 12-18 occur in section WL of South CR (Figure IX.3.a), because of a ca. 15 m thick basalt layer that disconformably overlies unit 10 in a (Figure IX.3.c.c).

Unit 12 The 12.5m thick unit of SL section is predominantly composed of alternating dolostones, limestones and marls. Bed thickness ranges from 25-170cm (average 110cm). Unit 12 comprises two groups of limestones: Planktonic foraminiferal mudstone/wackestone and peloidal packstone/grainstone, topped by a 110cm thick rudist biostrome. These limestone lithologies are well comparable to a 180 cm interval dominated by rudists in section SY.

Unit 13 The approximately 4m thick unit (SL section) comprises predominantly thin bedded marly limestones (rich planktonic foraminifera and pelagic crinoids) with lenticular flints. In section SY, the 7.1m thick unit 13 comprises massive limestones (average 120cm) with miliolids, bioclasts and rudists.

Unit 14 this unit is approximately 22m thick in section SL and 7.7m thick in section SY. It is mainly composed of massive limestones or dolomitized limestones, alternating with marls in the lower part of the unit (section SL, arranged in 100-350cm with average of 120cm). Bioturbation and lamination are most common sedimentary structures in the massive limestones of SY section, while rudist biostromes characterize unit 14 in SL section.

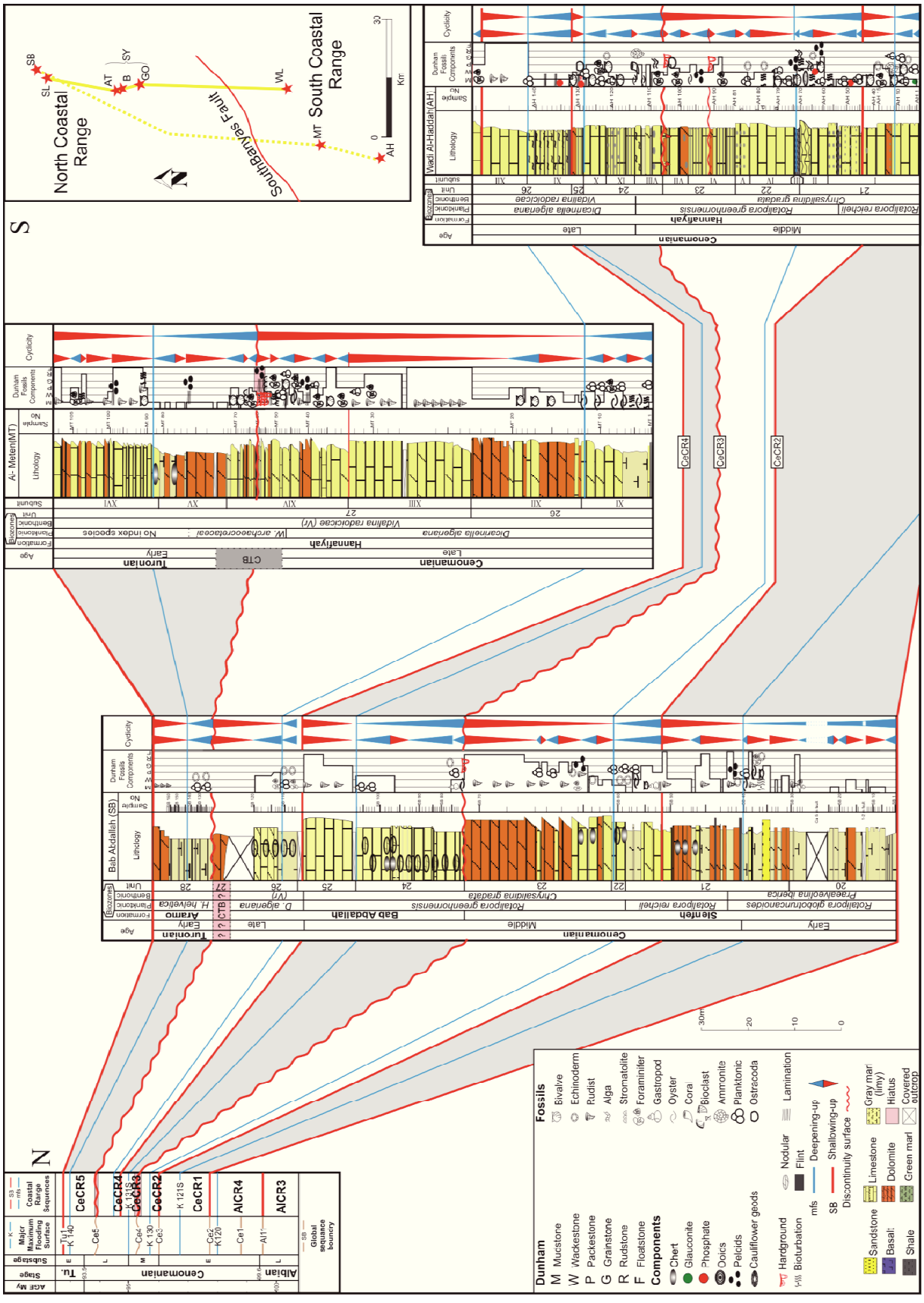
North Coastal Range
South Coastal Range
Southbanyas Fault
SB
SL
AT
B
SY
GO
WL
MT
AH
Km
S
N
Cenomanian
Turonian
Hannayah
Bab Abdallah
Sienfen
Aramo
Middle
Late
Early
Wadi Al-Haddar(AH)
Bab Abdalleh (SB)
A- Metem(MT)
Lithology
Sample No
Dunham Fossils Components
Cyclicity
Biozones
Unit
Subunit
Age
Formation
Planktonic
Benthonic
CeCR5
CeCR4
CeCR3
CeCR2
CeCR1
AlCR4
AlCR3
Fossils
Dunham
Components
Sandstone
Limestone
Dolomite
Basalt
Shale
Green marl
Covered outcrop
Gray marl (limy)
Hiatus
Nodular
Flint
Lamination
Deepening-up
Shallowing-up
Discontinuity surface
Hardground
Bioturbation
Global sequence boundary
Coastal Range Sequences
Major Maximum Flooding Surface
Substage
Stage
AGE My

Figure IX.3.b (previous page) N-S running correlation of the Coastal Range sequences AlCR3 to TuCR1 from (red lines) in the Bab Abdallah, Al-Meten and Wadi- Al-Haddah sections and maximum flooding surfaces of the Arabian Plate (blue lines); 3rd order global sequence boundaries (Al11- Ce5 brown lines) after ardenbol et al., 1998 Sharland et al., 2001, 2004; Ogg, 2004a; Haq and Al-Qahtani, 2005).

Unit 15 This ca. 6m thick unit of limestones comprises 70-80cm thick beds in section SL. Benthonic foraminifera form the most important fossils and peloids are the most important non-skeletal grains. This characteristic unit is represented in the SY section by 265cm thick thin bedded limestones, topped by a hardground (Figure IX.3.c.b).

Unit 16 is composed of ca. 4.8m thick alternating dolostones and fossiliferous limestones in the SL section. Bed thickness ranges from 50 to 130cm (average 120cm). The limestones hold benthonic foraminifera and abundant oysters in the upper 120cm. This unit correlates with 2.4m thick alternating dolostones and limestones in the SY section (Figure IX.3.c.b).

Age: Mouty and Saint-Marc (1982) attributed an (Albian) age for the Ain El Beida and Blaatah formations. Benthonic foraminifera of the limestones of these formations indicate Early Albian (*Mesorbitolina subconcava* zone) and Late Albian (*Neoiraqia convexa* zone).

IX.3.3 Slenfeh Formation (North and South CR) and Hannafiyah Formation (South CR)

The Slenfeh Formation is represented by massive and bedded limestones, dolostones with marly intercalations, occasionally with flint lenses. Seven units (17-23) where defined in the North CR, while in the South CR, we did not collect units 20 and 21 of Slenfeh Fm. The lowermost part of Hannafiyah Fm. in the south (AH section) is correlated with the uppermost Slenfeh Fm in the North CR (Figure IX.3.b).

Unit 17 in section SL comprises basal 7m light brown soft marls alternating with two horizons of platy marly limestones (the upper rich in oysters). While, the upper 15m of this unit consists of platy marly limestones, only its uppermost part has few chert pebbles. Among very rare non-skeletal grains, planktonic foraminifera are by far the most important skeletal grains. Additionally, some fragments of pelagic echinoids and thin-shelled molluscs have been found. The 22m thick unit of section SL correlates with


a
a1
a2
a3
Paleokarstic surface
I
II
III
IV
V
VI
VII
VIII
IX
Albian Basalt
AlCR2
ApCR2
AlI
b
c
d

Figure IX.3.c (previous page)- Coastal Range outcrop sections. (a) Overview of Wadi Al-Haddah quarry showing the mid-upper Cenomanian succession of Hannafiya Formation. (a1) unit III: the mfs of sequence CeCR2, probably corresponding with the P/B Break Event (Jarvis, 2006); (a2) Inoceramus pictus of unit III (a3) Lyropecten (Aequipecten) arlesiensis of unit III; (a4) Major paleokarstic surface corresponding with SB CeCR3(b) The irregular (erosion) surface AI11 corresponds with SB AlCR4of Sayno section. (c) Ca. 20m Late Albian basalt of South Coastal Range (Wadi-Layoun). (d) Cyclic stacking of the Late Aptian units in the Wadi-Layoun section with the SB ApCR2.

6m in SY section and with1.5m of limestones, disconformably overlying the basalt of section WL.

Unit 18 The 12.5m thick unit in section SL is predominantly composed of massive dolostones, forming cliff walls. Their thickness ranges from 120 to 360cm (average 210cm). This unit is an important marker bed, comprising nodular flints and cauliflower-shaped cherts (Figure IX.3.d.c). Unit 18 has similar thicknesses in WL and SY sections, however, the lower part in section SY is marked by a 30cm thick phosphatic bed.

Unit 19 consists of massive dolostones with intercalations of dolomarls. The approximately ca. 50m thick unit comprises unfossiliferous dolomite with flint lenses and chert nodules (Figure IX.3.d.b). Only the lower part of this unit is measured in sections SL and WL.

Unit 20 This unfossiliferous 19m thick unit comprises alternating limy and dolomitic marls with flint lenses at the base. Bed thickness ranges from 30 to 240cm (average 80cm) in SB section.

Unit 21 The ca. 37m thick unit consists of 80-390cm (average 150cm)-thick beds of alternating dolomites, marls, limestones with rudists, bivalves, benthonic and planktonic foraminifera. The lower part of unit 21 in section SB (North CR) includes ca. 2 m limestone interval with quartz (Figure IX.3.b), whilethe upper 8 m of this unit are correlated with ca. 26m, composed of 10-20 cm-thick beds of limestones (with thin bands of chert nodules) in the south (here: subunits **I-II** of AH section). The latter hold planktonic foraminifera, thin wall mollusks and green algal debris (Figures 3, 4a).

Unit 22 is composed of 2m thick nodular limestones rich in planktonic foraminifera and chert nodules (section SB). The comparable unit of the South CR comprises 80cm black shale with *Lyropecten (Aequipecten) arlesiensis* and large inoceramids shells (Figure IX.3.c.a2) is overlain by 12m thick bedded limestones (10-20cm thick beds) with

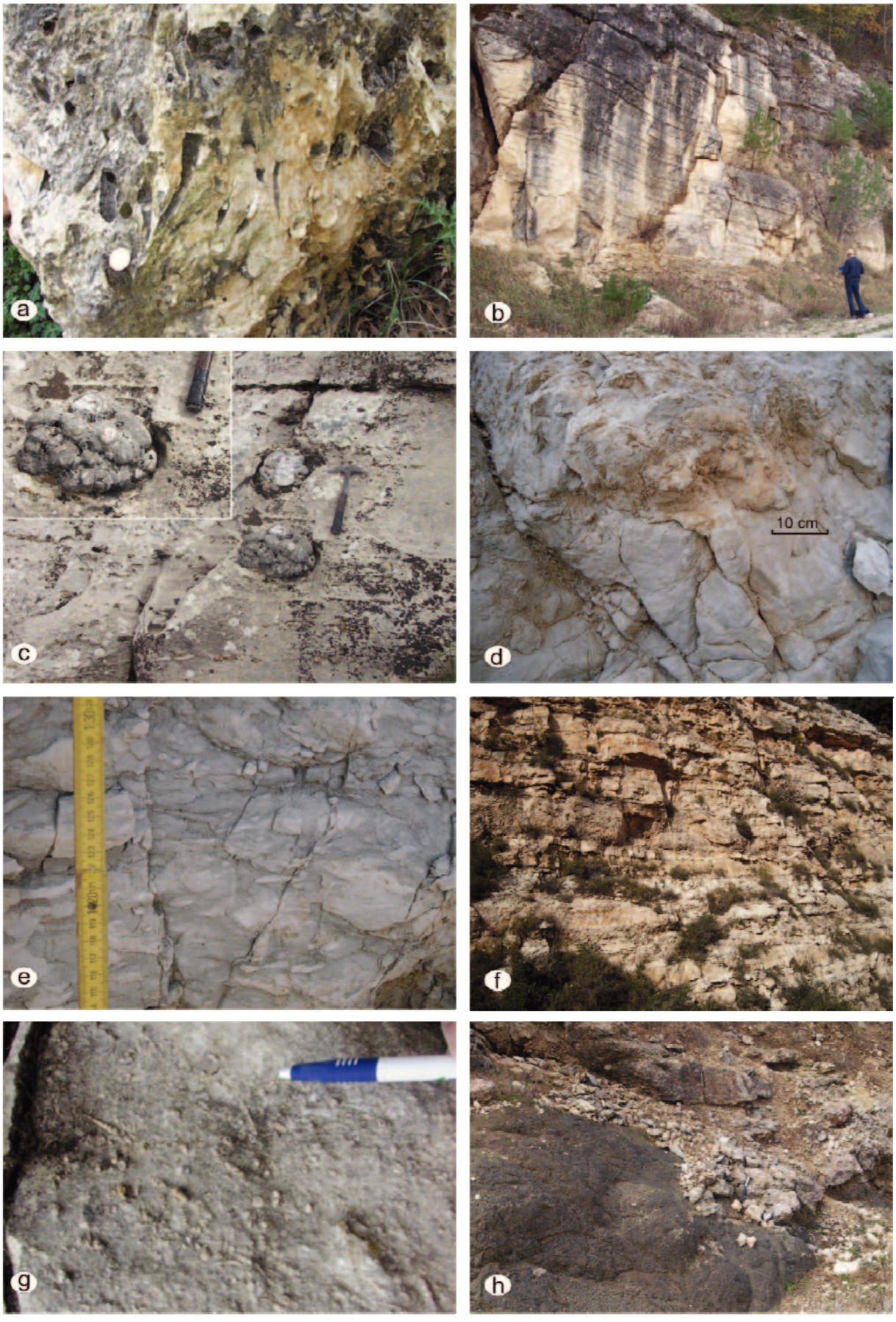
a
b
c
d
10 cm
e
f
g
h

Figure IX.3.d (previous page) Coastal Range outcrop sections. (a) rudist interval of Ein El-Beidah formation of section SL (unit 14). (b) Cliff wall of dolostones with flints unit 19 of SY section. (c) Cliff wall of dolostones with nodular and cauliflower-shaped cherts (unit 18 of SL section). (d) Marly limestones rich in large oysters (unit 26 of MT section). (e) intensely bioturbated marly limestones interpreted as a condensed of the transgressive of unit 26 of MT section. (f) Unit 27 (the upper part of subunit XIV) of Al-Meten quarry showing the ?Cenomanian-Turonian succession of the upper Hannafiya Formation. (g) limestone interval rich in Turritella sp. of unit 24 (section SB). (h) The Early Albian Basalt of Joubet Barghal north Coastal Range.

planktonic foraminifera, thin wall mollusks and chert nodules in the upper part. Unit 22 correlates with subunits **III- V** (section AH).

Unit 23 is a 31m thick unit, composed of an approximately 190-600cm (average 260cm)-thick rudist bed with few intercalations of limestones (wackestone with planktonic foramini-fera). This unit correlates with subunits **VI - VII** of section AH (South CR). The upper boundary of subunit **VII** is denoted by a regional unconformity marked by a distinctive paleokarstic surface (Figures 3, 4a).

Age: Mouty and Saint-Marc (1982) attributed a Late Albian-lower/Middle Cenomanian age to the Slenfeh Formation in the North CR. In this study, that was stratigraphically correlated with the Slenfeh and the lower Hannafiyah Fm.

IX.3.4 Bab Abdallah Formation (North CR) and Hannafiyah Formation (South CR)

Units 24 to 27 represent a more than 100m thick succession of alternating well bedded limestones, marls with flint nodules and massive rudistic dolomitized
limestones that were attributed to the Bab Abdallah Fm. in the North CR. This interval correlates with ca. 200m thick succession in the South CR of the Hannafiyah FM. (Figures IX.3.b, IX.3.c.a).

Unit 24 This approximately 23m thick unit comprises 160-380cm (average 240cm) thick beds of nodular marly limestones. The base of unit 24 is marked by abundant oysters, gastropods (*Turritella* sp.) and planktonic foraminifera, while chert nodules are more frequent in the upper 9m of section SB. In section AH (South CR), this unit (subunits **VII -** X) comprises 18m thick marls and nodular limestones (with corals, mollusks, green algae, ammonites and benthonic and planktonic foraminifera).

Unit 25 This approximately 20m thick massive dolomitized limestone interval is composed of rudist bondstones (bed thiicknesses between 180-310cm)in the North CR

(section SB). It was correlated with a 1m massive dolomite bed at the base of subunit **XI** in the AH section.

Unit 26 consists of ca. 50m thick marls and nodular limestones with abundant oysters, pelagic mollusks and planktonic foraminifera in section SB. It is correlated with subunits **XI- XII** in sections AH and MT. The latter are composed of well bedded limestones (wacke-/packstoneswith bed-thickness of 30-100cm), containing oysters, echinoderms, and foraminifera (benthonic and planktonic). These limestones are overlain by marls rich of planktonic foraminifera and oysters.

Unit 27 comprises approximately 50m thick massive dolostones and limestones (rudists boundstones). The thickness of individual beds range between 1-8m (average 4m) in sections SB and MT (subunits **XII- XIII**). Only in the MT section, the overlying subunits **XIV, XV, and XVI** are present and are composed of 25m thick platy limestones and dolostones, overlain by 37m thick massive bedded fossiliferous limestones, alternating with marls, dolomitic limestones and dolostones (Figures 3, 5f). Benthonic foraminifera, mollusks, stromatolithes (bindstones) and rudist bioclasts are frequent only in wacke-/packstones and pack-/floatstones. The Cenomanian Turonian boundary (CTB) is supposed to be in the platy limestones above, based on maximum values of $\delta^{13}C$ (see Chapter, Figure IX.3.d.f).

Unit 28 has a total thickness of 20m and is composed of 5-10cm thick alternating limestones and flints, containing pelagic echinids, thin-walled mollusks and planktonic foraminifera. These marly limestones are argillaceous in some intervals and are overlain by 3m massive limestones with rudists. This unit forms the base of the **Turonian Aramo Formation**."

Age: Most previous authors attributed a mid-Late Cenomanian age for the Bab Abdallah and Hannafiyah Formations and a Turonian age for the Aramo Formation (e.g. Mouty and Saint-Marc 1982). This is well comparable with our results; in addition to an earliest Turonian age for the uppermost Hannafiyah Formation (MT section).

IX .4 BIOSTRATIGRAPHY

Biostratigraphic control in the mainly shallow water carbonates of the Coastal Range of Syria is difficult. Planktonic foraminifera reflect in shallow environments high stress conditions, as indicated by generally low diversity, dwarfing and sporadic presence of index species. However, several intervals of the studied Aptian-Early Turonian succession show more diverse and abundant assemblages and allow for a good resolution, when all biostratigraphic data (benthic and planktic foraminifera plus macrofossils) are combined (Figure IX.4.1.a).

IX.4.1 Benthic foraminifera Biostratigraphy:

Numerous benthonic foraminifera are useful index fossils of the Cretaceous carbonate platforms (Loeblich & Tappan 1988). They show a widespread distribution, high diversity and abundance in the studied sections of the Coastal Range (Figures 7- 14) and thus are important for the biostratigraphic subdivision. Based on the concepts of Velic` (2007), Ogg et al. (2008a), Schroeder et al. (2010), and Ghanem et al. (2012) the following seven biozones (overlapping most planktonic zonal boundaries - Figure IX.4.1.a) were defined:

IX.4.1.1 The Early Aptian Pseudocyclammina vasconica range zone.

Diagnosis*:* This biozone is defined by the total range of the zonal markers *Pseudocyclammina vasconica* and *Voloshinoides murgensis,* according to the range of co-occurring benthic foraminifera in the Tethys and the Adriatic platform (Velić, 2007; Ogg and Ogg, 2008a, Figure IX.4.1.a) .

Description: This biozone spans a long Early Aptian stratigraphic interval. However, the lower part of the Early Aptian is missing, based on sequence stratigraphic interpretation (compare sequence ApCR1). In addition to the zonal marker species, the following taxa occur within the *P. vasconica* range zone of the present study**:** *Voloshinoides murgensis*, *Sabaudia minuta, Sabaudia auruncensis, Vercorsella*

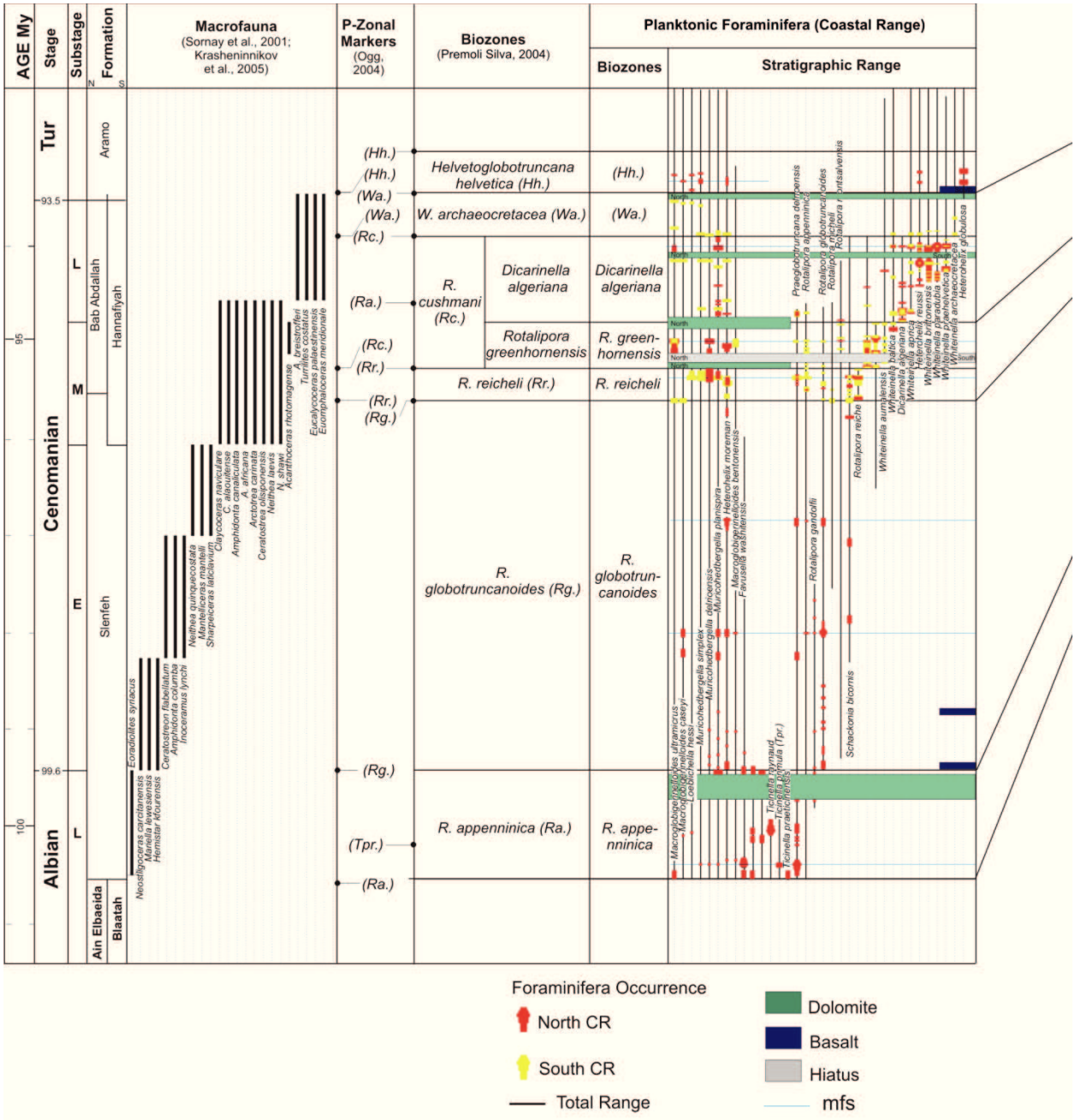

Figure IX.4.1.a: Stratigraphic concept and standard Biozones (planktonic and benthonic foraminifera). Red/ yellow dots represent the foraminiferal occurrence of North/ South Coastal Range, thick line indicates the total Range of foraminifera species and the blue line is the Maximum flooding surfaces.
(Figure continued on next page.)

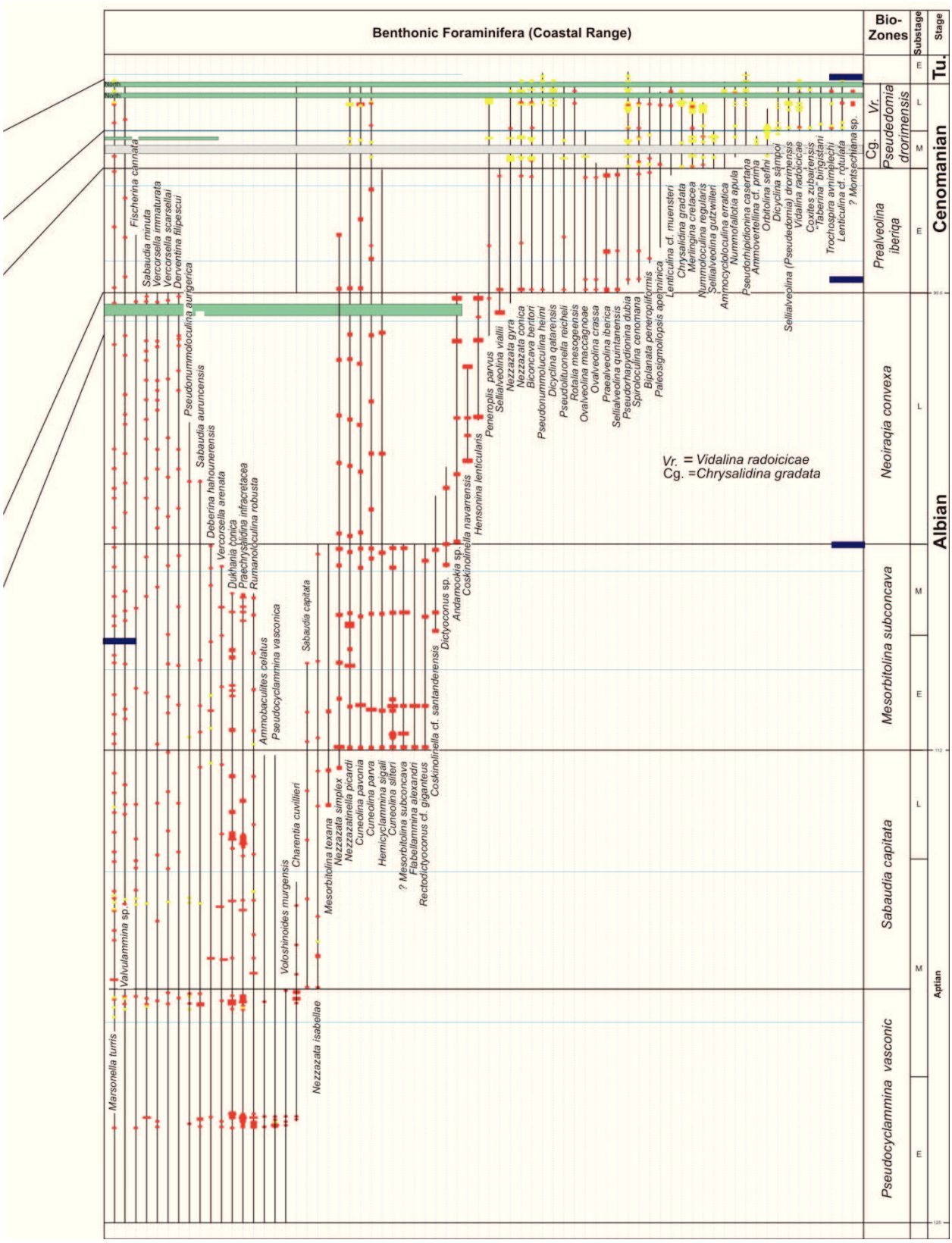
Benthonic Foraminifera (Coastal Range)
Bio-Zones
Substage
Stage
Cenomanian
Albian
Aptian
Tu.
Vr.
Cg.
Pseudedomia dorimensis
Prealveolina iberiga
Neoiraqia convexa
Mesorbitolina subconcava
Sabaudia capitata
Pseudocyclammina vasconic
Vr. = Vidalina radoicicae
Cg. =Chrysalidina gradata
Fischerina cannata
Sabaudia minuta
Vercorsella immaturata
Vercorsella scarsellai
Derventina filipescui
Pseudonummoloculina aurigerica
Sabaudia auruncensis
Deberina hahouenensis
Vercorsella arenata
Dukhania conica
Praechrysalidina infracretacea
Rumanoloculina robusta
Ammobaculites celatus
Pseudocyclammina vasconica
Sabaudia capitata
Voloshinoides murgensis
Charentia cuvillieri
Nezzazata isabellae
Marsonella turris
Valvulammina sp.
Mesorbitolina texana
Nezzazata simplex
Nezzazatinella picardi
Cuneolina pavonia
Cuneolina parva
Hemicyclammina sigali
Cuneolina silleri
? Mesorbitolina subconcava
Flabellammina alexandri
Rectodictyoconus cf. gigantteus
Coskinolinella cf. santanderensis
Dictyoconus sp.
Andamookia sp.
Coskinolinella navarrensis
Hensonina lenticularis
Peneroplis parvus
Sellialveolina viallii
Nezzazata gyra
Nezzazata conica
Biconcava beritori
Pseudonummoloculina heimi
Dicyclina qatarensis
Pseudolituonella reicheli
Rotalia mesogeensis
Ovalveolina maccagnoae
Ovalveolina crassa
Praealveolina iberica
Sellialveolina quintanensis
Pseudorhapydionina dubia
Sphaeroloculina cenomana
Biplanata peneropliformis
Paleosigmoilopsis apenninica
Lenticulina cf. muensteri
Chrysalidina gradata
Merlingina cretacea
Nummoloculina regularis
Sellialveolina gutzwilleri
Ammocyclocloculina erratica
Nummofallotia apula
Pseudorhipidionina casertana
Ammovertellina cf. prima
Orbitolina sefini
Dicyclina sampoi
Sellialveolina (Pseudedomia) dorimensis
Vidalina radoicicae
Coxites zubairensis
"Taberina" bingistani
Trochospira avnimelechi
Lenticulina cf. rotulata
? Montsechiana sp.

Figure IX.4.1.b: Benthonic foraminifera of the Early Aptian *Pseudocyclammina vasconica* zone: (1 and 2) *Praechrysalidina infracretacea*, (1) [ls], (2) [es] (Ain Tina). (3) *Hemicyclammina* sp. [es] (Sayno). (4, 5 and 6) *Pseudocyclammina vasconica*, (4) [as], (5) [sls], (6) [es] (Sayno). (7 and 8) *Ammobaculites celatus*, (7) [ls], (8) [as] (Sayno). (9) *Nezzazatinella* sp.? [ses] (Sayno). (10) *Vercorsella* sp.[os] young megalospheric form (Sayno). (11) *Pseudorhapydionina* sp.? [ses] (Sayno). (12, 16, and 17) *Charentia cuvillieri*, (12) [sas], (16) [as], (17) [es] (Sayno). (13) *Voloshinoides* cf*. murgensis* [ses] (Sayno). (14) *Sabaudia capitata* [os] young megalospheric form (Sayno). (15) *Dukhania conica* [ls] (Sayno). (18) *Vercorsella* cf. *immaturata* [os] young megalospheric form (Sayno).(19) *Sabaudia auruncensis* [os] young megalospheric form (Sayno). (20) *Pseudonummoloculina aurigerica* [as] (Sayno). (21 and 22) *Rumanoloculina robusta* [as] (Sayno). (23) miliolid indet [sas] (Sayno). (24) *Cuneolina* sp. [os] young megalospheric form (Sayno). (24) *Vercorsella arenata* [os] young megalospheric form (Sayno): as= axial section; sas= subaxial section; es= equatorial section; ses= subequatorial section; ob= oblique section; ts= transversal section; ls= logitudinal section.

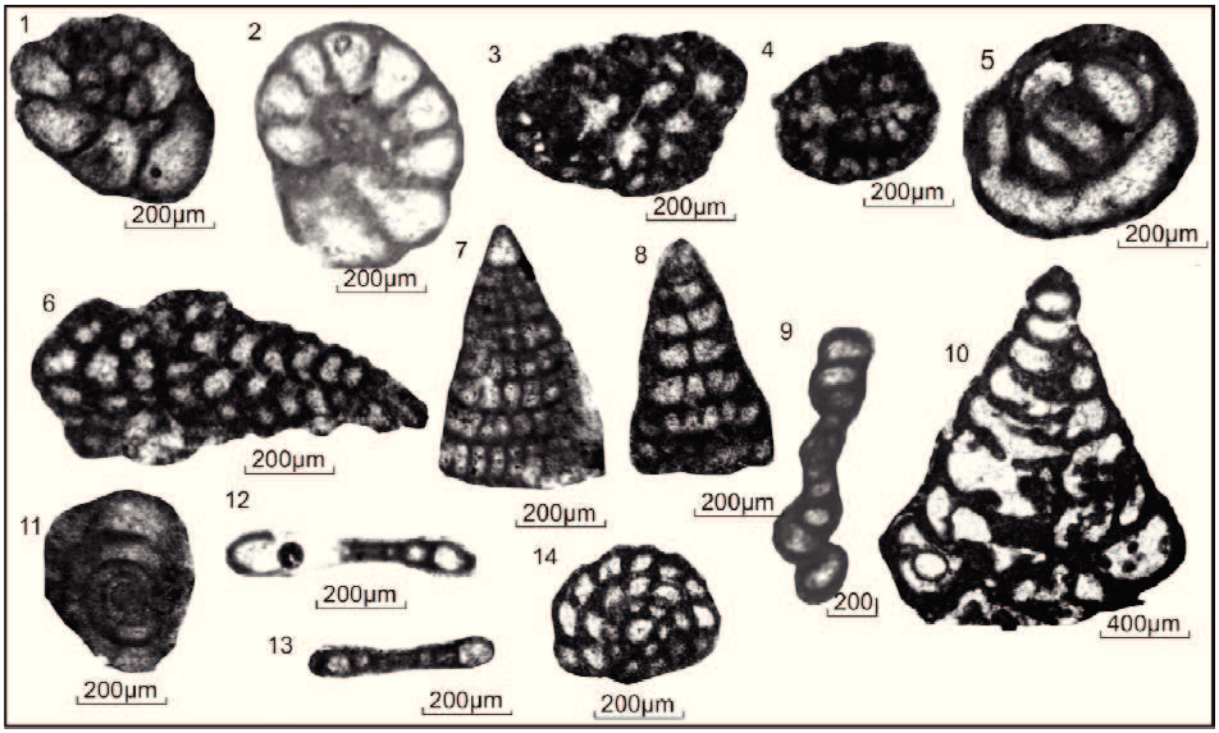

Figure IX.4.1.c: Benthonic foraminifera of the Late Aptian Assemblage zone: (1and 2) *Nezzazatinella picardia*, (1) [as], (2) [sas] (Sayno). (3) *Voloshinoides cf. murgensis* [sas] (Sayno). (4) *Cuneolina sliteri* [sas] (Sayno). (5) *Pseudonummoloculina aurigerica* [sas] (Sayno).(6 and 7) Vercorsella scarsellai, [os] young megalospheric form (6) (Sayno), (7) (Sayno). (8) *Vercorsella arenata*, [os] young megalospheric form (Sayno). (9) *Derventina filipescui* [sas] (Sayno). (10) *Praechrysalidina infracretacea*, [ls] (Sayno)(11, 12 and 13) *Vidalina* cf. *radoicicae,* (11) [ses], (12, 13) [sas] (Sayno). (14) *Nezazzata* sp. [es] (Sayno): as= axial section; sas= subaxial section; es= equatorial section; ses= subequatorial section; ob= oblique section; ts= transversal section; ls= logitudinal section.

arenata, Vercorsella immaturata, Rumanoloculina robusta, Ammobaculites celatus, Dukhania conica, Praechrysalidina infracretacea, Charentia cuvillieri, Pseudonummoloculina aurigerica, Derventina sp., including few miliolids. Mouty and Saint-Marc (1982) described two marker species (*Palorbitolina lenticularis* and *Choffatella decipiens*) from units 1 and 3 (Figures IX.3.a, IX.4.1.a, IX.4.1.b).

Correlation: The benthonic assemblages of the *P. vasconica* range zone of the CR correlates well with the Early Aptian benthonic foraminiferal assemblages of the Adriatic platform and Tethyan realm, described by Loeblich and Tappan (1988), Velić (2007) and Ogg et al. (2008b). Therefore it is comparable to the stratigraphic range of the *Palorbitolina lenticularis* zone of the Arabian platform (Schroeder et al., 2010).

Age and Occurrence*:* The Early Aptian *P. vasconica* range zone documents the first benthonic foraminifera of the Cretaceous succession of the Coastal Range. It is


1
200 µm
2
200 µm
7
200 µm
6
200 µm
3
200 µm
4
200 µm
5
200 µm
11
200 µm
10
300 µm
8
200 µm
9
200 µm
14
200 µm
16
200 µm
12
200 µm
13
200 µm
15
200 µm
17
200 µm
19
200 µm
18
200 µm
20
200 µm
21
200 µm
22
200 µm
23
200 µm
25
200 µm
24
200 µm
26
200 µm
27
200 µm

Figure IX.4.1.d (previous page)- Benthonic foraminifera of the Early Albian *Mesorbitolina subconcava* zone: (1, 2 and 3) *Flabellammina cf. alexanderi*, (1 and 3) [es], (2) [as] (Sayno). (4) *Peneroplis* sp.,? [es] (Sayno). (5 and 6) *Sabaudia capitata*, [as] (Sayno). (7) *Sabaudia minuta* [as] (Sayno). (8 and 9) *Debrina hahounerensis*, (8) [es], (9) [as] (Sayno). (10) *Orbitolina* (Ms) cf. *texana* [as] through a megalospheric form (Sayno). (11) *Derventina filipescui* [as] (Sayno). (12) *Nezazzatinella icardi*, [sas] (Sayno). (13) *Cuneolina parva*, [os] through a young megalospheric form (Sayno). (14) *Nezazzata isabellae* [es] (Sayno). (15) *Vercorsella* sp., [as] (Sayno). (16, 17 and 18) *Cuneolina sliteri*, [os] through a young megalospheric form (Sayno).(19) *Voloshinoides* sp., [os] through a young megalospheric form (Sayno). (20 and 21) *Vecorsella immaturata*, (20) [as], (21) [ts] (Sayno). (22) *Vecorsella arenata*, [as] (Sayno). (23) *Dictyoconus* sp.? [as] (Sayno). (24) *Nezazzatinella* sp., [sas] (Sayno). (25) *Rumanoloculina robusta* [as] (Sayno). (26) *Orbitolina* sp. [as] through a megalospheric form (Sayno). (27) *Hemicyclamina sigali* [es] (Sayno): as= axial section; sas= subaxial section; es= equatorial section; ses= subequatorial section; ob= oblique section; ts= transversal section; ls= logitudinal section.

recorded from 22m thick green marls, dolostones and limestones, representing units 1, 2, 3 and 4 (Bab Janneh Formation) of sections SY and WL (Figures IX.3.a, IX.4.1.a).

IX.4.1.2 The Late Aptian *Sabaudia capitata* interval zone.

Diagnosis: The lower boundary of this interval zone has been determined by the FO of *S. capitata* and *Nezzazata isabellae*. The FO of *Nezzazatinella picardi*, *Cuneolina parva* and *C. pavonia* mark the upper boundary of this biozone (Figure IX.4.1.a).

Description: The benthonic index fossils of the Late Aptian (*Mesorbitolina parva* and *M. texana*) biozones (Ogg and Ogg, 2008a; Velić, 2007; Schroeder et al., 2010, Figure IX.4.1.a) are not present in the studied sections. We therefore suggest the *S. capitata* interval zone as index zone for the Late Aptian. Besides the FO's of the two marker species, this biozone is characterized by the LO's of *Voloshinoides murgensis, Pseudocyclammina vasconica* and *Ammobaculites celatus*. Moreover, the *S. capitata* zone is associated with rich assemblages of the following wide range species: *Charentia cuvillieri*, *Dukhania conica, Praechrysalidina infracretacea, Sabaudia minuta*, *Sabaudia auruncensis*, *Vercorsella arenata*, *Vercorsella immaturata*, *Rumanoloculina robusta*, *Pseudonummoloculina aurigerica* (Figures IX.4.1.a, IX.4.1.c).

Correlation: The Late Aptian *S. capitata* interval zone is equivalent to the stratigraphic range of the following two biozones of the Arabian platform: *Mesorbitolina parva* and *M. texana* biozones (Schroeder et al., 2010).


1
200µm
2
200 µm
3
200 µm
4
250µm
5
200µm
6
400 µm
7
200 µm
8
200µm
9
200 µm
10
250µm
11
250µm
12
250µm
13
250µm
14
200µm
15
250µm
16
250µm
17
250µm
18
200µm
19
200µm
20
250µm
21
200 µm
22
200 µm
23
200 µm
24
200µm
25
200 µm
26
200µm
27
28
200µm
29
250µm
30
250µm
31
250µm
32
200 µm
33
200 µm
34
250µm
35
250µm
36
250µm
37
250µm
38
200 µm

Figure IX.4.1.e: Benthonic foraminifera of the Late Albian *Neoiraqia convexa* zone: (1 and 33) *Pseudonummoloculina aurigerica* [sas] (Sayno). (2, 3 and 4) *Cuneolina pavonia*, (2) [os] through the megalospheric form (Sayno), (4) [ls] (Slenfeh). (4) *Dokhania conica*, [ls] (Sayno). (6 and 7) *Praechrysalidina infracretacea*, (6) [ls], (7) [es] (Sayno). (8 and 9) *Derventina filipescui* [sas], (8) (Sayno), (9) (Slenfeh). (10) *Coskinolinella navarrensis*, [os] (Slenfeh). (11 and 12) *Sabaudia minuta* , [os] through the megalospheric form (Slenfeh). (13) *Hensonina lenticularis*, [as] (Slenfeh). (14, 17 and 18) *Spiroloculina* sp., (14) [sas] (Sayno), (15) [as] (Slenfeh), (18) [es] (Sayno). (16 and 16) *Andamookia* sp. [os] (Slenfeh). (19) *Rumanoloculina robusta*, [sas] (Sayno). (20) *Vecorsella* sp., [os] megalospheric form (Slenfeh). (21) [es] (Sayno). (3) *Coskinolinella* cf*. santanderensis*, [os] (Sayno). (22) *Nezzazata isabellae* [as] (Sayno). (23 and 24) *Nezzazata simplex*, 23 [as], [sas] (Sayno). (25) *Nezzazatinella picardia* [sas] (Sayno). (26) miliolid indet, [as] (Sayno). (27 and 28) textulard foraminifera, (27) [es], (28) [ls] (Slenfeh). (29, 30 and 31) *Bolivinopsis* sp., (29, 30) [ls], (31) [es] (Slenfeh). (32) *Vercorsella* sp. [os] young the megalospheric form (Sayno). (34 and 35) *Vidalina* sp. [es] (Slenfeh). (36 and 37) *Voloshinoides* sp.? [ls] (Slenfeh). (38) *Vecorsella arenata*, [os] through the megalospheric form (Sayno): as= axial section; sas= subaxial section; es= equatorial section; ses= subequatorial section; ob= oblique section; ts= transversal section; ls= logitudinal section.

Age and Occurrence: The *S. capitata* interval zone represents a Late Aptian interval in the northern part of Coastal Range (section SY). It is represented by shallow marine limestones intercalating with green marls and dolomites and occurs in 30m of units 5 and 6 in the upper Bab Janneh Formation of section SY (Figure IX.4.1.a).

IX.4.1.3 The Early Albian *Mesorbitolina subconcava* range zone:

Diagnosis*:* Interval of the total range of *Mesorbitolina subconcava* (Velić, 2007; Ghanem et al., 2012).

Description: The following Early Albian index taxa, such as *Mesorbitolina texana*, *Cuneolina sliteri, C. pavonia, C. parva, Dukhania conica, Praechrysalidinainfracretacea, Flabellammina alexandri, Hemicyclammina sigali, Sabaudia minuta, Nezzazata simplex*, *N. isabellae, Vercorsella arenata*, *V. immaturata* and *Nezzazatinella picardi* as well as some miliolids, *Dictyoconus* sp., and different *Orbitolina* spp. occur in the *Mesorbitolina subconcava* zone (Figures IX.4.1.a, IX.4.1.d).

Correlation: The benthonic foraminifera assemblage described coincides with the *Mesorbitolina subconcava* biozone of South Pamyrides after Ghanem et al. (2012) and the same zone in the Adriatic Platform (Velić, 2007) (Figure IX.4.1.a).

Age and Occurrence: The *M. subconcava* zone comprises the Early to Middle Albian (Velić, 2007; Ghanem et al., 2012). The *M. subconcava* biozone is evident in 65-m-thick

limestones (units 7- 10) in the northern part of the North CR of the Ain-Elbeida Formation of section SY (Figure IX.3.b).

IX.4.1.4 The Late Albian *Neoiraqia convexa* taxon-range zone

Diagnosis: Total range zone of zonal marker (Velić, 2007; Ghanem et al., 2012).

Description: The base of this assemblage zone is defined by the FO of zonal marker, *Andamookia* sp. and the LO's of *Cuneolina sliteri*, *Hemicyclammina sigali, Debarina hahounerensis, Nezzazata isabellae, Mesorbitolina texana, M. subconcava, Flabellammina alexandri* and *Rectodictyoconus* sp. The top corresponds to the FO of Early Cenomanian species (*Praealveolina iberica, Pseudolituonella reicheli, Biconcava bentori* and *Nezzazata conica*). This zone is additionally associated with *Coskinolinella navarrensis, C. santanderensis* and *Hensonina lenticularis.* Moreover, further taxa of wide stratigraphic range like: *Dukhania conica, Praechrysalidina infracretacea, Nezzazata simplex, Nezzazatinella picardi, Cuneolina pavonia, C. parva, Vercorsella arenata*, *V. immaturata, Derventina filipescui, Spiroloculina* sp., *Rumanoloculina* cf. *robusta, Fischerina* sp., *Sabaudia minuta, Bolivinobsis* sp., *Vercorsella* sp., *Vidalina* sp., *Voloshinoides* sp., and few miliolids occur in that biozone (Figures IX.4.1.a, IX.4.1.e).

Correlation: The zone is equivalent to both biozones: *Valdanchella dercourti* partial range zone and The *Neoiraqia* taxon-range zone of Velić (2007). It is delineated by the overlapping ranges of co-occurring species (Loeblich and Tappan, 1988; Ogg et al., 2008b; Velić, 2007, Figure IX.4.1.a).

Age and Occurrence: In the North CR this biozone is represented by Late Albian restricted shallow marine limestones with differing foraminiferal diversities. It occurs in the upper Ain-Elbeida Formation (units 10-16), composed of (ca. 42m) thick limestones, marly limestones and dolomitic limestones in section SY and by 53 m-thick limestones and dolostones in section SL.

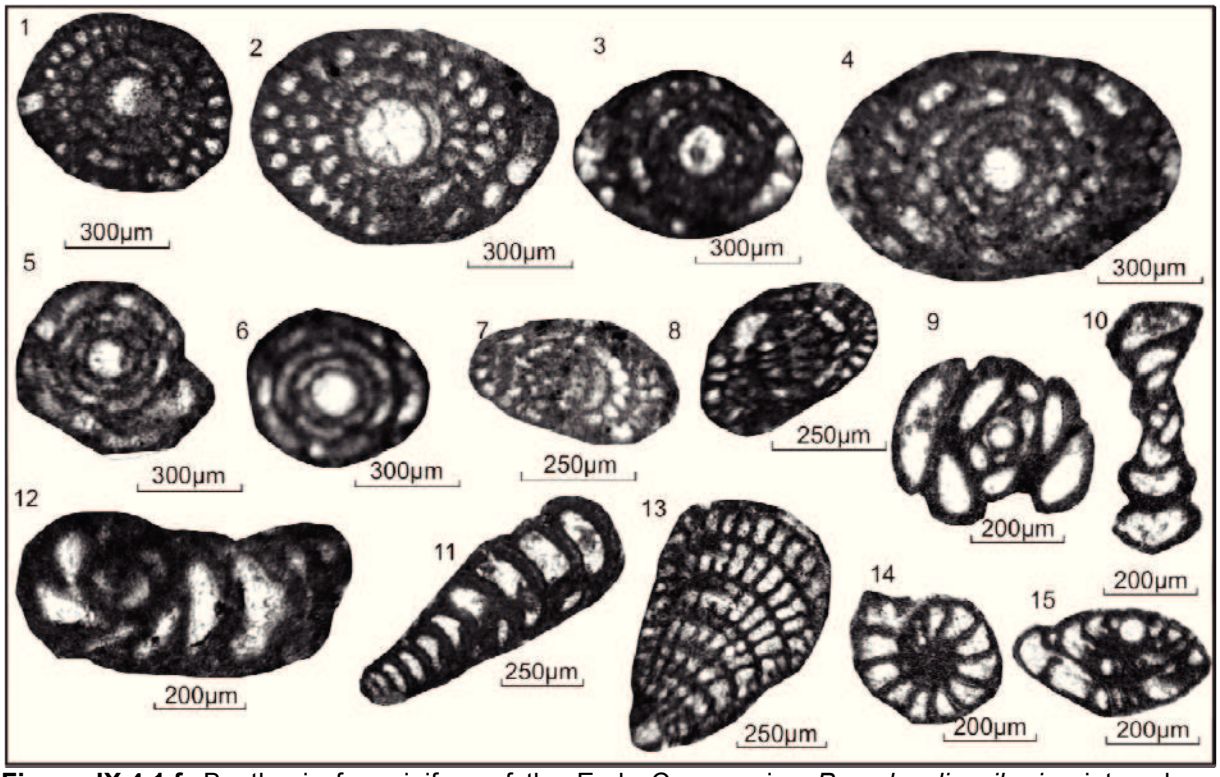

Figure IX.4.1.f: Benthonic foraminifera of the Early Cenomanian *Praealveolina iberica* interval zone: (1and 2) *Praealveolina iberica* [os] (Slenfeh). (3, 4 and 5) *Sellialveolina viallii*, (3 and 4) [as], (5) [ses] (Slenfeh). (6, 7 and 8) *Ovalveolina crassa*, (6) [ses] (Sayno), (7 and 8) [ts] (Slenfeh). (9) miliolid indet [as] (Sayno). (10) *Fischerina cannata*, [es] (Sayno). (11) *Pseudolituonella reicheli* [ls] (Slenfeh). (12) *Pseudorhipidionina dubia*, [es] (Slenfeh). (13) *Cuneolina parva* [os] the megalospheric form (Slenfeh). (14) *Biconcava bentori*, [sas] (Sayno). (15) *Nezazzata simplex* [sas] (Sayno): as= axial section; sas= subaxial section; es= equatorial section; ses= bequatorial section; os= oblique section; ts= transversal section; ls= logitudinal section.

IX.4.1.5 The Early Cenomanian *Praealveolina iberica* interval zone

Diagnosis: Total range zone of the zonal marker. Furthermore, this biozone is determined by the range between the FO of *Praealveolina iberica* and the FO of *Chrysalidina gradata, Selliaveolina gutzwilleri,* (Ogg and Ogg, 2008a; Vicedo et al., 2011; Ghanem et al., 2012).

Description: Besides the zonal marker, additional foraminifera (known as Cenomanian index taxa) occur, such as: *Nezzazata gyra, N. conica, Biconcava bentori, Ovalveolina crassa, Selliaveolina viallii, S. quintanensis, Peneroplis parvus, Biplanata peneropliformis*, *Dicyclina qatarensis, Pseudonummoloculina heimi, Pseudorhapydionina dubia,* and *Pseudolituonella reicheli.* They co-occur with some wide range species: *Nezzazata simplex, Cuneolina pavonia, C. parva, Nezzazatinella*


1
400µm
2
400µm
3
7
400µm
400µm
4
400µm
5
400µm
10
400µm
6
400µm
8
400µm
9
400µm
11
400µm
12
400µm
13
400µm
14
400µm
15
200µm
16
200µm
17
400µm
27
18
400µm
19
400µm
20
400µm
21
200µm
22
200µm
24
400µm
23
400µm
25
200µm
26
200µm
200µm
28
200µm
29
200µm
30
400µm
31
200µm
32
200µm
33
200µm
34
400µm
35
400µm
36
200µm
37
200µm
38
200µm
39
200µm
40
200µm

Figure IX.4.1.g: Benthonic foraminifera of the Middle Cenomanian *Chrysalidina gradata* partial zone: (1, 2, 3, 4 and 7) *Sellialveolina gutzwilleri*, (1) [as], (2, 3 and 7) [sas], (4) [ses] (Wadi Al-Haddah). (5, 6, 8, 9 and 10) *Sellialveolina quintanensis*, (5 and 8) (6) [os], (9) [ses] (Wadi Al-Haddah). (11 and 12) *Ovalveolina maccagnoae*, (11) [ses] (Wadi Al-Haddah), 12 (6) [os] (Bab-Abdallah). (13 and 14) *Nummoloculina regularis*, (13)[as], (14) [ses] (Wadi Al-Haddah). (15 and 16) *Biconcava* cf. *bentori*, (15) [ses] (16) [ses] (Wadi Al-Haddah). (17, 18 and 19) *Chrysalidina gradata* [ls] (Wadi Al-Haddah). (20 and 21) *Dicyclina sampoi*, (20) [ses], (21) [as] (Wadi Al-Haddah). (22) *Cuneolina* sp. [as] (Wadi Al-Haddah). (23 and 24) *Ammovertellina cf. prima* [sas] (Wadi Al-Haddah). (25, 26, 27 and 29) *Merlingina cretacea*, (25, 29) [es], (26, 27) [os] (Wadi Al-Haddah, Bab-Abdallah). (28 and 33) *Nezazzata gyra*, (28) [es] (33) [os] (Wadi Al-Haddah). (30) Dicyclina sp. [os] (Bab-Abdallah). (31and 32) *Nezazzatinella picardi*, [sas] (Wadi Al-Haddah). (34 and 35) miliolid indet, [sas] (Bab-Abdallah, Wadi Al-Haddah). (36, 37 and 38) *Pseudorhapydionina dubia*, (36) [os], (Bab-Abdallah). (37, 38) [ses] (Wadi Al-Haddah). (39 and 40*)* *Spiroloculina cenomana*, [as] (Wadi Al-Haddah). as= axial section; sas= subaxial section; es= equatorial section; ses= subequatorial section; os= oblique section; ts= transversal section; ls= longitudinal section.

Correlation: This biozone is equivalent to the *Praealveolina iberica* biozone in the South Palmyrides proposed by Ghanem et al (2012); it is also coincided with the *Conicorbitolina conica/Conicorbitolina cuvillieri* range zone of the Adriatic platform of Velić (2007). *picardi, Nummoloculina* sp.*, Fischerina* sp.*, Marsonella* sp. and miliolids div. spp. (Figures Figures IX.4.1.a, IX.4.1.f).

Age and Occurrence: The *Praealveolina iberica* interval zone spans the restricted Early Cenomanian shallow marine carbonates of the uppermost Ain-Elbeida to Slenfeh Formations (units 17- 21). It is represented by 109m thick limestones in section SL (North CR).

IX.4.1.6 The Middle Cenomanian *Chrysalidina gradata* partial range zone

Diagnosis: Interval range of the zonal marker to the FO of *Vidalina radoicicae*.

Description: This biozone is defined by the FO of the index fossil *Chrysalidina gradata,* associated with a rich assemblage of further Cenomanian benthonic foraminifera like *Selliaveolina gutzwilleri, Ovalveolina maccagnoae, Merlingina cretacea, Nummoloculina regularis*, *Nezzazata gyra, N. simplex, N. conica, Biconcava bentori, Biplanata peneropliformis*, *Orbitolina sefini*, *Dicyclina qatarensis, Nummofallotia apula, Peneroplis parvus, Pseudonummoloculina heimi, Pseudorhipidionina casertana*, *Pseudorhapydionina dubia, Spiroloculina cenomana* and *Rotalia mesogeensis.* These species co-occur with some wide range species: *Cuneolina pavonia, C. parva, Nezzazatinella picardi, Valvulammina* sp.*, Marsonella* sp. and miliolids div. sp. (Figures IX.4.1.a, IX.4.1.g).


1
500 µm
2
500 µm
3
500 µm
4
500 µm
5
400 µm
6
400 µm
7
400 µm
8
400 µm
9
400 µm
10
300 µm
11
300 µm
12
150 µm
13
150 µm
14
300 µm
15
400 µm
16
400 µm
17
250 µm
18
250 µm
19
300 µm
20
500 µm
21
400 µm
22
400 µm
23
400 µm
24
400 µm
25
400 µm
26
400 µm
27
300 µm
28
200 µm
29
300 µm
30
300 µm
31
200 µm
32
300 µm
33
300 µm
34
400 µm
35
400 µm
36
200 µm
37
125 µm
38
300 µm
39
500 µm
40
300 µm
41
500 µm
42
300 µm
43
300 µm
44
200 µm
45
300 µm
46
150 µm
47
150 µm
48
300 µm
49
500 µm
50
300 µm

Figure IX.4.1.h: Benthonic foraminifera of the Late Cenomanian *Vidalina radoicicae* range zone: (1 and 2) *Sellialveolina drorimensis*, (1) [es], (2) [sas], (Al-Meten). (3 and 4) *Chrysalidina gradata*, [ls], (Al-Meten). (5, 6, 7 and 9) *Orbitolina sefini*, (5, 6) [as], (7) [os], (9) [sas], (Wadi Al-Haddah). (8) "*Taberina" bingistani* [ses] (Wadi Al-Haddah). (10) *Peneroplis parvus* [es](Al-Meten, Wadi Al-Haddah). (11) *Coxites zubairensis* [sas] (Al-Meten). (12) *Binconcava bentori* [sas] (Al-Meten, Wadi Al-Haddah, Slenfeh/Bab-Abdallah). (13, 21 and 22) *Merlingina cretacea*, (13) [sas], (21) [es], (22) [as], (Al-Meten, Wadi Al-Haddah). (14) *Montsechiana* sp.? [es] (Slenfeh/Bab-Abdallah). (15, 16, 44 and 45) *Pseudorhipidionina casertana*, (15) [es], (16) [as], (44, 45) [os], (Wadi Al-Haddah). (17 and 18) *Dicyclina* sp., (17) [ses], (18) [sas], (Slenfeh/ Bab-Abdallah). (19) *Ammocycloloculina erratica* [sas] (Al-Meten). (20, 48, 49 and 50) *Dicyclina qatransis* (20) [sas], 48, 50) [as], (49) [ses], (Al-Meten). (23, 24 and 32) *Nezzazata gyra*, (23, 24) [sas] (Wadi Al-Haddah), (32) [sas] (Al-Meten). (25 and 26) *Pseudolituonella reicheli* (25) [ls], (26) [as], (Wadi Al-Haddah). (27) *Trochospira avnimelechi* [ses] (Slenfeh/ Bab-Abdallah). (28) *Lenticulina* cf. *rotulata* [sas] (Wadi Al-Haddah). (29 and 30) *Lenticulina* cf. *muensteri*, (29) [sas], (30) [es] (Bab-Abdallah). (31) *Lenticulina* sp. [sas] (Wadi Al-Haddah). (33) *Nezzazata conica* [sas] (Al-Meten). (34) *Nezzazatinella picardi* [as] (Slenfeh/Bab-Abdallah). (35)*Nezzazata* sp. [as] (Wadi Al-Haddah). (36 and 37) *Nummofallotia* cf. *apula,* (36) [os], (37) [es] (Al-Meten). (38) *Pseudonummoloculina heimi* [es] (Al-Meten). (39, 40 and 41) *Biplanata peneropliformis* [as]. (42 and 43) *Pseudorhapydionina* cf. *dubia*, (42) [es], (43) [as] (Al-Meten). (46) miliolids indet [as] (Al-Meten). (47) *Vidalina radoicicae* [es] (Al-Meten): as= axial section; sas= subaxial section; es= equatorial section; ses= subequatorial section; os= oblique section; as= axial section; sas= subaxial section; es= equatorial section; ses= subequatorial section; os= oblique section; ts= transversal section; ls= longitudinal section.

Correlation: The described biozone correlates with the *Chrysalidina gradata* partial range zone and the *Broeckinella (Pastrikella) balcanica* zone of the Adriatic platform described by Velić (2007). It also correlates with the mid-Cenomanian marker species of the Tethyan realm of Ogg et al. (2008b). This biozone is comparable with the lower part of *Selliaveolina* (*Pseudedomia*) *drorimensis* range zone in the South Palmyrides (Ghanem et al., 2012, Figure IX.4.1.a).

Age and Occurrence: The Middle Cenomanian *Chrysalidina gradata* partial range zone of Coastal Range is determined by the FO of *Chrysalidina gradata* to the FO *Vidalina radoicicae* (Ogg and Ogg, 2008a). This biozone represents Middle Cenomanian 76m thick marly limestones and limestones of the Coastal Range in the Hannafiyah Fm. in section AH (units 22-24) and a ca. 80 m-thick succession of limestones, intercalated with marls and dolostones in section SB (60m of Slenfeh Fm. and 20 of Bab Abdellah Fm. units 22-25) (Figure IX.3.b).

IX.4.1.7 The Late Cenomanian *Vidalina radoicicae* range zone

Diagnosis*:* Total range zone of the zonal marker.

Description: The *Vidalina radoicicae* is delineated by the total range of the zonal marker together with *Selliaveolina drorimensis* and *"Taberina" bingistani,* originally

defined on Tethyan Carbonate Platforms (Loeblich and Tappan, 1988; Velić, 2007). This biozone is associated with several other benthonic taxa like: *Orbitolina sefini*, *Dicyclina sampoi, D. qatarensis, Biplanata peneropliformis*, *Pseudorhapydionina dubia, Pseudorhipidionina casertana*, *Montsechiana* sp.?, *Chrysalidina gradata, Nummofallotia apula, Spiroloculina cenomana, Ammocycloloculina erratica, Trochospira avnimelechi, Nezzazata gyra, N. conica, Nezzazatinella picardi, Biconcava bentori, Lenticulina* cf. *rotulata, L.* cf. *muensteri Pseudonummoloculina heimi, Nummoloculina regularis, Cuneolina pavonia, C. para* and miliolids div. sp. (Figures IX.4.1.a, IX.4.1.h).

Correlation: The *Vidalina radoicicae* range zone correlates with the same zone of the Adriatic platform (compare Velić, 2007).

Age and Occurrence: According to Velić (2007), the *Vidalina radoicicae* biozone comprises the Upper Cenomanian. It is identified within a 35m thick succession of marls and limestones of the Hannafiyah Formation (section AH units 24-27), 110m thick of marls, dolostones and limestones of the Hannafiyah Formation (Al-Meten section MT, Figure IX.3.b) and 15m of marly limestones and limestones of Bab Abdellah Formation of section SB (units 26-27).

IX.4.2 Planktic foraminifera Biostratigraphy:

A frequent appearance of planktonic foraminifera was noticed in units 12 to 26 of sections SL, AH and MT. The high variety of planktonic foraminifera allows to define seven biozones, based on the first (FO) and last occurrence (LO) of several index taxa. They range from latest Albian to Early Turonian and are well comparable to the standard global assemblages of planktonic foraminifera (Ogg and Ogg, 2008; Premoli Silva and Verga, 2004).

IX.4.2.1 *Rotalipora appenninica* zone (latest Albian)

Diagnosis: Interval zone of *Rotalipora appenninica*.

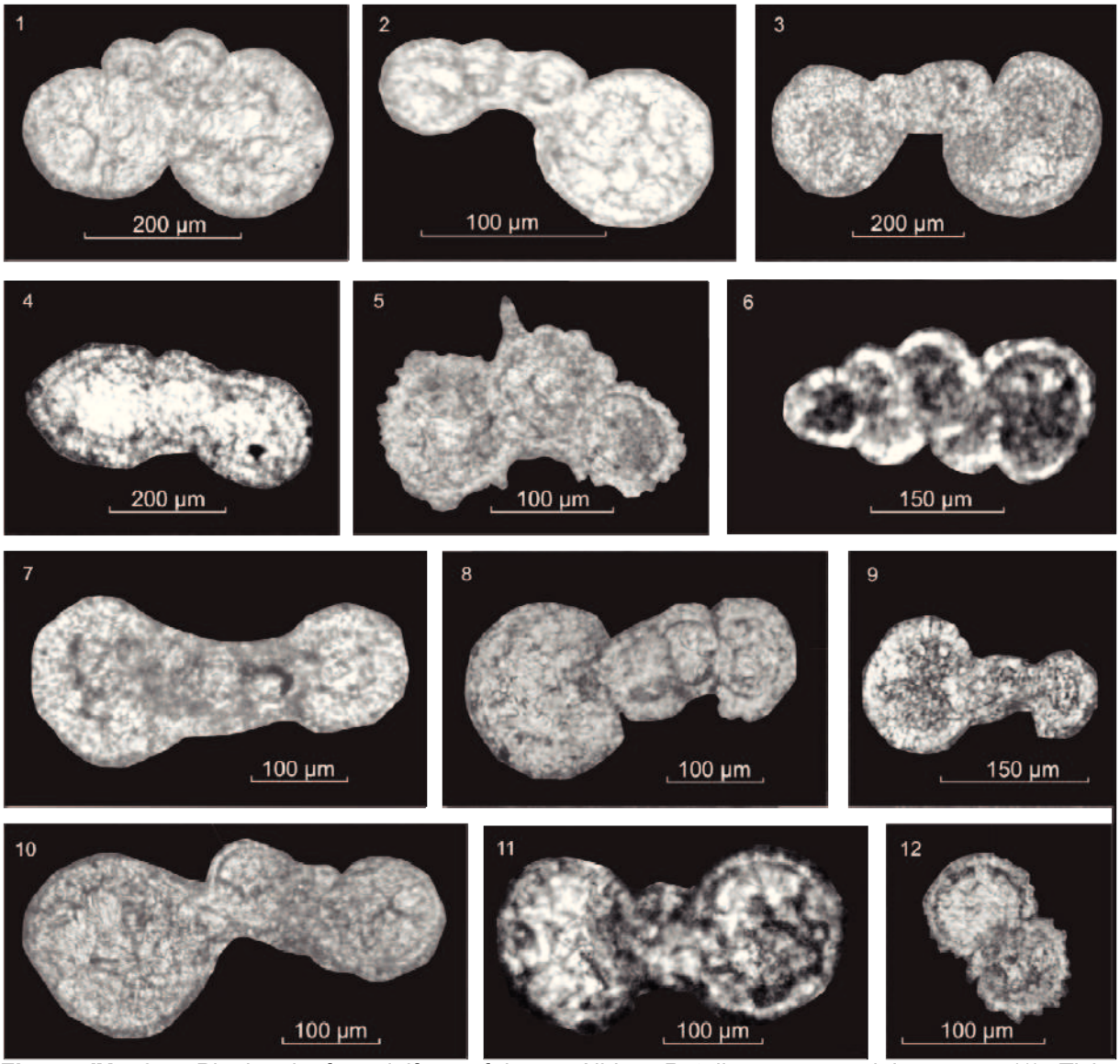

Figure IX.4.2.a: Planktonic foraminifera of latest Albian *Rotalipora appenninica* zone: (1) *Ticinella madecassiana* [as] (SL). (2 and 10) *Muricohedbergella planispira* [as] (SL). (3) *Ticinella praeticinensis* [as] (SL). (4) *Ticinella raynaudi* [sas] (SL). (5 and 12) *Favusella washitensis* [as] (SL). (6) *Heterohelix moremani* [ts] [as] (SL). (7) *Macroglobi-gerinelloides ultramicrus* [as] (SL). (8) *Muricohedbergella albiana* [as] (SL). (9 and 11) *Muricohedbergella* sp. [sas] (SL): as= axial section; sas= subaxial section; ts= transversal section.

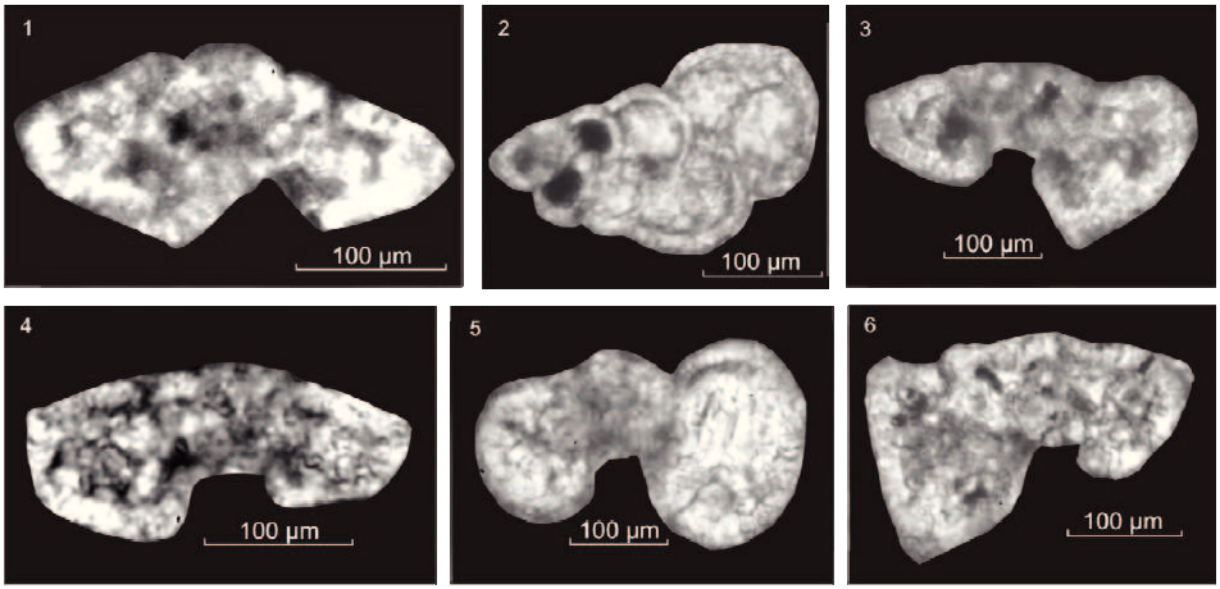

Figure IX.4.2.b: Planktonic foraminifera of Early Cenomanian Rotalipora globotruncanoides zone: (1) *Rotalipora* cf. *globotruncanoides* [as] (SB). (2) *Heterohelix moremani* [ts] (SB). (3) *Praeglobotruncana* cf. *delrioensis* [as] (SB). (4) *Rotalipora montsalvensis* [sas] (SL). (5) *Muricohedbergella delrioensis* [sas] (SL). (6) *Rotalipora gandolfi* [sas] (SL): as= axial section; sas= subaxial section; ts= transversal section.

Description: The marly limestones of that biozone are characterized by the FO of *Rotalipora appenninica,* associated with the Late Albian index species such as *Muricohedbergella albiana*, *Ticinella raynaudi* and *T. madecassiana* (Premoli Silva and Verga, 2004, Premoli Silva, et al. 2009). Those co-occur with some wide range species: *Muricohedbergella planispira*, *Heterohelix moremani, Rotalipora gandolfii, Macroglobigerinelloides ultramicrus* and *Favusella washitensis* (Figures IX.4.1.a, IX.4.2.a).

Correlation: The described assemblage holds several index species of the *Rotalipora appenninica* zone of the standard global planktonic foraminifera (Ogg and Ogg, 2008; Premoli Silva and Verga, 2004).

Age and Occurrence: Premoli Silva and Verga (2004) and Ogg et al. (2008) attributed a latest Albian age for that biozone. In the present study, the *Rotalipora appenninica* biozone occurs in a 50-m-thick succession of marly limestones, limestones and dolostones, corresponding with units 12- 16 of the Ain Elbeida Formation in section SL (Figure IX.3.a).

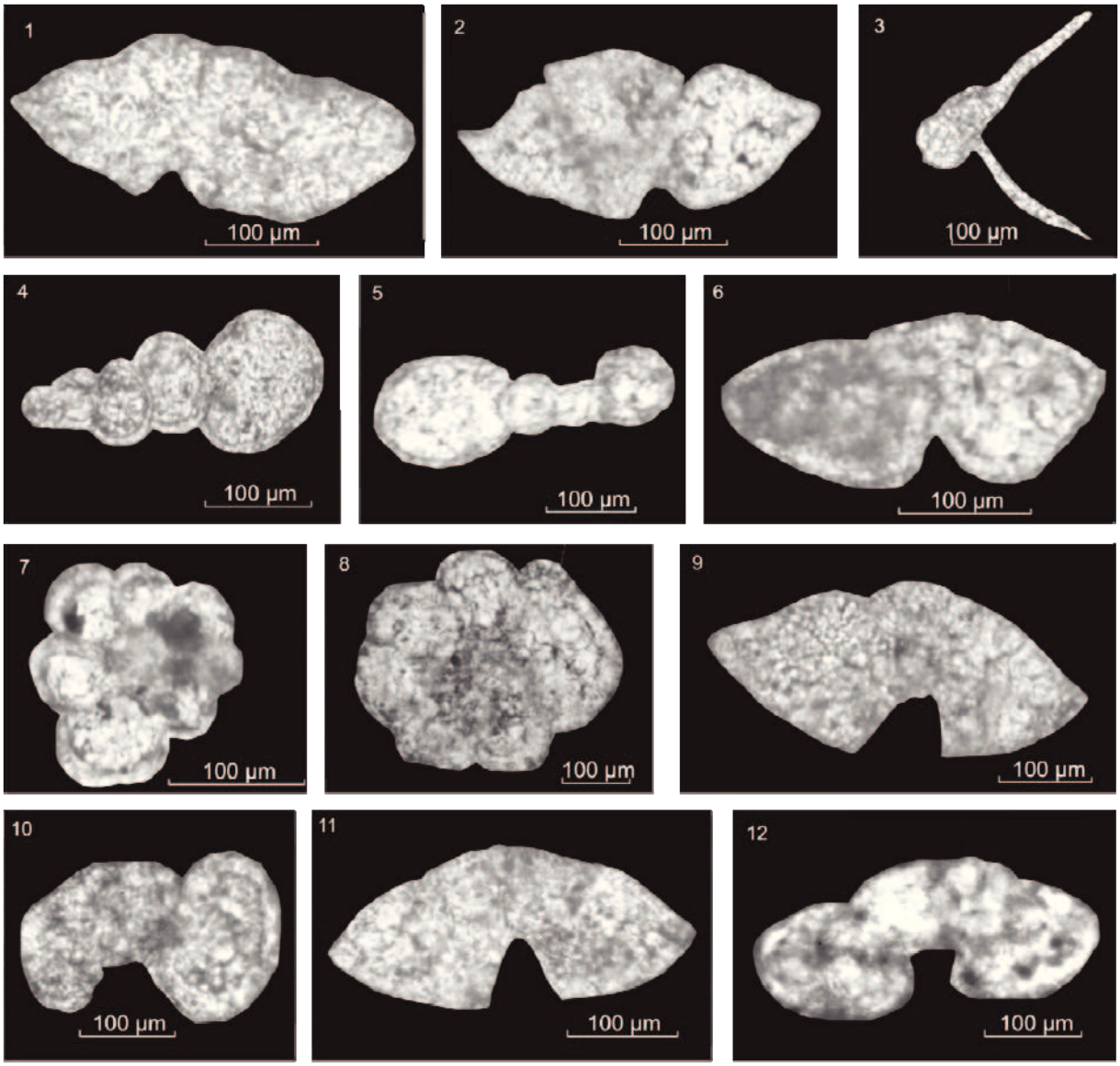

Figure IX.4.2.c: Planktonic foraminifera of early Middle Cenomanian *Rotalipora reicheli* zone: (1, 8, 9 and 11) *Rotalipora reicheli*, (1, 9, 11) [as] (AH), [es] (SB). (2 and 6) *Rotalipora appenninica* [as] (AH). (3) *Schackoina bicornis* [sas] (AH). (4) *Heterohelix moremani* [ts] (AH). (5) *Macroglobigerinelloids caseyi* [as] (AH). (7) *Macroglobigerinelloids ultramicrus* [es] (AH). (10) *Muricohedbergella delrioensis* [as] (SB). (12) *Praeglobotruncana delrioensis* [as] (SB): as= axial section; sas= subaxial section; es= equatorial section; ts= transversal section.

IX.4.2.2 *Rotalipora globotruncanoides* zone (Early Cenomanian)

Diagnosis: Interval zone comprising the range between the FO of the zonal marker to the FO of *Rotalipora reicheli.*

Description: The following planktic foraminifera co-occur together with the zonal marker: *Rotalipora globotruncanoides, R. gandolfii, R. montsalvensis, Macroglobigerinelloides ultramicrus*, *M. "caseyi", Heterohelix moremani,*

Muricohedbergella planispira and *Praeglobotruncana delrioensis* (Premoli Silva and Verga, 2004, Premoli Silva, et al. 2009, Figures IX.4.1.a, IX.4.2.b).

Correlation: The described *Rotalipora globotruncanoides* zone of the Coastal Range correlates with the same zone of the standard global planktonic foraminifera (Premoli Silva and Verga, 2004; Ogg and Ogg, 2008).

Age and Occurrence: The *Rotalipora globotruncanoides* zone corresponds to the Early Cenomanian (Premoli Silva and Verga, 2004; Ogg and Ogg, 2008). This biozone is evident in 79 m thick marly limestones, alternating with limestones and dolomites of units 17- 19 and the lower part of unit 20 of the Slenfeh Formation in sections SL and SB.

IX.4.2.3 *Rotalipora reicheli zone* (Middle Cenomanin)

Diagnosis: Total range zone of the zonal marker (Ogg and Ogg, 2008).

Description: This zone is delineated by *Rotalipora reicheli*, associated with *R. montsalvensis, R. appenninica, R. micheli, R. globotruncanoides, Macroglobigerinelloides"caseyi"*, *M. ultramicrus, M. bentonensis, Heterohelix moremani, Praeglobotruncana delrioensis, Muricohedbergella planispira M. simplex, M. delrioensis, Loeblichella hessi* and *Schackoina bicornis* (Premoli Silva and Verga, 2004, Premoli Silva, et al. 2009) (Figures IX.4.1.a, IX.4.2.c).

Correlation: The *Rotalipora reicheli* biozone in the Syrian CR correlates with the standard global zone, defined by Premoli Silva and Verga (2004) and Ogg and Ogg (2008) (Figure IX.4.1.a).

Age and Occurrence: This biozone was attributed to the early Middle Cenomanian according to Premoli Silva and Verga (2004) and Ogg and Ogg (2008). The *Rotalipora reicheli* biozone appears in 24m thick marly limestones in the upper part of Slenfeh Formation (unit 21 of section SB). It also occurs in 13m thick chalky limestones of unit 21 of Hannafiyeh Formation (lower part of section AH).

IX.4.2.4 *Rotalipora cushmani* zone (Late Cenomanian)

The *R. cushmani* total range zone corresponds to the upper Middle to Late Cenomanian (Premoli Silva and Verga, 2004; Ogg and Ogg, 2008). This biozone contains two

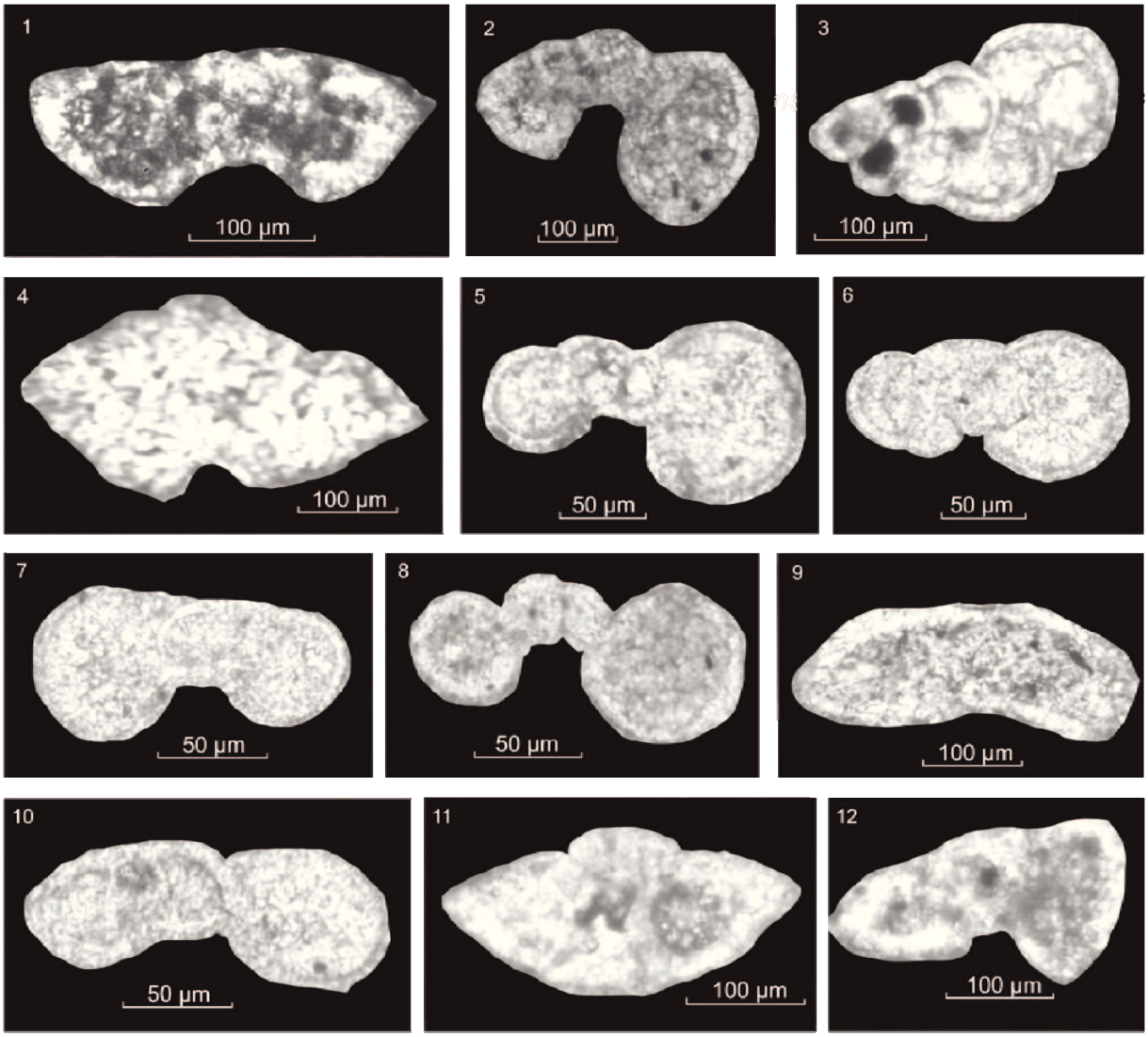

Figure IX.4.2.d: Planktonic foraminifera of late Middle Cenomanian Rotalipora *greenhornensi* subzone (*Rotalipora cushmani* zone): (1) *Rotalipora greenhornensis* [as] (SB). (2) *Muricohedbergella delrioensis* [as] (SB). (3) *Heterohelix moremani* [ts] (SB). (4) *Rotalipora cushmani* [as] (AH). (5 and 6) *Loeblichella hessi*, (5) [as], (6) [sas] (AH). (7 and 10) *Muricohedbergella simplex* [as] (AH). (8) *Muricohedbergella planispira* [as] (AH). (9) *Rotalipora montsalvensis* [sas] (SB). (11) *Rotalipora appenninica* [as] (AH). (12) *Rotalipora* sp. [as] (SB): as= axial section; sas= subaxial section; ts= transversal section.

subzones: *Rotalipora greenhornensis* Subzone and *Dicarinella algeriana* Subzone, both defined by Premoli Silva and Verga (2004) (Figure IX.4.1.a).

A- Rotalipora greenhornensis Subzone (late Middle Cenomanian)

Diagnosis: Interval subzone ranging from the FO of *Rotalipora greenhornensis* and *R. cushmani* to the FO of *Dicarinella algeriana*.

Description: the *Rotalipora greenhornensis* subzone is delineated by the sub-zonal marker together with *R. cushmani,* associated with *R. montsalvensis, R. appenninica, Muricohedbergella planispira, M. simplex, Heterohelix moremani, Praeglobotruncana delrioensis, Macroglobigerinelloides bentonensis, M. ultramicrus* and *Loeblichella hessi* (Premoli Silva and Verga, 2004, Premoli Silva, et al. 2009) (Figures 6, IX.4.2.).

Correlation: This subzone is comparable with the Middle Cenomanian part of *R. cushmani* zone of Premoli Silva and Verga (2004) and Ogg and Ogg (2008), and correlated with the *Rotalipora greenhornensis* subzone after Premoli Silva and Verga (2004).

Age and Occurrence: The *Rotalipora greenhornensis* subzone indicates the late Middle Cenomanian (Premoli Silva and Verga, 2004). It occurs in 47m of chalky limestones with chert and dolostones from the uppermost part of unit 21 to unit 24 of Hannafiyeh Formation of section AH. This subzone is also present in units 22- 25 of Slenfeh Formation and Bab Abdallah Formation of section SB.

B- *Dicarinella algeriana* Subzone (Late Cenomanian)

Diagnosis: Interval subzone comprising the range between the FO of the *Dicarinella algeriana* to the FO of *Whiteinella archaeocretacea* or the LO of *Rotalipora cushmani*.

Description: The FO of *Dicarinella algeriana* is accompanied by the gradual disappearance of Genus *Rotalipora* to the end of this Subzone and by the diversification of species of *Whiteinella,* including *W. baltica, W. aprica, W. paradubia, W. praehelvetica, W. aumalensis,* associated with *W. brittonensis,Heterohelix reussi, H. moremani, Rotalipora cushmani, R. montsalvensis, Muricohedbergella planispira, Macroglobigerinelloides bentonensis, M. ultramicrus* and *Praeglobotruncana delrioensis* (Figures IX.4.1.a, IX.4.2.e).

Correlation: Both, the marker species and the planktonic assemblage correlate with the upper *Rotalipora cushmani* zone, defined by Ogg and Ogg (2008a) and correlate with the *Dicarinella algeriana* subzone according to Premoli Silva and Verga (2004).

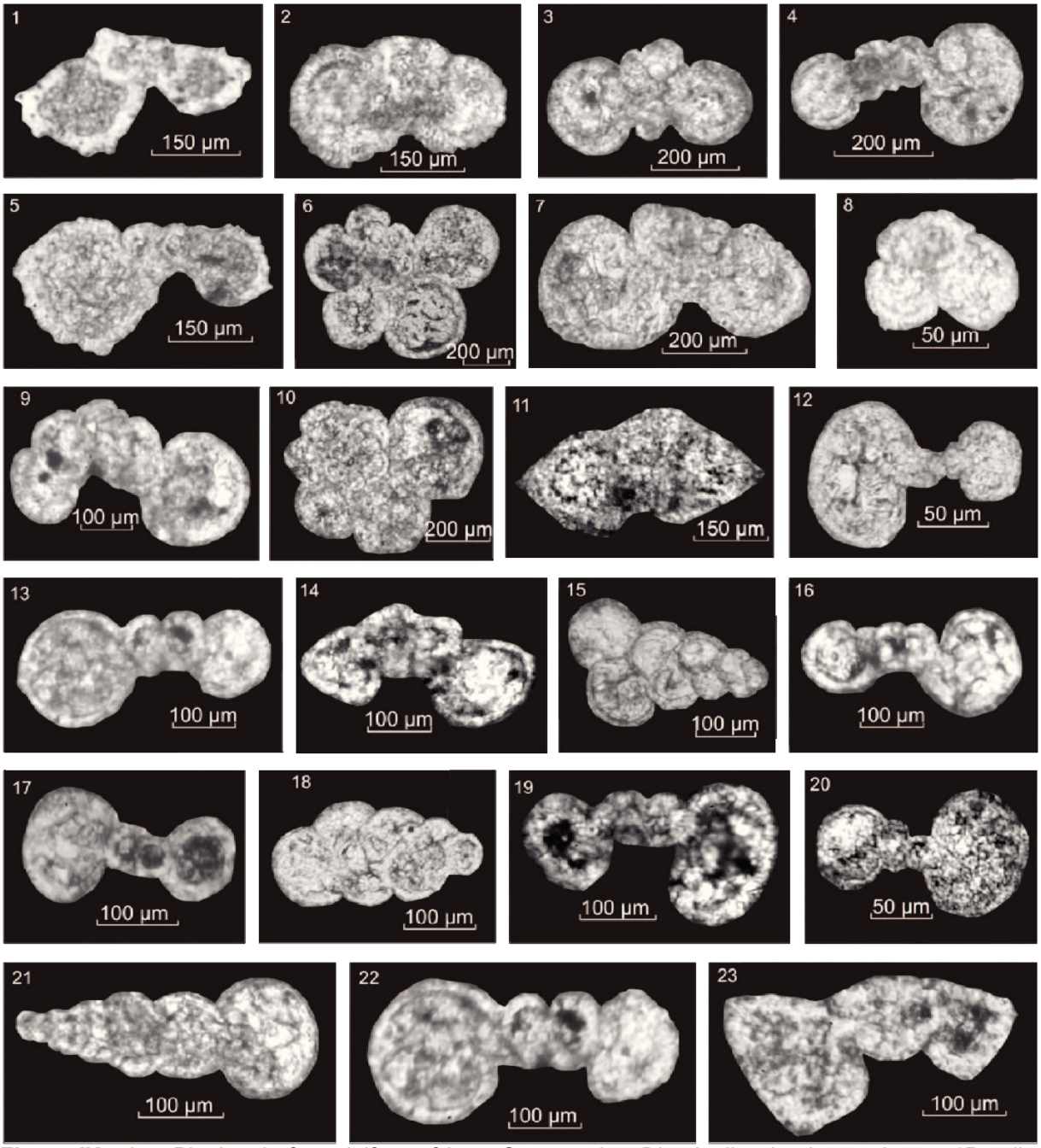

Figure IX.4.2.e: Planktonic foraminifera of Late Cenomanian *Dicarinella algeriana* subzone (*Rotalipora cushmani* zone): (1 and 5) *Dicarinella algeriana* [as] (SB). (2 and 3) *Whiteinella baltica* [as] (SB). (4, 7 and 13) *Whiteinella praehelvetica* [as] (SB). (6 and 10) *Whiteinella* sp. [es] (SB). (8) *Whiteinella* cf. *paradubia* [sas] (AH). (9) *Whiteinella brittonensis* [as] (SB). (11) *Rotalipora* cf. *cushmani* [as] (AH). (12 and 20) *Macroglobigerinelloides bentonensis* [as], (12) (SB), (20) (AH). (14) *Praeglobotruncana delrioensis* [as] (SB). (15 and 21) *Heterohelix reussi* [ts] (AH). (16 and 19) *Muricohedbergella planispira* [as] (AH, SB). (18) *Heterohelix moremani* [ts] (SB). (22) *Whiteinella aprica* [as] (AH). (23) *Rotalipora* sp. [as] (AH): as= axial section; sas= subaxial section; es= equatorial section; ses= subequatorial section; ob= oblique section; ts= transversal section.

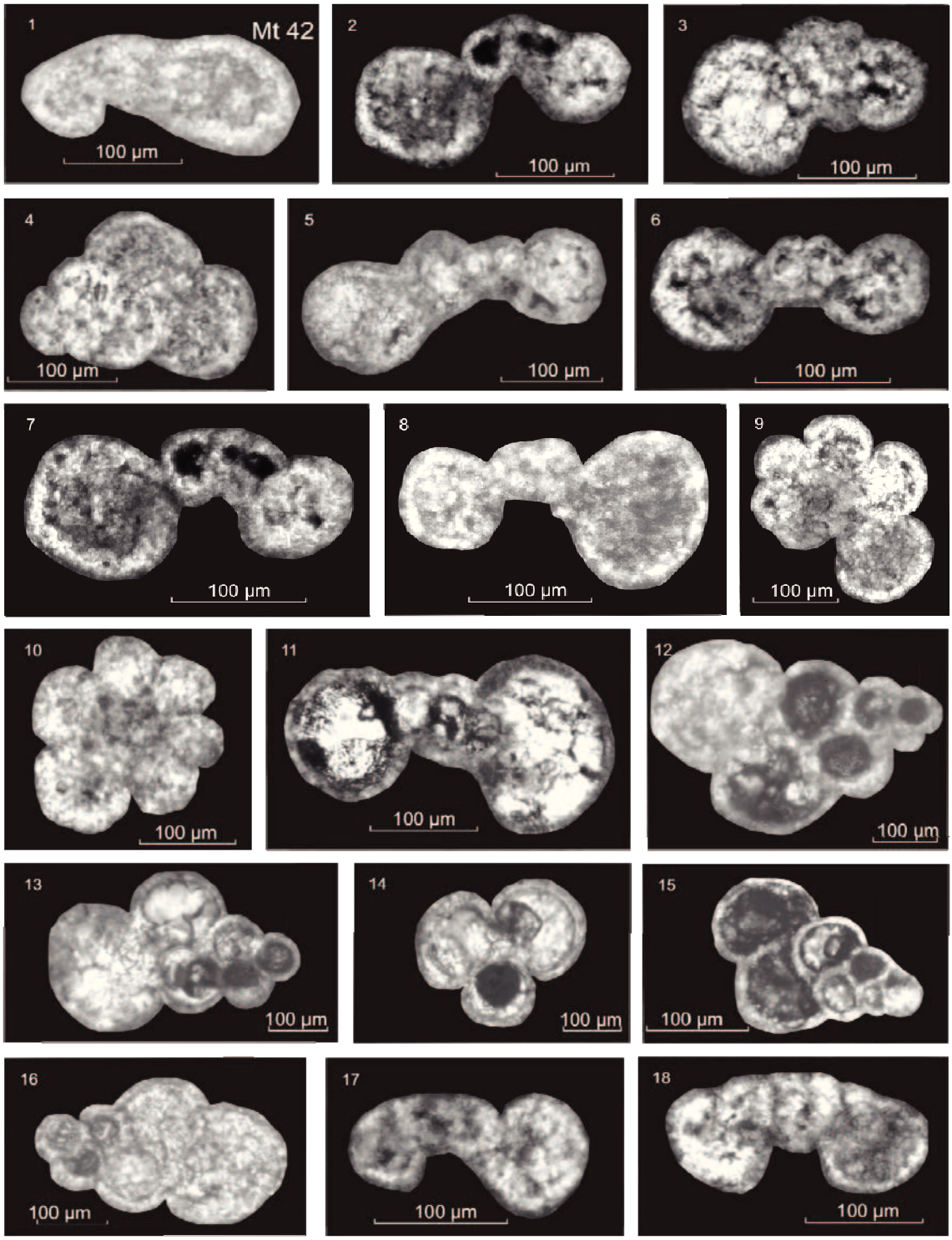

Figure 19: Planktonic foraminifera of latest Cenomanian Early Turonian *Whiteinella archaeocretacea* zone and *Helvetoglobotruncana helvetica* zone: (1 and 9) *Whiteinella archaeocretacea* [as], [es] (MT). (2, 7, 11 and 18) *Muricohedbergella delrioensis* [sas] (MT). (3) *Whiteinella baltica* [as] (MT). (4 and 15) *Heterohelix moremani* [ts] (MT, SB). (5) *Whiteinella* cf. *praehelvetica* [sas] (MT). (6) *Whiteinella aprica* [as] (MT). (8) *Muricohedbergella planispira* [as] (MT). (10) *Hedbergella* sp. [ses] (AH). (12, 13 and 14) *Heterohelix globulosa* [ts], (14) [es] (SB). (16) *Heterohelix reussi* [ts] (SB): as= axial section; sas= subaxial section; es= equatorial section; ses= subequatorial section; ob= oblique section; ts= transversal section.

Age and Occurrence: The *Dicarinella algeriana* subzone corresponds to the Late Cenomanian (Premoli Silva and Verga, 2004). It occurs in units 24- 27 of the Hannafiyeh Formation of section AH and units 26- 27 of Bab Abdallah Formation (section SB).

IX.4.2.5 *Whiteinella archaeocretacea* Zone (latest Cenomanian to earliest Turonian)

Diagnosis*:* This biozone is defined by the FO of the zonal markers.

Description: This zone is delineated by *Whiteinella archaeocretacea,* associated with *W. baltica, W. aprica, W. praehelvetica, Heterohelix moremani, H. reussi, Muricohedbergella planispira, M. delrioensi* and *Hedbergella* sp. (Figure IX.4.2.f).

Correlation: This biozone coincides with the Cenomanian - Turonian boundary interval (Ogg and Ogg, 2008) and was correlated with the *W. archaeocretace* biozone after Premoli Silva and Verga (2004).

Age and Occurrence: The *W. archaeocretace* biozone corresponds to the Cenomanian - Turonian boundary (Premoli Silva and Verga, 2004; Ogg and Ogg, 2008). It is appears in 30m of platy limestones of unit 27 of Hannafiyeh Formation, including the upper dolostones of unit 27 of Bab Abdallah Fm. (Figures IX.3.b, IX.4.2.f). The overlying (pelagic) limestones of the Aramo Formation contain associations of younger planktonic foraminifera (*Helvetoglobotruncana helvetica* zone).

IX.4.2.6 *Helvetoglobotruncana helvetica* Zone (Early Turonian)

Diagnosis: This interval zone is here defined by the first occurrence of *Hetrohelix globolusa* - the nominal taxon is missing.

Description: This zone is delineated by associated index forms such as the *Hetrohelix globolusa*, *H. reussi. H. moremani, Hedbergella* sp., and *Muricohedbergella delrioensis* (Figure IX.4.2.f).

Correlation: This biozone in the North CR correlates with the *Helvetoglobotruncana helvetica* zone, defined by Premoli Silva and Verga (2004) and Ogg et al. (2008) (Figure IX.4.1.a).

Age and Occurrence: This biozone was attributed to the Early Turonian (Premoli Silva and Verga, 2004; Ogg and Ogg, 2008). It was evidenced in ca. 20m thick white limestones of Aramo Formation in the upper part section Slenfeh (Figures IX.3.b, IX.4.2.f).

IX.5 SEQUENCE STRATIGRAPHY

The Aptian-Early Turonian succession at the Coastal Range is characterized by a cyclic organization at different scales of sequences and cycles. Each of these hierarchical cycles and their bounding surfaces are interpreted to be unique chronostratigraphic entities that developed through rising–falling sea level. The here defined sequences are based on the lateral comparison of stratigraphic sections and their stacking patterns within a high resolution biostratigraphic frame. The applied genetic model of sequence stratigraphy is derived mainly from field observations and thin section analysis. A multitude of high frequency cycles and (half) cycles are defined by changes of the depositional environments that are expressed in different sedimentary facies associations. Comparisons with the “global sequence stratigraphy” (Hardenbol et al., 1998; Ogg and Ogg, 2008) and the “Arabian Platform sequence stratigraphy” (Sharland et al., 2001, 2004; van Buchem et al., 2010, 2011), allows to interprete eleven Coastal Range sequences (two Aptian 2nd order sequences (ApCR1 and 2), four Albian 2nd order sequences (AlCR1-4), and five Cenomanian to Early Turonian 3rd order sequences (CeCR1-5). These sequences are tied by biostratigraphic criteria to the Arabian maximum flooding surfaces (K) of van Buchem et al. (2010, 2011), to the global sequences boundaries of Ogg et al. (2008), and to sequence boundaries of the neighbouring South Palmyrides (Ghanem et al., 2012). The here described 2nd/3rd order sequences are composed of higher frequency (half) cycles (Figures IX.3.a, IX.3.b, IX.5). Their vertical stacking patterns and lithologic characteristics (including microfacies data) support our new sequence stratigraphic

interpretations, including some “Syrian mfs” (e.g. K81S). A major outcome of this study is a unified sequence stratigraphic model, which significantly increases the chronostratigraphic resolution for the Aptian-Cenomanian succession of Coastal Range (western Syria).

IX.5.1 Sequence ApCR1 (including K80)

The Upper Jurassic carbonate rocks are separated from the overlying Lower Aptian by a regional unconformity that forms the lower boundary of the first Lower Cretaceous (Aptian) sequence of the Coastal Range (ApCR1). This sequence corresponds to the lower Bab Janneh Formation (units 1-4) in the North Coastal Range of section SY and in the South CR (section WL). A lower Aptian age is confirmed by benthonic foraminifers assemblages of the long range *Pseudocyclammina vasconica* biozone (compare Figures IX.4.1.a, IX.5).

Sequence ApCR1 represents two Lower Aptian shallowing/deepening-up cycles in both sections SY and WD (Figures IX.3.a, IX.4.2.d). The basal cycle of section SY represents a deepening-up trend with green marls (rich in bivalves and echinids). The overlying limestones are composed of grainstones to packstones with bioclasts, ooids, benthonic foraminifera and green algae that are attributed to a shallowing-up cycle (unit 2 of section SY). A second shallowing/deepening-up cycle above correlates with a major mfs (maximum flooding surface) that was compared with mfs K80 of van Buchem et al. (2010), based on biostratigraphic comparisons. Dolomite-limestone intercalations above are characterized by high energetic microfacies (grainstones) with benthonic foraminifera, bioturbations and may thus form the shallowest part of ApCR1 of section SY. They correlate with sandy limestones/sandstones and dolomitic limestones of section WL (Figures IX.3.a, IX.4.1.d).

The lower Aptian sequence boundaries Ap1 to Ap3 of Ogg et al. (2008) are comparable to the disconformable lower contact of ApCR1 at the Upper Jurasic- Lower Aptian boundary of the Coastal Range. Mfs K80 of van Buchem et al. (2010) is interpreted to correlate with the upper green marls above (Figure IX.3.a).

IX.5.2 Sequence ApCR2 (including K81S)

The lower boundary of the ApCR2 in the North CR (section SY) is determined by a hardground surface, associated with a thin caliche interval. This boundary coincides with the Early/Late Aptian boundary and is comparable with the global sequence boundary Ap5 according to Ogg et al. (2008a, b) (IX.3.a, IX.4.1.d).

Sequence ApCR2 is correlated with the upper Bab Jahaneh Formation and the lower part of Ain Elbeida Formation in the SY section, and with the upper Bab Jahaneh Formation in the WL section of the South Coastal Range. Up to five shallowing/ deepening-up cycles can be recognized in the North Coastal Range (SY section) that are comparable with only one deepening-up cycle in the South Coastal Range (section WL). The lower three cycles of section SY are composed of fossiliferous green marls intercalated with thin bedded fine to coarse grained limestones. The latter hold mollusks, ooids, bioclast and benthonic foraminifera. The shallowing-up cycles include marls and dolostones in the North CR. In the South CR (section WL) fossiliferous green marls with thin deltaic? sandstones prevail in section WL (Figure IX.3.a).

The global mfs between SB`s Ap5 and of Ap6 of Ogg et al. (2008) is correlated with ammonite-bearing limestones (with planktonic foraminifera) of section SY, respectively with a mollusk-rich interval of the upper green marls of section WL (Figure IX.3.a) and to marls of the lower Zbeideh Formation of the Southern Palmyrides (K82S) (Figure IX.5).

IX.5.3 Sequence AlCR1 (including K82S)

The lower boundary of AlCR1 may be erosional, as evidenced by mixing of caliche and synsedimentary karstic filling (section SY). It is, moreover, delineated by a rapid facies change from a stromatolitic (laminated) and dolomitic facies (below) to intertidal/shallow subtidal limestones (above); the latter are attributed to a deepening-up cycle (Figure IX.3.a). In section WL, however, the lower boundary of AlCR1 is obscured by covered outcrop. The Early Albian sequence boundary AlCR1 correlates well with SB Al1 of Ogg et al. (2008b), based on biostratigraphic comparisons.

Sequence AlCR1 corresponds to the lower part of the Ain Elbeida Formation in the northern CR and to most of the Blaatah Formation in the South CR. It is represented by

a major deepening/shallowing-up cycle in both sections SY and WL. The transgressive part in section SY is characterized by thin bedded oolithic grainstones to packstones. These limestones hold benthonic foraminifera, green algae and bioclasts, indicating open lagoonal environments. The overlying shallowing-up subcycle contains packstone-wackestones with miliolids, laminated dolo-peloidal or pure dolostones (Figure IX.3.a).
In section SY the mfs K83S of sequence AlCR1 is delineated on top of an interval of nodular limestones, containing *Orbitolina* spp. of *Mesorbitolina subconcava* zone**.** Mfs K83S may correlate with the mfs of sequence Al1of the Tethyan realm (Ogg et al., 2008).

IX.5.4 Sequence AlCR2 (including K100)

SB AlCR2 has been identified in both studied sections SY and WL by a sharp vertical facies change from dolostones (including restricted peritidal carbonates) to pure limestones that represent mid-ramp environments (Figure IX.3.a). This SB is correlated with the Early Albian global SB Al3 of Ogg et al. (2008).
The varying sediments of sequence AlCR2 (including basaltic rocks) represent the upper part of the Early Albian Ain Elbeida Formation (section SY), correlated with the upper part of Blaatah Formation (underlying the basalt Mouty et al., 1992 of section WL (Figures IX.3.a, IX.4.1.d).
The cyclic stacking patterns of sequence AlCR2 of both sections SY and WL exhibits three shallowing/deepening-up cycles in section SY (plus two deepening-up cycles). They are correlated with one minor deepening/shallowing-up cycle in section WL. The latter is composed of thin to massive well bedded and nodular limestones with abundant benthonic foraminifera, bioclasts, ooids and echininids in the nodular beds. Within the three cycles of section SY several rhytmically beds of dolostones and dolomitized limestones with rudists are intercalated (Figure IX.3.a).
In both sections SY and WL a major intra-AlCR2 hiatus is represented by volcanic rocks: An up to 3m thick basalt (Joubet Barghal, Figure IX.3.d.h) was dated 108.9my (+/- 2.6) by Mouty et al. (1992); it is overlain by ca. 50m thick late Albian strata of sequence ALCR3 that are, however, completely missing in the South CR. Instead, an up to 24m thick basalt flow rests disconformably on early Albian limestones of the

Blataah Formation and is disconformable overlain by Early Cenomanian marls of the Slenfeh Formation in section WL (Figures IX.3.a, IX.5). Consequently, we assume a major hiatus around 108.9my that comprises a shorter interval (intra-AlCR2) in the North CR and a much longer interval (AlCR2 to AlCR3) in the south, based on sequence stratigraphic comparisons (Figures IX.3.a, IX.5). On a global scale that intra-Albian volcanic-derived hiatus spans a maximum-interval from Al3 to Al 8 (Ogg et al., 2008); moreover, mfs K90 of van Buchem et al. (2011) lies within that hiatus (Figure IX.5).

Mfs K100 is represented in section SY by nodular limestones with planktonic foraminifera. This mfs lies directly above the Middle/Late Albian boundary, defined by the lower boundary of the *Neoiraqia convexa* zone (Figure IX.4.1.a) and the *Simplorbitolina manasi* zone of Schroeder et al (2010) respectively. It is correlated with K100 (ca. 106 Ma) of van Buchem et al. (2011) and was also evidenced from the South Palmyrides. In the South CR, however, we found no biostratigraphic evidence for that interval, including the whole overlying sequence Al CR3 (Figures IX.3.a, IX.5).

IX.5.5 Sequence AlCR3 (including K110)

Sequence boundary AlCR3 in the North CR is formed by a sharp facies change from rudist–bearing dolostones to open lagoon and inner shelf environments. It may correlate with the Late Albian SB Al8 of Ogg et al. (2008) (Figure19). In the South CR (section WL) no age-equivalent sediments of sequence AlCR3 were evidenced and thus indicate that the 24m thick basalts of section WL (including the hiatal surfaces at its base and top) may have formed contemporaneously, due to sequence stratigraphic interpretations (Figure IX.4.1.d). The basal disconformable contact of the basalts accounts for a correlation with SB AlCR3 (Figures IX.3.a, IX.5).

Sequence AlCR3 corresponds to the upper Ain Elbeida Formation of sections SY and SL. Sequence AlCR3 is composed of one major deepening/shallowing cycle that was subdivided into up to seven smaller cycles (Figure IX.3.a). Three smaller deepening-up and four smaller shallowing-up half-cycles of section SL correlate with one smaller deepening-up cycle and five shallowing-up half-cycles (including one smaller deeping-

up cycle: Figure IX.3.a). The deepening-up cycles of both sections are composed of nodular and well-bedded to laminated, micritic limestones (wacke-/packstone, with planktonic foraminifera). On the other hand, the shallowing-up half-cycles are composed of massive limestones and dolostones with rudists, often characterized by interbedded laminated and bioturbated limestones (Figure IX.3.a).

The Late Albian mfs K110 (van Buchem et al., 2011) corresponds in both sections of the North CR (Slenfeh and Sayno) to an interval rich in planktonic foraminifera of the middle *Rotalipora appenninica* zone. Towards the South Palmyrides, a major hiatus spans that interval (Figures IX.3.a, IX.5).

IX.5.6 Sequence AlCR4 (including K120)

The Late Albian SB AlCR4 is represented by a hardground surface in section SY (Figure IX.3.c.c), while in section SL (southern CR), a major facies change from intertidal to subtidal environments is interpreted to represent that surface. SB AlCR4 lies in the uppermost *Neoiraqia convexa* zone, and thus is well comparable to the global Late Albian SB Al11 of Ogg et al. (2008) and to SB CePL1 of the South Palmyrides (Figures IX.3.a, IX.5).

The Late Albian to Early Cenomanian sequence AlCR4 corresponds to the uppermost Ain Elbeida Formation and lower Slenfeh Formation of both sections SY and SL of the North CR. In the South CR the lower part is missing, due to the hiatus on top of the basalt (section WL Figures IX.3.a, IX.4.1.c).

Sequence AlCR4 is composed of five deepening-up cycles and four shallowing-up cycles in section SL that are correlated with three deepening-up and three shallowing-up subcycles of section SY and with two shallowing-up cycles of section WL (Figure IX.3.a). The lower deepening-up cycles of both sections SY and SL are composed of well-bedded, fine-grained limestones (wacke-/packstones with benthonic foraminifera, green algae and peloids), while the upper deepening-up cycle(s) consist of limestones and marly limestones with planktonic foraminifera. Most shallowing-up cycles are characterized by massive dolomites (with minor lamination), flints, chert nodules and

cauliflower quartz geodes (possibly replacing supratidal evaporates of the late highstand (Chowns and Elkins, 1974) (Figures IX.3.a, IX.3.d.a).

The rapid increase of planktonic foraminifera in unit 17 of sections SY and SL (*Rotalipora globotruncanoides* biozone) corresponds to mfs K120 (van Buchem et al., 2011). It is also evidenced from the South Palmyrides (Ghanem et al., 2012, Figure IX.5)

IX.5.7 Sequence CeCR1 (including K121S)

SB CeCR1 was defined on the top of a massive carbonate unit composed of dolostone-dominated facies. It lies in the middle *Rotalipora globotruncanoides* biozone and thus is well comparable to the lower Cenomanian SB Ce2 of Ogg et al. (2008) (Figure IX.5).

Sequence CeCR1 corresponds to the middle Slenfeh Formation of section SB (Figure IX.3.b) and is composed of five shallowing/deepening-up cycles. The shallowing-up cycles are characterized by unfossiliferous marls, dolostones, marls with rudists and chert nodules, and sandstones in section SB, whereas the deepening-up cycles are marked by marly limestones and limestones (mudstones to packstones with benthonic foraminifera) at the base and by planktonic foraminifera at the top. In the South CR (AH section), the uppermost CeCR1 is represented by two deepening-up subcycles (chalky limestones rich planktonic foraminifera) and only one minor shallowing- up subcycle (an interval of dolostones and limestones with benthonic foraminifera).

The mfs K121S of sequence CeCR1 corresponds to a marly limestone bed, rich in planktonic foraminifera. The latter indicated the upper *Rotalipora globotruncanoides* biozone, and thus corresponds to a major mfs sensu Ogg et al. (2008) between SB`s Ce2 and Ce3 (Figures IX.3.a, IX.3.b, IX.5).

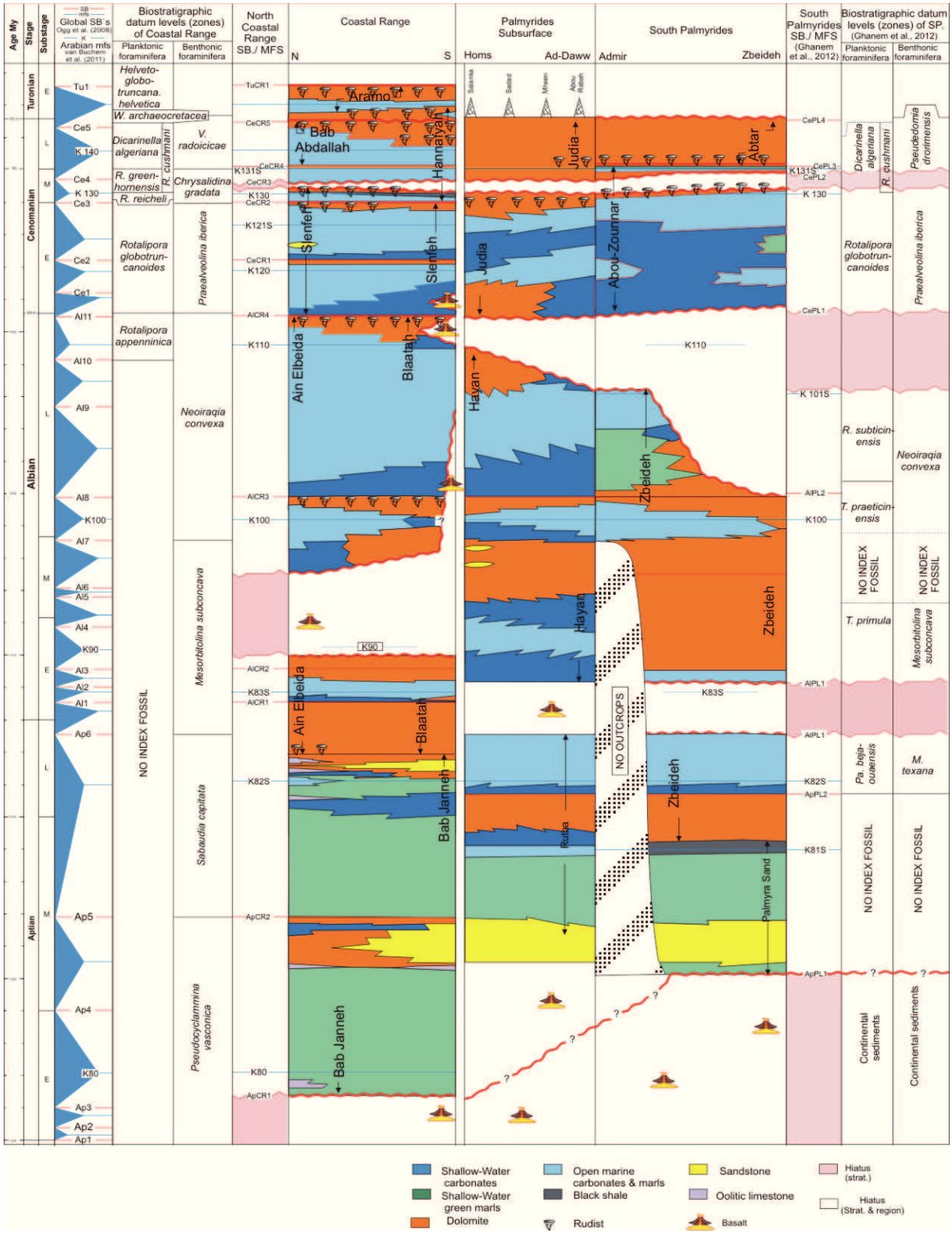

Figure IX.5: Correlation chart of the Aptian-Early Turonian succession based on integrated bistratigraphy and depositional sequences in the Coastal Range (N-S), South Palmyrides of Ghanem et al. (2012) and the subsurface area in between (Ad-Daww and Homs Depressions). Comparison with regional and global sequence boundaries and maximum flooding surfaces on the left. (The subsurface data was provided from the Syrian Petroleum Company).

IX.5.8 Sequence CeCR2 (including K130)

SB CeCR2 is situated at the top of unit 21 that is formed by massive limestones rich in rudists (Figure IX.3.b), which proves for ephemeral deposits and is overlain by more open shelf sediments. This SB lies ca. 15 m above the Early middle Cenomanian boundary of section SB, within the *Rotalipora reicheli* zone and was compared with the global sequence boundary Ce3 according to Ogg et al. (2008) (Figures IX.3.b, IX.5).

Sequence CeCR2 coincides with the upper part of Slenfeh Formation in the northern CR (section SB) and with the lower Hannafiyah Formation in the southern CR (section AH, Figure IX.3.b). We identified four deepening-up cycles in section SB, corresponding to eight deepening-up (half) cycles and plus six shallowing-up cycles in section AH. The deepening-up cycles of both sections are composed of intermediate to thick bedded limestones and marls with thin-walled mollusks, planktonic foraminifera and ammonites, while the shallowing-up subcycles contain massive dolostones rich in rudist in section SB. In section AH, they are composed of dolostones and limestones with benthonic foraminifera and bivalves. Two shallowing-up cycles are topped by two karstic horizons, due to subaerial exposure (Figures IX.3.a, IX.3.c.a); the upper karstification bed represents SB CeCR3 (Figure IX.3.b).

A major Middle Cenomanian mfs sensu Ogg et al. (2008) of the sequence Ce3 coincides with mfs K130 of the Eastern Arabian plate after van Buchem et al. (2011). This mfs corresponds in the CR to nodular limestones at the base of unit 22, rich in planktonic foraminifera of the basal *Rotalipora greenhornensis* subzone of section SB, and to a conspicuous black shale interval (subunit **III** of section AH) with *Lyropecten* sp. and inoceramids (Tröger, pers. comm.) (Figures IX.3.b, IX.3.c.a).

IX.5.9 Sequence CeCR3 (including K131S)

SB CeCR3 is regionally significant and recognized by a paleokarstic surface in the upper R. greenhornensis subzone (section AH, Figures IX.3.a, IX.3.c.a). This unconformity was correlated with the major global SB Ce4 sensu Ogg et al. (2008) and Hardenbol et al. (1998), and may correspond with a similar exposure surface in Iran

(Hajikazemi et al. 2010), Sinai (Gertsch et al., 2010), Egypt (Wilmsen and Nagm 2011) and NW Europe (Wilmsen et al., 2005)(Figure IX.5).

Sequence CeCR3 corresponds to the lower part of Bab Abdallah Formation (section SB), and to the middle part of Hannafiyah Formation in the AH section. It is composed of (nodular) limestones with local flint layers. Vertical stacking patterns reflect three deepening-up and one shallowing-up (half) cycles in the North CR (section SB). They correspond with three deepening-up and one shallowing-up (half) cycles in the South CR (section SB - Figure IX.3.b).

The deepening-up cycles of section AH are characterized by alternating marls (rich in oysters) and limestones with chert nodules and flint lenses (bivalves, corals, ammonites, benthonic and planktonic foraminifera), while nodular limestones, occasionally dolomitized, with planktonic foraminifera prevail in section SB. The shallowing-up cycles indicate regressive trends from shallow shelf to very restricted environments, as indicated by dolostones, rich in rudists (both sections AH and SB).

The upper Middle Cenomanian mfs K131S corresponds in section AH to an interval rich in planktonic foraminifera of the uppermost Rotalipora greenhornensis subzone (Figure IX.3.b).

IX.5.10 Sequence CeCR4 (including K140)

A sharp facies change between massive dolostones (rich in rudists) and overlying nodular limestones with planktonic foraminifera reflects SB CECR4 in the northern and southern CR (Figure IX.3.b). This SB is suggested to lie between both SB`S Ce4 and Ce5 of Ogg et al. (2008) (Figures IX.3.b, IX.5).

Sequence CeCR4 is composed of (nodular) limestones, marls and dolomites; the latter prevail in the upper parts. It corresponds to the upper part of Bab Abdallah Formation of section SB, and to the upper part of Hannafiyah Formation in both sections AH and MT. In the North CR (section SB), sequence CeCR4 is composed of three deepening-up and one shallowing-up cycles (corresponding to the upper part of Bab Abdallah Formation from a section that was previously collected by Mouty and Saint-Marc, 1982).

In the South CR (section MT), sequence CeCR4 a total of 10 deepening-up and 16 shallowing-up (half) cycles were identified (Figure IX.3.b).

The deepening-up cycles in South CR are characterized by nodular and well bedded limestones and marly limestones with chert nodules and flint lenses (especially in the lowermost part), while the upper part of the sequence is characterized by a lagoonal environment. The deepening subcycles of North CR are composed of nodular limestones and marly limestones (with planktonic foraminifera and ammonites). The shallowing-up subcycles are *attributed* by restricted lagoon facies (bioclastic wackestone). They consist of abundant rudist limestones (in both South and North CR) and dolostones, overlain by thin bedded to platy limestones with benthonic foraminifera, mollusks, stromatolites, laminated packstones and dolomites (section MT - Figures IX.3.b, IX.5).

Sequence CeCR4 ranges from the early Late Cenomanian to the Latest Cenomanian (*Dicarinella algeriana* subzone). The rapid increase of planktonic foraminifera in all three sections AH, MT and SB at the middle *Dicarinella algeriana* subzone corresponds to the major Arabian mfs K140 sensu van Buchem et al. (2011); it correlates to the global mfs between SB`s Ce4 and of Ce5 of Ogg et al. (2008).

IX.5.11 Sequence CeCR5

Several thin hardgrounds within the platy limestones of subunit XVI of section MT (South CR) delineate SBCeCR5, coinciding with similar karstic surfaces in the Eastern Arabian Plate (van Buchem et al., 2011). It lies few meters above the base of *Whiteinella archaeocretacea* biozone. The sequence boundary is defined by a sharp facies change from the uppermost dolostones of Bab Abdallah Formation to the deeper shelf limestones of Aramo formation (units 27 and 28 of North CR – Figure IX.3.b). This boundary lies directly below the Cenomanian - Turonian boundary and is comparable with the global sequence boundary Ce5 according to Ogg et al. (2008) (Figures IX.3.b, IX.5).

Sequence CeCR5 is composed of four deepening-up cycles and seven shallowing-up cycles in section MT that are correlated with one deepening-up and shallowing-up cycles of section SB (Figure IX.3.b). The deepening-up subcycles of South CR (MT section) comprises limestones with bivalves (abundant oystars) or planktonic foraminifera, and marls. These transgressive deposits are correlated with deeper shelf limestones and flints with planktonic foraminifera, pelagic echinids, sponges and phosphatic grains in the North CR (Aramo Formation). The overlying massive limestones with rudists indicate restricted environments during a shallowing-up cycle(s) of sequence CeCR5 of both, North and South CR.

The mfs of sequence CeCR5 coincides with an argillaceous marly limestone bed, rich in planktonic foraminifera and siliceous sponges. It represents the lower *Helvetoglobotruncana helvetica* biozone, and thus corresponds to a major mfs sensu Ogg et al. (2008) between SB`s Ce5 and Tu1 (Figures IX.3.a, IX.5).

IX.6 CARBON ISOTOPE STRATIGRAPHY

Carbon isotope fluctuations may reflect global oceanic perturbations and thus are useful proxies for stratigraphic interpretations of shallow water carbonate successions (Parente, et al., 2007). Several authors tested the carbon isotope signals of various Cretaceous carbonate platforms (Grötsch et al., 2002, Vahrenkamp, 1996, 2010) and contributed to an Albian to Turonian reference curve that was recently summarized by Jarvis et al. (2006), where boreal bioevents and global oceanic perturbations are correlated with carbon isotope excursions. Although not all of the here described events occur in the Tethyan Realm (Parente, et al., 2007; Ghanem et al., 2012) several major events of Jarvis et al. (2006) and Kennedy et al. (2004) are well comparable on a global scale.

The studied isotope samples are from four sections of the Coastal Range, spanning a late Albian to Early Turonian interval (Figure IX.6). To exclude diagenetic alteration, all samples were selected from micritic lithologies (after microscopical investigations). The correlation of the four studied sections SL, SB AH, and MT with other references allows for biostratigraphic comparisons and the determination of C_{org}-

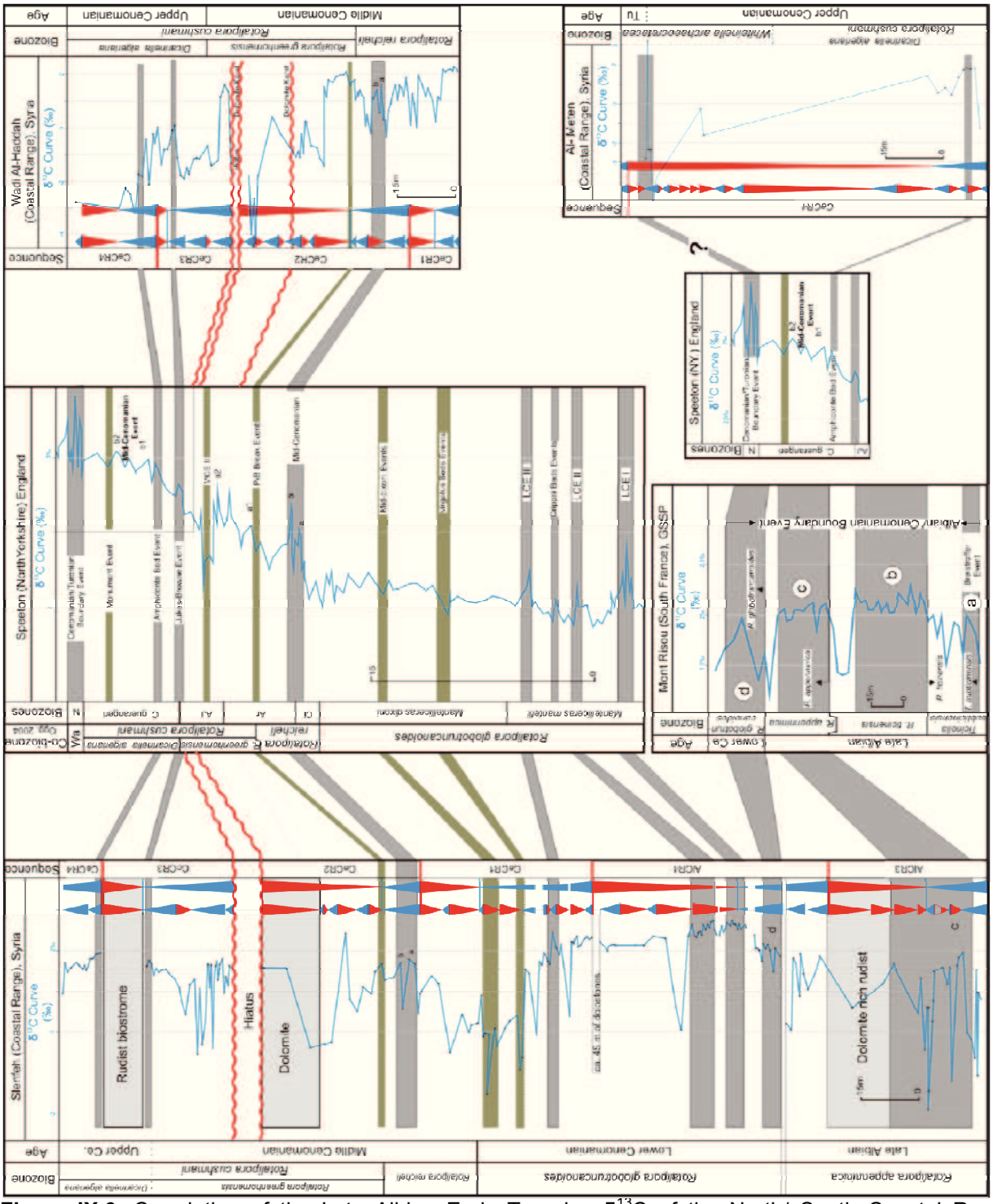

Figure IX.6: Correlation of the Late Albian Early Turonian $\delta^{13}C$ of the North/ South Coastal Range sequences (AlCR3-CeCR4) with the GSSP (global boundary stratotype section and point) of Mont Risou (Kenday et al., 2012) and the Cenomanian events of England (Jarvis e al., 2006).

rich intervals that correlate with major global events (Figure IX.6). We follow Allan and Matthews (1982) for the interpretation of carbon isotope values in a sequence

stratigraphic context. The latter authors suggested that negative $\delta^{13}C$ values may be associated with shallowing, due to alteration by meteoric fluids that resulted in increasing isotopically light carbon from soil zone CO_2 during sea-level fall and subaerial exposure.

IX.6.1 Sequence stratigraphy and diagenetic influence in isotope signature

The late Albian-Cenomanian strata of the Coastal Range were deposited in shallow marine to hemipelagic environments. $\delta^{13}C$ values range from -1.9‰ to 2.5‰ in the northern sections SL/SB and from -4.3‰ to 3.2‰ in the southern sections AT and MT (Figure IX.6) and thus reflect a characteristic range known from marine limestones, dolomitic limestones, and marls (Jenkyns et al., 1994).The carbon isotope record of 6 stratigraphic sequences (Al CR3 to CeCR4) comprises the late Albian to Cenomanian succession of the Coastal Range (Figure IX.5). The main negative isotope excursions are occurring during an interval with several subaerial exposures (compare Hajikazemi et al., 2010).

The late Albian $\delta^{13}C$ excursion during the early *R. appenninica* zone reached maximum values of ca. 2‰ and was compared with peak c of the same age of Mont Risou (Kennedy et al., 2004); it represents the upper part of the Albian/Cenomanian Boundary Event. The following decline of $\delta^{13}C$ values is equivalent to shallower water depths during the upper part of sequence AlCR3 (including dolomitic lithologies).

Sequence AlCR4 starts with similar carbon isotope values during the uppermost *R. appenninica* zone (around 1.5‰), increasing to a first peak during the lowermost *R. globotruncanoides* zone that was correlated with peak d of the Mont Risou (Figure 20). A short decline of the $\delta^{13}C$-values above is followed by rising $\delta^{13}C$-values (around 2.5‰ – Figure IX.6). This interval was subdivided into two positive plateaus (Figure IX.5), probably equivalent to LCE I and LCE II of Jarvis et al. (2006). A short term decrease of $\delta^{13}C$ is correlated with deepening during AlCR4, whereas the topmost 45 m of dolostones have not been sampled (Figure IX.3.b, compare unit 19 of sections SL and SY). Within the upper part of sequence CeCR1, a short positive excursion was correlated with LCE III, while both Events, virgatus and Mid-dixoni of Jarvis et al. (2006)

are reflected by two characteristic negative excursions in the Coastal Range, all within the upper *R. globotruncanoides* zone (Figure IX.6).

At the lower part of sequence CeCR2 (mid *Rotalipora reicheli* biozone), a characteristic double-peak (around 1.8‰) was correlated with peaks a and b of the Mid Cenomanian Event after Jarvis et al. (2006). This event was evidenced from limestones n the North CR, while in the South CR, this event occurs within a 5cm thick bed of marly clays and the overlying marly limestone interval. The P/B Break Event of Jarvis et al. (2006) correlates with a minor increase of $\delta^{13}C$-values at the base of the *R. greenhornensis* zone and is well comparable to a small positive excursion within 40- 60 cm thick black shales, rich in inoceramids and further bivalves (mfs of CeCE2, compare Figure IX.3.c.a) of section AH that correlates with characteristic pelagic marls in section SL (Figure IX.6). In the southern section AH, an abrupt decline of $\delta^{13}C$ coincides with two karstic surfaces and highstand deposition in between, followed by a hiatus above that occurs in both regions, North and South CR (Figure IX.6).

Sequence CeCR3 above is characterized by slightly decreasing $\delta^{13}C$ values, corresponding to a deepening (half) cycle that coincides with the FO of *Dicarinella algeriana* and *Whiteinella* sp. The increasing $\delta^{13}C$ values above reach maximum values of 1.8‰ that are correlated with the Jukes-Browne Event of Jarvis et al. (2006). Dolomitic lithologies prevail in a major rudist biostrome above that correspond to the HST of sequence CeCR3.

Sequence CeCR4 corresponds to the upper *Dicarinella algeriana* zone and may include the expected Cenomanian Turonian Boundary within platy limestones at the top of section MT (Figures IX.3.a, IX.6). Furthermore, it marks an inflection in the long-term $\delta^{13}C$ trend from slightly rising to decreasing values. The short-term rising excursion of the Amphidonte Bed Event of Jarvis et al. (2006) was correlated with a small maximum of $\delta^{13}C$ values during the lower *Dicarinella algeriana* biozone of the upper Cenomanian. Maximum $\delta^{13}C$ values occur in the uppermost platy limestones of sequence CeCR4 of section MT (Figure IX.6) that were correlated with the Cenomanian-Turonian Boundary Event (OAE2).

IX.6.2 Major oceanic events of the Coastal Range (OAE1d, LCE I-III, MCE, P/B break event)

The combination of various biostratigraphic markers (benthonic, planktonic foraminifera (this study), ammonites, inoceramid bivalves (Sorny et al., 2001; and Krasheninnikov et al., 2005) with carbon isotope signals is employed to establish a high-resolution correlation of the latest Albian to the Late Cenomanian successions of the North and South Coastal Range of Western Syria.

IX.6.2.1 OAE1d Event

In the succession studied, a double positive peak near the Albian - Cenomanian boundary (ACB) is correlated with peak c of the GSSP (Global boundary stratotype section and point) of Mont Risou (Gradstein et al., 2004; Kennedy et al., 2004). This correlation is supported by the FO of *Rotalipora appenninica* in the North CR, while the FO of *Rotalipora globotruncanoides* of section SL (North CR) correlates to peak d of the GSSP. The latest Albian to lower Cenomanian boundary of Western Syria is characterized by thick interval from the pelagic limestones of unit 12 to the pelagic marls of unit 17 with the massive dolostones rich in rudists in the middle (Figures IX.3.a, IX.4.1.a, IX.6).

IX.6.2.2 Lower Cenomanian Events (LCEs) I-III

The Lower Cenomanian $\delta^{13}C$ curve of the CR is marked by three well defined positive excursions. In section SL, LCE I reaches 2.73‰; it occurs in light gray marls with *Neostlingoceras cracitanensis* (Sorny et al., 2001) equal to the lower *Mantelliceras mantelli* zone (Jarvis et al., 2006). Following a short decline at the top of the marls above, LCE II attains $\delta^{13}C$ values up to 2.72‰; this excursion is equivalent to chalk-like clayey soft limestones (rich of calcispheres) with flint and cauliflower nodules at the top. In the lower part of section SL, the LCE III occurs within marly limestones of unit f (Figure IX.3.b) with positive $\delta^{13}C$ values (up to 2.47‰); it is supplemented biostratigraphically by a characteristic macrofauna (*Mantelliceras mantelli, Sharpeiceras*

laticlavium, Neithea quinquecostata, *Inoceramus lynchi* after Krasheninnikov et al. (2005) and planktonic foraminifera (upper *R. globotruncanoides* zone –Figures IX.3.a, IX.4.1.a, IX.6).

IX.6.2.3 The Mid- Cenomanian Event (MCE)

The Mid- Cenomanian Event is documented from sections in England, Germany (Wilmsen, 2007), Spain (Paul et al., 1994), Morocco (Gertsch et al., 2010) and Italy (Luciani and Cobianchi, 1999), where it corresponds to the lower part of the middle Cenomanian *Rotalipora reicheli* biozone (Paul et al., 1994; Jarvis et al., 2006; Gertsch et al., 2010). The $\delta^{13}C$ signature of the MCE in both South and North CR is represented by small $\delta^{13}C$ peaks (+1.8‰), that correlate to the mfs of the first cycle of CeCR4. The marker bed of this event is characterized by thin bed of clay with *Rotalipora reicheli*.

IX.6.2.4 Planktonic/Benthonic (P/B) Break event

This Event is characterized by a rapid increase of planktonic foraminifera marking the base of *Rotalipora greenhornensis* subzone (*R. cushmani* biozone) (Paul et al., 1994; Jarvis et al., 2006). However, in the Coastal Range of Syria decreasing δ13C values exhibit an increase of planktonic foraminifera in this interval and above. *Rotalipora* becomes much more abundant within the planktonic foraminiferal assemblages (Jarvis et al., 2006). *Rotalipora cushmani* and *R. greenhornensis* first appear at this level marking the base of the *R. greenhornensis* subzone (*R. cushmani* zone). The marker bed of this event is characterized by the occurrence of small bivalve *Lyropecten* (*Aequipecten*) *arlesiensis* and large *Inoceramus pictus* (South CR - Figure IX.3.c.a) together with the *Rotalipora* spp. in both CR areas.

IX.6.2.5 Jukes-Browne Event

The middle Late Cenomanian is marked by a small maximum in $\delta^{13}C$ values between the lower *Dicarinella algeriana* subzone and the upper *R. greenhornensis* subzone

(Figures IX.4.1.a, IX.6). It represents a good reference for the base of the Upper Cenomanian (Jarvis et al., 2006).

IX.6.2.6 Amphidonte Bed Event

The early Late Cenomanian of the Coastal Range is marked by oyster beds with *Amphidonte* sp. (North CR Krasheninnikov et al., 2005). A similar Upper Cenomanian oyster event, is also present in the South CR in both sections MT and AH (Figure IX.6). The $\delta^{13}C$ excursion of the oyster event may equivalent to the *Amphidonte* Bed Event of Jarvis et al. (2006).

IX.6.2.7 Cenomanian Turonian Boundary Event (OAE2)

The Cenomanian Turonian Boundary Event (OAE_2) carbon isotope record is unknown from shallow-water environments. However, the lagoonal carbonate rocks of Coastal Range correlates with similar platform position in Italy, Portogal, western Moroco, Spain and Mexico. The $\delta^{13}C$ excursion was observed to be comparable with deep-water sections (Parente et al., 2007; Parente et al., 2008; Elrick et al., 2009; Gertsch et al., 2010). Regardless of the negative diagenatic values, the maximum positive δ13C value may be spanning the Cenomanian Turonian Event (Jarvis et al. 2006). The δ13C curves of the section MT shows abrupt breaks such as a pronounced positive excursion of 3.2‰ correlating to shallow marine platy limestones within the *Whiteinella archaeocretacea* bizone interval (Figures IX.4.1.a, IX.6).

IX.7 CONCLUSIONS

This regional stratigraphic review of the Aptian - Early Turonian succession made use of the largest data base available to date in the Coastal Range. The biozonation schemes allow for a much improved regional understanding in the particular phylogenetic lineages of the benthonic and planktonic foraminifera. Benthonic foraminifera are presented in eight associations from Aptian to Early Turonian; 1) the Early Aptian *Pseudocyclammina vasconica* range zone; 2) The Late Aptian *Sabaudia capitata* interval Zone; 3) *Mesorbitolina subconcava* range Zone; 4) The Late Albian *Neoiraqia*

convexa taxon-range zone; 6) The Early Cenomanian *Praealveolina iberica* interval zone; 7) The Middle Cenomanian *Chrysalidina gradata* partial range zone; 8) The Late Cenomanian *Vidalina radoicicae* range zone. Six planktonic foraminiferal biozones are identified from the latest Albian to Early Turonian; 1) latest Albian *Rotalipora appenninica* zone; 2) The Early Cenomanian *Rotalipora globotruncanoides* zone; 3) The Middle Cenomanian *Rotalipora reicheli* zone; 4) The late Middle- Late Cenomanin *Rotalipora cushmani* zone (the late Middle Cenomanin *Rotalipora greenhornensis* Subzone and the Late Cenomanin *Dicarinella algeriana* Subzone); 5) The Cenomanain Turonian boundary zone *Whiteinella archaeocretacea* Zone; 6)The Early Turonian *Helvetoglobotruncana helvetica* zone.

Correlation of the vertical organism's diversity exhibit larger diversities of Aptian-Albian benthonic foraminifera in the North CR, contrasting to low diversities in the coeval strata of the South CR (probably due to shallower water depths). The lower transgressive and the early highstands of the Middle Cenomanian - Early Turonian sequences (South CR) are characterized by high diversities and frequencies of larger benthonic foraminifera. Furthermore, the Late Cenomanian late highstands of the South CR are characterized by thick rudist biostromes. For the North CR, in contrast, deeper shelf conditions are assumed.

Our new stratigraphic observations of the Aptian – Early Turonian carbonate platforms of the northwestern Arabian Plate of Syria (Coastal Range and the Palmyrides:Ghanem et al., 2012) allow for comparisons with those of the Eastern Arabian Plate, recently summarized by van Buchem et al. (2011). Although the detailed lithologic evolution and depositional geometry of both areas differ, the timing of several flooding surfaces and major incisions are well comparable. In contrast to the Eastern Arabian Plate, with extended shallow platforms (including sand-dominated successions e.g. during the Albian), coeval platforms of the Northwestern Arabian Plate (e.g. Syria) are much narrower with a steeper gradient; as a consequence, the extended sandy accumulations of East Arabia favored flourishing *Orbitolina* –assemblages that are, however, of minor importance in northwest Arabia. As a consequence, the biotic communities of Syria record many faunal similarities with those of the South European platforms, described e.g. from the Adriatic Plate.

A composite $\delta^{13}C$ isotope reference curve is proposed for the Coastal Range, which is calibrated by good biostratigraphic controls in both, shallow- marine (benthonic foraminifera) and hemipelagic deposits (planktonic foraminifera). Several isotopic events of the CR are well comparable to global biotic and abiotic events: OAE1d, LCEs, MCE, (P/B) break Jukes-Browne, Amphidonte Bed and OAE2.

The exceptional outcrop quality, displays detailed facies patterns from peritidal to mid-ramp environments. The regional correlating of Coastal Range with Levant, Arabian plates and Tethyan realm reveal similar large-scale depositional patterns, within the limits of the biostratigraphic resolution. These correlations suggest that each of the major episodes of the 2nd order sea-level rise are comparable with MFS K80 to MFS K140 of the Arabian Plate (van Buchem et al., 2011; Haq and Al-Qahtani, 2005). The calibration of our sequence-stratigraphic model with global sequences (Hardenbol, et al., 1998; Ogg et al., 2008), combined to the available time resolution, only the Cenomanian sequences boundaries CeCR1 to CeCR5 appear to have clear interbasinal equivalents, while ApCR.1, AlCR3 CeCR4 and CeCR5 are delineated by major disconformities.

IX.8 Acknowledgements

The authors sincerely thank Prof. Dr. Esmeralda Caus for here help and controlling the benthonic foraminifera. We thank Dr. Christian Scheibner for his suggestions. We wish to thank the Syrian Petroleum Company for their generosity in providing data used in this study.

IX.9 REFERENCES

Allan, J, R., and R.K. Matthews 1982. Isotope signatures associated with early meteoric diagenesis. Sedimentology, v. 29, p. 797-817.

Alsharhan, A. S., and A. E. M. Nairn 1997. Sedimentary Basins and Petroleum Geology Of The Middle East (2 ed.). Elsevier. p. 471. ISBN 978-0-444-82465-3.

Boudagher-Fadel, M. K. 2009. The taxonony and evolution of the foraminiferal genus *Buccicrenata* Loeblich and Tappan. Micropaleontology, 47(2), 168-172.

Chowns, T. M., and J. E. Elkins 1974. The origin of quartz geodes and cauliflower cherts through the silicification of anhydrite nodules. Journal of Sedimentary Petrology, v. 44, no. 3, p. 885-903.

Dunham, R. J. 1962. Classification of carbonate rocks according to depositional texture. In: Ham WE (ed) Classification of carbonate rocks. A symposium. APG Memoir, v. 1, p. 108-171.

Elrick, M., R. Molina-Garza, R. Duncan, and L. Snow 2009. C-isotope stratigraphy and paleoenvironmental changes across OAE2 (mid-Cretaceous) from shallow-water platform carbonates of southern Mexico: Earth and Planetary Science Letters, v. 277, no. 3-4, p. 295-306.

Flügel, E. 2004. Microfacies of Carbonate Rocks: Analysis, Interpretation and Application. Springer. Berlin Heidelberg New York.

Gale, A.S., W.J. Kennedy, J.A. Burett, M. Caron and B.E. Kidd 1996. The Late Albian to Early Cenomanian succession at Mont Risou near Rosans (Drome, SE France): An integrated study (ammonites, inoceramids, planktonic foraminifera, nannofossils, oxygen and carbon isotopes). Cretaceous Research, v. 17, p. 515-606.Gerdes, K. D., P. Winefield, M. D. Simmons and C. Van Oosterhout 2010. The influence of basin architecture and eustacy on the evolution of Tethyan Mesozoic and Cenozoic carbonate sequences. Geological Society, London, Special Publications, v. 329, no. 1, p. 9-41.

Gertsch, B., T. Adatte, G. Keller, A. A. A. M. Tantawy, Z. Berner, H. P. Mort and D. Fleitmann 2010. Middle and late Cenomanian oceanic anoxic events in shallow and deeper shelf environments of western Morocco. Sedimentology, v. 57, no. 6, p. 1430-1462.

Ghanem, H., M. Mouty, J. Kuss 2012. Biostratigraphy and Carbon-isotope stratigraphy of the uppermost Aptian to Late Cenomanian strata of the Southern Palmyrids, GeoArabia, v. 17, p. 155-184.

Grötsch, J., I. Billing, V. Vahrenkamp 2002. Carbon-isotope stratigraphy in shallow-water carbonates: implications for Cretaceous black-shale deposition.- Sedimentology, 45/4, 623-634.

Hajikazemi, E., I.S. Al-Aasm and M. Coniglio 2010. Subaerial exposure and meteoric diagenesis of the Cenomanian-Turonian Upper Sarvak Formation, southwestern Iran. Geological Society, London, Special Publications, v. 330, no. 1, p. 253-272.

Haq, B. U., and A. M. Al-qahtani 2005. Phanerozoic cycles of sea-level change on the Arabian Platform Rationale for an Arabian Platform Cycle Chart, v. 10, no. 2, p. 127-160.

Hardenbol, J., J. Thierry, M. B., J. Farley, T. Graciansky, P. C. de, and P. R. Vail 1998. Cretaceous sequence chronostratigraphy. In: de P.-C. Graciansky, J. Hardenbol, T. Jacquin, and P.R. Vail, Eds., Mesozoic and Cenozoic Sequence Stratigraphic Framework of European Basins. SEPM (Society for Sedimentary Geology) Special Publication 60, p. 3-13.

Immenhauser, A., and R. W. Scott 1999. Global correlation of middle Cretaceous sea-level events. Geology.

Jarvis, I. A. N., A. S. Gale, H. C. Jenkyns and M. A. A. Pearce 2006. Secular variation in Late Cretaceous carbon isotopes : a new δ13C carbonate reference curve for the Cenomanian – Campanian (99 . 6 – 70 . 6 Ma), v. 143, p. 561-608.

Kennedy, W. J., A. S. Gale, J. A. Lees and Caron M. 2004. The Global Boundary Stratotype Section and Point (GSSP) for the base of the Cenomanian Stage, Mont Risou, Hautes-Alpes, France. Episodes, v. 27, no.1, p. 21-32.

Krasheninnnikov, V. A., J. K. Hall, F. Hirsch, C. Benjamini and A. Flexer (Ed.), 2005. Geological framework of the Levant, Volume I: Cyprus and Syria., p. 165-416.

Kuss, J., A. Bassiouni, J. Bauer, M. Bachmann, A. Marzouk, C. Scheibner and F. Schulze 2003. Cretaceous – Paleogene Sequence Stratigraphy of the Levant Platform (Egypt, Sinai, Jordan). In: E. Gili, H. Negra and P. Skelton (Ed.), North African Cretaceous Carbonate Platform Systems, Nato Science Series, p. 171-187.

Loeblich, A. R. and H. Tappan 1988. Foraminiferal genera and their classification, Van Nostrand Reinhold Co., New York, 970 p.

Luciani, V. Cobianchi, M. (1999) The Bonarelli level and other black shales in the Cenomanian–Turonian of the northeastern Dolomites (Italy): calcareous nannofossil and foraminiferal data. Cretaceous Res., 20, 135–167.

Mouty, M., and P. Saint-Marc 1982. Le Cretace Moyen du Massif Alaouite (NW Syrie). Cahiers Micropal., Paris, v. 3, p. 55-69.

Mouty, M., D. Delaloye, D. Fontignie, O. Piskin and J.J. Wagner 1992. The volcanic activity in Syria and Lebanon between Jurassic and Actual. Schweizersche Mineralogische und Petrographische Mitteilungen, v. 72, p. 91-105.

Ogg, J.G. and G. Ogg 2008. Mid- Late Cretaceous Charts.
https://engineering.purdue.edu/Stratigraphy/charts/Timeslices/4_Mid-Cret.pdf
https://engineering.purdue.edu/Stratigraphy/charts/Timeslices/3_Late_Cret.pdf

Alsharhan, A.S. & Nairn, A.E.M., 1997. Sedimentary Basins And Petroleum Geology Of The Middle East, Elsevier. 979p.

Blomeier, D., Scheibner, C. & Forke, H., 2008. Facies arrangement and cyclostratigraphic architecture of a shallow-marine, warm-water carbonate platform: the Late Carboniferous Ny Friesland Platform in eastern Spitsbergen (Pyefjellet Beds, Wordiekammen Formation, Gipsdalen Group). Facies, 55(2), pp.291-324.

Boudagher-fadel, M.K., 2009. The taxonony and evolution of the foraminiferal genus Buccicrenata Loeblich and Tappan. Micropaleontology, 47(2), pp.168-172.

Chowns, T.M. & Elkins, J.E., 1974. The origin of quartz geodes and cauliflower cherts through the silicification of anhydrite nodules. Journal of Sedimentary Petrology,

Flügel, E., 2004. Microfacies of Carbonate Rocks: Analysis, Interpretation and Application, Springer. Berlin Heidelberg New York.

Friedrich, O., 2010. Benthic foraminifera and their role to decipher paleoenvironment during mid-Cretaceous Oceanic Anoxic Events – the “anoxic benthic foraminifera” paradox. Revue de Micropaléontologie, 53(3), pp.175-192.

Gale, A.S. et al., 1996. The Late Albian to Early Cenomanian succession ˆ me , SE France) : at Mont Risou near Rosans (Dro an integrated study (ammonites , inoceramids , planktonic foraminifera , nannofossils , oxygen and carbon isotopes). Sciences-New York, pp.515-606.

Gerdes, K.D. et al., 2010. The influence of basin architecture and eustacy on the evolution of Tethyan Mesozoic and Cenozoic carbonate sequences. Geological Society, London, Special Publications, 329(1), pp.9-41. Available at: http://sp.lyellcollection.org/cgi/doi/10.1144/SP329.2 [Accessed March 15, 2012].

Gertsch, B. et al., 2010. Middle and late Cenomanian oceanic anoxic events in shallow and deeper shelf environments of western Morocco. Sedimentology, 57(6), pp.1430-1462.

Hajikazemi, E., Al-Aasm, I.S. & Coniglio, M., 2010. Subaerial exposure and meteoric diagenesis of the Cenomanian-Turonian Upper Sarvak Formation, southwestern Iran. Geological Society, London, Special Publications, 330(1), pp.253-272.

Haq, B.U. & Al-qahtani, A.M., 2005. Phanerozoic cycles of sea-level change on the Arabian Platform Rationale for an Arabian Platform Cycle Chart. , 10(2), pp.127-160.

Hardenbol, J., Thierry, J., Farley, M. B., J. & T., Graciansky, P. C. de, Vail, P.R., Mesozoic and Cenozoic Sequence Chronostratigraphic Framework of European Basins.

Immenhauser, A. & Scott, R.W., 1999. Global correlation of middle Cretaceous sea-level events. Geology.

Jarvis, I.A.N. et al., 2006. Secular variation in Late Cretaceous carbon isotopes : a new δ 13 C carbonate reference curve for the Cenomanian – Campanian (99 . 6 – 70 . 6 Ma). , 143, pp.561-608.

Krasheninnikov, V.A., J.K. Hall, F. Hirsch, C.B. and A.F. (Eds. ., 2005. No Title Geological framework of the Levant, Volume I: Cyprus and Syria. , pp.165-416.

Loeblich, A.R. & Tappan, H.N., 1988. Foraminiferal genera and their classification, Van Nostrand Reinhold Co.

Mouty, M. and Sait-Marc, P., 1982. Le Cretace Moyen du Massif Alaouite (NW Syrie). Cahiers Micropal., Paris, 3, pp.55-69.

Parente, M., Frijia, G. & Di Lucia, M., 2007. Carbon-isotope stratigraphy of Cenomanian-Turonian platform carbonates from the southern Apennines (Italy): a chemostratigraphic approach to the problem of correlation between shallow-water and deep-water successions. Journal of the Geological Society, 164(3), pp.609-620.

Paul C.R.C., Mitchell S.F., Marshall J.D., keary P.N., Gale A.S., Duane A.M., D.P.W., 1994. Mid-Cenomanian Event Paul 94.pdf. , pp.707-738.

Schroeder, R. et al., 2010. Revised orbitolinid biostratigraphic zonation for the Barremian – Aptian of the eastern Arabian Plate and implications for regional stratigraphic correlations. GeoArabia, (1948), pp.49-96.

Sharland, P.R., R. Archer D.M. Casey, R.B. Davies, S.H. Hall, A.P. Heward, A.D. Horbury and M.D. Simmons 2001. Arabian Plate sequence stratigraphy. GeoArabia Special Publication 2, Gulf PetroLink, Bahrain, 371 p., with 3 charts. Sharland, P.R., D.M. Casey, R.B. Davies, M.D. Simmons and O.E. Sutcliffe 2004. Arabian Plate Sequence Stratigraphy. GeoArabia, v. 9, no. 1, p. 199-214.

Velić, I., 2007. Geologia Croatica Stratigraphy and Palaeobiogeography of Mesozoic Benthic Foraminifera of the Karst Dinarides (SE Europe). Geologia Croatica.

Verga, D. & Premoli Silva, I., 2002. Early Cretaceous planktonic foraminifera from the Tethys: the genus Leupoldina. Cretaceous Research, 23(2), pp.189-212.

Wilmsen, M. & Nagm, E., 2011. Depositional environments and facies development of the Cenomanian–Turonian Galala and Maghra el Hadida formations of the Southern Galala Plateau (Upper Cretaceous, Eastern Desert, Egypt). Facies, 58(2), pp.229-247.

Parente, M., G. Frijia, and M. Di Lucia, 2007, Carbon-isotope stratigraphy of Cenomanian-Turonian platform carbonates from the southern Apennines (Italy): a chemostratigraphic approach to the problem of correlation between shallow-water and deep-water successions: Journal of the Geological Society, v. 164, no. 3, p. 609-620.

Parente, M., G. Frijia, M.D. Lucia, H.C. Jenkyns, R.G. Woodfine, R.G. Woodfi and F. Baroncini 2008. Stepwise extinction of larger foraminifers at the Cenomanian- Turonian boundary : A shallow-water perspective on nutrient fl uctuations during Oceanic Anoxic Event 2 (Bonarelli Event): Geology, v. 2, p. 715-718.

Paul C.R.C., S.F. Mitchell, J.D. Marshall, P.N. keary, A.S. Gale, A.M. Duane and P. W. Ditchfield 1994. Mid-Cenomanian Event Paul 94.pdf. Cretaceous Research.

Premoli Silva, I. and D. Verga 2004. Practical Manual of Cretaceous Planktonic Foraminifera. In D. Verga, R. Rettori (Eds.), International School on Planktonic Foraminifera: Perugia, Italy, Tipografia Ponte Felcino, Universities of Perugia and Milan, 3th Course, p. 283.

Premoli Silva, I., M. Le Caron, R. M. Leckie, M.R. Petrizzo, D. Soldan and D. Verga 2009. Paraticinella Gen and Taxonomic Revision of Ticinella Bejaouaensis Sigal 1966. Journal of Foraminiferal Research, v. 39, no. 2, p.126-137.

Schroeder, R., F.S.P. van Buchem, A. Cherchi, D. Baghbani, B. Vincent, A. Immenhauser and B. Granier 2010. Revised orbitolinid biostratigraphic zonation for the Barremian – Aptian of the eastern Arabian Plate and implications for regional stratigraphic correlations. In F.S.P. van Buchem, M.I. Al-Husseini, F. Maurer and H.J. Droste. Barremian – Aptian stratigraphy and hydrocarbon habitat of the eastern Arabian Plate. GeoArabia v. 1, p. 49-96.

Sharland, P. R., R. Archer D.M. Casey, R.B. Davies, S.H. Hall, A.P. Heward, A.D. Horbury and M.D. Simmons 2001. Arabian Plate Sequence Stratigraphy. GeoArabia Special Publication 2, Gulf PetroLink, Bahrain, 371 p.

Sharland, P.R., D.M. Casey, R.B. Davies, M.D. Simmons and O.E. Sutcliffe 2004. Arabian Plate Sequence Stratigraphy. GeoArabia, v. 9, p. 199-214.

Sornay, J., M. Mouty and H. Gauthier 2001. Les ammonites du Ce´nomano-Turonien de la Chaıˆne coˆtie`re (Jibal As-Sahilyeh) de Syrie. Ge´ologie Me´diterrane´enne v. 28, p. 243-257.

van Buchem, F.S.P., M.I. Al-Husseini, F. Maurer, H.J. Droste and L.A.Yose 2010. Sequence-stratigraphic synthesis of the Barremian-Aptian of the eastern Arabian Plate and

implications for the petroleum habitat. In: Van Buchem, F.S.P., et al. (eds.) Barremian – Aptian Stratigraphy and Hydrocarbon Habitat of the Eastern Arabian Plate. GeoArabia Special Publication 4, Gulf PetroLink, Bahrain, 1, 9-48.

van Buchem, F.S.P., M.D. Simmons, H.J. Droste and R.B. Davies 2011. Late Aptian to Turonian stratigraphy of the eastern Arabian Plate – depositional sequences and lithostratigraphic nomenclature. Petroleum Geology, v. 17, p. 211-222.

Velić, I. 2007. Geologia Croatica Stratigraphy and Palaeobiogeography of Mesozoic Benthic Foraminifera of the Karst Dinarides (SE Europe). Geologia Croatica, v. 60, no. 1, p. 1-113.

Verga, D., and I. Premoli Silva 2002. Early Cretaceous planktonic foraminifera from the Tethys: the genus Leupoldina. Cretaceous Research, v. 23, no. 2, p. 189-212.

Vahrenkamp, V. C. 1996. Carbon isotope stratigraphy of the upper Kharaib and Shuaiba Formations; implications for the Early Cretaceous evolution of the Arabian Gulf region.- AAPG Bull., v. 80/5, p. 647-662.

Vahrenkamp, V. C. 2010. Chemostratigraphy of the Lower Cretaceous Shu'aiba Formation: A d13C reference profile for the Aptian Stage from the southern Neo-Tethys Ocean. GeoArabia Special Publication 4, Barremian – Aptian stratigraphy and hydrocarbon habitat of the eastern Arabian Plate, (van Buchem, Al-Husseini, Maurer and Droste, Eds.), p. 107-137.

Wilmsen, M., B. Niebuhr and M. Hiss 2005. The Cenomanian of northern Germany: facies analysis of a transgressive biosedimentary system: Facies, v. 51, no. 1-4, p. 242-263.

X. CONCLUSIONS

The Aptian to Early Turonian succession of the North Levant platform of the Southeastern Tethys (West Syria) has been studied in detail using a combination of lithostratigraphy, biostratiography, chemostratigraphy and sequence stratigraphy. The research focused in the stratigraphic development of the Aptian to Early Turonian North Levant platform. The evolution of the carbonate platform was influenced by global perturbations as well as by local tectonic and volcanic activity, summarized in the following paragraphs:

A chronostratigraphic framework of the studied sections is carried out, based on new lithostratigraphic and biostratigraphic results. The studied sections are investigated by integrating and correlating the field observations, the facies analysis, and the biostratigraphic data. High resolution is a principle requirement for the estimation of any event or process in the stratigraphic record. Benthonic and planktonic foraminifera are the essential parameters of the separate independent biozonations. Although the foraminiferal communities of the North Levant exhibit many faunal similarities with those of the South European platforms, several taxa are restricted to the North Arabian shelf.

Carbon isotope analyses have been carried out in order to use the $\delta^{13}C$ values for stratigraphic objectives. The positive $\delta^{13}C$ excursions, which have been observed worldwide close to the OAE1, have been identified in the sections investigated. Careful correlation of stable isotope data within a high resolution biostratigraphic framework led to reliable local correlation of the marl and limestone intercalations, and to their biostratigraphic position. . Several hiatuses and their regional extension from the South Palmyrides to the Coastal Range were detected with different parameters such as $\delta^{13}C$ peaks, biotic gaps and volcanic events.

The lithofacies and biofacies characteristics and the distribution of the skeletal and non-skeletal components reflect an ecological development from the carbonate platform to the deeper ramp conditions. The shallow lagoonal facies mainly occur in the early transgressive and the late regressive stages of individual cycles, while the deeper ramp marls characterize the late transgressive and the maximum flooding surface (mfs). The result of this facies investigation and its radioactive record allow to identify 12 Syrian 2^{nd} and/or 3^{rd} order sequences of the Aptian – Early Turonian deposits, connected to the

South Levant platform (Sinai, especially for the Albian to Early Turonian) and to the major 2nd order Arabian and to the 3rd order global sequences.

The combination between facies, sea level change and different types of hiatuses observed in the area enabled to reconstruct a detailed evolution of the paleogeography throug the Aptian to Early Turonian, as documented in two newly refined paleogeographic maps.

XI. APPENDIX

Supplementary material, including all investigated sections, boreholes, sample lists, biostratigraphy, microfacies, chemostratigraphic data, sequence stratigraphy, reprints of the already published manuscripts in addition to a schedule overview of the platform evolution during the Early-Middle Cretaceous rifting of the North Arabia, is provided in the enclosed CD.

XII. REFERENCES

Allan, J, R., and R.K. Matthews 1982. Isotope signatures associated with early meteoric diagenesis. Sedimentology, v. 29, p. 797-817.

Al-Maleh, A.KH. M. Mouty, T. Sawaf, G. Brew and M. Barazangi 2000. Mesozoic depositional trends in the northern Arabian Platform in Syria; regional and tectonic implications. GeoArabia, v. 5, no. 1, p. 30-31.

Alsharhan, A. S., and A. E. M. Nairn 1997. Sedimentary Basins and Petroleum Geology Of The Middle East (2 ed.). Elsevier. p. 471.

Blomeier, D., Dustira, A., Forke, H., and C. Scheibner, 2010. Environmental change in the Early Permian of NE Svalbard: from a warm-water carbonate platform (Gipshuken Formation) to a temperate, mixed siliciclastic-carbonate ramp (Kapp Starostin Formation).

Bachmann, M., A. M. Bassiouni and Kuss, J., 2003, Stratigraphic modelling, graphic correlation and cyclicities of mid-Cretaceous platform carbonates - northern Sinai, Egypt. Palaeogeography, Palaeoclimatology, Palaeoecology 200, 131-162.

Best, J.A., M. Barazangi, D. Al-Saad, T. Sawaf and A. Gebran 1993. Continental margin evolution of the northern Arabian platform in Syria. American Association of Petroleum Geologists Bulletin, v. 77, no. 2, p. 173–193.

Blomeier, D., Scheibner, C., and Forke, H., 2008. Facies arrangement and cyclostratigraphic architecture of a shallow-marine, warm-water carbonate platform: the Late Carboniferous Ny Friesland Platform in eastern Spitsbergen (Pyefjellet Beds, Wordiekammen Formation, Gipsdalen Group): Facies, v. 55, no. 2, p. 291-324.

Boudagher-Fadel, M. K. 2009. The taxonony and evolution of the foraminiferal genus Buccicrenata Loeblich and Tappan. Micropaleontology, 47(2), 168-172.

Bowman, S.A., 2011. Regional seismic interpretation of the hydrocarbon prospectivity of offshore Syria: , no. 3, p. 95-124.

Brew, G., and Barazangi, M., 2001. Tectonic and Geologic Evolution of Syria: GeoArabia, v. 6, no. 4. p. 289–318.

Brew, G., Best, J., Barazangi, M., and Sawaf, T., 2003. Tectonic evolution of the NE Palmyride mountain belt, Syria: the Bishri crustal block: Journal of the Geological Society, v. 160, no. 5, p. 677-685.

Brew, G., Litak, R., and Barazangi, M., 1999. Tectonic Evolution of Northeast Syria : Regional Implications and Hydrocarbon Prospects: GeoArabia, v. 4, no. 3.

Caron, C., and M. Mouty 2007. Key elements to clarify the 110 million year hiatus in the Mesozoic of eastern Syria: GeoArabia, v. 12, no. 2, p. 13- 36.

Caron, M. 1985. Cretaceous planktic foraminifera. In H.M. Bolli, J.B. Saunders and K. Perch-Nielsen (Eds.). Plankton Stratigraphy. Cambridge University Press, p. 17-86.

Chaimov, T., M. Barazangi, D. Al-Saad, T. Sawaf and A. Gebran 1992. Mesozoic and Cenozoic deformation inferred from seismic stratigraphy in the southwestern intracontinental Palmyride fold-thrust belt, Syria. Geological Society of America Bulletin, v. 104, no. 6, p. 704–715.

Chowns, T. M., and J. E. Elkins 1974. The origin of quartz geodes and cauliflower cherts through the silicification of anhydrite nodules. Journal of Sedimentary Petrology, v. 44, no. 3, p. 885-903.

Demicco, R. V., and L. A. Hardie 1994. Sedimentary structures and early diagenetic features of shallow marine carbonate deposits: Society of Economic paleontologists and Mineralogists Atlas Series v.1, p. 255.

Dunham, R. J. 1962. Classification of carbonate rocks according to depositional texture. In: Ham WE (ed) Classification of carbonate rocks. A symposium. APG Memoir, v. 1, p. 108-171.

Dubertret, L., 1955. Géologie des roches vertes du nord-ouest de la Syrie et du Hatay (Turquie). Not. et Mém. sut le Moyen Orient, v. 6, Paris, p. 179.

Elliott, G.F., 1962. More microproblematica from the Middle East: Middle East, Micropaleontology, v. 8, no. 1, p. 29-44.

El-Motaal, E.A., and Kusky, T.M., 2003. Tectonic evolution of the intraplate s-shaped Syrian Arc fold- thrust of the Middle East Region in the context of the plate tectonics: Syria, The 3rd International Conference on the Geology of Africa, v. 157, no. 2, p. 139-157.

Elrick, M., R. Molina-Garza, R. Duncan, and L. Snow 2009. C-isotope stratigraphy and paleoenvironmental changes across OAE2 (mid-Cretaceous) from shallow-water platform carbonates of southern Mexico: Earth and Planetary Science Letters, v. 277, no. 3-4, p. 295-306.

Flügel, E. 2004. Microfacies of Carbonate Rocks: Analysis, Interpretation and Application. Springer. Berlin Heidelberg New York.

Ferry, S., Y. Merran, D. Grosheny and M. Mroueh 2007. The Cretaceous of Lebanon in the Middle East (Levant) context [Le Crétacé du Liban dans le cadre du Moyen-Orient (Levant)]. Carnets de Géologie, p. 38-42.

Friedrich, O. 2010. Benthic foraminifera and their role to decipher paleoenvironment during mid-Cretaceous Oceanic Anoxic Events – the “anoxic benthic foraminifera” paradox. Revue de Micropaleontologie, v. 53, p. 175-192

Gale, A.S., W.J. Kennedy, J.A. Burett, M. Caron and B.E. Kidd 1996. The Late Albian to Early Cenomanian succession at Mont Risou near Rosans (Drome, SE France): An integrated study (ammonites, inoceramids, planktonic foraminifera, nannofossils, oxygen and carbon isotopes). Cretaceous Research, v. 17, p. 515-606.

Gardosh, M. a., Garfunkel, Z., Druckman, Y., and Buchbinder, B., 2010a. Tethyan rifting in the Levant Region and its role in Early Mesozoic crustal evolution: Geological Society, London, Special Publications, v. 341, no. 1, p. 9-36.

Gardosh, M. a., Garfunkel, Z., Druckman, Y., and Buchbinder, B., 2010b. Tethyan rifting in the Levant Region and its role in Early Mesozoic crustal evolution: Geological Society, London, Special Publications, v. 341, no. 1, p. 9-36.

Gerdes, K.D., Winefield, P., Simmons, M.D., and Van Oosterhout, C., 2010. The influence of basin architecture and eustacy on the evolution of Tethyan Mesozoic and Cenozoic carbonate sequences: Geological Society, London, Special Publications, v. 329, no. 1, p. 9-41.

Gertsch, B., T. Adatte, G. Keller, A. A. A. M. Tantawy, Z. Berner, H. P. Mort and D. Fleitmann 2010. Middle and late Cenomanian oceanic anoxic events in shallow and deeper shelf environments of western Morocco. Sedimentology, v. 57, no. 6, p. 1430-1462.

Gradstein, F.M., J.G. Ogg and A.G. Smith 2004. A Geologic Time Scale 2004. Cambridge University Press, 589 p.

Gradstein, F. M., Ogg, J. G., Schmitz, M., & Ogg, G. (2012). The Geologic Time Scale 2012 2-Volume Set. Elsevier Science, 1144p.

Ghanem H., and Kuss, J., (subm.). Stratigraphic control of the Aptian - Early Turonian sequences of the Levant Platform (Northwest Syria - Coastal Range). Geoarabia.

Ghanem, H., M. Mouty, J. Kuss 2012. Biostratigraphy and Carbon-isotope stratigraphy of the uppermost Aptian to Late Cenomanian strata of the Southern Palmyrids, Geoarabia, v. 17, p. 155-184.

Grötsch, J., I. Billing, and V. Vahrenkamp 2002. Carbon-isotope stratigraphy in shallow-water carbonates: implications for Cretaceous black-shale deposition.- Sedimentology, 45/4, 623-634.

Hajikazemi, E., I.S. Al-Aasm and M. Coniglio 2010. Subaerial exposure and meteoric diagenesis of the Cenomanian-Turonian Upper Sarvak Formation, southwestern Iran. Geological Society, London, Special Publications, v. 330, no. 1, p. 253-272.

Homberg, C., and Bachmann, M., 2010, Evolution of the Levant margin and western Arabia platform since the Mesozoic: introduction: Geological Society, London, Special Publications, v. 341, no. 1, p. 1-8.

Haq, B. U., and A. M. Al-Qahtani 2005. Phanerozoic cycles of sea-level change on the Arabian Platform - Rationale for an Arabian Platform Cycle Chart, GeoArabia, v. 10, no. 2, p. 127-160.

Hardenbol, J., J. Thierry, M. B., J. Farley, T. Graciansky, P. C. de, and P. R. Vail 1998. Cretaceous sequence chronostratigraphy. In: de Graciansky, P.-C. , J. Hardenbol, T. Jacquin, and P.R. Vail, Eds., Mesozoic and Cenozoic Sequence Stratigraphic Framework of European Basins. SEPM (Society for Sedimentary Geology) Special Publication 60, p. 3-13.

Joachimski, M.M. 1994. Subaerial exposure and deposition of shallowing upward sequences: Evidence from stable isotopes of Purbeckian peritidal carbonates (basal Cretaceous), Swiss and French Jura Mountains. Sedimentology, v. 41, p. 805-824.

Immenhauser, A., and R. W. Scott 1999. Global correlation of middle Cretaceous sea-level events. Geology, v. 27; no. 6; p. 551–554.

Jarvis, I., G.A. Carson, M.K. Cooper, M.B. Hart, P.N. Leary, B.A. Tocher, D. Horne and A. Rosenfeld 1988. Microfossil assemblages and the Cenomanian-Turonian (late Cretaceous) oceanic anoxic event. Cretaceous Research, v. 9, p. 3-103.

Jarvis, I., A. S. Gale, H. C. Jenkyns and M. A. A. Pearce 2006. Secular variation in Late Cretaceous carbon isotopes : a new δ13C carbonate reference curve for the Cenomanian – Campanian (99 . 6 – 70 . 6 Ma), Geol. Mag., v. 143, p. 561-608.

Kennedy, W. J., A. S. Gale, J. A. Lees and Caron M. 2004. The Global Boundary Stratotype Section and Point (GSSP) for the base of the Cenomanian Stage, Mont Risou, Hautes-Alpes, France. Episodes, v. 27, no.1, p. 21-32.

Kazmin, V.G., 2002, The late Paleozoic to Cainozoic intraplate deformation in North Arabia : a responce to plate boundary-forces: EGU Stephan Mueller Special Publication Series, v. 2, p.123–138,.

Krasheninnnikov, V. A., J. K. Hall, F. Hirsch, C. Benjamini and A. Flexer (Ed.), 2005. Geological framework of the Levant, Volume I: Cyprus and Syria., p. 165-416.

Kuss, J., A. Bassiouni, J. Bauer, M. Bachmann, A. Marzouk, C. Scheibner and F. Schulze 2003. Cretaceous – Paleogene Sequence Stratigraphy of the Levant Platform (Egypt, Sinai, Jordan). In: E. Gili, H. Negra and P. Skelton (Ed.), North African Cretaceous Carbonate Platform Systems, Nato Science Series, p. 171-187.

Kozlov, V. V. (assisted by A. V. Artyemov, and A. F Kalis), 1966a. The geological map of Syria. Scale 1:200,000. Sheets I-36-XIX, I-37-XIII (Trablus, Homs). Explanatory Notes. Technoexport, USSR, 68 p.

Loeblich, A. R. and H. Tappan 1988. Foraminiferal genera and their classification, Van Nostrand Reinhold Co., New York, 970 p.

Luciani, V. Cobianchi, M. 1999. The *Bonarelli* level and other black shales in the Cenomanian–Turonian of the northeastern Dolomites (Italy): calcareous nannofossil and foraminiferal data. Cretaceous Res., 20, 135–167.

Luiciani, V., M. Cobianchi and H.C. Jenkyns 2004. Albian high-resolution biostratigraphy and isotope stratigraphy: The Coppa della Nuvola pelagic succession of the Gargano Promontory (Southern Italy). Eclogae Geologicae Helvetiae v, 97, p. 77-92.

Luiciani, V., M. Cobianchi and C. Lupi 2006. Regional record of a global oceanic anoxic event: OAE1a on the Apulia Platform margin, Gargano Promontory, southern Italy. Cretaceous research, v. 27, p. 754-772.

Ma, G.S.-K., Malpas, J., Xenophontos, C., Suzuki, K., and Lo, C.-H., 2011. Early Cretaceous volcanism of the Coastal Ranges, NW Syria: Magma genesis and regional dynamics: Lithos, v. 126, no. 3-4, p. 290-306

Mamet, B., and Preat, A., 2005. Microfaies D'une Lentille Biohermale la Limite Eifelien/ Givetien (Wellin, Bord Sud du Sznclinorium de Dinant): Sciences-New York,, p. 85-111.

Mouty, M. 1997. Le Jurassique de la chaîne des Palmyrides, Syrie centrale. Bulletin of the French Geological Society, France, v. 168, no. 2, p. 181-186.

Mouty, M., A.KH. Al-Maleh and H. Abou-Laban 2002. Le Crétacé moyen la chaîne des Palmyrides (Syrie centrale). Geodiversitas, Paris, v. 25, p. 429-443.

MMouty, M., A.KH. Al-Maleh, H. Abou-Laban and Y. Al-Joubeli 1983. The geological study of the Palmyridean chain through typical geological sections. The General Establishment of Geology and Mineral Resources. Ministry of Oil, Syrian Arab Republic.

Mouty, M., D. Delaloye, D. Fontignie, O. Piskin and J.J. Wagner 1992. The volcanic activity in Syria and Lebanon between Jurassic and Actual. Schweizersche Mineralogische und Petrographische Mitteilungen, v. 72, p. 91-105.

Mouty, M., and P. Saint-Marc 1982. Le Cretace Moyen du Massif Alaouite (NW Syrie). Cahiers Micropal., Paris, v. 3, p. 55-69.

Ogg, J.G. 2004a. Mid- Late Cretaceous Charts. http://norges.uio.no/timescale /Late_Cretaceous.pdf and, http://norges.uio.no/timescale/Early_Cretaceous.pdf.

Ogg, J.G. 2004b. Mid- Late Cretaceous Charts. In F.M. Gradstein, J.G. Ogg and A.G. Smith (Eds.), A Geologic Time Scale 2004. Cambridge University Press, 589 p.

Ogg, J.G. and G. Ogg 2008. Mid- Late Cretaceous Charts.
https://engineering.purdue.edu/Stratigraphy/charts/Timeslices/4_Mid-Cret.pdf
https://engineering.purdue.edu/Stratigraphy/charts/Timeslices/3_Late_Cret.pdf

Ogg, J. G., G. Ogg and F. M.Gradstein 2008. The Concise Geologic Time Scale. Cambridge University Press.

Parente, M., G. Frijia, and M. Di Lucia, 2007. Carbon-isotope stratigraphy of Cenomanian-Turonian platform carbonates from the southern Apennines (Italy): a chemostratigraphic approach to the problem of correlation between shallow-water and deep-water successions: Journal of the Geological Society, v. 164, no. 3, p. 609-620.

Parente, M., G. Frijia, M.D. Lucia, H.C. Jenkyns, R.G. Woodfine, R.G. Woodfi and F. Baroncini 2008. Stepwise extinction of larger foraminifers at the Cenomanian- Turonian boundary : A shallow-water perspective on nutrient fl uctuations during Oceanic Anoxic Event 2 (Bonarelli Event): Geology, v. 2, p. 715-718.

Paul C.R.C., S.F. Mitchell, J.D. Marshall, P.N. keary, A.S. Gale, A.M. Duane and P. W. Ditchfield 1994. Mid-Cenomanian Event. Cretaceous Research, v.15, p. 707-738.

Philip, J., 2003, Peri-Tethyan neritic carbonate areas: distribution through time and driving factors: Palaeogeography, Palaeoclimatology, Palaeoecology, v. 196, no. 1-2, p. 19-37.

Ponikarov, V.P. 1966. The geology of Syria. Explanatory Notes on the Geological Map of Syria, scale 1:200 000. Ministry of Industry, Syrian Arab Republic.

Ponikarov, V.P., V.G. Kazmin, I.A. Mikhailov, A.V. Razvaliayev, V.A. Krasheninnikov, V.V. Kozlov, E.D. Soulidi-Kondtatiyev and V.A. Faradzhev 1966. The Geological map of Syria. 1:1,000,000. Explanatory Notes. Technoexport, USSR, 111 p.

Préat, A., and D. Carliez 1996. Microfacies et cyclicité dans le Givétien supérieur de Fromelennes (Synclinorium de Dinant, France). Annales de la Société géologique de Belgique, v. 117, p. 227-283.

Préat, A., and B. Mamet 1989. Sédimentation de la plateforme carbonatée Givétienne franco-belge. Bulletin des centres de recherches Exploration-production Elf Aquitaine, v.13 no.1, p.47-86.

Premoli Silva, I. and D. Verga 2004. Practical Manual of Cretaceous Planktonic Foraminifera. In D. Verga, R. Rettori (Eds.), International School on Planktonic Foraminifera: Perugia, Italy, Tipografia Ponte Felcino, Universities of Perugia and Milan, 3th Course, p. 283.

Premoli Silva, I., M. Le Caron, R. M. Leckie, M.R. Petrizzo, D. Soldan and D. Verga 2009. Paraticinella Gen and Taxonomic Revision of *Ticinella bejaouaensis* Sigal 1966. Journal of Foraminiferal Research, v. 39, no. 2, p.126-137.

Sari, B., and S.Özer 2001. Facies Characteristics of the Cenomanian – Maastrichtian Sequence of the Beydaglari Carbonate Platform, Korkuteli Area , Western Taurides , Turkey: Turkish J. Earth Sci. v. 43, p. 37-41.

Sawaf, T., D.Al-saad, A.L.I. Gebran, M. Barazangi, J.A. Best, and T.A. Chaimov 1993, Stratigraphy and Structure of Eastern Syria across the Euphrates depression. Tectonophysics, v. 220, no. 1–4, p. 267-281

Schulze, F., Kuss, J., and Marzouk, A., 2005, Platform configuration, microfacies and cyclicities of the upper Albian to Turonian of west-central Jordan: Facies, v. 50, no. 3-4, p. 505-527.

Schroeder, R. and M. Neumann 1985. Les grands foraminifères du Crétacé moyen de la region Méditerranéenne. Geobios, Mémoire Spécial 7, p. 1-160.

Schroeder, R., F.S.P. van Buchem, A. Cherchi, D. Baghbani, B. Vincent, A. Immenhauser and B. Granier 2010. Revised orbitolinid biostratigraphic zonation for the Barremian – Aptian of the eastern Arabian Plate and implications for regional stratigraphic correlations. In F.S.P. van Buchem, M.I. Al-Husseini, F. Maurer and H.J. Droste. Barremian – Aptian stratigraphy and hydrocarbon habitat of the eastern Arabian Plate. GeoArabia v. 1, p. 49-96.

Seber, D., M. Barazangi, T. Chaimov, D. Al-Saad, T. Sawaf and M. Khaddour 1993. Upper crustal velocity structure and basement morphology beneath the intracontinental Palmyride fold-thrust belt and north Arabian platform in Syria. Geophysical Journal International, v. 113, no. 3, p. 752–766.

Segev, A., 2009. 40Ar/39Ar and K–Ar geochronology of Berriasian–Hauterivian and Cenomanian tectonomagmatic events in northern Israel: implications for regional stratigraphy: Cretaceous Research, v. 30, no. 3, p. 810-828.

Segev, a., and Rybakov, M., 2010. Effects of Cretaceous plume and convergence, and Early Tertiary tectonomagmatic quiescence on the central and southern Levant continental margin: Journal of the Geological Society, v. 167, no. 4, p. 731-749.

Sharland, P. R., R. Archer D.M. Casey, R.B. Davies, S.H. Hall, A.P. Heward, A.D. Horbury and M.D. Simmons 2001. Arabian Plate Sequence Stratigraphy. GeoArabia Special Publication 2, Gulf PetroLink, Bahrain, 371 p.

Sharland, P.R., D.M. Casey, R.B. Davies, M.D. Simmons and O.E. Sutcliffe 2004. Arabian Plate Sequence Stratigraphy. GeoArabia, v. 9, p. 199-214.

Shatsky, V. N., Kazmin, V. G., and Kulakov, V. V., 1966. The Geological map of Syria. Scale 1:200,000. Sheets I-37-XIX and I-36-XXIV (Al-Latheqiyeh and Hama). Explanatory Notes. Technoexport, USSR, p107.

Sornay, J., M. Mouty and H. Gauthier 2001. Les ammonites du Cenomano-Turonien de la Chaıˆne coˆtie`re (Jibal As-Sahilyeh) de Syrie. Geologie Mediterraneenne v. 28, p. 243-257.

Sigal, J. 1966. Contribution a` une monographie des Rosalines. 1. Le genre Ticinella Reichel, souche des Rotalipores. Eclogae Geologicae Helvetiae, v. 59, p. 186-217.

Stampfli, G.M., J. Mosar, P. Favre, A. Pillevuit and J.-C. Vannay 2001. Permo-Mesozoic evolution of the western Tethyan realm: The Neotethys/East-Mediterranean connection. In P.A. Ziegler, W. Cavazza, A.H.F. Robertson and S. Crasquin-Soleau (Eds.), Peritethys, Memoir 6: Peritethyan Rift/Wrench Basins and Passive Margins, IGCP 369. Memorial Museum of Natural History, v. 186, p. 51-108.

Stampfli, G.M., and Borel, G.D., 2002. A plate tectonic model for the Paleozoic and Mesozoic constrained by dynamic plate boundaries and restored synthetic oceanic isochrons: v. 196, p. 17-33.

Stampfli, G.M., and Borel, G., 2003, AAPG International Conference: Science, v. 2, no. 1, p. 1-6.

van Buchem, F.S.P., M.I. Al-Husseini, F. Maurer, H.J. Droste and L.A.Yose 2010. Sequence-stratigraphic synthesis of the Barremian-Aptian of the eastern Arabian Plate and implications for the petroleum habitat. In: Van Buchem, F.S.P., et al. (eds.) Barremian – Aptian Stratigraphy and Hydrocarbon Habitat of the Eastern Arabian Plate. GeoArabia Special Publication 4, Gulf PetroLink, Bahrain, 1, 9-48.

van Buchem, F.S.P., M.D. Simmons, H.J. Droste and R.B. Davies 2011. Late Aptian to Turonian stratigraphy of the eastern Arabian Plate – depositional sequences and lithostratigraphic nomenclature. Petroleum Geology, v. 17, p. 211-222.

Velić, I. 2007. Geologia Croatica Stratigraphy and Palaeobiogeography of Mesozoic Benthic Foraminifera of the Karst Dinarides (SE Europe). Geologia Croatica, v. 60, no. 1, p. 1-113.

Verga, D., and I. Premoli Silva 2002. Early Cretaceous planktonic foraminifera from the Tethys: the genus *Leupoldina*. Cretaceous Research, v. 23, no. 2, p. 189-212. ..

Vahrenkamp, V. C. 1996. Carbon isotope stratigraphy of the upper Kharaib and Shuaiba Formations; implications for the Early Cretaceous evolution of the Arabian Gulf region.- AAPG Bull., v. 80/5, p. 647-662.

Vahrenkamp, V. C. 2010. Chemostratigraphy of the Lower Cretaceous Shu'aiba Formation: A d13C reference profile for the Aptian Stage from the southern Neo-Tethys Ocean. GeoArabia Special Publication 4, Barremian – Aptian stratigraphy and hydrocarbon habitat of the eastern Arabian Plate, (van Buchem, Al-Husseini, Maurer and Droste, Eds.), p. 107-137.

Wilmsen, M., B. Niebuhr and M. Hiss 2005. The Cenomanian of northern Germany: facies analysis of a transgressive biosedimentary system: Facies, v. 51, no. 1-4, p. 242-263.

Wilson, P.A. and R.D. Norris 2001. Warm tropical ocean surface and global anoxic during the mid- Cretaceous period. Nature, v. 412, p. 425-429.